INVESTIGATING THE MECHANISMS THAT REGULATE THE ESTABLISHMENT OF POLARITY DURING ZEBRAFISH NEURAL TUBE FORMATION

Gemma Clare Girdler

UCL

Submitted for the degree of PhD

I, Gemma Girdler, confirm that the work presented in this thesis is my own. Where information has been derived from other sources, I confirm that this has been indicated in the thesis.

ABSTRACT

The establishment of apico-basal polarity and lumen formation are fundamental steps during vertebrate neural tube development. In zebrafish embryos, the lumen is generated *de novo* from a solid rod structure. Prior to this, the neural cells acquire apico-basal polarity when they undergo mirror-symmetric division and one daughter cell crosses the midline (C-division). This specialised division must be tightly regulated in time and space for correct neural tube morphogenesis. I have shown that delaying convergence in wild-type tissue results in C-divisions occurring at the right time but in the wrong place and the generation of neural tube duplications. This uncoupling of individual cell behaviours from tissue morphogenesis suggests that an intrinsic timer controls cell polarisation and C-division during neurulation.

I have tested this hypothesis by heterochronic cell transplantation. I have found that both younger and older transplanted cells polarise according to their age, show a decreased ability to cross the midline during neurulation, and that older cells can generate ectopic lumens within the host neuroepithelium. These results all support the idea that an intrinsic timer controls cell polarisation and lumen formation. They suggest that the timer begins even before cells are specified as neural, and can resist many environmental signals during gastrulation and neurulation that could reset it.

I have also investigated the role of the environment in neural cell polarisation by examining the establishment of polarity of cells in embryos with abnormal neural tube morphogenesis, and in extreme ectopic locations both in the embryo and in 3D culture. Cells can polarise in all these environments, although polarisation can be delayed by 1hour by severe morphogenetic defects. Lastly I have found that cells do not monitor time by counting the number of cell cycles and that cell polarisation does not even require mirror-symmetric cell division. Overall my results highlight the importance of mechanisms that coordinate cell intrinsic programmes with morphogenetic movements and environmental signals, both in time and space, for correct embryogenesis.

ACKNOWLEDGEMENTS

There are many people that I would like to thank for helping me during my PhD, without whom I would not have made it to the end, nor had such a fun time getting there. Firstly I would like to thank my supervisor Jon for giving me the freedom to work independently but always offering invaluable guidance whenever I needed it. I have been proud to be a part of his lab.

Secondly huge thanks go to the past and present members of the Clarke lab, not only for their help, scientific advice and technical assistance in the lab, but also for keeping me amused and entertained throughout my PhD. Paula, Claudio, Marcel, Dave, Una and Clare - I feel lucky to have made such good friends, and to have shared so many funny moments about all sorts of stuffs!

Thank you to all the members of the fish groups at UCL for useful discussions and sharing reagents, especially when we had run out in the Clarke lab! In particular, I would like to thank Masa Tada for passing on his valuable knowledge and teaching me molecular biology when I wasn't even his student, I am really grateful. Likewise, thanks also to everyone at King's for their kind welcome when we moved to the MRC centre, and the several excellent parties! Thank you to all the Masters, Undergrad and PhD rotation students in the Clarke lab for offering their help with my experiments and analysis.

Thank you also to Mum and Dad for all their encouragement and support, especially during the last few months. To the rest of my family and friends, I thank you for being there for me over the course of my PhD.

Lastly I would like to thank Tom for support, patience and motivation in making this PhD possible. I can't wait to marry him in two weeks time!

TABLE OF CONTENTS

TABLE OF FIGURES

LIST OF SUPPLEMENTARY MOVIES

Movie 1. Dorsal view time-lapse movie of young cells (labelled with H2B-RFP), transplanted into an older host embryo (labelled with H2B-GFP and Pard3-Cherry). At the start of the time-lapse most donor cell nuclei are located at the basal edge of one side of the host neural rod. During the time-lapse the host neural rod polarises as Pard3-Ch becomes localised to the midline of the neural rod. Young cells move away from the basal surface of the rod towards the midline, where some divide. Frames are every 5minutes.

Movie 2. A combined time-lapse movie of three wild-type embryos undergoing neurulation labelled with Pard3-GFP to compare the time of apical polarisation between embryos. In all embryos Pard3-GFP accumulates at the midline at a similar time. The time-lapses are each a single z-level through the neural rod in transverse view. All time-lapses are at the level of the hindbrain, and embryos were imaged simultaneously. Frames are every 5.5minutes.

Movie 3. A combined time-lapse movie of one wild-type and one SB-treated embryo undergoing neurulation to compare the time of Pard3-GFP polarisation between embryos. The time-lapse reveals that puncta of Pard3-GFP appear later in the SB-treated embryo compared to wild-type. Embryos were imaged simultaneously. The time-lapses are each a single z-level through the neural primordium in transverse view at the level of the hindbrain. Frames are every 6.5minutes.

Movie 4. A time-lapse movie showing an ectopic cluster of cells labelled with H2B-RFP and Pard3-GFP from 13-20hpf. The separate channels are shown side-by-side. The nuclei are constantly changing place throughout the movie. Pard3-GFP first appears as puncta scattered throughout the cluster, which then over time coalesce towards the centre. The time-lapses show a maximum projection of several z-levels through the cluster. Frames are every 5minutes.

Movie 5. Time-lapse movie of a 15th cycle embryo labelled with mem-GFP and H2B-RFP. Many cells divide close to the midline showing that cell division has recovered sufficiently. The time-lapses are a small projection of 3 z-levels (5µm apart in depth) through the neural primordium in transverse view. The time-lapse was at the level of the hindbrain. Frames are every 5minutes.

Movie 6. Time-lapse movie of two cell divisions in a 15th cycle embryo labelled with Pard3-GFP and H2B-RFP. Both cells divide close to the midline in the medio-lateral axis, and the medial daughter cell crosses the midline, to form two pairs of cells. Frames are every 5minutes.

Movie 7. A combined time-lapse movie of one wild-type and one division-blocked embryo undergoing neurulation to compare the time of Pard3-GFP polarisation between embryos. The time-lapse reveals that puncta of Pard3-GFP accumulate at the midline at the same time in the both embryos. Embryos were imaged simultaneously. The time-lapses are each a single z-level through the neural primordium in transverse view. Both time-lapses were at the level of the hindbrain. Frames are every 5minutes.

CHAPTER 1 GENERAL INTRODUCTION

The development of an organism requires the tight coordination of many processes such as cell division, morphogenesis, and patterning. Events must occur both at the right time and in the right place for embryogenesis to proceed successfully. A huge amount of research has been fruitfully directed at discovering the molecules that direct spatial organisation of cell fates and those that instruct cell behaviour, but little is known about how the sequence and timing of events is controlled. My project aims to determine whether apical polarisation and a specialised cell division, critical to zebrafish neural tube morphogenesis, are regulated by spatial cues or a timing mechanism.

1.1 MORPHOGENESIS

Morphogenesis is the process of how an organism takes its shape and is one of the fundamental aspects of embryogenesis. Despite this importance however, surprisingly little research has been directed at documenting how organs take shape, and also at investigating which proteins and genes are necessary for normal morphogenesis. Morphogenesis requires the coordinated movements of many cells with each other; furthermore these movements must be coordinated with the other fundamental processes of embryogenesis, such as proliferation, differentiation, and spatial patterning. One of the morphogenetic movements that has been best studied is primary neurulation in amniotes, which generates the neural tube, the precursor structure of the brain and spinal cord. Primary neurulation has been intensely studied in mice, with the discovery of over 100 different gene mutations that all give rise to neural tube defects (NTDs) (Copp *et al.* 2003; Copp *et al.* 2010). This vast array of genes includes members of several different signalling pathways and genes necessary for several different cellular behaviours, suggesting that the tight coordination of many different cellular processes during neurulation is extremely important. At the start of primary neurulation the neural plate thickens, it then begins to fold and bend inwards at hinge points in the plate (fig 1.1A). During this rolling processes, the coordinated infolding of a large number of cells together results in a long groove developing down the length of the epithelium. Towards the end of neurulation the two edges of the neural plate meet at the dorsal midline, and fusion occurs to join the two sides of the neuroepithelium together thus creating a tube that is separated from the original epithelium (Colas *et al.* 2001; Copp *et al.* 2003).

Salivary gland development in *Drosophila* is a second example of a morphogenetic process

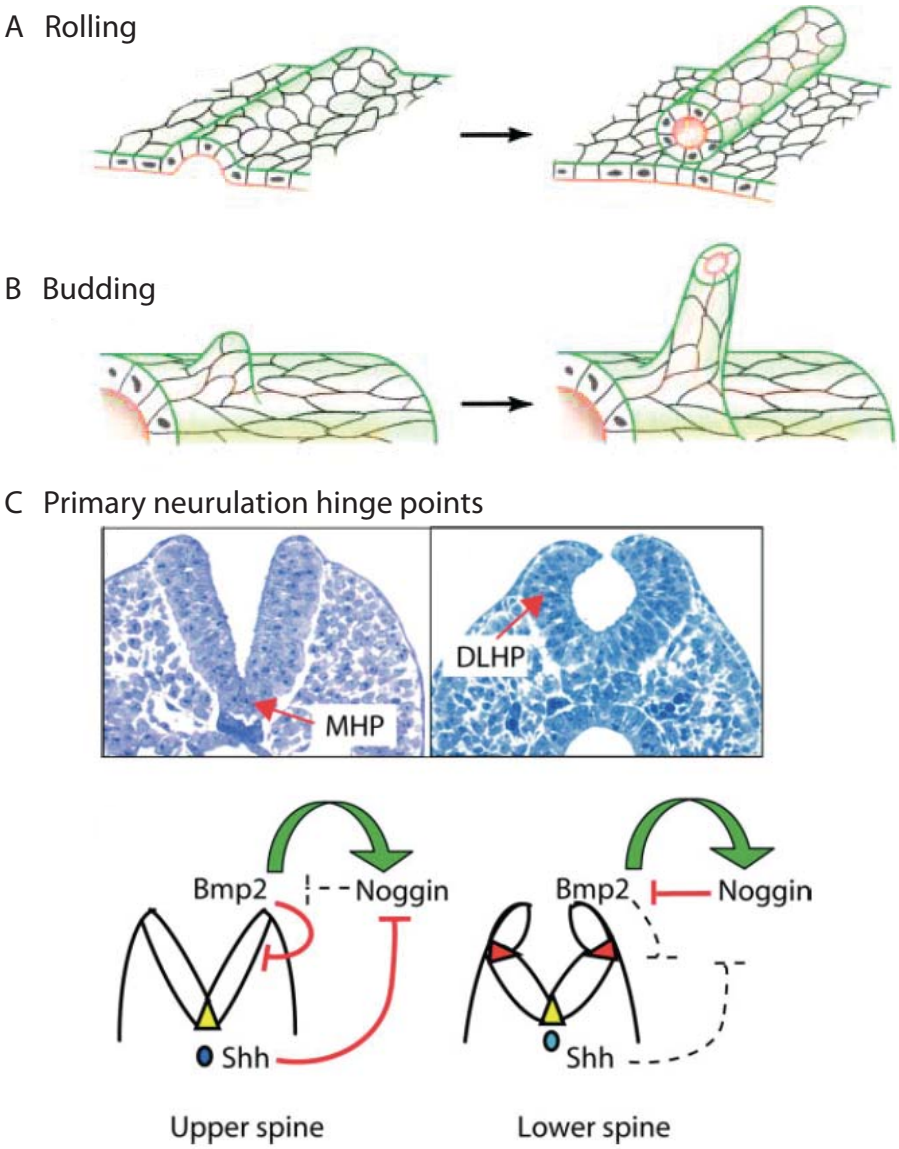

Figure 1.1 Primary neurulation is an example of the morphogenetic mechanism of rolling an epithelial sheet to form a tube.

A) Rolling is one morphogenetic mechanism of tube formation from a polarised epithelium. A groove forms down the length of the epithelial sheet by invagination. The sheet continues to rolls up and a tube is formed when the edges of the invaginating sheet fuse.
B) Budding is a second morphogenetic mechanism of tube formation but involves the invagination of a smaller group of cells in an epithelium to form an extension of the already existing lumen.
C) Transverse sections through the rolling neural plate to reveal the median hinge point (MHP) and the paired dorsolateral hinge points (DLHPs).
D) Molecular interactions between Shh signalling from the notochord and BMP signalling in the neural plate control the formation of hinge points during primary neurulation. Yellow triangles, MHP; red triangles, DLHPs; green arrows, stimulatory interactions; red lines, inhibitory interactions; dashed lines, inactive influences.
Figures A and B adapted from Lubarsky and Krasnow (2003)
Figures C and D adapted from Copp and Greene (2010)

involving tubulogenesis that is beginning to be characterised. In the salivary gland the forms by a slightly different mechanism compared to primary neurulation as a small group of cells invaginates to form a local infolding in the epithelial surface in a process called budding (fig 1.1B). Although the scale of the infolding differs between the two systems, they share common mechanisms of epithelial remodelling, including cell shape changes and cytoskeletal rearrangements. I will use these two examples to describe two of the cellular mechanisms that drive morphogenesis, cell elongation and apical constriction of cells.

Cellular mechanisms of morphogenesis

Cell elongation

The elongation of neural plate cells can be considered to be the first cell shape change to occur during primary neurulation. The epithelial cells extend along their apico-basal axis to form a sheet of columnar cells, and this elongation is accompanied by a concurrent decrease in the width of the neural plate (Schoenwolf 1983). The microtubule cytoskeleton appears to partly drive cell elongation, because after microtubule depolymerisation using nocodazole, the height of cells in the neural plate decreases by approximately 25% (Schoenwolf *et al.* 1987). The microtubule cytoskeleton in epithelial cells is coordinated by γ-tubulin, which acts as a microtubule nucleation centre to organise the microtubules in the apico-basal axis of the cell (Gunawardane *et al.* 2000). It has been shown that the localisation of γ-tubulin close to the apical surface is important for apico-basal cell elongation (Lee *et al.* 2007), and that the protein responsible for the correct distribution of γ-tubulin is the actin binding protein Shroom3 (Lee *et al.* 2007).

The elongation of cells before bending is not just a phenomenon restricted to neuroepithelial cells, as it also occurs during *Drosophila* salivary gland formation. The secretory cells of the salivary gland change in shape from cuboidal to columnar as they elongate to form a placode. This is an essential first step in correct gland morphogenesis, although little is known so far about how the cell shape changes are driven and regulated (Andrew *et al.* 2000).

Apical constriction of cells

The apical constriction of cells is a second cell shape change that is common in the folding of epithelial sheets. It not only occurs during primary neurulation, but also during gastrulation in both *Xenopus* (Hardin *et al.* 1988) and *Drosophila* (Leptin *et al.* 1990). In primary neurulation, cells at specific locations in the midline of the neural plate and along

the lateral edges of the folding neural plate adopt a wedge shape caused by the apical surfaces of the cells contracting (Schoenwolf *et al.* 1984). These cells form the hinge points (fig 1.1C) and they facilitate the bending and folding of the neural plate. BMP and Shh signalling determines the location of the dorsolateral hinge points (DLHPs) within the neural plate (fig 1.1D), but the apical constriction of cells itself appears to be mostly regulated by the actin cytoskeleton, and in particular the same Shroom family of actin binding proteins that regulate cell elongation during neurulation. Shrooms are able to cause apical constriction when expressed in a heterologous system (Haigo *et al.* 2003), and knockdown of Shroom activity prevents the formation of hinge points needed for bending of the neural plate (Haigo *et al.* 2003). Therefore it is not surprising that mice lacking Shroom display neural tube defects (Hildebrand *et al.* 1999).

Proteins that interact with actin and that may be involved in apical constriction include the small GTPases Rho and Rac. Mice mutant for p190RhoGAP exhibit many abnormalities in brain development, including NTDs (Brouns *et al.* 2000), suggesting that it is important to control the level of Rho signalling during neurulation. The precise mechanisms of how the different brain abnormalities arise remains unclear, but it would be interesting to find out if p190RhoGAP has any role in apical constriction. There is stronger evidence for the requirement of Rac in apical constriction, as Rac is required for the Shroom mediated apical constriction of neural plate cells during *Xenopus* neurulation (Haigo *et al.* 2003).

During the budding process of the salivary gland, the dorsal and posterior most cells of the placode undergo apical constriction and begin to internalize. Other cells of the placode then follow the lead of this initial group to form a tube that is continuous with the outside of the embryo. One component that is necessary for apical constriction and the concurrent invagination of placode cells is the transcription factor, *forkhead*, because in *forkhead* mutants, the salivary glands completely fail to invaginate (Myat *et al.* 2000). In summary, the process of apical constriction is common to both rolling and budding tubulogenesis, and appears to be able to drive morphogenesis, likely in concert with other mechanisms, to reshape a polarised epithelium into a tube (Sawyer *et al.* 2009).

Cell division and morphogenesis

The mechanisms that regulate cell division are critical to normal embryonic development. As well as being responsible for growth (i.e. proliferation), cell division is also used as a mechanism to increase cell diversity (through asymmetric divisions) and has been proposed to contribute to the shaping of tissues during morphogenesis. There are only a

few examples in the literature of how cell division can drive morphogenesis, which are discussed below.

A number of years ago it was proposed that spatial control of proliferation is important for cell shape changes during primary neurulation. Cells in the median hinge point adopt a wedge-shape morphology, and it has been proposed that an extension in the length of the cell cycle in this region helps to drive the changes in addition to apical constriction. This hypothesis is supported by studies in chick showing that median hinge point cells have longer gap and DNA synthesis phases of the cell cycle compared to more lateral neural plate cells, and a shorter mitotic phase (Smith *et al.* 1987). Moreover, the humpty dumpty mutant mouse that has elevated proliferation in the ventral neural tube has the NTD exencephaly (Kim *et al.* 2007). This mutant phenotype is rescued by loss of the cell cycle regulator E2f1, suggesting that abnormal proliferation is the main cause of the NTD. Lastly, the spina bifida mouse model, *curly tail*, has a dorso-ventral imbalance in cell cycle phase in the posterior neuropore region, with more cells in G0/G1 in the notochord and, and more cells in S-phase dorsally compared to wild-type. It has been proposed that this reduced proliferation ventrally is one of the early events that leads to the curly tail phenotype (Copp *et al.* 1988a; Copp *et al.* 1988b). It is currently unclear in general how unregulated proliferation causes NTDs apart from affecting hinge point formation, but one interesting idea is that abnormal cell division and premature differentiation of cells could alter the mechanical properties of the neural plate and thus prevent bending. Alternatively cell proliferation may be needed for fusion of the neural folds, as this region must undergo extensive remodelling during fusion (Copp *et al.* 2010).

During zebrafish neurulation cell division is also crucial for the correct morphogenesis of the neural tube. Prior to lumen formation, cells undergo a characteristic cell division close to the midline of the solid neural rod during which they acquire apico-basal polarity (Tawk *et al.* 2007). This generates pairs of daughter cells with mirror-image polarity and it directs the localisation of apical proteins to the midline of the rod (Tawk *et al.* 2007). It is essential that cells undergo this mirror-symmetric C-division at the right time and place to ensure that the apical ends of cells are at the embryonic midline and that a single lumen subsequently forms in the centre of the tube. In embryos with delayed convergence of the neural tissue towards the midline such as in the zebrafish PCP pathway mutant *trilobite* (Sepich *et al.* 2000), mirror-symmetric cell divisions that usually occur at the midline in wild-type embryos instead occur in ectopic lateral locations either side of the midline (Tawk *et al.* 2007). As apical proteins are deposited at the abscission plane of daughter cells undergoing this division, this leads to the generation of bilateral ectopic apical planes

and consequently, duplicated neural tubes (Tawk *et al.* 2007). This example indicates the powerful morphogenetic influence of cell division for neural tube morphogenesis.

During many morphogenetic processes such as tissue elongation, cell divisions are oriented along a particular axis. It is thought that elongation of the body axis during and after gastrulation is largely driven by cell intercalation (Keller 2002), although some research has shown that cell division may act as part of the driving force for morphogenesis. The best evidence comes from studies of germband extension in *Drosophila*, during which the whole germ band doubles in length and the posterior end folds back over itself. Imaging of cell divisions in the posterior germband during the early fast phase of extension showed that divisions were predominantly oriented along the antero-posterior axis, the direction of extension (da Silva *et al.* 2007). Furthermore blocking cell division reduced the rate of germband extension during this phase and also the overall extension (da Silva *et al.* 2007), showing that oriented cell divisions are necessary for efficient elongation, at least in the posterior part of the germband. Interestingly in the anterior part of the germband, no cell divisions occur during the fast phase of elongation (Foe 1989), indicating that more than one process can operate within the same tissue in different locations to drive the same morphogenetic movement.

The orientation of cell divisions and their contribution to axis elongation has been investigated in zebrafish embryos too. During zebrafish gastrulation when cells are undergoing convergence and extension movements towards the dorsal midline, cell divisions are mostly oriented along the antero-posterior axis. Cell division orientation is controlled by the planar cell polarity (PCP) signalling pathway, because knockdown of components of this pathway resulted in randomised division orientation (Gong *et al.* 2004). It was proposed that oriented cell divisions contributed to axis extension, because daughter cells of divisions occupied a smaller space in the antero-posterior space upon reduction of PCP signalling compared to controls (Gong *et al.* 2004). However, subsequent cell intercalation and movements that the cells underwent after division were not taken into account, and thus it is difficult to separate the contribution of cell division from intercalation. Moreover, blocking cell division during gastrulation does not cause an obvious reduction in the antero-posterior length of the embryo (Zhang *et al.* 2008), suggesting that oriented cell divisions may only play a small role in convergence and extension.

Finally the role of oriented cell divisions to determine organ shape has been investigated in the imaginal discs of *Drosophila*. The wing disc is split up into several different

compartments and clones of cells in these different compartments show characteristic shapes (Resino *et al.* 2002). Many clones are elongated in shape, and it is thought that restriction of cell division to certain areas within the disc determines the shape of the adult wing that forms from the disc (Gonzalez-Gaitan *et al.* 1994; Resino *et al.* 2002). Analysis of the relationship between cell division orientation and clone shape in two different areas of the wing disc revealed that cell divisions were oriented within the clones, and that this orientation was correlated with the direction of elongation of the clone (Baena-Lopez *et al.* 2005). In addition, Baena-Lopez and colleagues found that the PCP pathway is required for oriented cell division, because in PCP pathway mutants, clones of cells were more circular in shape and the resultant wing was wider and shorter than wild-type (Resino *et al.* 2002). Based on these observations they proposed that cell division orientation drives the shape of organs, rather than cell movements such as intercalation.

1.2 ESTABLISHMENT OF POLARITY

Polarity can be defined as asymmetry in cell shape or function and cellular polarity is a fundamental requisite for morphogenesis. Nearly all cells show some level of asymmetry or polarity, and this is manifest in the shape or cellular architecture of the cells. Although there is a huge diversity in the shape of cells in multicellular organisms, ranging from cuboidal epithelial cells to highly elongated neurons, polarity is essential for cells to adopt all these shapes and for their functional specialisation. The coordination of the polarity of individual cells within a tissue is necessary during the formation of many organs, including the CNS. Furthermore, once the cells are organised into a functional tissue and the three-dimensional (3D) structure of the organ is established, it is essential that cellular and tissue polarity are maintained for normal organ structure and function.

The importance of the maintenance of epithelial polarity and integrity is evident in diseases such as cancer, where loss of epithelial integrity is a hallmark of cancers deriving from several different organs. Many polarity proteins are mutated in cancer, and in fact the core polarity proteins Scribble, Lethal giant larvae, and Discs large were first discovered in *Drosophila* as tumour suppressor genes (Bilder *et al.* 2000). The loss of a polarised differentiated structure in cancer cells promotes increased proliferation and invasion into normal adjacent tissue. Moreover, loss of cell-cell contact is crucial for the increased cell motility of cancer cells during metastasis (Nguyen *et al.* 2007). A recent review on the relationship of tight junctions with breast cancer highlights that loss of tight junctions may promote cancer progression via several different mechanisms including loss of cell polarity, changes in cell fate and increased migration (Brennan *et al.* 2010). Finally, the loss of epithelial structure and polarity often correlates with a poor prognosis for the patient (Martin *et al.* 2004; Nguyen *et al.* 2007), indicating that understanding both how an epithelium is established and regulated is an important issue in our attempt to tackle and treat cancer.

The structure of a polarised epithelium

The most abundant type of polarised cell in mammals is the epithelial cell, which forms the building block of many organs including the vertebrate brain. All epithelia have several defining features. They are sheets of columnar shaped cells, connected to each other by tight cell-cell contacts, sitting on a basal lamina (fig 1.2). The cells of an epithelium have defined apico-basal polarity with an apical membrane facing the lumen of an organ (which is the ventricle or central canal in the brain and spinal cord) and a basolateral membrane

that contacts adjacent cells or the extracellular matrix laterally and the basal lamina basally. Between the apical and basolateral membranes exists a junctional belt of proteins that is crucial for the structural integrity of the epithelium. The junctions not only provide a point of cell-cell contact to anchor cells within the epithelium, but they also act as physiological barriers to prevent the flow of fluid between cells thus isolating the body from the outside environment. There are four main types of junction between the cells in most epithelia: tight junctions, adherens junctions, desmosomes and gap junctions (fig 1.2A). Although the junctional components in epithelial cells are relatively conserved across species, the precise arrangement of the junctions can differ (Knust *et al.* 2002). I have focussed upon the protein components of adherens and tight junctions, and their organisation in vertebrate epithelial cells.

The most apical junctions in mammalian epithelia are tight junctions. These are composed of the cytoplasmic scaffolding proteins Zonula adherens (ZO) -1, -2, and -3 and members of the Occludin, Claudin and JAM families of proteins (Hartsock *et al.* 2008). The occludins and claudins are both transmembrane proteins and have similar functions in the tight junction. They are both critical for the function of the paracellular permeability barrier that regulates the permeability and selectivity to ion movement between the cells of an epithelial layer (Tang *et al.* 2003). They also serve to separate the apico and basal membrane domains (Tsukita *et al.* 2001). ZO-1, -2, and -3 are members of the MAGUK (membrane associated guanylate kinase homologues) family of proteins, which through their multiple protein-protein interaction domains such as PDZ and SH3 domains, they can bind many proteins, including both adherens junction and tight junction components. They therefore likely act as scaffolding proteins and a link between adherens and tight junctions. In addition ZOs can interact with the actin cytoskeleton (Hartsock *et al.* 2008).

Just slightly more basal to the tight junctions lie adherens junctions. These are composed of transmembrane adhesion proteins such as E-Cadherin, and the intracellular group of proteins p120 catenin, β-catenin, and α-catenin (Nelson 2003). Adherens junctions mediate cell-cell adhesion, by the homophilic binding of the extracellular portions of Cadherins between adjacent cells in an epithelium. The catenins link the Cadherins to the actin cytoskeleton to stabilise the cell-cell contacts, either directly or via other actin binding proteins, and one study has highlighted a possible link of β-catenin to microtubules (Ligon *et al.* 2001). Cadherin-mediated cell-cell adhesion is essential for epithelial integrity, although remodelling of adherens junctions also provides a mechanism for epithelial cellular rearrangements and morphogenesis (Nishimura et al. 2009).

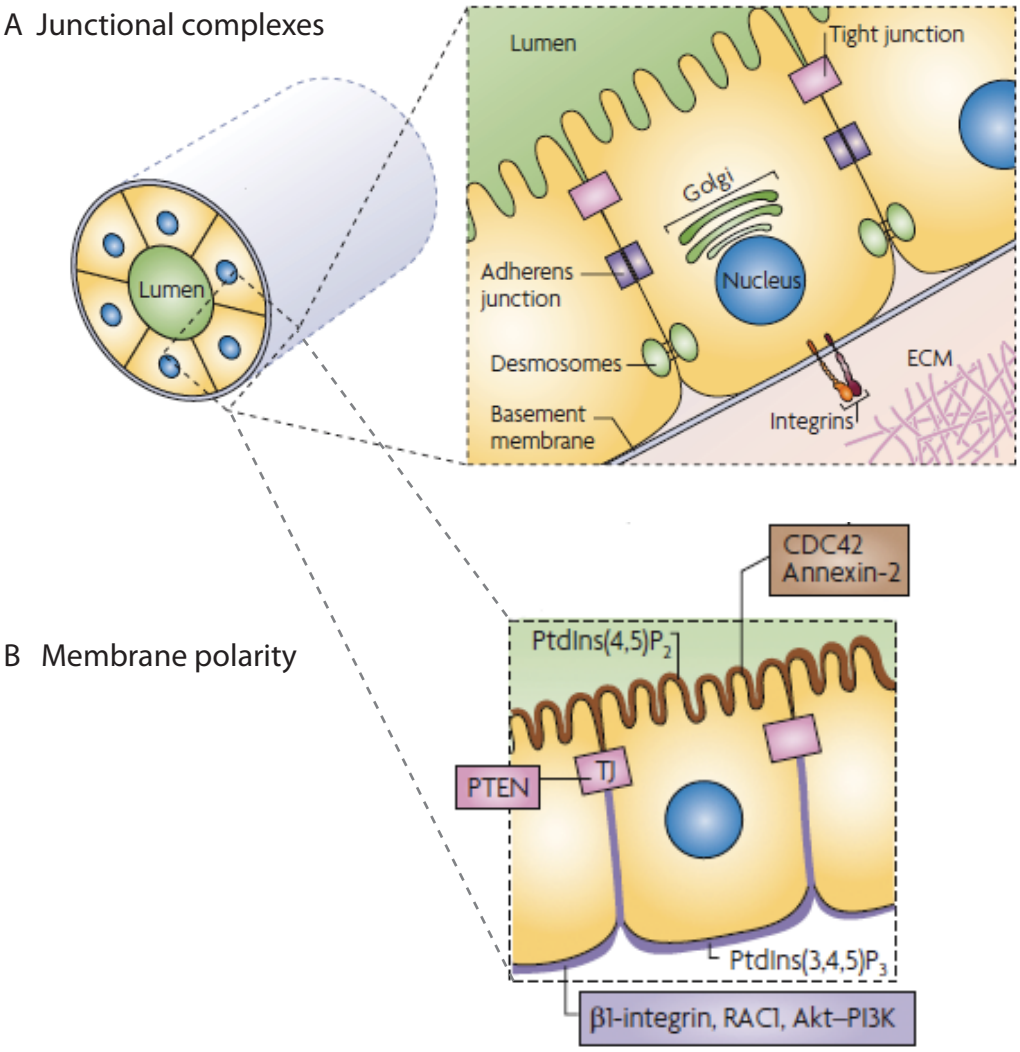

Figure 1.2 The distribution of junctional complexes and membrane polarity components in a tubular epithelium.

A) The epithelial cells that form tubes are strongly polarised with an apical side that faces the lumen and a basal side that sits on the basement membrane. The cells adhere to neighbouring cells by junctions and form a permeability barrier to solutes in the lumen. Tight juntions are positioned most apical in a tubular epithelium, adherens juntions are situated just basal to tight junctions, and desmosomes are present in the lateral membrane below adherens junctions. Integrins on the basal side of the cell interact with the basement membrane and extracellular matrix (ECM).

B) The correct localisation of specific phospholipids and signalling proteins is crucial for the maintenance of apico-basal polarity. PtdIns(4,5)P_2 is important for apical membrane identity, whereas PtdIns(3,4,5)P_3 partly specifies the baso-lateral membrane domains. The two membrane domains are separated by tight junctions (TJs), and PTEN localisation at TJs likely controls the localisation of PtdIns(4,5)P_2 to the apical membrane.
Figure adapted from Bryant and Mostov (2008)

Polarity proteins and their junctional localisation

The polarity proteins are a separate group of proteins to junctional components that are also essential for cellular polarity in many cell types including epithelia. They were first discovered in *C. elegans* and *Drosophila*, but since then, highly conserved homologues of polarity proteins in both structure and function, have been discovered in many species including mammals (Goldstein *et al.* 2007). The core polarity proteins form three main complexes, named the Par complex, the Crumbs complex and the Scribble complex. The Par and Crumbs complex are usually located at the apical domain of epithelial cells, but the Scribble complex localises to the lateral membrane (fig 1.3). Mutually antagonistic interactions between the three complexes are essential for both the establishment and maintenance of apico-basal polarity. The complexes are thought to act as scaffolding and signalling centres, to facilitate the coordinated regulation of the cytoskeleton, membrane trafficking and membrane composition necessary for cellular polarity (Goldstein *et al.* 2007).

The Par complex

The Par complex comprises four main proteins, Par3, Par6, atypical protein kinase C (aPKC), and Cdc42. It can be split into two subcomplexes: Par6-aPKC-Cdc42 and aPKC-Par3, the latter of which is often localised to tight junctions (Ebnet *et al.* 2001), partly through the binding of Par3 to JAM (Itoh *et al.* 2001). Disruption of the complex results in a dramatic loss of apico-basal polarity and tight junction structural integrity (Suzuki *et al.* 2002). Par6 and Par3 contain several protein-protein interaction domains, including PDZ domains (Tepass *et al.* 2001), through which they bind each other and several other polarity proteins, to order the proteins at the apical junctions (Hurd *et al.* 2003). Par6 provides an essential link between Par3 and the other complex components aPKC and Cdc42 (Joberty *et al.* 2000). aPKC is a Serine/Threonine kinase and its phosphorylation of several proteins including Par3 is essential for downstream polarity events (Iden *et al.* 2008). Overexpression of a dominant negative form of aPKC causes mislocalisation of Par3 in *Drosophila* showing that Par complex proteins are dependent upon each other for their correct localisation. Cdc42 is a small GTPase of the Rho family and has essential roles in cellular polarity in a number of different systems (Etienne-Manneville 2004). It can regulate both the actin and microtubule cytoskeleton, signalling pathways and even endocytosis, which are all processes essential for the establishment and maintenance of epithelial junctions and polarity (Etienne-Manneville 2004).

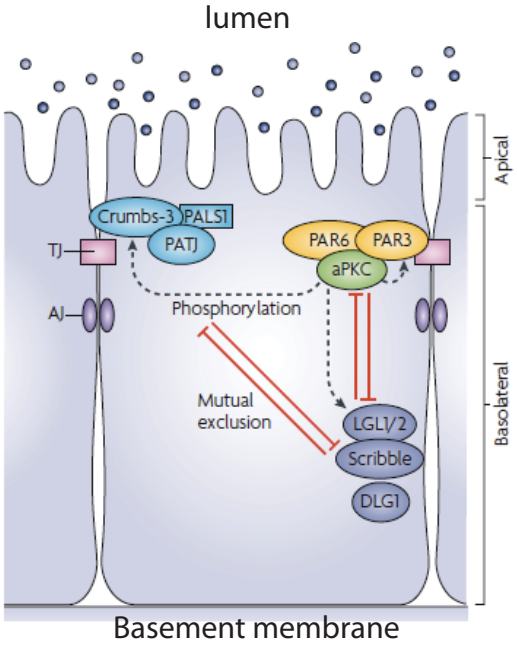

Figure 1.3 The distribution of the core apico-basal polarity complexes within an epithelial cell.

The three core polarity complexes that are essential for apico-basal polarity in epithelial cells are the Crumbs complex (Crumbs, PALS1 and PATJ), the Par complex (PAR6, PAR3 and aPKC, sometimes including Cdc42) and the Scribble complex (LGL1/2, Scribble, DLG). The Crumbs complex localises to or just above TJs, the Par complex localises predominantly at tight junctions (TJs) and the Scribble complex localises to the lateral membrane. Reciprocal inhibitory interactions between the complexes (red arrows), establish and maintain this asymmetric distribution of the complexes, partly mediated by phosphorylation of LGL by aPKC, which prevents the Scribble complex moving too far apical. Mutual exclusion between the the Crumbs and Scribble complexes also helps to maintain apico-basal polarity.
Figure adapted from Iden and Collard (2008)

The Crumbs complex

The Crumbs complex consists of three proteins: Stardust/Pals1, PATJ and Crumbs. Pals1 and PATJ are both cytoplasmic scaffolding proteins, whereas Crumbs is a transmembrane protein. The Crumbs complex is often located more apical to the Par complex (Roh *et al.* 2003), although it can also interact with tight junctions (Schluter *et al.* 2009). The Crumbs complex is required for the correct targeting of many proteins towards the apical end of the cell, including occludin, aPKC and ZO-1 (Roh *et al.* 2003), and the Crumbs complex may stabilise the apical localisation of the Par complex by directly interacting with Par6 (Hurd *et al.* 2003). In turn, the Crumbs complex appears to depend upon the Par complex for its stable localisation at the apical surface (Tanentzapf *et al.* 2003). The Crumbs complex may also play a role in determining apical membrane identity in the mature epithelium by recruiting spectrin skeletal components and the actin binding protein Dmoesin, which are both necessary for plasma membrane and epithelial integrity (Medina *et al.* 2002).

The Scribble complex

The Scribble complex consists of Lethal giant larvae (Lgl), Discs large (Dlg), and Scribble. Each protein is dependent upon the other proteins in the complex for its correct localisation to the basolateral membrane domain. The main function of the Scribble complex as a whole appears to be to antagonise the Par complex and thereby promote lateral membrane identity (Tanentzapf *et al.* 2003). Both Dlg and Scribble contain PDZ protein binding motifs and therefore likely act as scaffolds for proteins that need to be localised to the lateral membrane (Nelson 2003). An intriguing connection of Lgl with Syntaxin-a, a SNARE protein involved intracellular vesicular transport, suggests that Lgl may contribute to epithelial polarity by regulating exocytosis (Musch *et al.* 2002).

Establishment of epithelial polarity

In the many diverse systems in which polarisation is required for function, from single cells to multicellular epithelial sheets, there are several common basic steps in generation of polarity. Firstly, asymmetry of the cell must be broken. This is often in response to an external cue, such as cell-cell contact or contact with the extracellular matrix (ECM). The next three steps then occur over a similar time period, and are interrelated. Localised assembly of polarity complexes occurs at the surface landmark, the cytoskeleton is rearranged into a polarised network, and polarised trafficking and endocytosis establish different membrane domains. Finally, to enable the formation of a mature and functional epithelium with junctional complexes joining adjacent cells, individual cell polarity must be coordinated between cells in the tissue.

Most of the knowledge we have about generation of polarity in vertebrates comes from the study of polarised cell lines *in vitro*. In two-dimensional (2D) cultures, the establishment of polarity is often studied during assays such as wound healing and after a calcium switch that causes the disassembly of cell-cell junctions. In three-dimensional cultures, single cells are embedded within the matrix and over time they proliferate and generate a polarised cyst (Bryant *et al.* 2008). The generation of polarity has been studied *in vivo* in invertebrates, and because of the close conservation of the core polarity proteins, discoveries of how polarity is generated in flies is also relevant for studies of vertebrate polarity. I will mainly describe experimental evidence from cell culture studies and *Drosophila* cellularisation to highlight the main steps in the establishment of polarity.

Breaking symmetry

It has been difficult to isolate the factors involved in the initial symmetry breaking event using polarised cell cultures, partly because a 2D culture system itself provides a strong polarity cue. The monolayers of cells sit on a stiff substrate and are thus exposed to the culture medium on the opposite side, and they polarise according to this axis imposed on them. It is likely that cells *in vivo* do not receive such a strong cue during organogenesis. The use of 3D cultures for studying generation of polarity has therefore been more fruitful in determining how symmetry is broken, as the cells are completely surrounded by ECM and do not have such a strong environmental polarity cue. In this system, symmetry breaking can occur at or soon after the first division, either during cell division as polarity components are localised to the abscission plane of the daughter cells (Jaffe *et al.* 2008), or by cell-cell contact between the two daughter cells after division (Martin-Belmonte *et al.* 2007a). Another example of where cell-cell contact may provide the break in symmetry is shown in the repolarisation of epithelial cells after calcium switch. If calcium is removed from the medium, then epithelial cells lose their cell-cell contacts and the epithelium disassembles. However upon re-addition of calcium, the cells repolarise, and the cell-cell adhesion mediated by E-Cadherin provides the cue for the assembly of polarity complexes (Ebnet *et al.* 2004).

All cells have an actin cytoskeleton composed of actin filaments that are crosslinked by a variety of actin binding proteins. Myosin motors generate tension within the filamentous network that is important for maintaining the structure of the cell and for plasma membrane dynamics (Keller *et al.* 2002). It is likely that local changes in the relaxation or tension of the actin cytoskeleton provide the initial symmetry-breaking step, which could

occur either spontaneously or in response to an external cue. The local instability of the actin cytoskeleton at the cell cortex may facilitate cell polarity to spontaneously arise (Paluch *et al.* 2006), or the relaxation of the cell cortex may be an integral part of the polarisation process, exemplified during the polarisation of the *C. elegans* zygote (Munro *et al.* 2004).

It has also been proposed that polarity can arise spontaneously from small random fluctuations in the stability or localisation of polarity components within the cell that then are amplified by positive feedback mechanisms (Sohrmann *et al.* 2003). Studies in yeast have identified a complex consisting of a Cdc42 GEF (guanine nucleotide exchange factor), the scaffold protein, Bem1p, and a Cdc42 effector kinase that localises to random sites in the cell cortex during symmetry breaking (Kozubowski *et al.* 2008). The close proximity of the GEF and kinase results in a local increase in Cdc42-GTP at the cortex that breaks the symmetry in the cell (Kozubowski *et al.* 2008).

Localised assembly of polarity complexes

The localised assembly of polarity complexes at the specific polarisation landmark site has been investigated using epithelial wound healing as a model system. During the re-establishment of polarity after wound healing, polarity proteins are recruited in a particular order that begins with spot-like adherens junctions forming first at cell-cell contacts. These contain E-Cadherin and ZO-1 (Yonemura *et al.* 1995), and Par3 and aPKCλ are only recruited later to the tight junction (Suzuki *et al.* 2002). The same study showed that the Par complex was one of the last proteins recruited to the tight junctions, after Claudin-1, JAM and Occludin (Suzuki *et al.* 2002).

In contrast to the wound healing assays, the Par3 homologue Bazooka (Baz) appears to be one of the first proteins localised to the future adherens junction during *Drosophila* cellularisation (Harris *et al.* 2004). Its localisation to the apical domain can occur independently of aPKC and Par-6 but instead is reliant upon the cytoskeleton, and in particular, dynein mediated transport towards the apical side of the cell (Harris *et al.* 2005). This shows that despite conservation of the polarity proteins among various species, the precise order in which they are assembled during the establishment of polarity can vary across different systems.

Cytoskeletal rearrangements

Another step essential for polarity establishment is the rearrangement of both the actin and microtubule cytoskeleton, as this enables the initial asymmetry site to be reinforced and retained. In this step, the family of small GTPases seem to be important for localising modulators of the actin cytoskeleton such as Arp2/3 to the polarity landmark, which can then begin to remodel the cortical actin by promoting actin polymerisation (Fukata *et al.* 2001). How the microtubule cytoskeleton reorganises to become aligned in the apico-basal axis of the cell, with microtubule minus ends at the apical pole is not clear, but again polarity proteins and small GTPases may be important for this step. It has been shown that in migratory cells, Par3 binds the Rac GEF Tiam1, which in turn through aPKC stabilises microtubules to enable persistent migration (Pegtel *et al.* 2007), so a similar mechanism may exist to reorganise microtubules in the development of an epithelium.

Establishment of different membrane domains

Once the junctional complexes are stabilised, polarity proteins are localised to their correct locations, and the cytoskeleton is polarised, then the trafficking of proteins to specific membrane compartments can take place. In a genome wide screen for regulators of membrane traffic, all members of the Par complex were found to be regulators of endocytosis (Balklava *et al.* 2007), thus revealing a potential mechanism for how different membrane domains are generated during establishment of apico-basal polarity. Specifically aPKC, through its interaction with the endocytic protein Numb, could regulate endocytosis and membrane trafficking important in the generation of polarity, as in migrating cells, aPKC regulates the activity of Numb, and Numb function is essential for integrin-mediated cell migration (Nishimura *et al.* 2007).

Par3 may also help to establish membrane domains by directing the asymmetric distribution of phosphatidylinositol phosphates (PtdIns-Ps) that are crucial for correct membrane identity. The conversion of one form of PtdInsP to another is carried out by two groups of enzymes; PI3Kinases catalyse the generation of PtdIns(3,4,5)P_3 from PtdIns(4,5)P_2, whereas the phosphatase PTEN catalyses the reverse reaction as it removes a phosphate group from PtdIns(3,4,5)P_3 to generate PtdIns(4,5)P_2. Junctional proteins may control the localised distribution of the two different forms of PtdInsP by regulating the localisation of PTEN, as Par3-mediated localisation of PTEN to junctional membranes is also necessary for establishment of polarity in Madine-Darby Canine Kidney (MDCK) cells (Feng *et al.* 2008).

Maturation of the epithelium

In epithelial cells actin fibres arrange into a circumferential bundle close to the adherens junction, and microtubules orient along the apico-basal axis. These rearrangements help to convert the initial spot junctional complexes into the junctional belt of proteins close to the apical surface that is a hallmark of epithelial cells. Both Par3 and aPKC seem to be required for this step of organising the cytoskeleton, as depletion of aPKCλ inhibits the proper formation of cortical circumferential bundles of actin (Suzuki *et al.* 2002).

Maintenance of epithelial integrity

Many of the interactions between the core polarity components central to the initial establishment of polarity continue to be important for the maintenance of separate apical and basal domains. There are reciprocal exclusion mechanisms that prevent an apical complex invading the territory of a basal complex and vice versa (fig 1.3). For example, aPKC in the apical cortex inhibits the Scribble complex from localizing apically by phosphorylating Lgl and causing Lgl to dissociate from the cortex (Betschinger *et al.* 2003). This results in the Scribble complex only being functional in the basolateral membrane. Likewise, Lgl competes with Par3 for binding to Par6-aPKC, this sequestering the Par6 complex away from Par3 in the lateral cell cortex (Yamanaka *et al.* 2003). This means that the Par complex can only function in the apical cortex, away from Lgl. These reciprocal inhibitory interactions ensure that each complex is restricted to its respective membrane domains, and that these domains are not overlapping. Moreover, as the complexes each promote the expansion of the domain with which they are associated, then the apical and basal domains are maintained at a constant size.

Maintenance of the asymmetric distribution of the phospholipids (PtdInsPs) is also crucial for epithelial integrity (fig 1.2B). The importance of restricting PtdInsPs to their correct membrane compartment is illustrated by the rapid changes in polarity that occur after mislocalising PtdInsPs in the plasma membrane. Addition of exogenous PtdIns(4,5)P_2 to the basal membrane results in erroneous delivery of apical proteins to the basal membrane (Martin-Belmonte *et al.* 2007a). Conversely, exogenous addition of PtdIns(3,4,5)P_3 to apical membranes causes loss of apical identity and the trafficking of basal membrane to the basal surface (Gassama-Diagne *et al.* 2006). The core polarity complexes may control PtdInsPs localisation by binding PTEN, restricting it to the tight junction, and thus restricting PtdIns(3,4,5)P_3 to the basolateral membrane (von Stein *et al.* 2005).

In 3D culture, most epithelial cell lines form small cysts with an apical lumen in the centre. Two studies have revealed that the ECM component laminin orients cell polarity of MDCK cells via the small GTPase Rac1 and β1-integrin (O'Brien *et al.* 2001; Yu *et al.* 2005b). A striking inversion of polarity results if either the function of β1-integrin or Rac1 is inhibited, such that the apical surface of the cysts becomes misoriented towards the matrix. Further investigation into the molecular mechanism by which the inversion of polarity occurs revealed that the inversion is dependent upon RhoA and its downstream pathway components ROCK1 or Myosin II (Yu *et al.* 2008), because knockdown of any of these components restored the correct polarity of the cyst after inversion caused by Rac1 or β1-integrin. These studies highlight that ECM components are responsible for correct orientation of polarity *in vitro*.

One study has highlighted a role for the small GTPase Rab8 in maintenance of epithelial integrity. In cultured MDCK cells, Rab8 acts in membrane trafficking of vesicles towards the basolateral membrane (Huber *et al.* 1993). In the intestines of *rab8* knockout mice, proteins normally localised to the apical surface were found to be located intracellularly in lysosomes, likely having been endocytosed from the apical plasma membrane (Sato *et al.* 2007). These two observations suggest that polarised transport pathways within cells are essential for the maintenance of apical and basolateral membrane domains, together with the polarity proteins themselves.

Cell division and polarity

The coordination of cell polarity with cell division is an important feature of embryonic development in general as it provides an important mechanism for both generating cell diversity during development and for maintaining a pool of stem cells (Wang *et al.* 2005a). The unequal distribution of information in the form of cell fate determinants during mitosis gives rise to daughter cells with different compositions, in a process called asymmetric cell division (Ahringer 2003). Although study of asymmetric cell division has generated a wealth of knowledge about the interactions between different polarity proteins, it is not such a useful system for the study of how cell polarity is established. This is partly because in *Drosophila* neuroblasts, where asymmetric cell division has been best characterised, the neuroblasts inherit and maintain their axis of polarity during delamination from the overlying epithelium. Thus they do not establish a new axis of symmetry during cell division, but align the spindle and cell fate determinants with the polarity cues already present. There are a few examples in the literature of the concurrent establishment of cell polarity during cell division, which I briefly mentioned in the section

on symmetry breaking above. This however deserves a detailed mention, as the establishment of apical polarity through cell division is an important feature of zebrafish neural tube formation, and one upon which this thesis is focussed.

The analysis of cell division just prior to lumen formation in zebrafish neurulation provided the first observations that apical polarity could be established during cell division (Tawk *et al.* 2007). Examination of the distribution of Pard3-GFP in individual cells showed that Pard3-GFP became localised to the cleavage furrow or abscission plane between the daughter cells (Tawk *et al.* 2007). Pard3-GFP remained strongly localised to the medial ends of the two daughter cells, which resulted in the generation of pairs of sister cell with mirror-image apico-basal polarity (Tawk *et al.* 2007). The observation that daughter cells after cell division displayed a striking mirror-image appearance in both cell shape and behaviour was actually documented over thirty years ago in a study of 3T3 cells in culture (Albrecht-Buehler 1977). In this paper many daughter cells showed mirror-symmetry in their directional migration and organisation of their actin cytoskeleton for many hours after division (Albrecht-Buehler 1977). The biological significance of this mirror-symmetry was not known at the time, but it suggested that some behaviours of cells are determined at mitosis.

Recently, two independent studies of cyst formation from single-cell suspensions in 3D culture have proposed that the early stages of polarity establishment are coupled to cell division. One study used Caco-2 cells, an epithelial gut cell line (Jaffe *et al.* 2008), and the other used Madin-Darby Canine Kidney (MDCK) epithelial cells (Schluter *et al.* 2009). Single Caco-2 cells at the start of the culture did not show any signs of polarity, as aPKC was localised all around the cell periphery. However, after cell division ZO-1 and aPKC were localised between the two cells indicating the presence of an apical domain (Jaffe *et al.* 2008). Furthermore the apical surface appeared to be specified during cell division, because aPKC colocalised with tubulin at the midbody of the abscission site between the two daughter cells just after division (Jaffe *et al.* 2008). The second study followed the localisation of Crumbs3a (Crb3a) during the first cell division of MDCK cells in culture. The localisation of GFP-Crb3a changed from an intracellular cytosolic location close to the mitotic spindles in early mitosis, to being localised between the two daughter nuclei in late mitosis, and finally becoming solely present at the plasma membrane at the location where the two cells completed abscission (Schluter *et al.* 2009). This suggests that during mitosis, GFP-Crb3a is trafficked in vesicles to the abscission site between the two cells where upon exocytosis, apical membrane is generated, which subsequently allows the formation of a small lumen.

Although the establishment of polarity through cell division is emerging as a concept important for lumen formation *in vitro* and *in vivo*, there is still much to find out this is achieved. It has been proposed that local changes in cortex tension drive cell shape during cell division (DeBiasio *et al.* 1996), and as local changes in the cytoskeleton may also promote symmetry breaking, then this provides a possible link between polarity and cell division. Intracellular membrane trafficking is necessary for the completion of abscission, to bring vesicles to the cleavage site where they fuse with the plasma membrane to separate the two daughter cells (Skop *et al.* 2001; Shuster *et al.* 2002). If apical membrane determinants are contained in the vesicles trafficked to the fusion site, then establishment of membrane polarity would occur concurrently with completion of abscission. Finally, phosphoinositide signalling may provide a link between cell polarity and division, because when *Dictyostelium* cells divide, the phosphatase PTEN is localised to the cleavage furrow and the kinase PI3K functions at the cell poles (Janetopoulos *et al.* 2005). This generates a localised distribution of different phosphoinositides that is essential for cell division, in particular for cleavage furrow ingression and cytokinesis (Janetopoulos *et al.* 2005). As phosphoinositides can determine membrane identity (Gassama-Diagne *et al.* 2006), then this suggests another link between polarity and cytokinesis. It will be interesting to find out which, if any, of these molecular mechanisms are important for the targeting of apical proteins to the abscission plane between daughter cells.

1.3 LUMEN FORMATION

Lumen formation is a fundamental step during the organogenesis of many organs including the heart, gut and brain. Moreover the size and shape of the tubes are critical for correct functioning of many organs. Although the tubular architecture in the different organs can be widely different, they do all share one common feature, which is that the cells comprising the tube are polarised. The cells have an apical side facing the lumen and a basal side contacting a basal lamina or neighbouring cells. The morphogenetic mechanisms of tube formation vary enormously between the different tissues but ultimately all must end with the basic structure of a polarised epithelium surrounding a lumen. In fact, a lumen can only form after the cells of the tissue have acquired apico-basal polarity. The different morphogenetic mechanisms for tube formation largely fall into two categories, depending on when the cells of the tube become polarised. During wrapping, and budding, an already polarised epithelium is reshaped to form a tube, (fig 1.1A,B). However, a tube can be generated *de novo* from a solid unpolarised group of cells, such as during cavitation and hollowing (fig 1.4).

Knowledge of the cellular and molecular mechanisms of lumen formation mostly derives from studies using mammalian polarised cell lines in culture or invertebrate model systems. Culture systems, especially 3D culture systems, have provided an accessible system to carry out experiments, such as biochemical analysis and imaging studies that until recently have proved difficult in the embryo. Recently though the mechanisms of tube formation in vertebrates have been investigated through live imaging of neural tube formation and blood vessel formation. Culture systems have also been useful for studying the role of the environment in directing lumen formation as the culture medium can be manipulated in terms of its physical properties, such as stiffness, its constituent ECM components, and even the growth factors and signalling molecules present. I have previously highlighted the key cellular shape changes of lumen formation from a polarised epithelium in the description of primary neurulation in section 1.1, so will focus upon *de novo* tube formation in this section.

Mechanisms of *de novo* lumen formation

The three main mechanisms for forming a lumen from a group of unpolarised cells are cord hollowing, cell hollowing and cavitation (fig 1.4). Cavitation is traditionally defined as the formation of a tube from a solid group of cells by apoptosis of the central cells to form a luminal space. However, the integral role for apoptosis in creating a lumen is not

entirely clear, as even in systems where apoptosis is thought to be essential for lumen formation, blocking apoptotic cell death only delays lumen formation (Mailleux *et al.* 2007). Moreover, it has been proposed that cell death of lumenal cells is a mechanism for simply clearing unpolarised cells from the central lumen in MDCK cells (Martin-Belmonte *et al.* 2008), as an additional part of tubulogenesis. The initial events of cavitation may therefore be similar to cord hollowing, as polarisation of the outer cells does not depend upon apoptosis (Mailleux *et al.* 2007), and thus cavitation can be viewed as an extension or variation in cord hollowing in some senses (Andrew *et al.* 2009). Further research is needed to find out if apoptosis is a driving force for lumen formation or whether it just helps make the process more efficient by clearing up leftover cells. Evidence to support the latter model comes from studies of cells in culture plated upon small micropatterned areas of extracellular matrix (ECM). If cells are restricted in their cell extension by progressively patterning the substrate to a smaller and smaller area, cells can be forced to undergo apoptosis (Chen *et al.* 1997). This shows that loss of adhesion to the ECM can result in cell death and suggests that a similar mechanism may occur when cells become located in the centre of the cluster and thus detached from the ECM during lumen formation.

Cord hollowing is the formation of a lumen, de novo, between cells, whereas in cell hollowing the lumen forms within the cytoplasm of a single cell (Lubarsky *et al.* 2003). Therefore, not surprisingly, during both cord and cell hollowing, similar mechanisms and molecular machinery control lumen formation. The two main mechanisms are the synthesis of vesicles consisting of new apical membrane inside the cells, and their fusion with the plasma membrane. In this way, the cells become polarised and a lumen forms coincidentally.

Vesicle coalescence to form an intracellular lumen

Single cell hollowing is a mechanism commonly used for lumen formation in small diameter tubes, such as capillaries. Live imaging of the formation of endothelial tubes in the zebrafish revealed for the first time that endothelial tubes form *in vivo* by cell hollowing. These studies showed that small vesicles form within the cells, which gradually coalesce to form a large intracellular vesicle (Kamei *et al.* 2006). Eventually the large vesicle must fuse with the plasma membrane to form a channel through the cell that eventually joins up with the lumen in the neighbouring cell to form a continuous tube. The proteins involved in vesicle formation and coalescence have also been investigated using HUVEC cells in 3D culture as a model of angiogenesis. In this system, when the pinocytosis

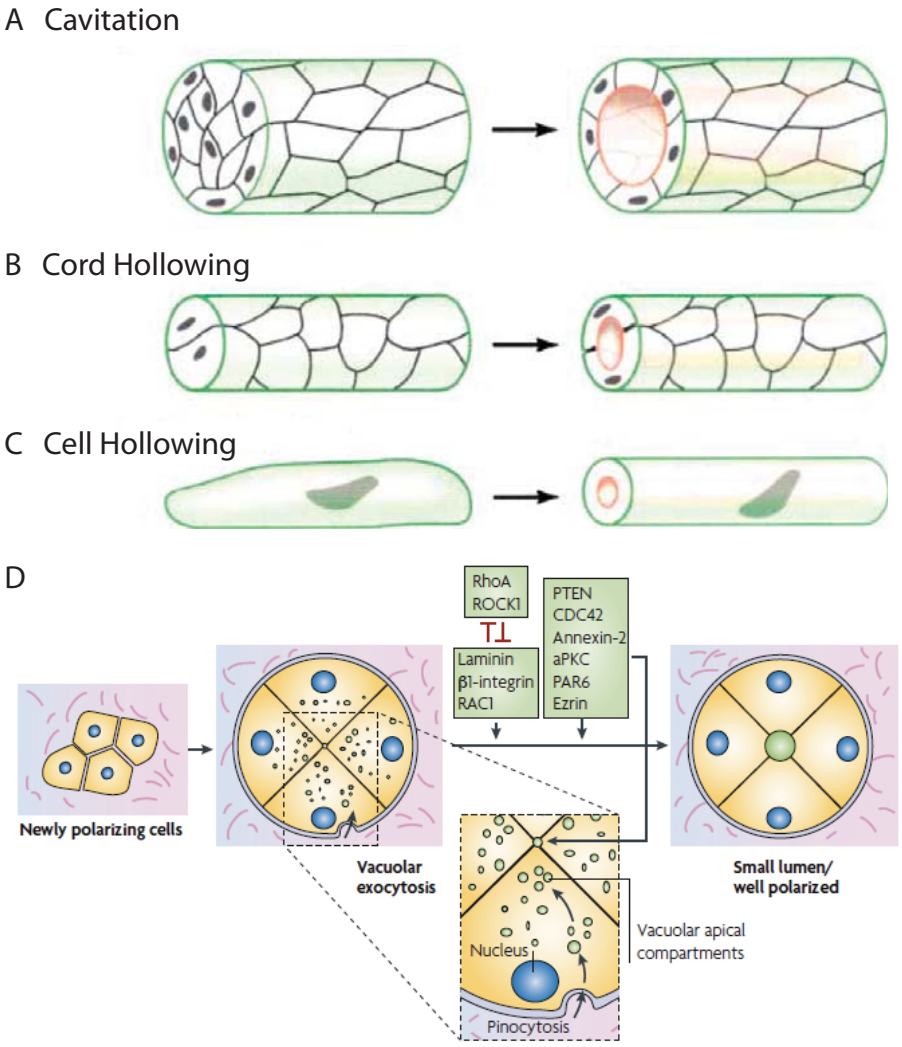

Figure 1.4 Morphogenetic mechanisms of *de novo* tube formation

A) During the process of cavitation a solid rod of cells is converted into a tube by apoptosis of centrally located cells to create a lumen. The outer cells must also acquire apico-basal polarity to form a tubular epithelium.
B) Cord hollowing is also the generation of a lumen from a solid rod of cells but this does not involve apoptosis, just generation of apical membrane in the centre of the rod comcomitant with cell polarisation.
C) Cell hollowing is the formation of a lumen in the cytoplasm of a single cell that extends down the length of the cell. It involves the biogenesis, coalescence and fusion of intracelullar vesicles to create a lumenal space bound by apical membrane.
D) *de novo* tube formation involved the generation of many intracellular vesicles that are trafficked towards the centre of the rod or cyst. Upon their fusion with the plasma membrane, apical membrane is deposited at the centre of the cyst, and the fluid released into the extracelullar space between the cells begins the formation of a small lumen. The proteins known to be involved in directing and orienting this process are highlighted in green and include both apical polarity proteins and basal cues.
Figures A-C adapted from Lubarsky and Krasnow (2002)
Figure D adapted from Bryant and Mostov (2008)

of plasma membrane was inhibited using specific antibodies to Integrins then lumen formation failed to occur (Davis *et al.* 1996). The small GTPases Cdc42 and Rac1 have also been implicated in vesicle coalescence because overexpression of dominant negative Cdc42 inhibited the early stages of vacuole formation, and overexpression of Rac1 caused vesicles to collapse inside the cells (Bayless *et al.* 2002).

A recent study of terminal branching in the *Drosophila* trachea has revealed a different model of cell hollowing in which vesicles do not coalesce within the cell to form one large vesicle that subsequently fuses to the plasma membrane. In the trachea lumen formation appears to be a directional process, as growth of a new lumen occurs inwards from one end of the cell. The lumen then extends through the cell as the cell itself elongates, by fusion of vesicles to the existing lumen all along the lumen length (Gervais *et al.* 2010). In this system both lumen formation and cell elongation depended upon an organised microtubule network, which in turn was controlled by asymmetric actin accumulation within the cell (Gervais *et al.* 2010).

Exocytosis to generate intercellular lumens

The exocytosis of vesicles with the plasma membrane is the main step in the formation of a lumen during cord hollowing. Upon vesicle fusion with the plasma membrane, the vesicles deliver apical membrane components and the fluid they contain to the space between cells. Thus the cells become polarised and a small intercellular lumen forms simultaneously. The continued delivery of vesicles to the same central location within a cluster of cells results in apical membrane and lumen enlargement and the generation of a single expanded lumen.

Some of the molecular components involved in vesicular exocytosis during cord hollowing have been identified from studies of cyst formation in 3D culture (fig 1.4D). The lipid phosphatase PTEN is one of the first proteins to localise to the newly formed apical membrane in MDCK cells (Martin-Belmonte *et al.* 2007a). The resulting enrichment of PtdIns(4,5)2 at the apical membrane then recruits Cdc42 via Annexin, which in turn binds aPKC thus directing the Par complex to the apical membrane (Martin-Belmonte *et al.* 2007a). Not surprisingly, when most of these components are knocked down in MDCK cells, lumen formation is disrupted, as the cysts display multiple lumens (Martin-Belmonte *et al.* 2007a). The biogenesis of apical membrane *per se* however is unaffected, as large intracellular vesicles that are positive for the apical marker gp135 are still generated.

Rather it is the delivery of these vesicles to the centre of the cyst and fusion with the plasma membrane that is disrupted.

Further work studying Caco-2 cells in 3D culture has shed light on the involvement of Cdc42 during cyst formation. In this system, Cdc42 does not seem to be important for the formation of the apical surface itself, but primarily for the organisation and co-ordination of spindle orientation during cyst morphogenesis. Knock down of *cdc42* by small interfering RNAs (siRNAs) resulted in multiple apical lumens that were intercellular but mislocalised away from the centre of the cluster of cells (Jaffe *et al.* 2008). These aberrant lumens formed primarily from a disruption in the spindle and cleavage furrow orientation of dividing cells, which then resulted in ectopic abscission sites and ectopic lumens because the apical proteins were still correctly targeted to the abscission sites (Jaffe *et al.* 2008). Thus during cyst growth after apical domain establishment at the 2-cell stage, the apical membrane is maintained at the centre of the cyst firstly, by orienting the mitotic spindle to produce an apico-basal oriented cleavage plane, and secondly by asymmetric abscission at the most apical end of the cells.

The role of Cdc42 in vesicle exocytosis has also been investigated during pancreas development *in vivo* (Kesavan *et al.* 2009). Interestingly upon knock out of Cdc42, there are two luminal defects. Some apical vesicles fail to fuse with the plasma membrane and form autocellular lumens, which is similar to the defect seen upon Cdc42 knockdown in MDCK cells. However, some small intercellular lumens are also generated, showing that fusion with the plasma membrane is not completely abolished but that coalescence of these lumens to form a single central multicellular lumen does fail (similar to the phenotype of Cdc42 knockdown in Caco-2 cells). Taking all of these studies together it appears that Cdc42 has important roles during vesicle exocytosis, both in regulating exocytosis itself and in coordinating cell behaviours such as cell division with the axis of polarity to ensure correct lumen formation.

1.4 DEVELOPMENTAL TIMERS

During embryogenesis, it is important that developmental events all occur in the correct order, that they occur at the same rate, and that the timing of events in different tissues in the embryo are coordinated. Changing any of these different elements may have disastrous effects upon morphogenesis during development. Research directed at discovering the factors controlling the timing of developmental processes has been limited, but some developmental timers have been uncovered that share certain properties, and so common mechanisms for measuring time are emerging. A couple of timers have been discovered that globally control the timing and synchrony of simultaneous developmental events over many different tissues. These may act as master timers to directly drive developmental events in specific tissues or to control separate tissue-specific timers. Alternatively, events in different tissues may be driven by different tissue specific timers that exist in series or parallel with each other. In this arrangement it would be essential that the timers interact with each other to ensure coordination of development across the embryo (reviewed in Johnson and Day, 2000).

I have classified the different developmental timers into three broad categories: clocks, switches or egg timers (fig 1.5), and have given an example of each timer that controls events in the whole embryo, and one that is tissue specific. Timers that are repetitive or cyclical in nature, such as the circadian rhythm, or somitogenesis oscillator I have classed as clocks. Timing mechanisms that involve step-wise and progressive changes between different phases of development, such as the heterochronic genes and *Drosophila* neuroblast temporal transition sequence, I have classified as switches. Finally, timers that are nonoscillatory, and activate a response after a defined time period, I have called egg timers. These include the timers that trigger the mid blastula transition during early embryogenesis, and the differentiation of oligodendrocytes. The links of these timers with the cell cycle and cell division are also highlighted, as this thesis investigates how a specialised cell division during zebrafish neuralulation is regulated in time and space.

Although classed as distinct categories, there are links between the different timers. An oscillatory clock may not measure time itself but provide a regular checkpoint to ask if a certain amount of time has elapsed. The actual passage of time in this situation may be measured by a concentration dependent egg timer. Alternatively, clocks might be considered to be a series of small egg timers, with the same response being elicited every time that the threshold value is reached.

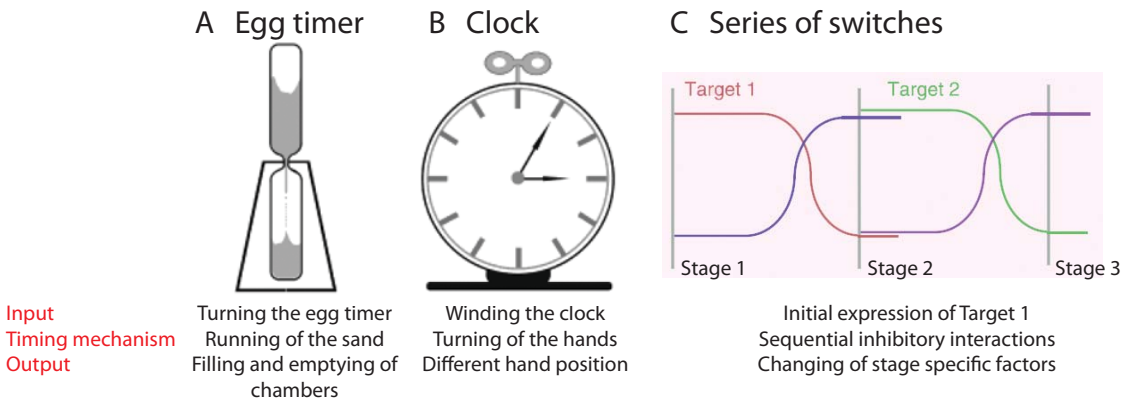

Figure 1.5 The three different types of developmental timing mechanisms.

A) An egg-timer mechanism is linear and is usually based upon the decrease or build-up of an intracellular factor that initiates a response when it reaches a threshold level. An example is the oligodendrocyte differentiation timer.

B) A clock mechanism is cyclical and is based upon a feedback loop that generates a repeated periodic expression or activation of intracellular factors. Examples include the somitogenesis clock and circadian rhythms.

C) A series of switches create a linear timing mechanism that generates sequential activiation of intracellular factors that each define a particular period in time. Example of this type of timer include the heterochronic genes and Drosophila neuroblast temporal fate determinants.
Figures adapted from Johnson and Day (2000) and Moss (2007)

Clocks

Developmental timers that have an oscillatory mechanism as their core component resemble clocks. Clock timers must involve feedback to generate the oscillations and also directionality to drive the clock forwards. Examples include the somitogenesis and circadian clocks, which both consist of a core of transcriptionally controlled oscillating factors that regulate periodic events during development (Pourquie 2003; Giudicelli *et al.* 2004; Gallego *et al.* 2007).

Circadian clock

A biochemical or physiological process has a circadian rhythm if it fluctuates or changes with a periodicity of approximately 24 hours in synchrony with the light-dark cycle of a day. In mammals, the circadian rhythms that exist in almost all peripheral tissues in the body are partly controlled by a master oscillator, which can continue operating as a clock in the absence of external stimuli (Gallego *et al.* 2007). Likewise, zebrafish have a similar central oscillator in the pineal gland, which modulates the production of melatonin as its output, and also controls circadian clocks in peripheral cells too. In mammals the clock can be reset by external light sensed by the retinal ganglion cells (Gallego *et al.* 2007), but the induction of rhythmic gene expression in mammalian cells lines after serum shock (Balsalobre *et al.* 1998), also suggests that individual cells are capable of producing circadian oscillations independently of the master oscillator. In zebrafish, most cells including the pineal gland, directly respond to light, as they are photoreceptive (Tamai *et al.* 2005). Moreover, rhythmic gene expression can be light entrained in explant cultures of *Drosophila* tissue (Plautz *et al.* 1997), suggesting that autonomous clocks exist in individual cells that can act together with a master circadian clock to generate a reliable circadian rhythm.

The basis of the circadian rhythm in mammals is a core transcriptional unit of two proteins CLOCK and BMAL1 and several feedback loops. Dimerisation of CLOCK and BMAL1 in the day drives transcription of both specific Day genes and also their negative regulators *period* (*per*) and *cryptochromes 1* and *2*. Per and the Cryptochromes in return inhibit CLOCK and BMAL1 (Kume et al. 1999), and this completes the negative feedback loop that drives the cyclical expression of *per* and the *cryptochromes*. Post-transcriptional modifications, including phosphorylation of these components, together with input from other circadian clock proteins combine to regulate the transcription and translation feedback loop so that it lasts 24hours and is synchronised with day and night (Gallego *et al.* 2007).

Zebrafish cells have circadian rhythms that operate in early embryogenesis (Vuilleumier *et al.* 2006; Dekens *et al.* 2008). Several reports have conflicting views upon how the clock is initially set up. One study proposes that clock components are maternally inherited and thus that the embryonic circadian clock is set by the mother (Delaunay *et al.* 2000). Another study shows that within the first 24 hours of development, zebrafish cells show an increase in expression of the clock gene, *per2*, in response to light exposure after the mid blastula transition (Ziv *et al.* 2006b). Both the time and length of the light exposure period during this first day affected the expression of a rhythmic gene in the pineal gland 3 days later suggesting that the circadian clock is set up in the first day of embryogenesis (Ziv *et al.* 2006b). Finally a third report suggests that *period1* transcription occurs independently of light with no maternal contribution (Dekens *et al.* 2008). These experiments highlight that there is much left to discover about the regulation of circadian rhythms, but however they are set up, their existence in the fish embryo suggests that they may be important for embryogenesis. It has been suggested that the early circadian rhythms are important for effective repair of DNA damage (Tamai *et al.* 2004), and even that the circadian clock gates the cell cycle during embryogenesis (Dekens *et al.* 2003).

Somitogenesis

An oscillating clock is part of the mechanism that regulates the periodic events of somitogenesis during vertebrate development. Somitogenesis is the process of formation of the segmental units of the trunk called somites, which are paired blocks of mesoderm that develop into skeletal muscle, the vertebrae, ribs and part of the trunk dermis (Pourquie 2001). They are formed from the presomitic mesoderm (PSM), which lies flanking the notochord and neural tube down the antero-posterior axis of the embryo. Somites form progressively from the PSM in an anterior to posterior direction as the body axis elongates, with a periodicity specific to each species, which is thirty minutes in the zebrafish (Holley *et al.* 2000b). The current model for somitogenesis is the "clock and wavefront model" (fig 1.6A), which was first proposed over thirty years ago as a theoretical explanation of how the correct segmentation of the PSM into somites arises (Cooke *et al.* 1976). It comprises two major components: an oscillating clock within the PSM that determines the time period of formation of one somite, and a moving gradient of morphogen that controls the anterior most position of the next somite. Waves of gene expression appear to sweep down the PSM, and where these reach the lowest concentration of morphogen, a somite forms (figure 1.6A).

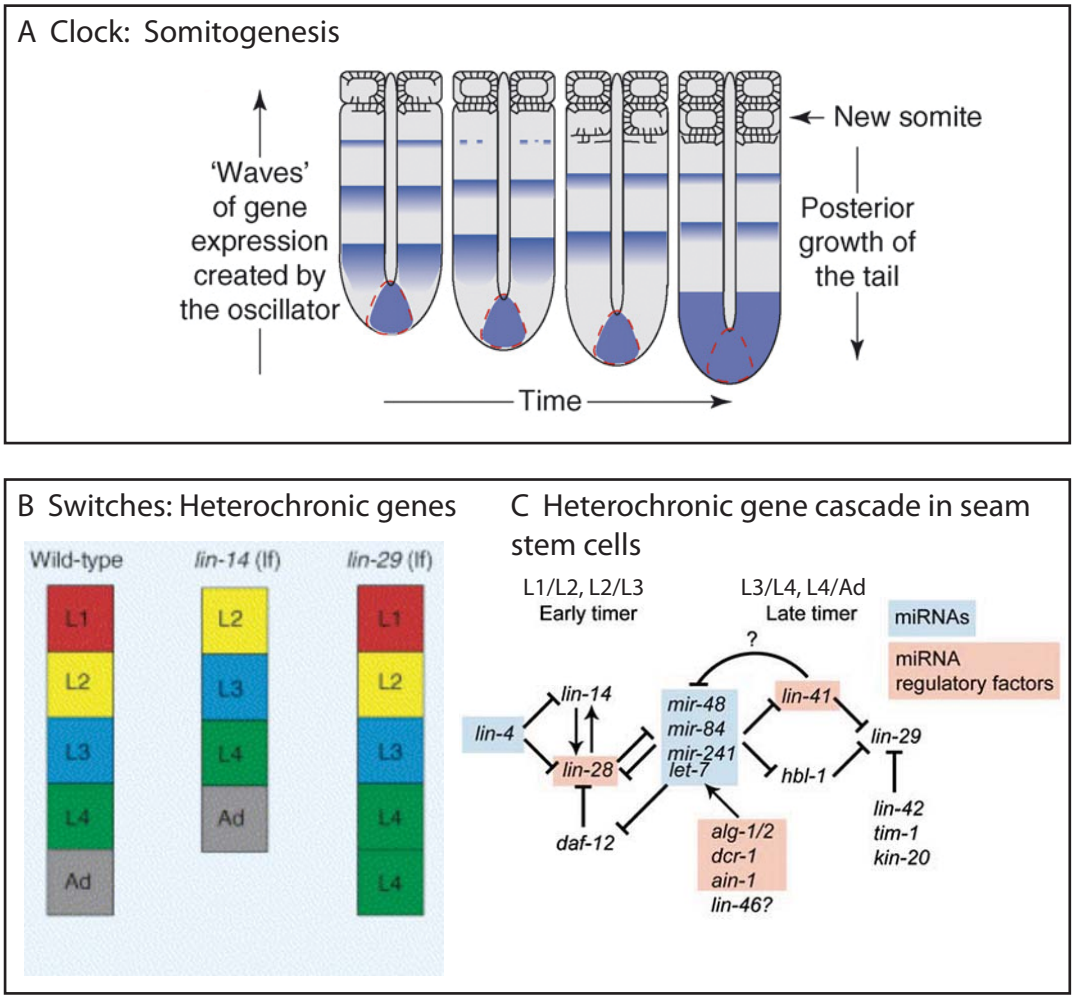

Figure 1.6 The "clock and wavefront" model of somitogenesis, and the *C. elegans* heterochronic gene cascade.

A) The somitogenesis clock creates waves of oscillating gene expression in the presomitic mesoderm. Where the wave meets the anterior end of the presomitic mesoderm a new somite forms. As the body axis elongates over time, new somites form sequentially, one every 30minutes in zebrafish.
B) Development in wild-type *C. elegans* proceeds through four larvals (L1-L4) moults before adulthood (Ad). Heterochronic gene mutants have either a precocious (lin-14 lf) phenotype where one developmental stage is skipped, in this case L1, or retarded phenotype (lin-29 lf) where stages are repeated and development does not progress to the next stage, which in this example is L4.
C) The heterochronic genes form a series of binary switches that control the different stages of development in time, by way of multiple inhbitory interactions between genes in the early and late timers. Many of the heterochronic genes are miRNAs, or miRNA regulators.
Figure A adapted from Mara and Holley (2007).
Figure B adapted from Abbott (2007)
Figure C adapted from Nimmo and Slack (2009)

The clock controls the timing of formation of each somite by oscillating between permissive and non-permissive states of somitogenesis. Components of the Notch pathway are at the core of the oscillator, as several pathway components oscillate in the PSM with a periodicity of the same as the time taken for the formation of each somite. These include *c-hairy1* (Palmeirim *et al.* 1997; Forsberg *et al.* 1998; McGrew *et al.* 1998), *her1* (Holley *et al.* 2002) and *lunatic fringe* (Forsberg *et al.* 1998; McGrew *et al.* 1998). Negative feedback loops comprising these components are thought to determine the period of oscillation. In the zebrafish, the negative feedback is proposed to be mediated at the transcriptional level by *her* genes, which once translated into protein, dimerise with each other (Cinquin 2007a), and act as repressors to inhibit their own transcription (Mara *et al.* 2007a). This model requires firstly that the Her proteins have a short half-life, so that upon their degradation, transcription from the *her* locus can begin again, and secondly that the Notch pathway is continually activated, which could be provided by DeltaD that is expressed in the PSM (Mara *et al.* 2007b). In mice, a feedback loop between Notch and its modulator Lunatic fringe may control the period of oscillation, although this feedback could be negative or positive in nature as both may generate oscillations in the PSM (Cinquin 2007b).

Components of the Wnt and FGF signalling pathways also oscillate in the PSM including *axin2* and *dickkopf* (Aulehla *et al.* 2003; Dequeant *et al.* 2006). The role of these genes in the somitogenesis clock remains controversial because *axin2* can continue to oscillate in a Notch pathway mutant, suggesting that the Wnt pathway may be upstream of Notch signalling (Aulehla *et al.* 2003), but then Axin2 mutants do not have any defects in somitogenesis (Yu *et al.* 2005a). It is currently unclear if the oscillating genes represent the output of the clock, rather than being part of the oscillator itself.

It is also still unclear which genes actually drive the oscillations, as it is experimentally hard to determine which genes are instructive for clock function and which genes are just permissive. Some components of the Notch pathway, such as DeltaD, Notch1 and Dll1 and are required to create the oscillations (Barrantes *et al.* 1999; Holley *et al.* 2000a), but do not oscillate in the PSM themselves. It is possible that these genes that act upstream of the oscillating genes and within the clock itself, but this is yet to be proven. Notch pathway genes in zebrafish seem to be required to maintain synchrony between the individual oscillating cells in the PSM, because upon their knockdown, gene expression of the ligand DeltaC in individual cells still occurs, but forms a salt-and-pepper distribution (Jiang *et al.* 2000). Moreover in Notch pathways mutants the first few somites form normally

suggesting that it takes a certain length of time for the oscillations to become unsynchronised (Conlon *et al.* 1995; van Eeden *et al.* 1996).

The last part of the somitogenesis clock that is important, but has been somewhat neglected in research, concerns how the clock is stopped when enough somites have been produced. Somite number is variable across different species, but it has been shown that in zebrafish, chicken, mouse and corn snake, the number of somites is controlled by the gradual shrinking of the PSM towards the end of somitogenesis (Gomez *et al.* 2008). In summary, somitogenesis is an example of how feedback with a signalling pathway creates oscillations, that when combined with morphogenetic movements of body axis extension, can generate a series of repetitive structures over time.

Egg timers

Another class of developmental timers that are not cyclical in nature, but are driven by a one-way flow of their components of time, are similar in nature to egg timers. They involve a build up or decrease in a product to a threshold level, often with reference to an initial developmental event. Once this threshold is reached then a response is elicited. An example of an egg timing-like mechanism in the whole embryo is the increasing nucleo-cytoplasmic ratio during early development essential for onset of the maternal to zygotic transition (MZT). A tissue specific egg timer is the intrinsic timer regulating the differentiation of oligodendrocytes.

Maternal to zygotic transition

In early embryonic development of most metazoans, the embryo goes through a series of rapid cleavage divisions, characterised by cell cycles consisting of only M and S phases, no accompanying cell growth, and little or no *de novo* transcription. During the cleavage divisions, because there is no zygotic transcription, the embryo must rely upon factors present in the egg to direct the first cell divisions and the initial specification of cell fate and patterning. Then after a certain time, the embryo changes from control by maternally deposited factors to synthesizing RNA and proteins from its own genes (Newport *et al.* 1982b; Tadros *et al.* 2009). In some species, this transition occurs at the same time as cell divisions become asynchronous, the cell cycle lengthens, and gap phases are introduced into the cell cycle, which in *Xenopus* is termed the mid blastula transition or MBT (Newport *et al.* 1982a). The timing of this switch during development has been most intensely studied in *Xenopus* embryos, and many experiments show results that are

consistent with an intrinsic timing mechanism involving an egg-timer type of memory that may have cyclinE as a core component.

MBT requires the coordinated change in many cellular behaviours, including cell division, cell motility and activation of transcription (Newport *et al.* 1982a). Therefore it seems logical that a single or common mechanism could control the timing in the switch of all these behaviours at MBT. The first proposal for a mechanism explaining the timing of MBT was that cells could monitor the number of cell cycles, by the increase in nucleo-cytoplasmic ratio as the embryo progresses through the cleavage cell divisions. This mechanism was proposed as an explanation of the result that zygotic transcription, division asynchrony, and increased cell motility that occur at the MBT were activated two cell cycles earlier than normal in polyspermic embryos (Newport *et al.* 1982a; Clute *et al.* 1995). A mechanism based upon the number of cleavages or rounds of DNA replication could not account for this result (Newport *et al.* 1982a; Clute *et al.* 1995). As neither transcription nor translation are required for the MZT (Clute *et al.* 1995), a nucleo-cytoplasmic timer model was proposed in which cytoplasm factors are titrated away from the nucleus or chromatin over time that could then relieve chromosomal repression (Prioleau *et al.* 1994). Alternatively, or in conjunction with this, maternal cyclins becoming depleted to a threshold level may enable cell cycle lengthening at the MBT (Edgar 1994). Thus the nucleo-cytoplasmic can be viewed as a type of egg-timer mechanism, because a factor must be decreased to a threshold level for the next events to occur.

Although a timer based upon a changing nucleo-cytoplasmic ratio can explain some experimental observations, other experiments show that it cannot be the only timer operating through the cleavage stages of embryogenesis. Events such as the degradation of CyclinE at the MBT are not stopped by inhibitors of DNA replication, therefore cannot be dependent upon the nucleo-cytoplasmic ratio (Howe *et al.* 1996). Moreover waves of contraction still happen in enucleated *Xenopus* eggs with the same timing as if cleavage divisions were occurring (Hara *et al.* 1980). MAP kinase activity may be a molecular component of this timer because increasing MAPK activity by over-expression of a constitutively active form of MAPK delays the degradation of CyclinE (Hartley *et al.* 1997). In summary, there does not seem to be one model that can account for how the timing of all events is regulated at the MBT, which suggests that several mechanisms may exist in parallel. Further investigation into the molecular mechanism of the timer may help to resolve these apparent differences in the MBT timer.

Oligodendrocyte and glial cell differentiation

A cell-type specific example of an egg timer is the counting part of timer that operates during glial cell development. During the formation of the nervous system, cells exit the cell cycle and differentiate at specific times during development. This is crucial for brain development to simply control total cell number, and also as part of the mechanism to generate the wide variety of both neurons and glia necessary that populate the brain. Only a little is known about the factors that control the timing of when cells must stop dividing and differentiate during development. It is thought that cell intrinsic mechanisms play a role in directing the time of differentiation of glial cells in the brain, and also in the oligodendrocytes that myelinate the axons of the optic nerve. Oligodendrocytes are generated from precursor cells (OPCs) that reside in the optic nerve over a six-week period after birth (Barres *et al.* 1992). The mechanism controlling when individual OPCs stop proliferating and differentiate has been investigated and thus far, results are consistent with an intrinsic timer consisting of two components: a timing component that measures elapsed time, and an effector component that initiates differentiation.

Early experiments monitoring the generation of oligodendrocytes in culture from single precursors were the first to suggest that an intrinsic timing mechanism could control oligodendrocyte differentiation. When cultured upon astrocyte monolayers, the precursors formed clones of cells by proliferative divisions before terminally differentiating (Temple *et al.* 1986). The size of the clone varied between different precursors, as the precursors could divide as little as once, or as many as eight times. Critically however, the clonal progeny always differentiated at the same time, even when cultured in separate wells (Temple *et al.* 1986). This showed that although the precursor cells were initially all different in their proliferative capacity, the clonal progeny from a single cell had the same differentiation timer, implying that the daughter cells inherited a timing mechanism from the mother cell. An obvious explanation of these results was that the cells somehow counted the number of cell cycles to know when to differentiate. However, this hypothesis was disproved in subsequent experiments that took advantage of the slower rate of division of precursor cells at a lower temperature. These experiments demonstrated that although the cells had a longer cell cycle, they differentiated after fewer divisions (Gao *et al.* 1997), showing that the timing mechanism was independent of the number of cell cycles, and must rely on a different mechanism to monitor elapsed time.

The molecular nature of the intrinsic timer is still largely unknown, but discovery of a couple of key regulators showed, perhaps unsurprisingly in hindsight, that components that stop the cell cycle are part of the timer. Two such components are the cyclin dependant kinase inhibitors $p27^{Kip1}$ and $p57^{Kip2}$. It has been shown that levels of $p27^{Kip1}$ rise over time reaching a plateau in concentration that coincides with the time of oligodendrocyte differentiation (Durand *et al.* 1997). Moreover, in $p27^{Kip1}$ KO mice oligodendrocyte precursors go through extra cell cycles before differentiating (Durand *et al.* 1998). Likewise, *in vitro* cultures of OPCs show increasing levels of $p57^{Kip2}$ over time, and the level of $p57^{Kip2}$ can regulate the number of cell cycles an OPC undergoes before differentiating (Dugas *et al.* 2007).

Although $p27^{Kip1}$ and $p57^{Kip2}$ are components of the timer, both the upstream components that control their levels and the downstream components that constitute the effectors of the timer are yet to be identified. Other components of the timer must exist because in the presence of mitogens OPCs can proliferate indefinitely (Barres *et al.* 1994), and environmental cues such as retinoic acid and thyroid hormone are required for OPCs to exit the cell cycle (Barres *et al.* 1994; Gao *et al.* 1997). One model is that once $p27^{Kip1}$ and $p57^{Kip2}$ reach a certain level, the OPCs become competent to respond to environmental factors.

There is evidence for a similar intracellular timer controlling the differentiation of glia in the mammalian brain, of which there are three major types: astrocytes, oligodendrocytes, and ependymal cells. Astrocytes have many functions in the brain, including supportive and homeostatic roles, oligodendrocytes provide the myelin sheath for neuronal axons, and ependymal cells line the ventricles of the brain and secrete CSF. In the brain, the different types of glia form at stereotypical times during brain development. In the rat, astrocytes appear first at E15-E16, a couple of days later ependymal cells being to differentiate, and lastly oligodendrocytes appear just before birth at E21 (Abney *et al.* 1981). Dissociated cell culture of glial precursors showed that, remarkably, the different glial cells differentiate at exactly the same time as they would *in vivo* (Abney *et al.* 1981). As the cells appeared to be able to make cell fate decisions on time in the absence of many of the environmental signals from the brain, this suggested that the timing of generation of the different types of glia was intrinsic to the precursor cells.

Developmental switches

The last type of timer consists of a series of developmental switches that control the change in potential of cells over time in a unidirectional manner. Switches do not depend

upon elapsed time, but one event is dependent upon the successful completion of the previous event. Examples of switches include the temporal transition determinants in *Drosophila* CNS neurogenesis and the heterochronic gene cascade in *C. elegans*. The temporal transition determinants in *Drosophila* are a series of transcription factors that are expressed in the neural progenitors of the CNS in a specific order that control the different types of neurons over time (Isshiki *et al.* 2001; Brody *et al.* 2005). The heterochronic genes form a sequential cascade of factors that coordinate the development of different tissues over time in the whole worm (Moss 2007).

Heterochronic genes

Genes that globally control the timing and synchrony of simultaneous developmental events over many different tissues may regulate cell-specific timers. The cell lineage of *C. elegans* is largely invariant and genetically coded, and does not rely on extrinsic signals. The correct timing of developmental events is therefore important and in *C. elegans* this is controlled by a group of genes, called heterochronic genes (reviewed in Moss, 2007). Heterochronic gene mutants were identified as either having a precocious phenotype in which developmental events are skipped, or a retarded phenotype in which events are repeated (fig 1.6B). These changes are usually linked to a particular stage in development and result in cells adopting fates characteristic of other stages and extreme deformation of the adult worm (Ambros *et al.* 1984). The heterochrony phenotype is characterised by the fact that a single mutation alters the strict stereotyped lineage of the worm across several tissues, but the cellular mechanism changed in each tissue may be different.

Many heterochronic genes have been identified, including lin-4 (Lee *et al.* 1993), and let-7 (Reinhart *et al.* 2000), both of which have become the founder members of large microRNA families (fig 1.6C). The function of microRNAs in this context is to repress cell fates (Olsen *et al.* 1999). Heterochronic genes act as switches that are precisely timed to specify particular cell fates at different developmental stages (Ambros 1989), and positive feedback loops between the genes are likely to be important to make the timing switches in the pathway robust (Moss 2007).

Temporal Identity transitions in Drosophila neuroblasts

During the formation of the central nervous system, a relatively small number of progenitor cells must give rise to a wide variety of neurons. One way to do this is to respond to changing environmental cues in space and time, but it appears that many neural progenitors in the *Drosophila* CNS change the type of neuron they generate with

time by following an intrinsic programme. The neural precursor cells, or neuroblasts, undergo multiple rounds of asymmetric cell division during neurogenesis, as at each division, the neuroblast renews itself and buds off a smaller ganglion mother cell (GMC). Generally, the GMC then goes on to divide once more before differentiating into two neurons or glia. During these asymmetric cell divisions, the neuroblasts sequentially express a series of transcription factors (Isshiki *et al.* 2001), which are inherited by the GMCs, and often determine the identity of the neurons or glia generated from the GMC (Isshiki *et al.* 2001; Grosskortenhaus *et al.* 2005). They are in order of expression, Hunchback (Hb), Krüppel, Pdm1 and Pdm2, and Castor.

The timely switch of expression from one transcription factor to the next is important for the correct temporal identity of neurons, but components controlling the progression through the series remain largely unknown. These components must however be intrinsic to the neuroblasts, because neuroblasts show the correct sequential expression of the transcription factors in culture (Brody *et al.* 2000; Grosskortenhaus *et al.* 2005). The transitions are coupled to the cell cycle, and cell division itself is an important trigger for changing from one transcription factor to the next (Grosskortenhaus *et al.* 2005). A component required for the *hb* to *krüppel* switch is *seven-up*, which is transiently expressed in neuroblasts coincident with the downregulation of *hb*. *seven-up* mutants show an increase in cells expressing *hb* and early markers at the expense of later born neurons (Kanai *et al.* 2005). A similar failure of the timer to advance occurs if *hb* is misexpressed beyond its normal temporal window (Isshiki *et al.* 2001; Pearson *et al.* 2003). Furthermore, if *hb* expression is downregulated later, the neuroblast resumes its normal cell lineage (Grosskortenhaus *et al.* 2005), showing that the neuroblast was temporarily kept in a young state.

One of the temporal transcription factors Castor, can be considered to be a switching factor itself because upon loss of Castor activity, *pdm* expression is maintained (Grosskortenhaus *et al.* 2006). Thus Castor is required to inhibit the expression of the previous factor *pdm*. In contrast, the other transcription factors Hb, Krüppel or Pdm do not seem to function in this manner because their loss of function simply leads to skipping of these temporal identities (Jacob *et al.* 2008).

After the last factor in the series, the expression of another transcription factor *grainyhead* is induced in late embryogenesis, whose expression is maintained in neuroblasts through to larval stages. Grainyhead appears to have a slightly different role in neurogenesis compared to the other transcription factors, as it controls the number of neurons formed

by regulating the balance between neuroblast proliferation and death in postembryonic stages (Cenci *et al.* 2005). In the thorax it acts to maintain the neuroblast in a mitotically active state, whereas in the abdomen it is responsible for enabling neuroblasts to undergo apoptosis in response to *abdominal-A* expression (Cenci *et al.* 2005). The mechanism of stopping proliferation at the right time is a crucial part of brain morphogenesis, and in *Drosophila* this seems to be linked to the earlier intrinsic sequence of temporal determinants that regulates cell fate during neurogenesis.

Developmental timers in nervous system development

The changing potential of neural progenitor cells over time to produce different types of neurons and glia may, in part, be controlled by a developmental timing mechanism. This has been investigated in the relatively simple system of the retina of the eye, which at the end of embryogenesis, contains a number of different cell types that can be identified by their characteristic morphology (Marquardt *et al.* 2002). These are generated at specific times during embryogenesis and a single progenitor cell is capable of sequentially generating all of the different cell types (Turner *et al.* 1987; Holt *et al.* 1988). Therefore retinal cell diversification appears to be controlled by time, and not by spatial patterning of different progenitors within the eye. Experiments in both zebrafish and *Xenopus* suggest that the precise order of neurogenesis is controlled by an intrinsic timing mechanism within the retinal precursors themselves (Rapaport *et al.* 2001; Kay *et al.* 2005), rather than a sequential set of inductive environmental cues, as detailed below.

Cell transplantation experiments in *Xenopus* have shown that young cells are not influenced to progress through neurogenesis early, either when transplanted into an older host tissue retina or when co-cultured with older cells (Rapaport *et al.* 2001). They appear to follow a schedule of gene expression according to their age, not their surrounding environment, indicating that an intrinsic timing mechanism may control sequential histogenesis. In zebrafish, retinal ganglion cell (RGC) neurogenesis normally occurs in a wave that begins near the optic stalk and subsequently progresses around the eye. It can be visualised by the gradual expansion of *ath5* expression, a marker for RGCs. Transplantation of cells from the ventronasal retina (that usually turns on *ath5* early), to a more temporal location where *ath5* expression appears later, resulted in the transplanted cells expressing *ath5* before the surrounding temporal cells in 30% of cases. This suggests that sequential induction of neurogenesis by cell-cell communication is not necessary for the wave of retinal neurogenesis, as transplanted cells can begin to express *ath5* and

differentiate before their neighbours, but that the timing of expression of *ath5* is intrinsic to cells.

Although the molecular mechanism of the developmental timer controlling retinal histogenesis is not known, the timer must be integrated with environmental signals because a number of different signalling pathways are crucial for the differentiation of certain retinal cell types (Kelley *et al.* 1995; Hyatt *et al.* 1997; Patel *et al.* 2000). It was hypothesized 20 years ago that a timer may act to change the ability of retinal precursors over time to respond to environmental signals (Watanabe *et al.* 1990), and subsequent experiments support this model (Rapaport *et al.* 2001). In this way, an intrinsic mechanism of cellular competence integrated with environmental cues could explain the histogenic order of retinal neurogenesis. This competence model may prove to be a common theme for the sequential generation of cell fates in other systems too.

The cell cycle and developmental timers

Cell division plays a role in some developmental timers, such as the temporal transition sequence of *Drosophila* neuroblasts. It has been shown that the switch from Hb to Krüppel, the first two transcription factors in the series, depends on cytokinesis, because neuroblasts arrested in G2 phase of the cell cycle continue to express *hb*, and do not switch to *Krüppel* expression (Grosskortenhaus *et al.* 2005). The switch was shown not to be dependant on cell cycle progression *per se*, because the same failure of *hb* downregulation was observed in neuroblasts that continue progressing through the cell cycle though cytokinesis is impaired (Grosskortenhaus *et al.* 2005).

Specific developmental transitions occur at certain cell cycles

During early embryonic development in both mouse and zebrafish, certain events occur at specific cell cycles. Cell lineage analyses of single zebrafish cells during gastrulation and neurulation has revealed that specific morphogenetic movements and the orientation of cell division are related to specific cell cycles. Kimmel and colleagues found that in the 15th cell cycle, cells generally move in a posterior-direction during epiboly, and then divide along the antero-posterior axis (Kimmel *et al.* 1994). However during cell cycle 16, cells change direction to move towards the dorsal midline as they undergo convergence extension movements and then divide in the neural keel or rod with a medio-lateral orientation to separate sister cells across the midline (Kimmel *et al.* 1994).

Similar correlations of developmental events with the cell cycle have been observed during mouse development. The first transcription of zygotic genes always occurs at the end of the first cycle (Ram *et al.* 1993; Christians *et al.* 1995). Then during the second cell cycle, prior to and immediately following DNA replication, two larger bursts of transcriptional activity representing general activation of transcription take place (Bolton *et al.* 1984). During the fourth cell cycle, the trophectoderm begins to become polarised (Fleming *et al.* 1993), and blastocoel cavitation takes place during the sixth cycle, when the embryo is at the 32cell stage.

Possible mechanisms for linking cell division to developmental timers

The cyclical repetitive nature of cell division, coupled with the necessity of cell division in embryonic development, leads to many possibilities for cell cycle components to part of developmental timers. During organogenesis, tissues must reach a certain size and stop proliferating. They may do this by simply monitoring the number of cells, or they may monitor cell size, especially during early development when upon every cell division, cells reduce in size. Finally cells may count the number of cell cycles they have undergone.

Experiments in the *Drosophila* wing imaginal disc and during early development in mouse, *Xenopus* and ascidian embryos show that it is unlikely that tissues or the embryo monitors the total cell number. During the development of the *Drosophila* wing imaginal disc cells, manipulating cell cycle components to either accelerate or slow cell proliferation resulted in compensatory changes in cell size, such that the clone or compartments of cells with the altered proliferation rate stayed the same size (Neufeld *et al.* 1998). Moreover, inhibiting mitosis but allowing DNA replication to continue in a clone of cells gave a similar result, as the clone consisted of fewer larger cells (Weigmann *et al.* 1997). These experiments not only argue monitoring of cell number is not important during organogenesis, but also that cell size is not important. They show that during development, mechanisms must exist to monitor overall volume of tissues, not volumes of individual cells.

There is also little evidence that cells count the number of cell divisions to monitor time. The timing of differentiation of OPCs and cardiac myocytes in culture appears to be intrinsic to cells, because clonal progeny all differentiate at the same time (Gao *et al.* 1997; Burton *et al.* 1999). However, experiments have shown that cells do not count the number of cell divisions because when OPCs and cardiac myocytes are cultured at 33°C instead of 37°C they divide more slowly, but still differentiate at the same time, even though they have undergone fewer cell cycles (Temple *et al.* 1986; Burton *et al.* 1999).

1.5 ZEBRAFISH NEURAL TUBE FORMATION

The process of neural tube formation, or neurulation is a very early event in the development of the embryo, and is arguably the first morphogenetic movement in development of the CNS. It is an important process to study because when the neural tube fails to close, neural tube defects (NTDs) arise, which are one of the most common congenital defects in human pregnancies, occurring at a frequency of 1 in every 1000 births (Copp *et al.* 2003). The most severe NTD is craniorachiscisis in which the neural tube is open down the whole length. NTDs may also be present at specific regions in the brain or spinal cord; for example in spina bifida only the sacral segments of the spine fail to close.

Morphogenetic mechanisms of neural tube formation

Primary and secondary neurulation in amniotes

In amniotes, the neural tube forms by one of two mechanisms depending on antero-posterior location. All of the brain and most of the spinal cord forms by primary neurulation, with only the most sacral spinal regions undergoing secondary neurulation. At the start of primary neurulation the neural plate thickens, then begins to fold and bend inwards at hinge points in the plate (fig 1.7A). Where the two edges of the neural plate meet at the dorsal midline, fusion occurs to join the two sides of the neuroepithelium together, thus creating a tube (Colas *et al.* 2001; Copp *et al.* 2003). In contrast, secondary neurulation begins with the aggregation of an unpolarised group of mesenchymal cells at the midline to form a solid rod. The cells must then acquire apico-basal polarity so that the rod can cavitate to form a tube (fig 1.7B).

The process of secondary neurulation is poorly understood, especially the mesenchymal to epithelial transition, perhaps partly because there appears to be variation in the mechanism among species and at different stages of embryogenesis. In chick embryos, the outer cells of the rod seem to elongate and adopt epithelial characteristics first, leaving a central core of unpolarised cells (Schoenwolf *et al.* 1980). Small lumens then form first at the interface of the two types of cells, which then develop into a larger central lumen as inner cells subsequently elongate and likely intercalate with the outer cells (Schoenwolf *et al.* 1980). In human embryos, multiple small lumens have also been observed, which must then coalesce together to from a single central lumen (Saitsu *et al.* 2004). In mice, two other mechanisms of lumen formation have been documented. One mechanism involves

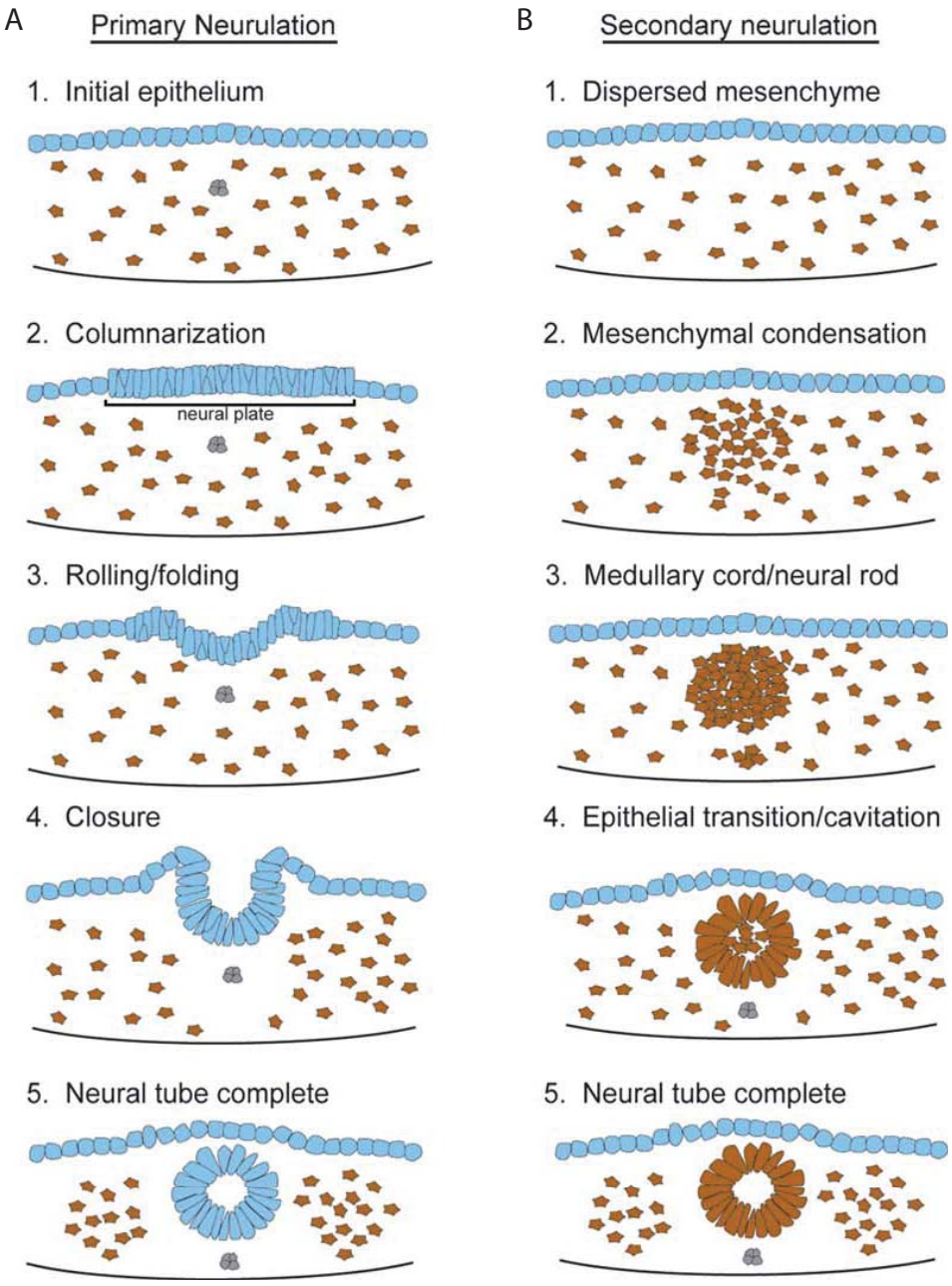

Figure 1.7 Primary and secondary neurulation in amniotes.

A) Primary neurulation begins when the existing polarised epithelial cells elongate in their apico-basal axis to form the neural plate. The neural plate then folds at the midline and rolls up. A tube is formed when the dorsal edges of the rolled neural plate fuse at the dorsal midline.
B) Secondary neurulation begins when mesenchymal cells aggregate at the midline and condense to form a solid neural rod. The cells then undergo a mesenchymal to epithelial transition and acquire apico-basal polarity necessary for the formation of a lumen from the solid rod to complete tube formation.
Figure taken from Lowery and Sive, 2004.

the formation of a small rosette structure with epithelial characteristics that expands over time as cells join the rosette to form the neural tube (Schoenwolf 1984). In the second mechanism, cells in the dorsal part of the rod first become epithelial, and then other cells join ventrally to form the rest of the neural tube (Lowery *et al.* 2004). Ultrastructural analysis of secondary neurulation in mouse suggests that junctional complexes are localised to the inner ends of cells at cavitation stages (Schoenwolf 1984), but the dynamic nature of cell polarisation and lumen formation during secondary neurulation remains completely unexplored.

Zebrafish neural tube morphogenesis

Zebrafish neurulation begins at the end of gastrulation when the dorsal ectoderm thickens to form the neural plate (Lowery *et al.* 2004). The tissue then converges towards the midline where it infolds to form the neural keel, an intermediate and transient primordium (fig 1.8A). During keel formation cells elongate along their superficial deep axis and thus begin to intercalate with their neighbours on the same side of the neural keel (Hong *et al.* 2006). These are the start of the large cell rearrangements that begin to convert the multilayered hindbrain neural plate into the single-layered neuroepithelium of the brain. It has been proposed that the cell-cell adhesion molecule N-Cadherin plays a role in this superficial-deep intercalation of neural plate and keel cells (Hong *et al.* 2006).

In the neural keel, the cells on the two sides of the neural plate meet and interdigitate across the midline at all dorso-ventral levels as their processes extend across the midline (Hong *et al.* 2006). As the keel rounds up to form a solid rod, further extensive cell rearrangements take place when cells divide at the midline and one daughter cell intercalates into the contralateral side of the neural rod (Kimmel *et al.* 1994; Concha *et al.* 1998; Geldmacher-Voss *et al.* 2003; Tawk *et al.* 2007). This results in two columns of cells, one on each side of the neural rod and thus clears cellular processes from lying across the midline (Tawk *et al.* 2007). A proper pseudostratified neuroepithelium with well-defined apico-basal polarity is subsequently established, with the apical surfaces of the epithelia on each side of the neural rod located at the embryonic midline. Finally the two sides of the rod separate to form a tube and complete neurulation (Lowery *et al.* 2004; Clarke 2009).

The description of zebrafish neurulation just given applies to hindbrain and spinal cord regions of the CNS. Morphogenesis of the forebrain during neurulation involves the evagination of the eye field, and is therefore more complex than in hindbrain and spinal

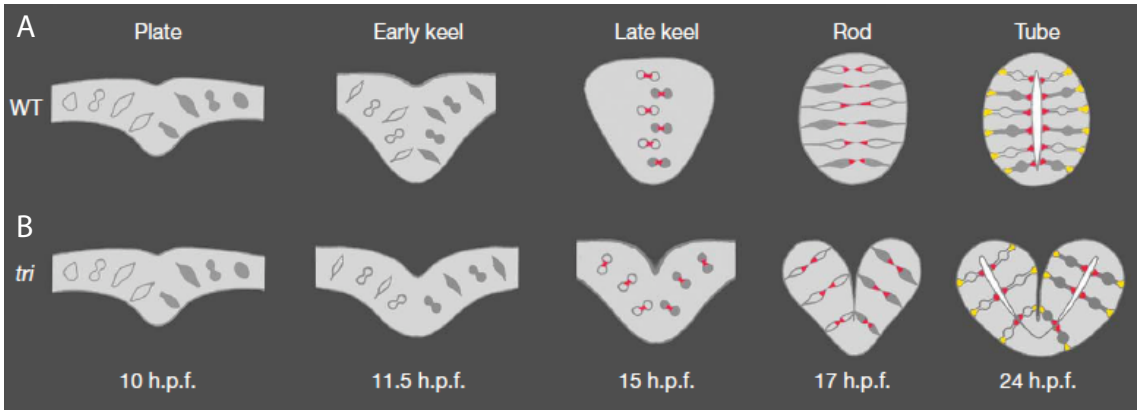

Figure 1.8 Zebrafish neural tube morphogenesis in wild-type and *trilobite* mutant embryos.

Diagrams to show the cellular organisation and behaviours at the different stages of zebrafish neurulation in transverse section.
A) At the beginning of neurulation, the neural plate is a multilayered tissue, that is not a conventional epithelium and does not have apico-basal polarity. Convergence of the neural plate and invagination of the tissue at the midline forms the neural keel. The keel then rounds up to form a solid rod, and the last step in neurulation is the opening of a lumen to form a tube. Cell divisions follow stereotypical patterns during neurulation especially in the late keel when cell divisions are localised close to the embryonic midline. These divisions separate sister cells across the midline and Pard3-GFP (red) accumulates at the cleavage plane or abscission site of cells during this crossing division. This results in pairs of daughter cells each with mirror-image polarity aligned into two columns within the neural rod. The apical proteins are thus localised to the midline of the neural rod and enable the formation of a proper neuroepithelium and the single central lumen to open.
B) At the beginning of neurulation in *trilobite* (*tri*) the neural plate is wider than in wild-type embryos. This means that at 15hpf, cells undergo mirror-symmetric cell divisions in ectopic lateral locations across the superficial-deep axis of the neural plate . This generates ectopic apical surfaces either side of the embryonic midline and leads to the formation of duplicated neural tubes, lying side by side.
Cells on the left and right sides of the plate are filled or in outline to emphasise that cells from one side of the plate contribute to both sides of the tube. The basal marker GFAP is shown in yellow.
Figure adapted from Clarke, 2009

cord regions. Tracking of cell nuclei during forebrain neurulation revealed that cells do not simply converge in a medio-lateral direction towards the midline. Instead the whole anterior neural plate contracts, with lateral cells moving in a posterior direction towards a focus at the hypothalamic anlagen that is initially located at the posterior most end of the anterior neural plate (England *et al.* 2006). The hypothalamic cells then subduct and move anteriorly underneath the eye field to emerge anterior to the telencephalon, while convergence narrows the neural plate (England *et al.* 2006). The eye field then begins to evaginate at the same time as diencephalic precursors move in an anterior direction along the midline and the telencephalic precursors move dorsally and medially to meet at the dorsal midline (England *et al.* 2006). Thus forebrain neurulation proceeds by mechanisms more complex than a simple neural keel, as the neural plate also folds to form lateral outpockets of tissue. Despite this complex morphogenesis, midline-crossing divisions similar to those in the hindbrain are evident in the diencephalon during neurulation (my unpublished observations), although they are probably not so prevalent in the forebrain as in the hindbrain. This indicates that although forebrain neurulation is complicated by the concomitant evagination of the eye fields, it does at least share some cell behaviours and mechanisms with neurulation in other brain regions.

Zebrafish hindbrain neurulation has features of both primary and secondary neurulation. Features similar to primary neurulation include the formation of a neural plate that converges towards the midline (Lowery *et al.* 2004). However, in contrast to the polarised epithelial structure of the *Xenopus* and amniote neural plate, the zebrafish neural plate is not a conventional epithelium, as the cells do not display obvious apico-basal polarity (Geldmacher-Voss *et al.* 2003; Hong *et al.* 2006; Tawk *et al.* 2007; Yang *et al.* 2009). Other features of zebrafish neurulation are more similar to secondary neurulation, such as the formation of a solid rod, which then opens to form a tube. The detailed mechanisms of how the posterior neural tube of amniotes cavitates during secondary neurulation are unclear, but as mentioned above a lumen forms in zebrafish by cell rearrangements, not apoptosis. The opportunity for excellent optical imaging of development in the zebrafish embryo has resulted in the emergence of neurulation in zebrafish as a useful model system for the study of the generation of polarity and lumen formation *in vivo*, with potential implications for the morphogenetic mechanisms of secondary neurulation.

Cell behaviours during the keel to tube transition

Neurulation requires the coordination of several cellular behaviours with tissue movements to ensure correct neural tube morphogenesis. In this section I will focus upon

the cell behaviours of cell division and polarisation that occur during the keel to rod stages of zebrafish neurulation, secondly describe in detail our current knowledge of how they are regulated, and finally highlight the importance of tightly coordinating cellular behaviour during neurulation.

Cell division

Cell division is tightly coupled to the morphogenetic movements of zebrafish neurulation. In the neural plate, cells divide aligned with the superficial deep axis of the plate, and as the tissue invaginates to form a keel, the orientation of division gradually changes though 90˚ to become aligned with the mediolateral axis (Tawk *et al.* 2007). The cell divisions at late keel and rod stages are characterised by their location close to the midline of the tissue and the separation of daughter cells across the midline to deposit one daughter cell on each side of the rod (fig 3.1B, Kimmel *et al.* 1994; Geldmacher-Voss *et al.* 2003; Tawk *et al.* 2007). The pairs of daughter cells stretch equally across the rod, and this leads to the generation of two columns of cells with the contact point of sister cells at the embryonic midline. This defines a seam in the centre of the rod, where the lumen will later form.

There are several important features to note about this midline crossing or C-division. Firstly, unless a cell undergoes this division, it cannot cross the midline and integrate into the other side of the neural rod. This was shown by time-lapse imaging (Concha *et al.* 1998), and also experimentally by blocking cell division and observing that cell crossing was abolished (Tawk *et al.* 2007). Secondly most neural progenitor cells in the hindbrain and anterior spinal cord undergo this division (Kimmel *et al.* 1994; Lyons *et al.* 2003). Thirdly, it occurs at the time when apico-basal polarity is being established in the neural tissue (Tawk *et al.* 2007), and generates pairs of daughter cells with mirror-image symmetry. This is crucial for neural tube morphogenesis and the generation of apical polarity as described below.

Mirror-symmetric cell division

The close relationship between this specialised midline-crossing division (C-division) and apical polarity was revealed by labelling neural cells with a GFP-fusion protein of Pard3 and imaging the establishment of polarity at the cellular level by time-lapse microscopy. Zebrafish Pard3 is the orthologue of the core polarity protein Par3 in *C. elegans,* and was originally called ASIP in zebrafish for aPKC isotype-specific interacting protein (von Trotha *et al.* 2006). It was observed that Pard3-GFP first became polarised within the cell during cytokinesis, as it localised to the cleavage furrow or abscission site of cells

undergoing C-division (Tawk *et al.* 2007). Pard3-GFP remains at the medial ends of the two daughter cells as they elongate across their respective sides of the neural rod (fig 1.8). The targeting of Pard3-GFP to the abscission site of pairs of daughter cells not only results in the two daughter cells acquiring mirror image polarity with respect to each other, but also in the localisation of Pard3-GFP to the midline of the neural rod (Tawk *et al.* 2007).

The mirror-symmetric inheritance of another apical component fusion protein, Pard6-GFP, has also been observed during midline crossing divisions (Munson *et al.* 2008) suggesting that this could be a common method for localising apical proteins to the midline. The delivery of apical proteins to the midline in this way facilitates the localisation of apical proteins to a single midline plane, and subsequently the formation of junctional contacts between cells on the same side of the rod generates two apical surfaces with a single central lumen between them. The functional importance of Pard3 for midline crossing behaviour has been investigated using morpholino knockdown of *pard3* and overexpression of Pard3-Δ6-GFP, which lacks the aPKC binding domain and is thus proposed to function as a dominant negative form of Pard3 (von Trotha *et al.* 2006). Pard3-Δ6-GFP does not localise to the cleavage furrow or prospective apical ends of cells during C-division, and both daughter cells remain on the same side of the midline (Tawk *et al.* 2007). Morpholino knock down of *pard3* similarly reduces the ability of cells to cross the midline (Tawk *et al.* 2007) suggesting that the mirror-image polarity of cells generated during C-division may be necessary for each daughter to integrate into the appropriate side of the neural rod.

The mirror-symmetric nature of polarisation of C-divisions has mostly been studied using overexpression of the fusion protein Pard3-GFP. One concern is that the fusion protein may not be representative of the localisation of the endogenous protein. However several different GFP fusion proteins expressed at the same concentration in neural keel and rod cells are not specifically enriched at the cleavage plane of cells undergoing mirror-symmetric C-division (Tawk *et al.* 2007), suggesting that this targeting is a real phenomenon. Moreover, Pard3-GFP accurately localises to the junctional belt close to the ventricular surface of cells in the neuroepithelium (fig1.9), which matches its predicted location usually associated with tight junctions in a mature epithelium (Hirose *et al.* 2002). Additionally, immunohistochemistry with a sample of Pard3 antisera showed that endogenous Pard3 was located to the midline of the neural rod with the same distribution as Pard3-GFP (Tawk *et al.* 2007). Finally the localisation of other apical components to the abscission plane of cells undergoing division has been reported during apical polarity

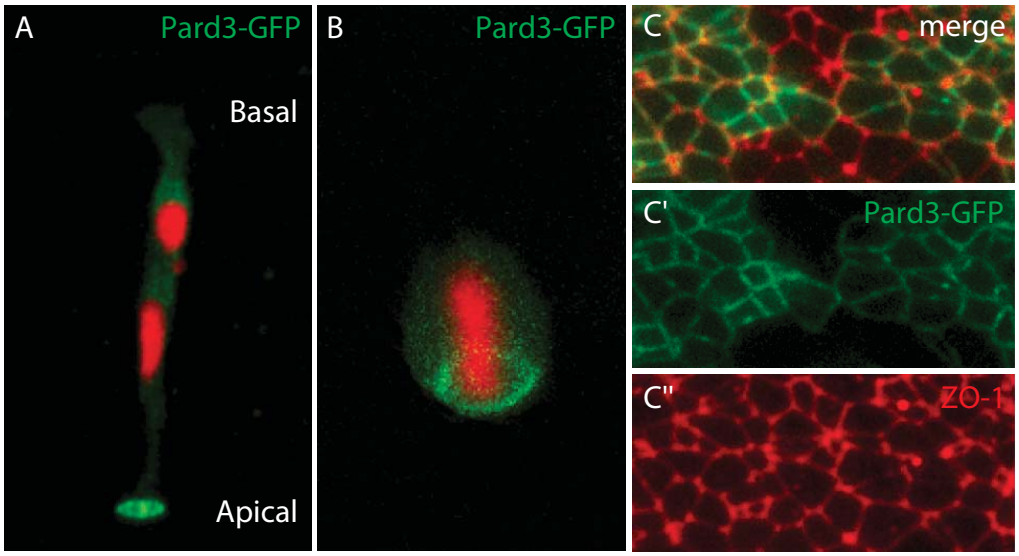

Figure 1.9 Pard3-GFP localises to junctional belts of neuroepithelial cells.

A) Confocal micrograph of two neuroepithelial cells labelled with H2B-RFP and Pard3-GFP. The cells have an elongated morphology and Pard3-GFP localises asymmetrically forming in a ring close to the lumenal or apical surface of the neuroepithelium.
B) Confocal micrograph of a neuroepithelial cell labelled with H2B-RFP and Pard3-GFP undergoing cell division. Pard3-GFP localisation in a ring is maintained when cells rounds up to divide at the apical or ventricular surface of the neural tube.
C-C") Confocal micrographs of the ventricular surface of the neuroepithelium labelled with Pard3-GFP and ZO-1. Both proteins show a similar reticular network pattern of localisation, which represents the belts of junctional proteins localised close to the ventricular surface that separate apical and basal membrane domains. Areas of colocalisation of the two proteins are yellow in C. Images kindly provided by Paula Alexandre

establishment in cyst formation in culture. The fusion protein GFP-Crumbs3a has been reported to localise to the abscission plane of cells in MDCK cells (Schluter *et al.* 2009), and endogenous aPKC localises to the midbody of Caco-2 cells undergoing division (Martin-Belmonte *et al.* 2007a; Jaffe *et al.* 2008; Schluter *et al.* 2009). This shows that cleavage plane targeting of apical proteins to the cleavage plane may be a common mechanism for establishing apical polarity. All of these observations strongly suggest that localisation of Pard3-GFP reflects that of the endogenous protein, and therefore that the fusion protein is a valuable tool to reveal the dynamic nature of cell polarisation.

Establishment of apico-basal polarity at the tissue level

The localisation of GFP fusion proteins Pard3 and Pard6 reveals that the acquisition of apico-basal polarity occurs during keel and rod stages of neurulation (Tawk *et al.* 2007; Munson *et al.* 2008). The generation of polarity has been also been studied by immunohistochemistry for polarity components including the tight junction component ZO-1, the adherens junction components N-Cadherin and β-catenin, the core polarity proteins aPKC and Nok (zebrafish PALS1 homologue) and the protein Lin7c that interacts with Nok (Wei *et al.* 2006). The first of these proteins to become expressed are ZO-1 and N-Cad, which show a scattered punctate distribution in the neural plate (Yang *et al.* 2009). Their localisation to puncta and not to a defined apical plane shows that an apical surface is not yet established in these cells, a finding which is further corroborated by the lack of any detectable specific aPKC staining (Geldmacher-Voss *et al.* 2003). As neurulation progresses and the two halves of the neural plate meet during neural keel stages, aPKC, β-catenin, ZO-1, Nok and Lin7c all become enriched at the midline, with the ventral most cells polarising first (Geldmacher-Voss *et al.* 2003; Yang *et al.* 2009). The density of midline labelling increases over time, and by rod and tube stages all junctional proteins studied become localised to the apical ends of neural progenitor cells (Geldmacher-Voss *et al.* 2003; Yang *et al.* 2009).

The punctate distribution of polarity components ZO-1 and N-Cad in the early neural keel suggests that focal accumulations of these two proteins appear before puncta of other polarity proteins such as Pard3-GFP and aPKC. Although the initial cellular localisation of the ZO-1 and N-Cad puncta is not clear, the puncta do progressively become localised at the midline through time, similar to other polarity proteins. It has been proposed that the function of later expressed apical-proteins such as aPKC, Lin7c and Nok is to stabilise the early ZO-1 and N-Cad puncta at the midline after cell rearrangements of neurulation have largely finished (Yang *et al.* 2009). This suggestion is based upon the observation that

premature overexpression of *lin7c* causes disorganised apico-basal polarity, which is assumed to result from premature stabilisation of ZO-1 and N-Cad in ectopic locations (Yang *et al.* 2009). This however was not directly tested and another interpretation of the data is that morphogenesis is uncoupled with the generation of polarity (see later in this section). Therefore although the distribution of different proteins involved in apical polarisation become polarised at different times during neurulation, the functional step-wise process of the maturation of apico-basal polarity during neurulation remains to be proven.

Why is mirror-symmetric cell division important?

Mirror-symmetric C-division is a stereotypical behaviour of nearly all neural cells in the zebrafish neural keel and rod. However its importance for correct neural tube morphogenesis is only beginning to be investigated. One way to do this is study the formation of the neural tube in the complete absence of cell division, which can be achieved by using pharmacological inhibitors to blocking cell division. Several groups have done this and have reported that zebrafish embryos form a normal neural tube with correct apico-basal polarity by 24hpf (Ciruna *et al.* 2006; Tawk *et al.* 2007; Nyholm *et al.* 2009). However a detailed analysis of neural tube morphogenesis in the absence of cell division has not been carried out, and given the specialised nature of this division, it might be expected to confer some advantage to the process of neural tube formation. In collaboration with Una Ren in the Clarke lab, I have begun to investigate in more detail how the neural tube forms in the absence of cell division, with a focus upon how apical polarity is generated in the rod (Chapter 6).

Importance of coordinating cell behaviours with morphogenesis

During zebrafish neurulation, individual cell behaviours such as cell division and intercalation are coordinated with the tissue movements of convergence towards the midline. This coordination is crucial for normal neural tube morphogenesis, which is revealed by the neural tube defects of embryos that have delayed convergence, such as the zebrafish PCP pathway mutant *trilobite* (*tri*). In *tri* mutants the neural plate converges more slowly than normal during neurulation (Sepich *et al.* 2000), and mirror-symmetric cell divisions that usually occur at the midline in wild-type embryos instead occur in ectopic locations either side of the midline before the neural primordium has even begun to form a keel at the midline (Tawk *et al.* 2007). These divisions occur across the superficial deep axis of the *tri* neural plate, and the two daughter cells stay in register (fig 1.8B). As the apical protein Pard3-GFP is deposited at the abscission plane of the two

daughter cells, they acquire mirror-image polarity and this leads to the generation of an apical plane halfway between the superficial and deep surfaces of the invaginating neural plate (fig1.8B, Tawk *et al.* 2007). By 24hpf, the tissue has undergone convergence and invagination at the midline to generate duplicated neural tubes, lying side by side, each with correct apico-basal polarity (Tawk *et al.* 2007).

A couple of other studies have suggested that manipulations in signalling pathways other than the PCP pathway can also cause the duplicated neural tube phenotype. It has been reported that ubiquitous overexpression of sonic hedgehog causes severe gastrulation defects and the formation of a bifurcated neural tube (Takamiya *et al.* 2006). In this case, the two neural tubes were completely separated at some antero-posterior levels. Embryos heterozygous for the mutant locus *half baked*, show a concomitant widening of the dorsal ectoderm and shortening of the body axis during gastrulation, which results in a broad neural primordium with ectopic neurons at the midline by 24hpf (McFarland *et al.* 2005). These observations are consistent with a neural tube duplication, because neurons form at the basal edge of the neural tube that in regions of duplication sit at the embryonic midline. Finally neural tube duplications can even arise when genes important for the convergence of the mesoderm, such as *has2* are knocked down (Tawk *et al.* 2007). The correlation of the occurrence of neural duplications with a convergence phenotype in all these different mutants suggests that any delay in convergence may cause neural tube duplications. I have tested this idea in Chapter 3, by investigating if surgically delaying convergence in wild-type embryos also generates neural tube duplications.

In *tri* embryos, the occurrence of mirror-symmetric C-divisions in ectopic lateral locations before the tissue has converged towards the midline suggests that the timing of mirror-symmetric cell division has become uncoupled from the morphogenetic tissue movements of convergent extension and invagination. Furthermore, the observations that cells undergo mirror-symmetric division on time, even though they are in the wrong place, lends itself to speculation that a cell intrinsic timing mechanism might control the time of cell division and polarisation during zebrafish neurulation. In this thesis I have tested this intrinsic timer hypothesis using heterochronic cell transplantation (Chapter 4).

THESIS AIMS

- To test if surgically delaying convergence in wild-type embryos generates neural tube duplications.
- To test the hypothesis that an intrinsic timer controls neural cell mirror-symmetric cell division and polarisation using heterochronic cell transplantation.
- To investigate the role of the environment in neural cell polarisation by studying the timing of cell polarisation in abnormal neural environments and in extreme ectopic locations both in the embryo and 3D culture.
- To investigate how the neural tube forms in the absence of cell division, with a focus upon how apical polarity is generated in the rod.

CHAPTER 2 GENERAL MATERIALS AND METHODS

Embryo care

Wild-type and transgenic zebrafish were maintained under standard conditions (The Zebrafish Book) on a 14-hour photoperiod in the UCL or KCL fish facility. Embryos were obtained either by natural matings, or by separate pairings of a single AB male with a Tupfel long fin (Tuplf) female. Separate pairings enabled embryos to be obtained at 12pm, as male and female fish in the same tank were separated with a divider until the time that embryos were required. All embryos were incubated at 28.5°C in fish water with methylene blue added, and staged according to published criteria (Kimmel *et al.* 1995).

Wild-type strains used were: AB Tubingen (UCL), Tuplf (UCL), King's College Wild-type (Kwt), and Shark Bait (KCL).
One transgenic line was used: Tg:(HuC:GFP) to visualise neurons (Park *et al.* 2000).
Two mutant lines were used: MZ*oep*$^{tz257/tz257}$ (Gritsman *et al.* 1999) and *trilobite*$^{m209/m209}$ (Jessen *et al.* 2002).

RNA synthesis

Plasmid DNAs were linearised by restriction enzyme digestion for 2 hours, extracted using phenol – chloroform – isoamyl alcohol mixture (25:24:1, Sigma, 77617), and precipitated at -20°C overnight in a solution of 100% ethanol and 0.05M Sodium acetate. The DNA was then centrifuged, washed in 70% ethanol, and resuspended in water ready for transcription. Sense-strand capped mRNA was transcribed with the mMESSAGE mMACHINE system (Ambion). RNA was purified on a spin column (Roche) and its concentration was measured using a spectrophotometer.

Microinjection

All embryo injections were carried out under a dissecting microscope using a glass microinjection needle mounted on a micromanipulator and attached to a Picospritzer (General Valve Corporation). All RNA and morpholinos were dissolved in RNase free water. RNA and morpholinos were injected at the 1-4 cell stage for ubiquitous expression, or into a subset of blastomeres at the 32-64cell stages for mosaic labelling of cells.

Pharmacological treatments

Cell-division blockade

To block cell division before or during neurulation, a combination of the cell division inhibitors aphidicolin (150μM, Sigma or Biomol) and hydroxyurea (20mM, Sigma) dissolved in 2.5% DMSO in embryo medium was used (Harris *et al.* 1991; Lowery *et al.* 2005; Lyons *et al.* 2005; Ciruna *et al.* 2006; Tawk *et al.* 2007).

Whole mount Immunohistochemistry

- Embryos were fixed in 4% paraformaldehyde in PBS (Sigma) for 2 hours, with gentle shaking, at room temperature, or overnight at 4°C.
- After fixation embryos were washed 3x 10mins in PBTr (PBS + 0.3-0.5% Triton-X-100) with gentle shaking.
- They were then dehydrated through 50% methanol in PBTr (10mins wash) to 100% methanol (3 x 5min washes) and placed at -20°C for at least 30mins, often overnight, to permeabilise the embryos.
- Next the embryos were rehydrated by a series of 5 minute washes through 75% methanol in PBTr, 50% methanol in PBTr, 25% methanol in PBTr, and finally washed 3 x 10mins in PBTr.
- After rehydration, embryos were incubated in blocking solution (IB, 10% normal horse, bovine or sheep serum, 1% DMSO in PBTr) for at least 1 hour at room temperature with gentle shaking.
- Embryos were incubated in primary antibody in IB, overnight at 4°C with gentle shaking.
- The next day, embryos were washed for at least 2 hours in PBTr, changing the solution every 30mins.
- Following this, embryos were incubated in secondary antibody in IB, overnight at 4°C with gentle shaking.
- Finally embryos were rinsed 3 x 5mins in PBTr, and washed in PBTr for at least 2 hours at 4°C with gentle shaking.

Primary antibodies used were α-ZO-1 (1:500, Zymed), α-GFAP (1:300, Dako), α-phospho histone H3 (1:500, Cell signalling, or Upstate), α-laminin (1:500, Sigma).
Secondary antibodies used were fluorescently conjugated α-mouse, α-rabbit or α-chick alexa-488, alexa-546, alexa-633 or alexa-647 (1:400, Molecular Probes).

In situ hybridisation

- Embryos were fixed in 4% paraformaldehyde at 4°C overnight with gentle shaking.

- Embryos were then washed in PBS 3x 5mins, before being dehydrated into 100% methanol by 3x 5min washes.
- Embryos were then rehydrated through a methanol series of 75%, 50%, 25% methanol in PBS, with 5min washes in each.
- After thorough washing in PBTw (0.1% Tween20 in PBS) embryos were incubated in hybridisation buffer (hyb) for 3-6hrs at 65°C.
- Then probes diluted in prewarmed hybridization buffer were added to the embryos, and left overnight at 65°C.
- The following day embryos were washed in the following solutions:

  5mins in 66% hyb mix, 33% 2x SSC at 65˚C

  5mins in 33% hyb mix, 66% 2x SSC at 65˚C

  5mins in 2x SSC at 65˚C

  20mins in 0.2x SSC +0.1% Tween-20 at 65˚C

  2 x 20mins in 0.1x SSC +0.1% Tween-20 at 65˚C (high stringency)

  5mins in 66% 0.2x SSC at +33% PBST at room temp

  5mins in 33% 0.2x SSC at +66% PBST at room temp

  5mins in PBST at room temp
- Embryos were put in blocking solution (PBST plus 5% sheep serum) for 2hrs at room temperature then the anti-DIG antibody (1:3000) was added to the embryos and left overnight at 4°C with gentle shaking.
- The next day embryos were washed with colouration buffer (to control the pH) and then the staining was revealed using NBT/BCIP. Embryos were kept in the dark at room temp until the blue staining was visible.
- The reaction was stopped by washing in PBS and fixing again for 20mins in PFA 4%.
- Finally embryos were dehydrated and then rehydrated in methanol and stored in 70% glycerol.

Probes used were dlx3 (1µg/ml), and pax2a (0.5µg/ml).

Counter-staining of whole-mount embryos

For particular experiments it was necessary to visualise the tissue structure of the brain in fixed specimens. To do this, embryos were incubated in nucleic acid stains To-Pro-3, Sytox green or Sytox orange for 1 hour after whole mount immunohistochemistry.
To-Pro (far red fluorescence, dilution 1:1000, T3605, Invitrogen).
Sytox green (green fluorescence, dilution 1:5000, S7020, Invitrogen).
Sytox orange (red fluorescence, dilution 1:5000, S11368, Invitrogen).

Confocal microscopy

Mounting

Embryos were mounted in 1.5% low melting point agarose (A9414, Sigma) in a chamber slide, which was placed in a large petri dish filled with embryo medium. Live embryos older than 18hpf were anaesthetized with tricaine/MS-222 (E102521, Sigma) using approximately a 1:20 dilution of the stock solution made according to the protocol in The Zebrafish Book. For dorsal view imaging, embryos were oriented with the area of interest uppermost, or for transverse view imaging embryos were mounted with the area of interest at the "equator" of the embryo.

Imaging

Embryos were imaged on a Leica SP2 or SP5 confocal microscope (Leica, GmBH Heidelberg, Germany), using a 20x, 40x or 63x long-working distance water immersion objective. For live imaging, a heated environmental chamber was used set at 28.5°C. For time-lapse imaging of neurulation, z-stacks of 10-20 sections covering a depth of 50-100µm were taken through the neural primordium every 5-10 minutes for approximately 8 hours.

Image Analysis

Raw confocal data was exported to ImageJ (NIH, http://rsbweb.nih.gov/ij/) for analysis. All images were compiled and analysed in ImageJ and Adobe Photoshop. Images were enhanced for presentation by adjustments of levels, brightness and contrast, and colour balance and saturation. Projections of a z-stack of images were maximum projections unless otherwise indicated. Numerical analysis was carried out in Microsoft Excel. Figures were constructed in Adobe Illustrator.

CHAPTER 3 DELAYING CONVERGENCE OF THE WILD-TYPE NEURAL PLATE BY SURGICAL SEPARATION GENERATES NEURAL TUBE DUPLICATIONS

3.1 INTRODUCTION

This chapter tests the hypothesis that ectopic mirror-symmetric divisions generated by delayed convergence of the neural plate are the primary cause of neural tube duplications in planar cell polarity (PCP) mutant embryos. This is in contrast to other work that has previously suggested that the phenotype of PCP mutants is caused by defective contralateral cell intercalation during neurulation (Ciruna *et al.* 2006).

Cell division and apico-basal polarity during zebrafish neurulation

A schematic illustrating the morphogenesis of zebrafish neurulation is shown in figure 3.1A. The neural plate first converges towards the midline and invaginates. During keel and rod stages, the cells undergo a specialized cell division at the midline and one daughter cell is deposited on each side of the midline (fig 3.1B). Once cells have undergone this division, a midline seam forms and the lumen of the neural tube opens shortly afterwards.

In zebrafish, the neural plate is not a conventional epithelium, as cells do not have well-defined apico-basal polarity. This is only established during neural keel stages when the two halves of the neural plate meet at the midline and many proteins that usually localise close to the apical ends of cells within an epithelium such as aPKC, Pard3, Par6, ZO-1, Nok and Lin7c all become enriched at the midline (Geldmacher-Voss *et al.* 2003; Tawk *et al.* 2007; Munson *et al.* 2008; Yang *et al.* 2009). By rod and tube stages, all these proteins become localised to the apical ends of neuroepithelial cells at the midline (Geldmacher-Voss *et al.* 2003; Tawk *et al.* 2007; Munson *et al.* 2008; Yang *et al.* 2009). The acquisition of apico-basal polarity happens coincidentally as with cell division as Pard3-GFP localises to the cleavage furrow, or later to the abscission plane, of cells undergoing C-division (Tawk *et al.* 2007). Pard3-GFP remains at the medial ends of the two daughter cells as they elongate across opposite sides of the neural rod and the two daughter cells therefore acquire mirror image polarity with respect to each other (fig 3.1C). Thus the midline crossing division itself orchestrates the establishment of apico-basal polarity during neurulation.

Figure 3.1. The midline crossing or C-division during neurulation generates daughter cells with mirror-image apico-basal polarity.

A) Schematic of neurulation in transverse view illustrating how the neural plate converges towards the midline to form a keel, then solid neural rod, and finally cavitates to give a tube. At keel stages, cells divide close to the midline and one daughter cell crosses to the contralateral side to form bilateral pairs of cells across the neural rod.

B) The midline crossing behaviour is shown in more detail in this time-lapse sequence of a cell labeled with membrane-GFP and H2B-RFP. Before dividing the cell is stretched past the midline of the neural rod, but it rounds up to divide at the midline with a parallel cleavage orientation with respect to the future midline (dotted lines). The medial daughter cell crosses the midline, stretches to extend the whole width of one side of the neural rod, and maintains contact with its sister cell.

C) Time-lapse sequence of a cells undergoing C-division and mirror-symmetrically inheriting Pard3-GFP. Before and during early mitosis Pard3-GFP is localised diffusely in the cytoplasm of cells. However in the late stages of mitosis (t=15min), Pard3-GFP becomes localised to the abscission plane between the two sister cells (arrowheads) as they separate, giving cells with mirror-image polarity.

In both time-lapses time points are relative to start of mitosis, yellow dots indicate the edges of the neural rod and the midline is shown by dotted lines. Images courtesy of Jon Clarke (A,C) and Una Ren (B).

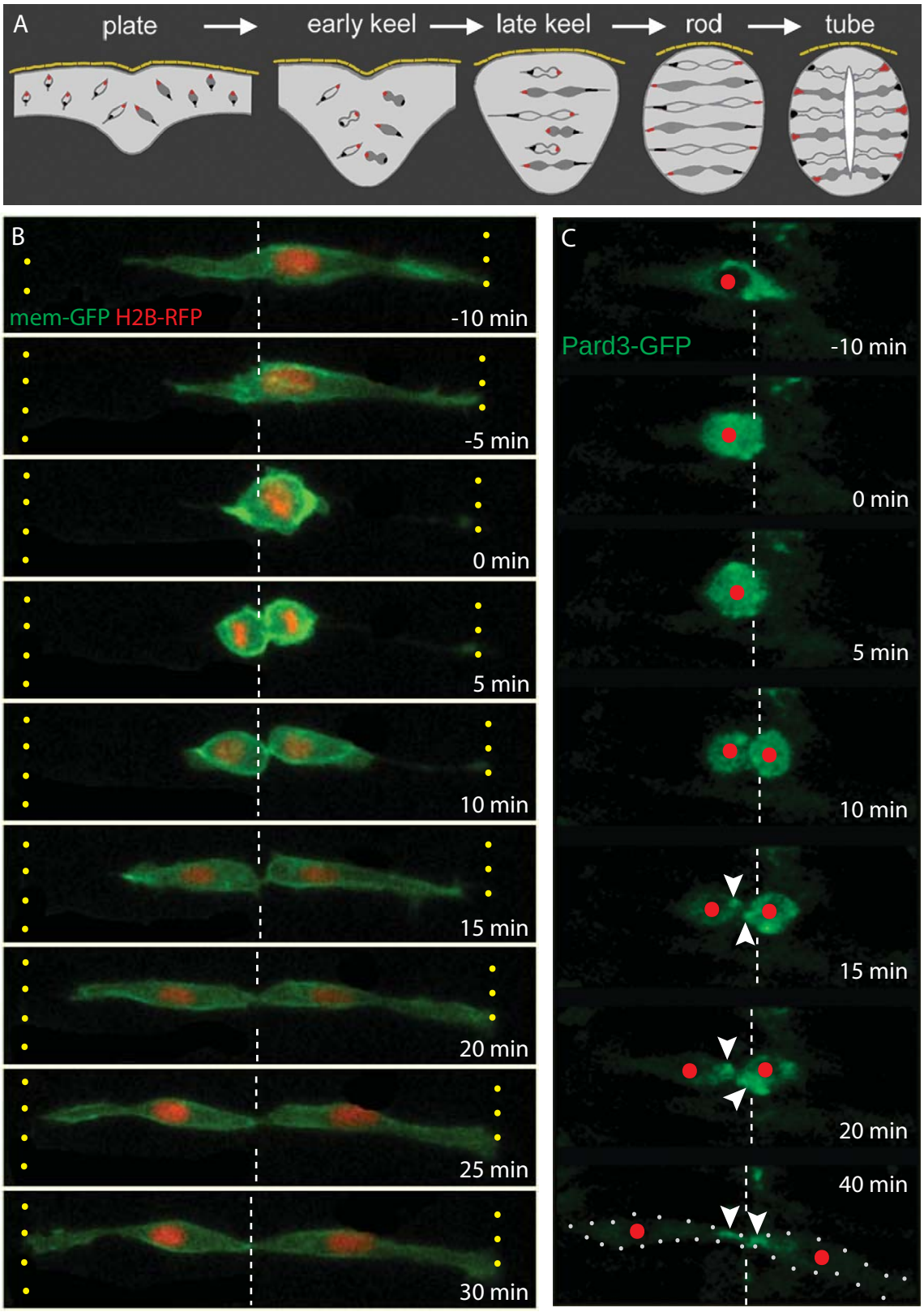

Figure 3.1. The midline crossing or C-division during neurulation generates daughter cells with mirror-image apico-basal polarity.

The occurrence of C-divisions must be tightly regulated to occur at a specific time and in a specific place during neurulation. One could imagine that if these divisions occurred far away from the midline, or with the wrong orientation, then cells might be unable to cross to the other side, and this could result in abnormal neural tube development. The Clarke lab and others have studied the importance of coupling cell division to the morphogenetic movements of neurulation in PCP signalling mutants.

The non-canonical Wnt PCP signalling pathway

The non-canonical Wnt PCP signalling pathway has been shown to be important for several processes during embryogenesis both in invertebrates and vertebrates. The pathway was initially discovered in *Drosophila*, when several mutants were identified that displayed disrupted hair cuticle and bristle orientation (Gubb *et al.* 1982). Since this initial paper, a group of genes has been identified which form a signalling pathway (the Wnt PCP pathway) that coordinates the pattern and polarity of cells within an epithelium with respect to each other and the body axes (Strutt *et al.* 2005; Jenny *et al.* 2006; Wang *et al.* 2007). In *Drosophila*, PCP signalling controls the local orientation of wing hairs in the pupa and adult (Wong *et al.* 1993; Adler *et al.* 1998) and controls the chirality of ommatidia in the eye (Zheng *et al.* 1995; Wolff *et al.* 1998). Similarly, in vertebrates, PCP components are involved in pattern formation, as they are required for hair bundle orientation in the mouse inner ear (Curtin *et al.* 2003; Wang *et al.* 2006), and for hair follicle orientation in skin (Devenport *et al.* 2008).

PCP signalling not only helps to organise cells or groups of cells with respect to each other, but it also plays important roles during morphogenesis. In vertebrates it has been suggested that it contributes to morphogenesis by controlling cell division orientation in the gastrulating zebrafish embryo (Gong *et al.* 2004). It is involved in the shaping and packing of cells in the *Drosophila* wing epithelium (Classen *et al.* 2005). Lastly, and most relevant to this thesis, PCP genes are necessary for coordinating cell movements within whole tissues, by directing convergence and extension during vertebrate gastrulation, neurulation and organogenesis (Tada *et al.* 2009). These convergence and extension movements are characterized by medial migration and intercalation of cells with their neighbours. Many different cell types undergo convergent extension movements including mesodermal cells during gastrulation, neural progenitors during neurulation (Wada *et al.* 2009), and ear precursors during organ of corti formation (Wang *et al.* 2005b). When a number of PCP genes, such as *vangl2*, *frizzled*, *scribble*, *flamingo*, *dishevelled* and *prickle*, are mutated, embryos are much shorter than normal, and directed

cell migration during gastrulation is disrupted (Tada *et al.* 2009). The zebrafish *vangl2* mutant is called *trilobite* (*tri*), and this has been studied in detail to elucidate the roles for PCP signalling in embryogenesis, in particular during neurulation.

Background to the *trilobite* mutant

The *tri* mutant was discovered in a screen for gastrulation defects. *tri* embryos are characterized by convergent extension defects during gastrulation (Jessen *et al.* 2002; Park *et al.* 2002), which persist during neurulation, causing the neural plate to converge more slowly than normal towards the midline (Sepich *et al.* 2000). This loss of PCP Wnt signalling also produces dramatic abnormal neural tube morphogenesis (Ciruna *et al.* 2006; Tawk *et al.* 2007). The two studies of Ciruna *et al* and Tawk *et al* examined the neurulation defects in detail, and produced some similar data, although the interpretation of this data was different in several important ways. These differences are outlined below.

The MZ*tri* and *Ztri* phenotypes

In the early stages of neurulation the neural primordium of *tri* embryos is wider than that of wild-type embryos in both studies (fig 3.2A-D). By the end of neurulation, the MZ*tri* neural primordium is still wider than wild-type, but it also displays an abnormal structure (fig 3.2E-G). Ciruna *et al* describe the structure as "*an outer pseudo-stratified neuroepithelial layer surrounding an ectopic mass of disorganized cells*" (fig 3.2F). However in Tawk *et al*, the central core of the Z*tri* mutant does not look so organised (fig 3.2G). When the structure of the primordium was analysed further using antibodies against apical protein aPKC and the basal marker GFAP, Tawk *et al* showed that the Z*tri* primordium has two apical midlines (fig 3.2J) compared to the single midline of a wild-type neural tube (fig 3.2H), and that the Z*tri* neural primordium consists of duplicated neural tubes, side by side (compare fig 3.2I to K). Upon further inspection of the MZ*tri* neural primordium the central mass of cells also does not look disorganised (fig 3.2L); rather the neuroepithelium has clear interfaces between the layers of the neuroepithelium (arrow heads in fig 3.2L), which look similar to the bilateral interfaces of the Z*tri* primordium (arrowheads in fig 3.2G). Therefore the MZ*tri* mutant also appears to have duplications of the neuroepithelium, that are similar to the duplications of Z*tri* embryos.

The role of PCP and cell division in *tri* mutants is disputed

Ciruna *et al* examined the neurulation abnormalities at the cellular level by time-lapse microscopy. They made the important observation that cell division has a critical role in generating the MZ*tri* phenotype. Although cells still underwent division, the behaviour of

Figure 3.2. The neural tube defects in MZ*tri* and Z*tri* are similar.

Transverse views of the neural primordium of wild-type and *tri* embryos at different stages of neurulation adapted from Ciruna *et al* (A,B,E,F,L) and Tawk *et al* (C,D,G-L).

A) A section at spinal cord level through the neural keel at 14hpf of a wild-type embryo.

B) The neural keel of MZ*tri* mutants is wider compared to wild-type embryos of the same age (compare to A).

C) A section through the neural keel of a wide type at posterior hindbrain level at 14hpf.

D) The neural keel of Z*tri* mutants is also wider compared to wild-type embryos (compare to B)

E) The neural rod of a wild-type embryo at 19hpf has a single midline surface.

F) By 19hpf, the neural primordium of *tri* mutants is abnormal in structure with a disorganized central core of cells.

G) The Z*tri* neural primordium also has an abnormal structure at 18hpf, although the central mass of tissue appears to be more organised.

H) At 24hpf, aPKC localises to a single apical midline (red arrow) in the wild-type neural tube.

I) GFAP highlights the basal edges of the neural tube in a wild-type embryo (yellow arrows).

J) aPKC labelling in a section of the Z*tri* neural primordium at 24hpf reveals two apical surfaces (two red arrows) either side of the embryonic midline.

K) GFAP labeling of the Z*tri* neural primordium from reveals duplicated neural tubes, side by side (four yellow arrows in L compared to 2 arrows in I).

L) Re-examination of a different section of the MZ*tri* mutant primordium suggests that the structure is remarkably similar to Z*tri,* with duplicated neural tubes and two apical surfaces (yellow arrowheads, compare to J and K).

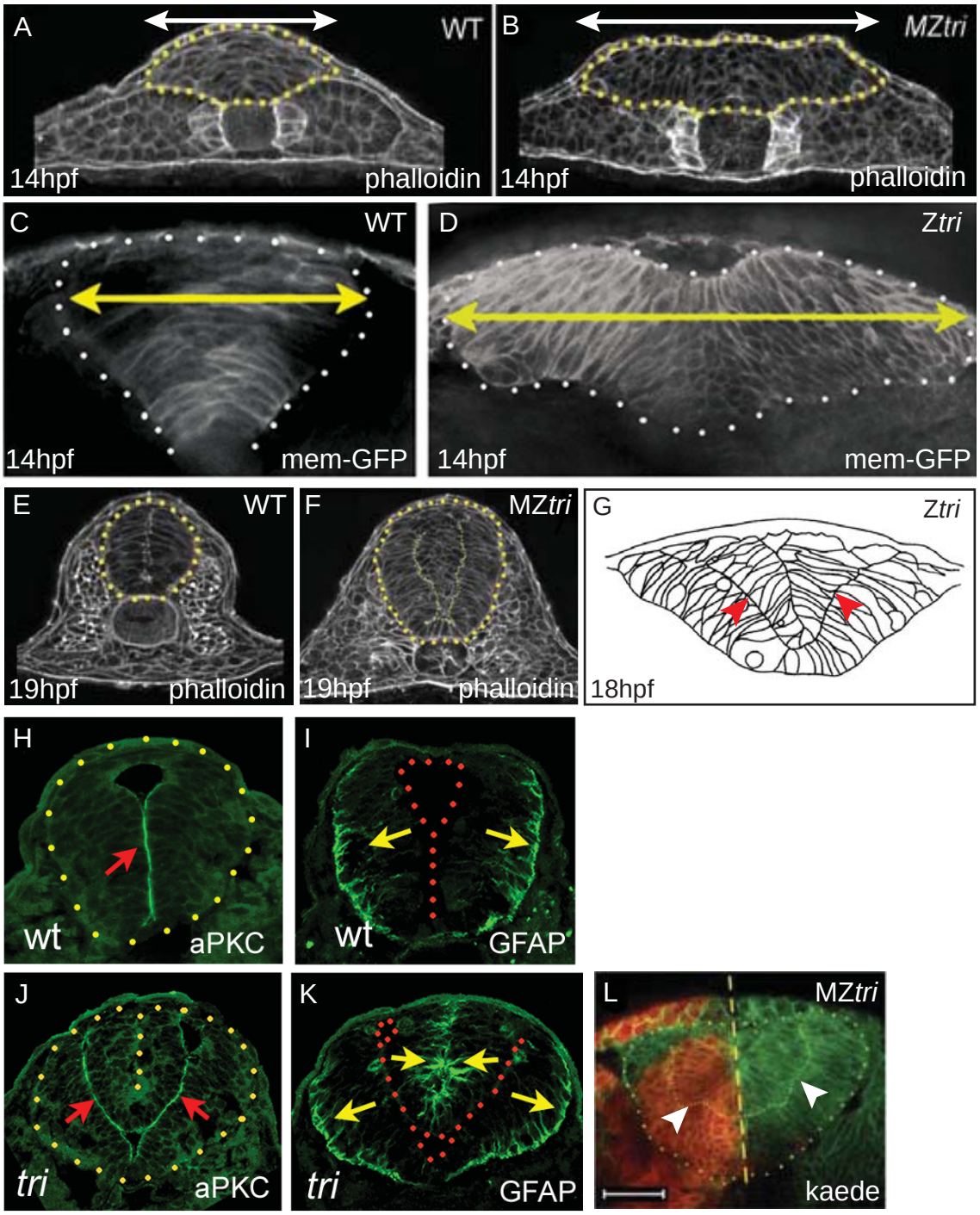

Figure 3.2. The neural tube defects in MZ*tri* and Z*tri* are similar.

daughter cells after division was abnormal. In wild-type embryos, the medial daughter crosses the midline and integrates into the contralateral side of the neural rod, resulting in bilateral pairs of cells (fig 3.1B). However in MZ*tri* embryos, cells did not cross the embryonic midline after division, and remained where they were formed on the same side of the neural primordium (fig 3.3A). Ciruna *et al* believed that these daughter cells accumulated outside of the neuroepithelium and formed the "ectopic mass" in the middle of the neural primordium seen in fig 3.2F. Thus they report that MZ*tri* cells fail to reintegrate into the neuroepithelium after mitosis (Ciruna *et al.* 2006).

At first this seems to be a reasonable argument, but on closer inspection of the data, the behaviour of cells and the tissue organisation in their figures does not match their description of events, even in wild-type embryos. For example, during neurulation, Ciruna *et al* write that *"cells divide apically and position daughter cells outside the neuroepithelium"*. However cells never appear to leave the neural primordium when dividing, they just round up within the tissue. They then claim that both daughter cells must reinsert into the neuroepithelium after division. In time-lapse analysis of cell division in MZ*tri* embryos, the daughter cell that is described as failing to reintegrate into the neuroepithelium (arrowhead in fig 3.3A), does not appear to be located outside the neural tissue. It is true that this daughter cell is ectopic in the sense that it remains on the same side of the embryonic midline and fails to intercalate into the contralateral side of the neuroepithelium, but only if the embryonic midline is considered to be the apical midline.

Finally, Ciruna *et al* attempted to relate these "intercalation" defects with cell polarity during neurulation. They looked at the subcellular localisation of PCP components, namely GFP-tagged Prickle (Pk). They found that GFP-Pk puncta were asymmetrically biased towards the anterior sides of neural cells. This polarity was lost during division and then re-established, and importantly, was absent in MZ*tri*. They attempted to link this apparent loss of antero-posterior PCP in MZ*tri* with the defects in medio-lateral cell intercalative behaviour by claiming that PCP components are required to repolarise cells after division, and then for directing cell reintegration. However they did not test if there is a causal relationship between these two events, and the relationship between polarity in the two different axes is unclear. In our lab, we studied proteins important for polarity in the apico-basal axis, and found that the *tri* defects can be explained in a different way (Tawk *et al.* 2007).

In our study the localisation of the Pard3-GFP fusion protein was imaged during

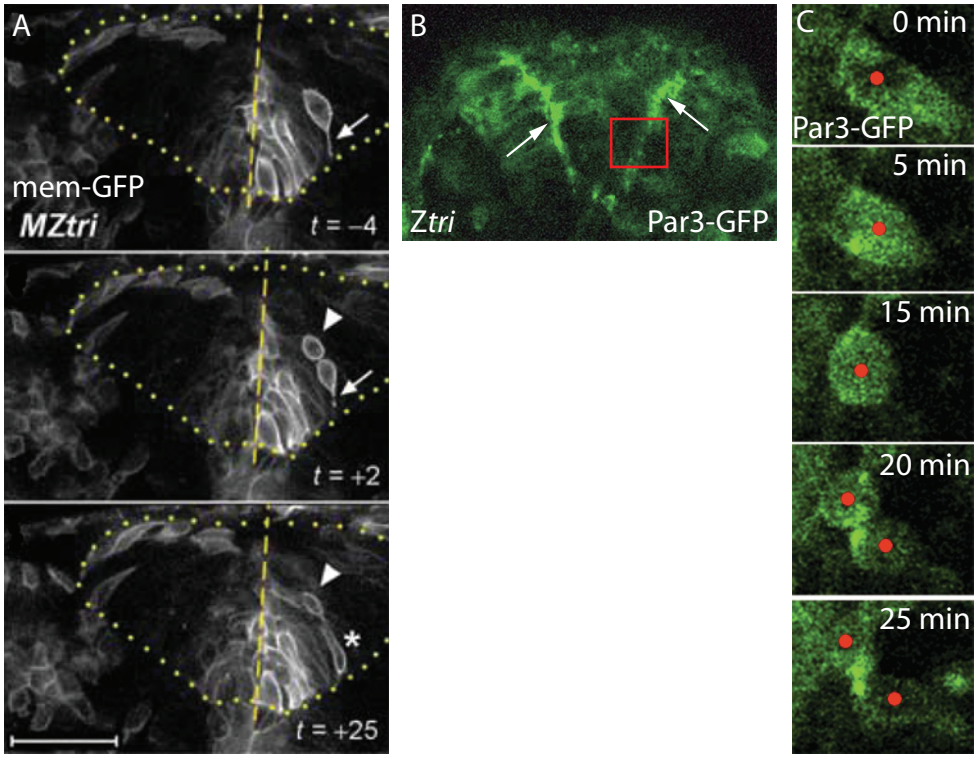

Figure 3.3. MZ*tri* and Z*tri* mutants both show ectopic cell divisions.

A) A time-lapse sequence from the MZtri mutant (Ciruna *et al*. 2006), showing a cell dividing in an ectopic location (arrow). The medial daughter cell (arrowhead in A) does not cross the midline by t=25.
B) A confocal section through the Ztri neural primordium at 18hpf reveals that Pard3 is localised to the two ectopic apical midlines (arrows in B, Tawk *et al*., 2007).
C) A confocal micrograph time-lapse sequence of cell division from the boxed area in B shows that Pard3 is mirror-symmetrically inherited during this ectopic cell division (Tawk *et al*. 2007). The cell division orientation is similar to the sequence in A, and the medial daughter cell also does not cross the midline by 25min after division.
Figure A adapted from Ciruna *et al*, (2006)
Figures B and C adapted from Tawk *et al*, (2007)

neurulation by time-lapse microscopy. We found that in wild-type embryos, cells establish apico-basal polarity as they undergo the midline-crossing division by mirror-symmetrically inheriting Pard3-GFP. As the two daughter cells extend equally across their respective side of the neural rod and Pard3-GFP is targeted to the medial ends of each cell, this positions the apical proteins at the embryonic midline. The coordination of many cells undergoing mirror-symmetric division in the neural rod creates two columns of cells, with the apical surfaces of the neuroepithelia located at the midline of the rod (Tawk *et al.* 2007). We found that in *tri* mutants, neural cells divided in ectopic locations, halfway between superficial and deep surfaces of the delayed neural plate, in the same location that the ectopic apical surfaces later form (fig 3.3B). Moreover these ectopic divisions were mirror-symmetric divisions (fig 3.3C), which led to ectopic apical surfaces and duplicated neural tubes forming.

If the observations of cell division and daughter cell behaviour described in Tawk *et al* are compared to those in Ciruna *et al*, they are almost identical (fig 3.3); it is just the interpretation that is different. Ciruna *et al* favour the hypothesis that the superficial-most daughter cells is extruded from the neuroepithelium and cannot reintegrate. In contrast, Tawk *et al* show that the superficial most daughter is not placed outside the neuroepithelium, but that it crosses the ectopic prospective apical surface, located halfway between superficial and deep surfaces of the neural primordium. Interestingly both studies show that the process of cell division is required for the neural defects, by observing rescue of the phenotype when cell division is blocked during neurulation. However, both proposed mechanisms have cell division as a central feature, so this experiment does not distinguish between either of the two proposed mechanisms.

3.2 AIM

In an attempt to solve this confusion of whether the neural defects seen in *tri* embryos are caused only by the convergence delay, or if loss of cell polarity and intercalation are the main defects, the aim of this chapter was to test if delaying tissue convergence in wild-type tissue results in neural tube duplications.
If duplications arise in an identical way to Z*tri* embryos, this would show that defective PCP signalling is not required to generate the duplication phenotype. It would strongly suggest that delayed convergence during neurulation is the principle cause of the neural tube defects in *tri* embryos, as Tawk *et al* propose. If neural tube duplications do not occur, this would indicate that reducing Wnt PCP signalling may disrupt processes other than convergence, such as cell intercalation and reintegration, as Ciruna *et al* propose.

3.3 METHODS

Surgical Separation of the brain down the midline

Wild-type embryos at neural plate stage (1somite, 10hpf) were mounted in low melting point agarose to immobilise the embryo. The embryos were oriented so that the first somite was facing up, in the middle of the embryo (embryo outline shows dorsal view in fig 3.4A). To separate the left side of the neural plate from the right, the neural plate was cut down the midline using a tungsten needle at midbrain, hindbrain or anterior spinal cord levels. The two sides of the neural plate come apart immediately after cutting, and effective separation was confirmed by observing yolk cells spill out from the wound (fig 3.4B). The embryos were left in the agarose at room temperature for about 30mins to help healing, and then incubated at 28.5°C. The embryos were either incubated overnight for assessment at the end of neurulation, or removed from the agarose after the wound had healed sufficiently so that yolk no longer was escaping, and remounted for time-lapse imaging. If incubated overnight, in the morning the embryos were released from the agarose and left to develop further for a few hours before imaging. I refer to embryos that have undergone this procedure as split-brain embryos.

In some experiments cell division was blocked after surgical separation of the neural tube by incubating embryos in embryo medium containing aphidicolin (100μM, from stock solution 1mg/ml in DMSO, Sigma) and hydroxyurea (20mM, Sigma).

In situ hybridisation

The standard *in situ* protocol was followed and the following probes and their concentration used in this chapter were:
dlx3 at 1μg/μl.
pax2a at 0.5μg/μl.

Convergence analysis

Convergence was analysed by measuring the distance between the two bands of *pax2a* and *dlx3* expression to give the width of the neural plate in wild-type and split-brain embryos at three different stages during early neurulation: 3 somites, 5 somites and 7 somites.

Antibodies used in this chapter

The standard immunohistochemistry protocol was followed, and the following primary antibodies and dilutions were used:
Anti ZO-1 at 1:500 (Zymed)
Anti GFAP at 1:300 (Dako, Z0344)
Anti phospho-histone H3 at 1:500 (Millipore, 06-570)

Kaede photoconversion

Embryos were injected at 1cell stage with Kaede mRNA for ubiquitous labelling. At 10hpf embryos were dechorionated, and mounted in agarose, with the neural plate facing up. The Kaede fluorophore was converted from green to red (Ando *et al.* 2002) by exposing one side of the embryo to UV light using a 10X objective on an epifluorescence Zeiss microscope. The neural plate was then subject to surgical separation down the midline, and the embryo left to develop overnight.

Confocal and time-lapse imaging

All confocal images in this chapter were acquired using an SP2 Leica laser scanning confocal microscope. Fixed antibody stained embryos were mounted in a dorsal view, and a stack of z-slices through the neural tissue was collected with a z-depth interval of 2-5µm. For time-lapse imaging, embryos were mounted for dorsal or transverse views through the neural tissue, and a z-stack of approximately 10 z-levels at 5-10µm intervals was captured every 5-7minutes.

Image processing

Fixed and time-lapse images were processed as described in the general methods using ImageJ. Transverse reconstructions of whole-mount immunostained embryos were carried out from a dorsal view stack of z-slices taken at 0.5-1µm intervals. The reconstruction was performed using the reslice command in ImageJ.

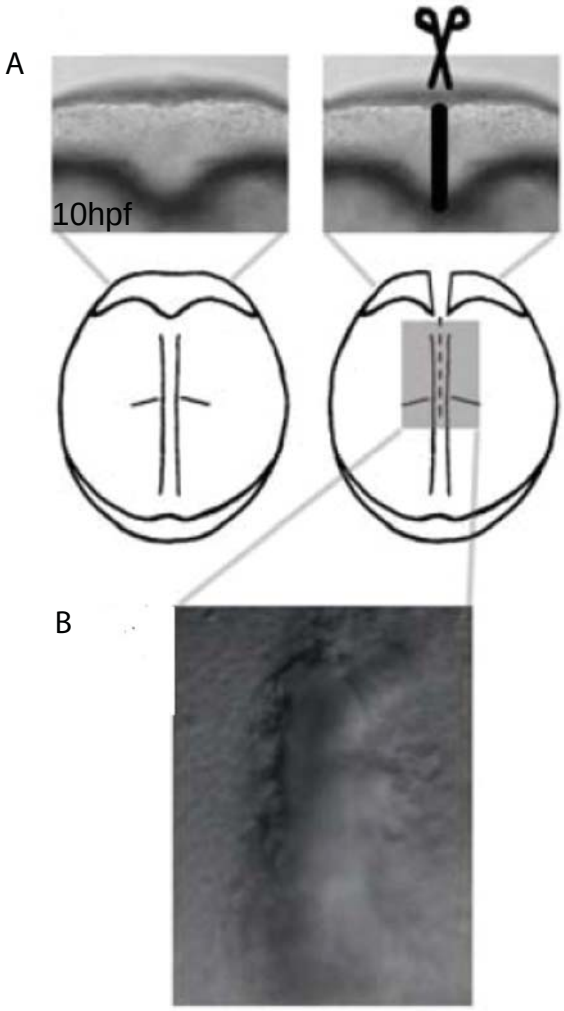

Figure 3.4. Schematic llustrating the technique for surgical separation of the neural plate in split-brain embryos.

A) At 10hpf, the neural plate was cut down the midline, at approximately the level of the first somite.
B) The tissues come apart immediately after cutting and yolk cells often spill out of the wound, ensuring that the cut extended through the whole depth of the neural plate.

3.4 RESULTS

The development of twinned neural tubes during zebrafish neurulation has only been reported in genetically mutant embryos that demonstrate delayed convergence (Tawk *et al.* 2007). If neural tube duplication is simply caused by delayed convergence, and does not result from loss of polarity after cell division and subsequent lack of cell intercalation as previously suggested (Ciruna *et al.* 2006), then delaying convergence in wild-type embryos should cause the same duplication phenotype. To test this hypothesis, we surgically divided the neural plate down the midline (fig 3.4). These embryos are subsequently referred to as split-brain embryos.

Tissue movements towards the midline are delayed in split-brain embryos.

The aim of the experiment to surgically divide the neural plate in half was to slow convergence of the neural plate towards the midline by creating a large wound in the centre of the neural tissue. I verified that convergence was delayed by assessing the width of the neural plate in split-brain embryos at different stages during neurulation, and compared it to the width of uncut wild-type embryos of the same age. The width of the neural plate was marked by *pax2a* and *dlx3* mRNA expression (Akimenko *et al.* 1994). As expected, the width of the neural plate decreases as neurulation progresses in both wt and split-brain embryos (figs 3.5A-F), as cells converge towards the midline. However when the progress of convergence between uncut and split-brain embryos is compared, it is evident that convergence is impaired in split-brain embryos. One hour after cutting (at 3somites), the neural plate width is slightly larger in split-brain embryos than wild-type (compare fig 3.5B to C), but by 2 hours after cutting (at 5somites), split-brain embryos have a much wider neural plate than uncut embryos (compare fig 3.5D to E). This wider neural plate of split-brain embryos remains at early neural keel stages (3hrs after cutting, or 7S, compare fig 3.6F to 3.6G), showing that convergence of the neural tissue towards the midline during neurulation is slower in split-brain embryos than in uncut embryos.

When the width of the neural plate in the experiment above was measured at the level of the otic vesicles in several different embryos (fig 3.5H), it was found to be quite variable in split-brain embryos. The variability in width could be explained by inconsistency in the size or location of the cut. If a small cut was made, then perhaps the wound heals quickly and the delay in convergence is minimal. Nonetheless the average width of the neural

Figure 3.5. Split-brain embryos have delayed convergence of the neural plate.

(A-G) Dorsal views of zebrafish embryos during the early stages of neurulation. To visualize convergent extension defects embryos were stained with *dlx3* (neural plate border and otic placodes, OP) and *pax2a* (midbrain hindbrain boundary, MHB) by *in situ* hybridisation. In all pictures double-ended arrows indicate the width of the neural primordium. Scale bar in A is 200μm. In all images anterior is up. WT indicates a wild-type embryo.

A) WT embryo at 1 somite stage (10.5hpf), has a wide neural plate at the beginning of neurulation. Surgical separation was carried out at this time.

B) WT embryo at 3 somites (11.5hpf), showing that the neural plate has decreased in width.

C) Split-brain embryo at 3 somites showing that the neural plate is wider than wild-type (B).

D) The neural tissue of a WT embryo at 5 somites (12.5hpf) has converged towards the midline and decreased in width (compare to B).

E) The neural plate of a split-brain embryo at 5 somites is considerably wider compared to a same age uncut WT embryo (compare to D).

F) During neural keel formation (7 somites, 12.5hpf), the neural primordium has continued to decrease in width.

G) At 7 somites, the neural primordium of split-brain embryo has hardly converged towards the midline, and remains much wider than an uncut embryo (compare to F).

H) The graph shows the average neural plate width of several uncut WT or split-brain embryos over time. At all time points the width of the neural plate in split-brain embryos is wider compared to uncut embryos. By 7somites the uncut embryo neural keel has converged to 135μm, whereas the split-brain width is still 200μm, showing that convergence is delayed. Error bars show the standard deviation.

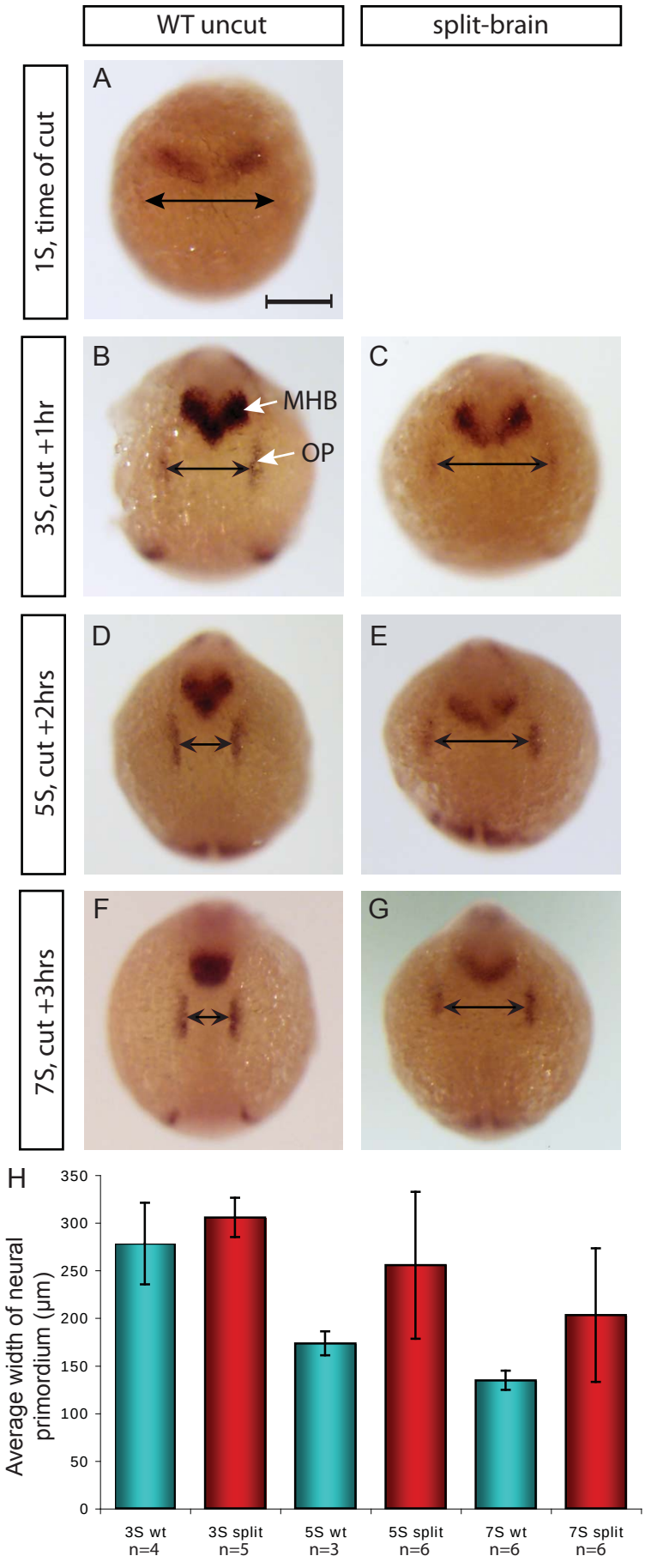

Figure 3.5. Split-brain embryos have delayed convergence of the neural plate.

primordium in split-brain embryos was still considerably larger in both 5S and 7S stage split-brain embryos (fig 3.5H), showing that the surgical cutting technique delays convergence effectively, and is a suitable technique for testing our hypothesis.

Splitting the wild-type neural plate down the midline generates duplicated neural tubes.

Analysis of split-brain embryos at 28hpf shows that surgical intervention efficiently generates the duplicated neural tube phenotype characteristic of *trilobite*/*vangl2* mutant embryos (fig 3.6). The extent of duplication varied between embryos possibly explained by the variation in the delay in convergence. In 22 out of 30 split-brain embryos, twinned neural tubes were evident for a considerable length of the hindbrain (fig 3.6A). Five out of thirty embryos had smaller islands or bridges of tissue, which likely represent a small duplication caused by a slight delay in convergence (fig 3.6B). Only 3 out of 30 split-brain embryos did not show a duplication phenotype (fig 3.6C). There were a couple of differences in the nature of the split-brain duplications compared to *trilobite*. In *tri* embryos the duplication is often present in the more dorsal region of the primordium not in the very ventral region (fig 3.2E,F) and the ventricles join in the ventral part, to give a V or Y-shaped ventricle (illustrated in the transverse schematic diagram of fig 3.6D). Similar duplications did occur in some split-brain embryos, as the duplication was evident in the dorsal focus (fig 3.6E), but not in the ventricle focus where a single midline ventricle was present (fig 3.6F). However most split-brain embryos showed a complete duplication in the dorso-ventral axis, illustrated in transverse section in the schematic diagram (fig 3.6G). This more severe duplication in split-brain embryos compared to *tri* embryos is probably because split-brain embryos have a greater convergence delay than *tri* mutants.

Another notable difference in the duplications between *tri* and split-brain embryos is that *tri* embryos only show duplications in the posterior hindbrain and anterior spinal cord, whereas in split-brain embryos, duplications can extend into the anterior hindbrain, and even as far anterior as the midbrain (fig 3.6G).

The neural tube duplications in split-brain embryos have well-defined apico-basal polarity.

To investigate the organisation of the duplications in split-brain embryos, embryos were immunostained with antibodies for markers of apico-basal polarity, namely ZO-1 (apical) and GFAP (basal). ZO-1 is a component of tight junctions that form at the ventricular side

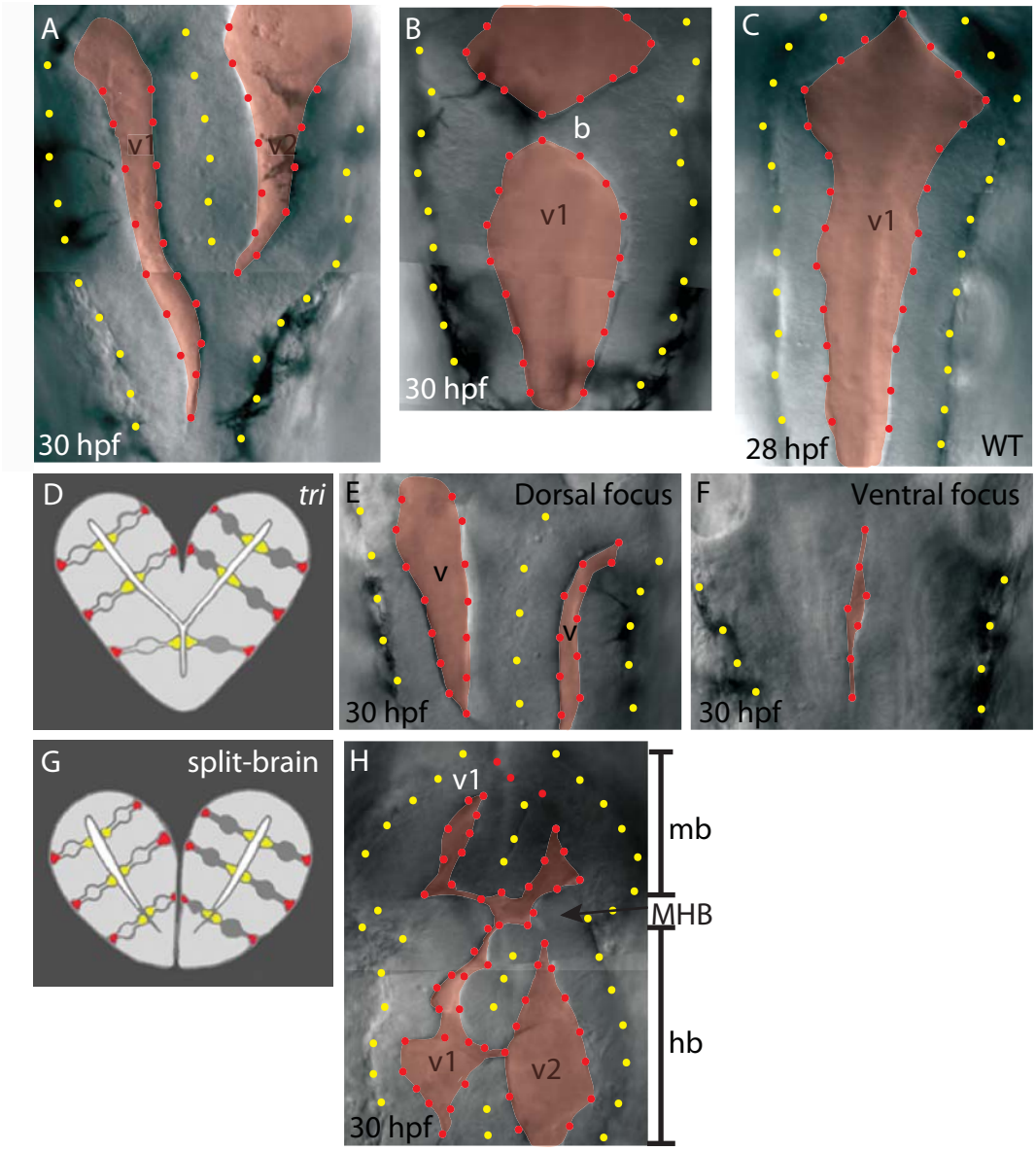

Figure 3.6. Surgical separation of the neural tube down the midline efficiently generates neural tube duplications.

Dorsal view DIC images of split-brain and uncut wild-type embryos with apical surfaces outlined with red dots, basal surfaces with yellow dots, and the ventricles (v) are shaded in red. In all pictures anterior is up.

A) A split-brain embryo with duplicated neural tubes, each tube has its own ventricle (v1 and v2) located on either side of the embryonic midline. This duplication is at the level of the hindbrain as it is posterior to the midbrain hindbrain boundary.

B) A split-brain embryo with an ectopic bridge of tissue spanning across the midline (b).

C) Uncut wild-type embryos always have a single neural tube with a one ventricle at the midline.

D) Schematic diagram of a transverse section of a typical duplication found in *trilobite (tri)* mutant. Observe the Y-shaped ventricle connected at the ventral region.

E) A split-brain embryo showing ventricle duplication in the dorsal region of the embryo.

F) Ventral focus of the same region in (E) showing that the duplication does not extend to the ventral most part of the neural primordium, thus forming a Y-shaped ventricle like *tri* embryos in figure (D).

G) Schematic diagram of a transverse section of a more severe duplication where the neural tubes lie side by side, and each of the duplicated ventricles are completely separate.

H) The duplications in split-brain embryos can extend anteriorly into the midbrain (mb). Midbrain hindbrain boundary (MHB) hindbrain (hb).

of the neuroepithelium (Shin *et al.* 2006), and GFAP is expressed in the basal (outer) endfeet of radial glial cells in the neuroepithelium (Tawk *et al.* 2007). GFAP and ZO-1 staining of an uncut embryo in dorsal view at 24hpf, reveals that the single neural has well-organised apico-basal polarity with GFAP highlighting the two basal edges of the tube (fig 3.7A), and ZO-1 outlining the single ventricle at the midline (fig 3.7C). In a split-brain embryo, the neuroepithelium still shows well-organised apico-basal polarity, but the GFAP staining reveals that the neural primordium splits into two neural tubes (n=2, fig 3.7B). ZO-1 staining of a split-brain embryo reveals that the ventricle bifurcates (fig 3.7D), and that towards the anterior end of the tissue the neuroepithelium is less organised. This is not surprising given the drastic surgery that split-brain embryos have undergone. Reconstructed transverse sections (fig 3.7E-J) further illustrate that each of the neural tubes in split-brain embryos have normal apico-basal organisation (fig 3.7F,H,J), when compared to the neural tube of an uncut embryo (fig 3.7E,G,I). GFAP staining reveals that in this split-brain embryo the two tubes are completely separate lying side by side (fig 3.7F). A magnified view of ZO-1 staining (indicated by the box in fig3.7H) shows that the two ventricles of split-brain embryos are also completely separate.

Cells do not cross the embryonic midline in regions of neural tube duplication in split-brain embryos

In the analysis of split-brain embryos thus far, the neural tube duplications appear similar to those of *tri* embryos. In MZ*tri* and Z*tri* duplications, cells are unable to cross the embryonic midline, and so each tube of the duplication arises from one side of the neural plate (Ciruna *et al.* 2006; Tawk *et al.* 2007). To see if cells in split-brain embryos also behave similarly and do not cross the midline in the regions of duplication, one side of the neural plate was labelled prior to surgical separation of the neural plate down the midline, and then the distribution of labelled cells was assessed at 30hpf. Unilateral labelling was achieved by converting the Kaede fluorophore from green to red on one side of the neural plate only. The bright field image of a split-brain embryo reveals the neural tube duplication (fig 3.8A), in which the basal (yellow) and apical (red) edges of the neural primordium are outlined. In the region where the neural tube is not split, cells cross the midline as normal, as red cells are present on both sides of the embryonic midline (fig 3.8B,C). However in the region of duplication, (bracket in fig 3.8B), red cells remain on the left side of the embryonic midline (fig 3.8B), only populating the left neural tube of the duplication (fig 3.8C). This failure of wild-type cells to cross the embryonic midline in regions of duplication, argues that the inability of cells to cross the midline in *tri* mutants is not caused by loss of PCP Wnt signalling preventing contralateral intercalation.

Figure 3.7. The neural tube duplications of split-brain embryos have normal apico-basal polarity.

(A-D) Whole mount dorsal view confocal projections of wild-type and split-brain embryos at the level of the hindbrain stained with GFAP (A,B) or ZO-1 (C,D) antibodies. In all pictures anterior is up.

(E-J) Transverse reconstructions were made from confocal z-stacks, at the approximate levels indicated by the dotted lines in A-D.

A) At 24hpf, GFAP is localised at the basal edges of the neural tube of an uncut embryo. Arrows indicate each side of the neural tube.

B) At 30hpf, a split-brain embryo has duplicated mirror-image epithelial organisation where the neural tube has split (compare 4 arrows in B to the 2 arrows in A).

C) In an uncut embryo at 24hpf, ZO-1 outlines the apical or ventricular surface at the midline of the neural tube.

D) The split-brain embryo displays a disorganized neural tube in which two bilateral domains of ZO-1 expression can be seen.

E) GFAP outlines the basal edges of the neural tube in an uncut embryo. v1 indicates one single ventricle.

F) GFAP staining of a split-brain embryo clearly shows two neural tubes lying side-by-side (compare to the single neural tube of E). v1 and v2 indicate duplicated ventricles.

G) The box in this copy of E shows the approximate area of magnification of the ZO-1 transverse reconstruction of the wild-type uncut embryo.

H) The box in this copy of F shows the approximate area of magnification of the ZO-1 reconstruction for the split-brain embryo.

I) ZO-1 outlines the single ventricle (v1) in an uncut embryo.

J) ZO-1 outlines the twinned ventricles of a split-brain embryo (v1 and v2), showing that the duplication has correct apico-basal polarity.

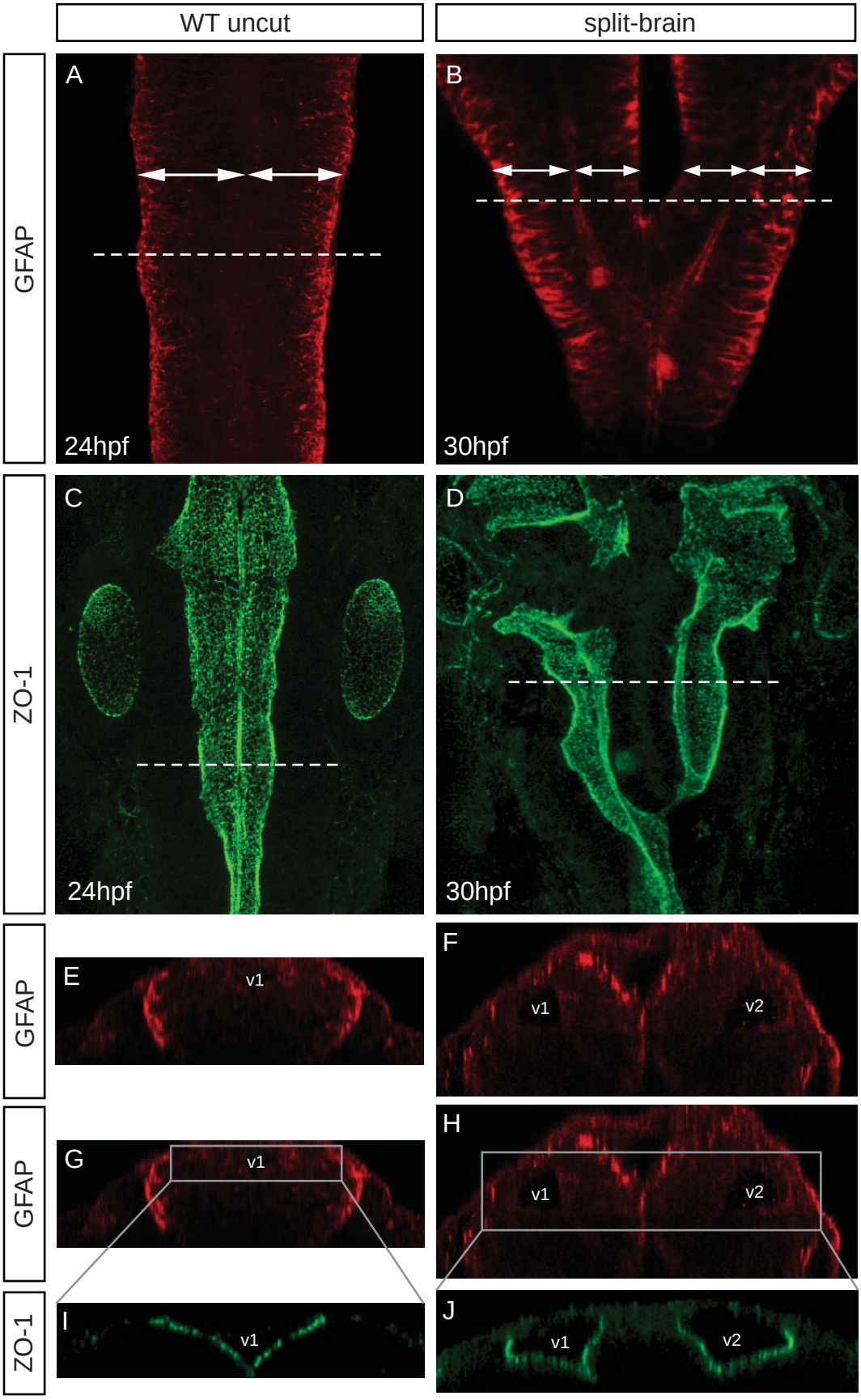

Figure 3.7. The neural tube duplications of split-brain embryos have normal apico-basal polarity.

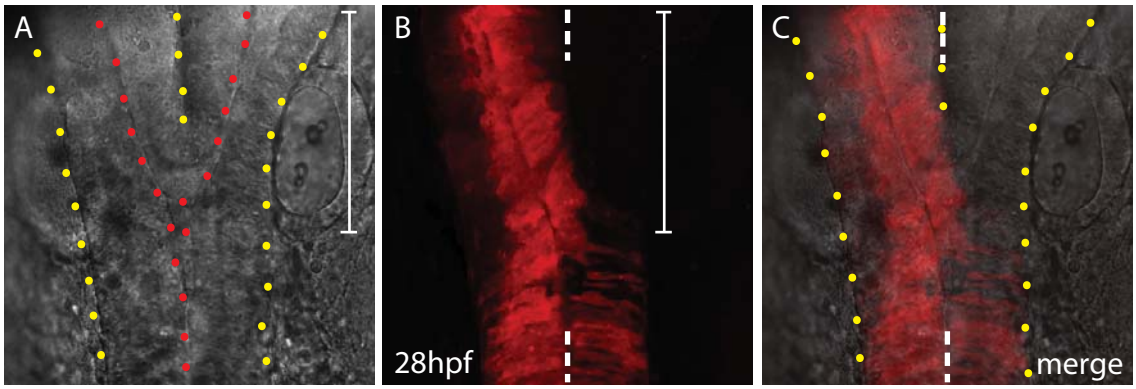

Figure 3.8. Neural progenitor cells in the region of duplication in split-brain embryos cannot cross the embryonic midline.

One side of the neural plate was labelled by photoconverting Kaede from green to red. Then the neural plate was cut down the midline and the resulting split-brain embryo was imaged from a dorsal view at 28hpf. Anterior is up in all images.
A) A bright field image shows that the neural tube shows a duplicated morphology in the anterior hindbrain (bracket in A). Red dots outline the apical surface, yellow dots the basal surface.
B) A confocal projection of neuroepithelial cells labelled with converted Kaede (red) in the same embro shows that red cells are bilaterally distributed where the neural tube is not duplicated. However they only populate the left side of the duplication (bracket indicates duplicated region). White dotted lines indicate the embryonic midline.
C) This merge panel confirms that cells have not crossed the embryonic midline in the region of duplication.

Neural tube duplications arise from ectopic C-divisions

In Tawk *et al*, we proposed that neural tube duplications in *tri* mutants arise from C-divisions occurring in lateral locations and generating ectopic apical midlines. Although we have observed that cells behave similarly regarding midline-crossing in split-brain and *tri* embryos, to confirm that split-brain duplications also result from ectopic C-divisions I examined the localisation of Pard3-GFP in uncut and split-brain embryos. At the end of neurulation (18hpf), wild-type embryos show a single midline localisation of Pard3-GFP (fig 3.9A), whereas split-brain embryos show two domains of Pard3-GFP by 21hpf, sandwiched between the superficial and deep edges of each side of the neural primordium (fig 3.9B). Next we analysed the location and orientations of cell divisions from 15-18hpf (the time when C-divisions normally occur) by time-lapse microscopy, to find out if cell divisions occur in the location where the apical surfaces subsequently form. The typical midline location of cell divisions in an uncut wild-type embryo during keel and rod stages are shown in dorsal view (fig 3.9C), and in the transverse schematic diagram (fig 3.9E). In split-brain embryos the two sides of the neural primordium are completely separated and hence cell divisions do not occur at the embryonic midline, but at the equivalent midline in each side of the split neural primordium (fig 3.9D). These ectopic cell divisions were oriented along the medio-lateral axis (equivalent to the superficial-deep axis) of each side of the neural primordium, illustrated in the transverse schematic diagram of the split-brain neural primordium (fig 3.9F). In this way, the orientation of divisions in each side is reminiscent of the C-divisions that normally occur at the midline in the single neural keel of uncut wt embryos, which also divide with a medio-lateral orientation (compare fig 3.9C with 3.9D).

Analysis of divisions was only possible in one split-brain embryo because following midline separation, embryos were very fragile and often did not survive being removed from the agarose, remounted and then imaged under the confocal microscope. This was true especially for embryos mounted for transverse confocal sections through the cut neural primordium, which is why the embryo analysed was imaged from a dorsal view. Only a few divisions could be analysed on one side of the neural primordium of the embryo shown in figure 3.9D, because cell divisions often did not occur in the plane of the confocal z-stack. Nonetheless, comparison of the positions of divisions (fig 3.9D) and the Pard3 ectopic apical surfaces of the same embryo (fig 3.9G) reveals that cell divisions coincide with Pard3-GFP localisation. Therefore Pard3-GFP localisation was examined in individual cells undergoing cell division by time-lapse microscopy. I found that Pard3-GFP was indeed localised to the abscission plane of dividing cells and remained at the medial

Figure 3.9. Split-brain duplications are caused by ectopic C-divisions

A) A transverse confocal section through a wild-type embryo reveals a single apical midline of Pard3-GFP at 18hpf (arrow).

B) A transverse confocal section through a split-brain embryo at 21hpf reveals bilateral apical localisation of Pard3-GFP (arrows), in contrast to the single midline of an uncut embryo.

C) The location of cell divisions (white dots and lines in C) in uncut embryos at keel and rod stages) is close to the embryonic midline where the apical surface will form. Most cell divisions are oriented in the medio-lateral axis of the neural rod.

D) Cell divisions in a split-brain embryo (white lines in B) are similarly located halfway between the medial and lateral edges of each side of the split primordium, which is outlined in blue dots.

E) Schematic transverse diagram illustrating the positions of cell divisions in a wild-type embryo at the midline of the neural keel.

F) Schematic transverse diagram illustrating the positions of cell divisions in a split-brain embryo.

G) A dorsal view confocal section of the same embryo in D shows that Pard3-GFP is localised halfway between medial and lateral edges of each side of the split neural primordium (white arrows), coinciding with the locations of divisions in D. Where the primordium is not split, Pard3-GFP localises at the apical midline seam at the embryonic midline (arrowhead).

H) A time-lapse sequence of cells dividing in the boxed area in G reveals that daughter cells inherit Pard3-GFP mirror-symmetrically after division. Pard3-GFP is concentrated at the abscission plane of a dividing cell (arrowhead in H at 15mins), and remains localised between the two daughter cells (arrowhead in H at 25mins). Time starts from the beginning of mitosis. Red dots indicate the positions of the nuclei.

(I) By 24hpf, a dorsal view confocal projection of a split-brain embryo clearly shows the continuous Pard3-GFP bilateral midlines (arrows) of the split neural primordium.

Yellow dots outline the basal edges of the neural primordium in A,B,F and H. In dorsal view pictures (C,D,G,I) anterior is up.

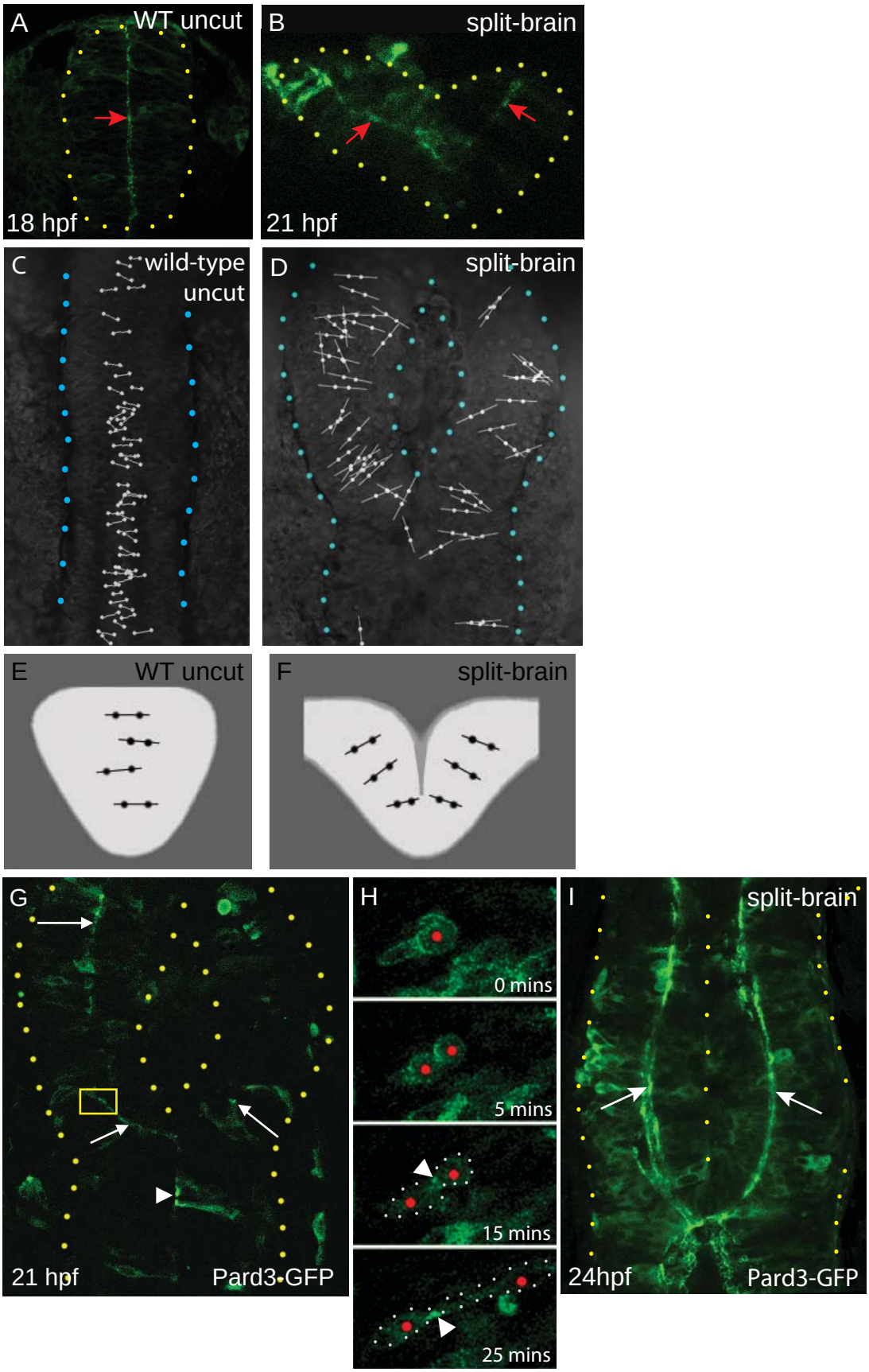

Figure 3.9. Split-brain duplications are caused by ectopic C-divisions.

ends of the daughter cells just after division as they elongated across a single side of the neural primordium (n=3, fig 3.9H). By 24hpf Pard3 localisation at the ectopic midlines is continuous and the duplication is obvious (fig 3.9I). This data confirms the presence of mirror-symmetric divisions in the ectopic Pard3 domains, and strongly suggests that they organise the neural duplication phenotype.

Reducing cell division rescues neural tube duplications

If ectopic cell divisions cause duplications then blocking cell division should rescue the duplication in split-brain embryos, just as it does in *tri* embryos, where 76% of embryos have a significant decrease in the duplication when divisions are reduced (Tawk *et al*, 2007). Inhibition of cell division in split-brain embryos significantly decreases the formation of duplicated neural tubes (χ^2 test, $p<0.05$, fig 3.10C). A notable 36% (10/28) of embryos were fully rescued, with no obvious duplication as observed by bright field microscopy (fig 3.10A). A further 36% (10/28) were partially rescued, such that only a small bridge or island of duplicated tissue was present (fig 3.10B), and the remaining 28% were not rescued as they still had obvious regions of duplicated neuroepithelium.

The proportion of embryos rescued by blocking cell division was a little lower than expected, so I reasoned that perhaps this was the result of inefficient cell division block. I analysed the efficiency of the pharmacological inhibition of cell division by comparing the numbers of mitotic figures at 24hpf in control embryos (fig 3.10D) versus those that had been incubated in the inhibitors from neural plate stage onwards (fig 3.10E). Mitotic figures were stained with an antibody to Phospho-histone H3, which labels cells in late G2 and M phases, and imaged in three different regions of the brain (n=1 for each category). Cell division was only decreased by 62% on average (fig 3.10F), which is probably the reason why the rescue of split-brain embryos was inefficient. Some of this work has recently been published in a paper from the Clarke lab (Tawk *et al.* 2007).

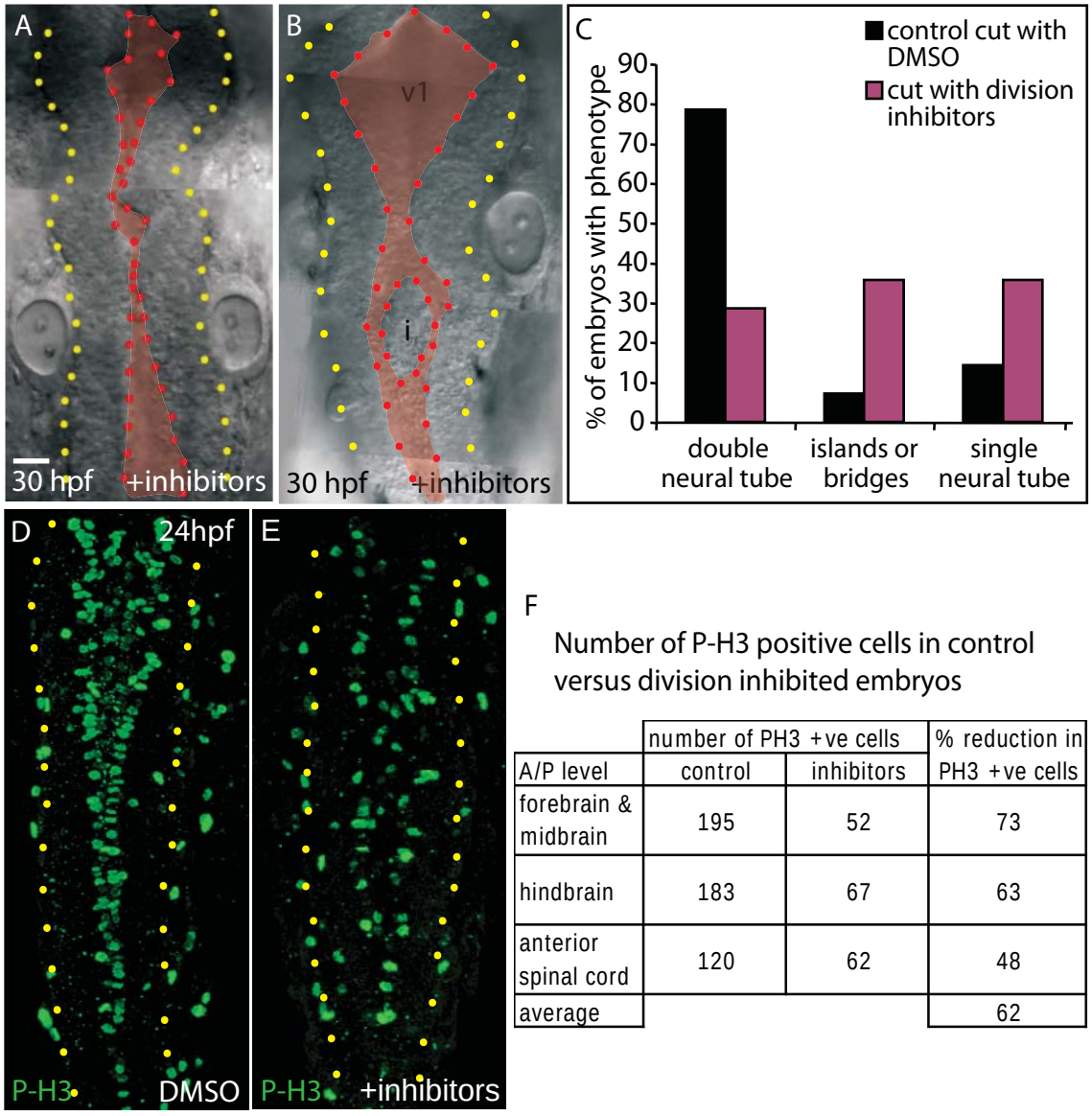

F

Number of P-H3 positive cells in control versus division inhibited embryos

	number of PH3 +ve cells		% reduction in
A/P level	control	inhibitors	PH3 +ve cells
forebrain & midbrain	195	52	73
hindbrain	183	67	63
anterior spinal cord	120	62	48
average			62

Figure 3.10. Cell division inhibitors rescue the neural tube duplications usually generated in split-brain embryos.

A) Dorsal view bright-field image of a split-brain embryo shows that inhibiting cell division throughout neurulation can completely rescue neural tube duplications. By 30hpf the embryos have a single neural tube with a central midline ventricle (shaded in red).
B) Dorsal view bright-field image of a split-brain embryo showing that inhibiting cell division throughout neurulation can partially rescue neural tube duplications so that only a small island of ectopic neural tissue (i) is formed.
C) The proportion of embryos with neural tube duplications is significantly reduced when cell division is blocked (χ^2 test).
D) Control embryos have many cells dividing at 24hpf, as shown by antibody staining for phospho-H3, which marks cells in early mitosis.
E) Inhibiting cell division during neurulation from 12hpf until 24hpf, reduces the number of phospho-H3 positive cells at 24hpf.
F) Table comparing number of phospho-H3 positive cells in 3 different areas of the brain in separate control and division inhibited embryos (n=1 for each category). Mitotic figures were reduced by 62% on average.
In all figures anterior is up and red dots outline the apical surfaces, yellow dots outline the basal edge of the neural tube. All images show a dorsal view of the hindbrain.

3.5 DISCUSSION

Neural tube duplications result from ectopic C-divisions

I have demonstrated that the neural tube duplications of split-brain embryos are caused by ectopic C-divisions (fig 3.11), which is exactly how we proposed the duplications arise in *tri* mutants (Tawk *et al.* 2007). This indicates that simply delaying convergence can cause these dramatic neurulation defects, and argues that PCP pathway mutants do not have additional defects in cell repolarisation and intercalation, as previously suggested (Ciruna *et al.* 2006). Ciruna *et al* reported that after cell division, the medial daughter cell was unable to reintegrate into the neural primordium in MZ*tri* embryos, and hence was extruded from the neural tissue. They failed to identify the ectopic duplicated epithelium, and therefore reasoned that the central tissue of the MZ*tri* primordium was outside the neuroepithelium, rather than being part of it. The duplication may have been obvious if they had analysed apico-basal polarity during neurulation, but even looking at the tissue structure by membrane-GFP clearly reveals the duplication in some of their figures, especially figs 2f, 2g and 3d (Ciruna *et al.* 2006). In their Kaede photoconversion experiment, they even note that surprisingly, cells in this central mass respect the embryonic midline, though they do not speculate on a reason for this. It would seem unlikely that if cells had lost polarity and been extruded from the tissue that they would look so organised. From our studies of *tri* and split-brain embryos, we would predict that a basal surface exists at the embryonic midline and this is why cells respect the embryonic midline.

Most of the MZ*tri* images in Ciruna *et al* look very similar to the Z*tri* pictures in Tawk *et al*, suggesting that the neural defects are formed by the same mechanism of ectopic cell division. However the structure of the MZ*tri* primordium is not consistent in the paper, as in some images the central mass of tissue does appear more disorganised (figs 1h and 1k in Ciruna *et al*, 2006). Perhaps the MZ*tri* phenotype is variable, or the structure of the neural primordium differs depending on the antero-posterior position within the embryo, but it is not mentioned in their paper. Ciruna *et al* used a maternal zygotic mutant of *tri* in their study, so it is possible that the MZ*tri* embryos have a different, more severe phenotype than the zygotic *tri* embryos, which we used in our studies. Nonetheless upon consideration of all the points above, my data does not support the proposed new role for Wnt PCP signalling in cell re-intercalation suggested by Ciruna *et al*. The neurulation defects of *tri* mutants can be explained by slow convergence of the neural plate leaving any other role for Wnt PCP signalling during zebrafish neurulation to be proven.

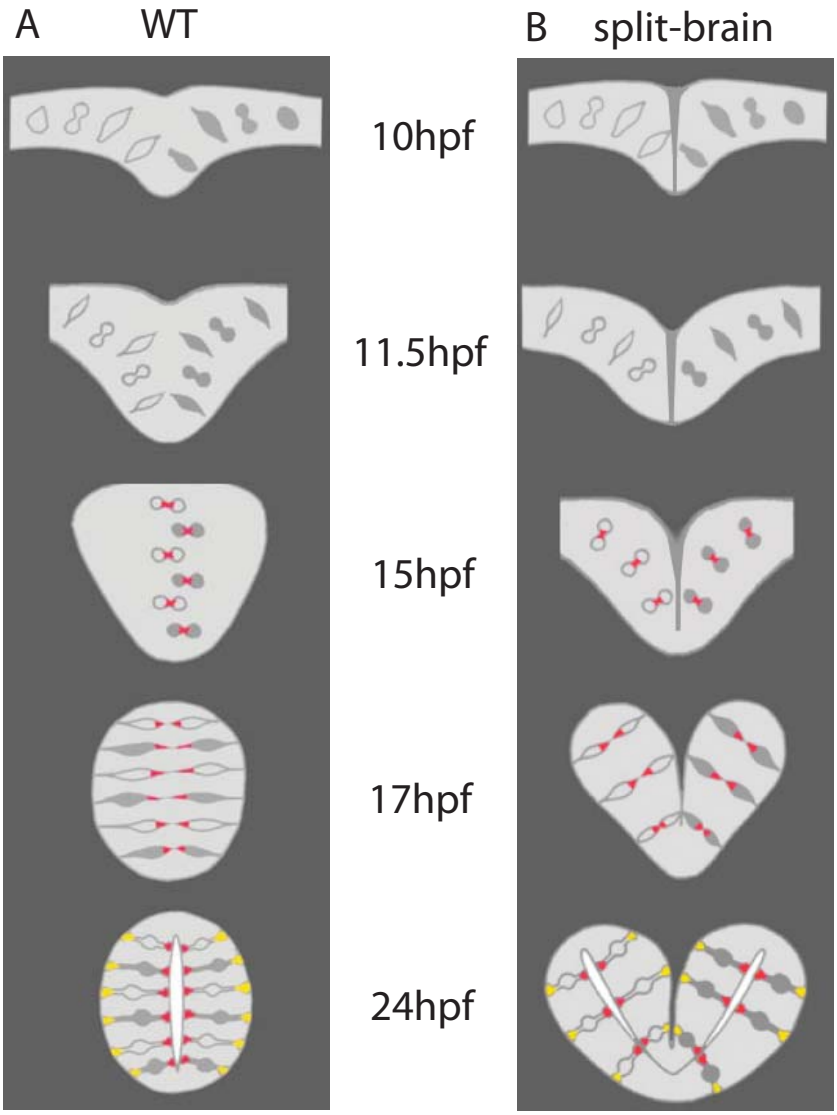

Figure 3.11. Schematic illustrating neurulation in wild-type and split-brain embryos.

A) In wild-type neurulation, cells undergo mirror-symmetric division at the midline at keel and rod stages. A single lumen has formed in the neural tube by 24hpf.
B) In split-brain embryos cells divide and polarise in ectopic locations because the neural primordium is split in half. This causes ectopic apical surfacesto form, and duplicated neural tubes to develop.
In both figures, Pard3 (apical) localisation is shown in red, and GFAP (basal) is shown in yellow.

The antero-posterior location of split-brain duplications suggests that the mechanism of neurulation is similar in midbrain and hindbrain regions.

In split-brain embryos, neural tube duplications were observed at all levels of the hindbrain, and occasionally in the midbrain. This is in contrast to *tri* mutants, which consistently exhibit duplications only in the posterior hindbrain and anterior spinal cord. This reveals a couple of interesting things. Firstly, the fact that duplications arise in more anterior brain regions indicates that the mechanism of neurulation in the midbrain is likely to be very similar to hindbrain regions. Secondly, it reveals that Wnt PCP signalling is probably more important for convergence in the posterior hindbrain and anterior spinal cord, than in more anterior regions. During normal neurulation, either other factors or pathways contribute to convergence in more anterior brain regions, or cells do not have to undergo such large convergence movements such that when convergence is slowed in *tri* mutants, the neural tube still manages to form normally.

An intrinsic timer may regulate neural progenitor cell division in time and space

In *tri* and split-brain mutants, neural cells undergo C-division in ectopic locations, before they have reached the embryonic midline. This implies that the location of cell division is not controlled by a signal from the midline, because otherwise cells would wait until they have reached the midline to divide. In *tri* and split-brain embryos, cell division and polarisation appear to have become uncoupled from the morphogenetic tissue movements of neurulation. This suggests that neural cells rely on a timing mechanism to know when to undergo C-division, not a spatial cue. I have investigated this intrinsic timer hypothesis in the rest of my thesis. It is an attractive idea, especially as neuroepithelial cells nearly always undergo the midline crossing division on their 16th zygotic cell division (Kimmel *et al.* 1994), suggesting that cells could possibly count divisions to know their age.

Although an indication that a timing mechanism could be involved, the observations made in *tri* and split-brain embryos do not exclude the possibility that surrounding tissues, such as mesoderm, send a signal at a certain time telling the cells when to divide. Nor do they exclude the idea that neuroepithelial cells reach a competence to respond to a polarising signal at a particular time, though this could be part of a timing mechanism. I investigate the contribution of the environment, the robustness of the timer, and its relationship to cell division in more detail in the next chapters.

A redundant mechanism exists for establishing cell polarity in the absence of cell division

In the studies of Ciruna *et al*, Tawk *et al*, and also in my experiments, blocking cell division rescues neural tube duplications to give a relatively well-organised single neural tube by 24hpf. Firstly this result suggests that mirror-symmetric cell division is responsible for the generation of mirror-image polarity. Secondly, the formation of a relatively well-organised neural tube also suggests that the cells are able to establish polarity in coordinated fashion in the absence of cell division. These results indicate that although neural cells usually acquire apical polarity at neural keel and rod stages as they undergo mirror-symmetric cell division, a redundant mechanism must exist for establishing cell polarity, other than mirror-symmetric cell division. I have not investigated the precise mechanism of the rescue of *tri* and split-brain embryos, but we are beginning to understand how cells behave and polarise in wild-type embryos when cell division is blocked (see chapter 6), which may then enable us to understand the mechanism of rescue in *tri* and split-brain embryos.

The function of the non-canonical Wnt PCP pathway during neurulation is conserved

The slow convergence of the neural plate and resultant neural tube duplications seen in fish PCP mutants suggests that the role of PCP signalling during neurulation in mice, frogs and fish is conserved. In *Xenopus*, Dishevelled is specifically required for convergence and extension in the midline to allow neural tube closure (Wallingford *et al.* 2002). Similarly in looptail mice, which have a mutation in *vangl2*, convergent extension defects in the paraxial mesoderm and the neuroepithelium before neurulation cause the neural folds to be widely spaced apart, preventing later closure (Ybot-Gonzalez *et al.* 2007). The PCP pathway thus appears to be necessary for efficient convergence of the neural plate in fish, frogs, and mice, even though the modes of neurulation in these species are quite different. This result unifies the role of the PCP pathway in neurulation across diverse animal groups.

CHAPTER 4 HETEROCHRONIC CELL TRANSPLANTATION SHOWS THAT AN INTRINSIC TIMER CONTROLS THE ESTABLISHMENT OF APICAL POLARITY

4.1 INTRODUCTION

The formation of an organ is a complex process, as it requires cells to adopt certain fates and to organise in a specific manner. Cells must undergo complex cell behaviours, all of which must be coordinated with surrounding cells to enable the tissue to develop a specific 3D architecture essential for correct function. Many factors are involved in directing the behaviour of cells during organogenesis, and these may be both intrinsic and extrinsic to the cell. Intrinsic programmes are able to direct cellular behaviour in the absence of environmental cues and may be a function of a cell's clonal history. Conversely, extrinsic cues from the surrounding environment may signal to cells and direct their behaviour. During embryogenesis, both intrinsic and extrinsic factors combine to direct and coordinate the wide variety of cell behaviours necessary to generate an organism from a single cell. The relative contribution of intrinsic or extrinsic factors varies within different cell or tissues, as research has shown that either intrinsic or extrinsic cues can be dominant in directing certain behaviours. This chapter investigates the hypothesis that an intrinsic mechanism controls the timing of neural cell polarisation during zebrafish neural tube development. Several observations have led us to derive this hypothesis and these are detailed below.

Basis of the timer hypothesis for cell polarisation

The hypothesis that an intrinsic mechanism controls the time of C-division and cell polarisation during neurulation mainly derives from observations of cell division in embryos with delayed convergence of the neural plate towards the midline (Chapter 3 and Tawk *et al*, 2007). In these embryos, at approximately 15hpf when cells would normally undergo C-division at the midline of the neural keel and rod, many neural cells are still located in ectopic lateral positions, far from the midline. However, the neural cells still divide and polarise at the correct time, irrespective of their ectopic location (Tawk *et al.* 2007), implying that the local environment of the keel is not important for the temporal control of C-division.

Other evidence that an intrinsic programme governs zebrafish neural cell behaviour and cell division comes from cell lineage tracing studies during late gastrulation and neurulation, in which specific cell behaviours were found to be related to specific cell cycles (Kimmel *et al.* 1994). In the 15th cell cycle, cells generally move in posterior direction as they undergo epiboly, but during cell cycle 16, cells change their direction to move towards the dorsal midline as they undergo convergence extension movements (Kimmel *et al.* 1994). In addition, Kimmel and colleagues found that on their 15th cell division, cells generally divided oriented along the antero-posterior axis, but that on their 16th cell division, cells divided with a medio-lateral orientation that separated sister cells across the midline (Kimmel *et al.* 1994). These observations clearly show that cell behaviours change with time, and also that cell behaviours are strongly correlated with specific cell cycles.

Heterochronic transplantation as a tool to test cell autonomy and age

In order to determine whether extrinsic or intrinsic factors are important for a certain developmental processes, cells or tissue can be transplanted into a different environment. This recipient site may either be a different location to test the role of spatial signals for the behaviour under test, or be a different age to test if temporal factors are the key regulators of the process.

During CNS development in both vertebrates and invertebrates, neural precursors change over time to generate different types of neurons with age. Several groups have begun to investigate which factors are important for controlling these progressive changes over time, by testing if a cell's age is important for specific neuronal behaviours. One cell behaviour that has been investigated by heterochronic cell transplantation is the dendritic targeting of granule cells (GCs) in the olfactory bulb. The dendritic tree of GCs is targeted either to superficial or deep laminae in the olfactory bulb (Mori *et al.* 1983; Orona *et al.* 1983), and this targeting depends on the specific location and age of the GC progenitor cells in the sub ventricular zone of the brain. In neonatal mice, anterior GC progenitors in the subventricular zone send dendrites to the superficial layers, but in adult mice, the dendrites of anterior progenitors are targeted to the deep lamina (Kelsch *et al.* 2007). When anterior neonatal GCs were transplanted into an anterior location in the adult, most neonatal anterior GCs showed dendritic targeting to superficial layers, typical of their age (Kelsch *et al.* 2007). This indicates that precursors are committed to generate GCs with a specific dendritic tree, even when placed in an environment that normally generate GCs

with the opposite branching pattern. Thus the environment does not play an important role in dendritic targeting of GC precursors.

In zebrafish, heterochronic cell transplantation been used to test the autonomy of cell movements during gastrulation. At a particular time point in gastrulation, endodermal cells switch from random walk movements to directed migration towards the dorsal midline of the embryo (Pezeron *et al.* 2008). When older or younger heterochronic cells were transplanted into a host embryo, they always showed migration movements typical of the host embryo age (Pezeron *et al.* 2008). This shows that directed and random migration of cells during gastrulation is governed by environmental signals, and not by the age of the cells.

The above two examples illustrate that heterochronic transplants can reveal if cell behaviours are governed by intrinsic or extrinsic factors. Therefore it should be a suitable technique to use in the study of cell polarisation during zebrafish neurulation.

4.2 AIMS AND HYPOTHESIS

Use a heterochronic transplant strategy to test:
(1) If heterochronic cells polarise Pard3-GFP according to their age or at the same time as surrounding host cells.
(2) If heterochronic cells divide with an orientation typical of their age or their environment.
(3) The ability of heterochronic cells to cross over the midline to the contralateral side of the neural rod. Since cell division has previously been determined to be necessary for a cell to cross the midline (Tawk *et al.* 2007) this will provide an indirect measure of whether cells undergo C-division at the correct time and place.

Hypothesis

My hypothesis is that an intrinsic timer controls the timing of mirror-symmetric C-division and cell polarisation during zebrafish neural tube morphogenesis.

If the hypothesis is true then donor cells should undergo division and polarisation either earlier or later than host cells, possibly in ectopic locations, and thus be unable to cross the midline.

If donor cells divide and polarise at the same time as host cells, and are therefore able to cross the midline with the same frequency as isochronic cells, this will disprove the hypothesis and indicate that the environment controls the timing of polarity establishment.

4.3 METHODS

Heterochronic cell transplantation method

Preparation for transplantation

Wild-type embryos were used for all transplants. For control isochronic transplants both donor and host embryos were collected at 9.30am. For heterochronic transplants, donor and host embryos were laid 3 hours apart at 9.30am and 12.30pm.
Donor embryos were labelled by injection of RNA encoding H2B-RFP (100pg) and either membrane-GFP (memGFP, 100pg) or Pard3-GFP (100pg) at the 1-2 cell stage.
Host embryos were collected at the 1-4cell stage, and incubated at 28.5˚C in parallel with the donor embryos.

To position embryos during cell transplantation, an agarose plate consisting of 6 rows of wells was used. This was prepared in advance of cell transplantation by placing the well mould in the lid of a 100mm Petri dish, pouring 1.2% agarose around the mould, and allowing it to set.

One hour before embryos were the correct age for transplantation, donor embryos were selected as the most bright and uniformly fluorescent embryos. (N.B. Young donors could not be selected in this way, as it is too early after RNA injection for fluorescence to be visible). Both host and donor embryos were manually dechorionated in agarose-coated Petri dishes and then transferred to the agarose transplantation plates containing fish water supplemented with penicillin and streptomycin (Sigma, 50x stock diluted 1:100) ready for transplantation. Donor and host embryos were placed in alternating rows of wells for ease of transplantation.

Cell transplantation technical details

- All cell transplantations were carried out at blastula stages (see fig 4.1B-D for the precise stages of donor and host embryos for the different types of transplants)
- The transplantation apparatus consisted of a micropipette attached to a micrometer drive-controlled Hamilton syringe by mineral oil-filled polyethylene tubing. The micropipette was mounted on a micromanipulator by the side of the dissecting scope.
- The tip of the micropipette needle was broken using forceps to a diameter just larger than that of a donor cell (typically 10-15µm).

- Approximately 10-20 cells were extracted from the donor embryo and drawn into the micropipette by turning the micrometer drive.
- Cells were then expelled into the host embryo by turning the micrometer drive in the opposite direction.

Further details on cell transplantation can be found in the zebrafish book (Whitlock *et al.* 2000) and in excellent published videos (Deschene *et al.* 2009; Kemp *et al.* 2009a).

For isochronic and young into old heterochronic transplants, as host embryos were approximately shield stage donor cells could be targeted one side of the prospective hindbrain (fig 4.1A-C), which was important for the analysis of midline crossing at 24hpf. For old into young transplants, host embryos were too young cells for accurate, unilateral targeting to the hindbrain (fig 4.1D), so the location of transplanted cells was assessed at 10-11hpf, and only unilateral transplants were used for further analyses.

Post transplantation and analysis

After transplantation, embryos were left to recover for 30mins on the bench, before being carefully transferred to an agarose-coated Petri dish containing fish water supplemented with antibiotics for incubation at 28.5°C.

For analysis of cell polarisation, host embryos were fixed in 4% PFA at a specific time during neurulation when the polarity of host and donor cells should be different. Cells should show polarised Par3-GFP at 17.5-18hpf, but Pard3-GFP should not be polarised at 14.5-15hpf. Therefore old hosts were fixed at 17.5-18hpf, and young hosts at 14.5-15hpf. Embryos were later washed in PBS and imaged the following day.

To analyse midline crossing, embryos were anaesthetised and mounted for live confocal imaging at 22-24hpf, or fixed for imaging later.

For all fixed imaging, embryos were counter-stained with To-Pro dye (dilution 1:1000, Invitrogen, T3605) in order to label all nuclei and thus show the location of transplanted cells within the brain.

Transplantation cell crossing analysis

I have used midline crossing as an indirect measure of whether cells have undergone C-division at the normal time and place. I analysed cell crossing at 22-24hpf because the time-period of C-divisions has finished, and most cells will not have divided again (P. Alexandre, personal communication). As all transplants were initially unilateral, the ability of cells to cross the midline was assessed by counting the number of cells on each

side of the neural tube. Only cells that were integrated into the neural tube were counted. This was repeated for 20-40 embryos for each type of transplant.

The percentage of cells crossing the midline was calculated by:

$$\frac{\text{number of cells on contralateral side}}{\text{total number of cells}} \times 100$$

This percentage can be extrapolated to give the percentage of successful C-divisions that have occurred in each embryo:

$$\%\ \text{successful C-divisions} = 2 \times \%\ \text{of cells crossing the midline}$$

The data were displayed for each type of transplant as box plots, constructed using a program on the "Statistics to Use" website (Kirkman 1996). The box plot shows the minimum value, lower quartile, median value, upper quartile and maximum value for each set of data. The box part of the graph is defined by the interquartile range, which is a measure of the variation in the data. Suspected outliers are shown as unfilled circles and defined by Tukey as being either $1.5\times IQR$ or more above the third quartile or $1.5\times IQR$ or more below the first quartile.

Isochronic antero-posterior transplantation data analysis

The locations of isochronic transplanted cells in each embryo were categorised into hindbrain or midbrain and diencephalon. Similar to heterochronic transplants, the ability of cells to cross the midline was assessed by counting the number of cells on each side of the neural tube.

Statistical analysis

Student's t-test was used to test for a significant difference between the percentage of successful C-divisions in isochronic compared to division-blocked isochronic transplants, as the data were of a Gaussian distribution.

The Kolmogorov-Smirnov (KS) test was used to test for a significant difference between the percentages of C-divisions in isochronic transplants and each type of heterochronic transplant because the data were of a skewed distribution (Kirkman 1996). The skewed distributions of heterochronic transplantation data were visualised using frequency histograms and were also determined as part of the online KS test (Kirkman 1996).

The Chi-squared test (GraphPad Prism) was used to test for a significant difference between the cell division orientations of young transplanted and host cells from a 3 by 2 contingency table of C, D or oblique angled divisions for the two types of cells.

Separate Chi-squared tests (GraphPad Prism) were used to test for significant differences between the Pard3-GFP polarisation state of heterochronic transplanted cells compared to isochronic transplanted cells at 15hpf and 18hpf.
Calculation of Pearson's rank correlation coefficient (Excel) was used to detect if the number of transplanted cells had any effect on the efficiency of midline crossing.

Immunohistochemistry

Antibodies used in this chapter and their concentrations are detailed below:
Anti ZO-1 (1:500, Zymed)
Anti GFAP (1:500, Dako)
Anti phospho-histone H3 (1:500, Upstate)

Confocal and time-lapse imaging

Confocal images in this chapter were acquired using an SP2 or SP5 Leica laser scanning confocal microscope. Fixed embryos were mounted in a dorsal view, and a stack of z-slices through the transplanted cells was collected with a z-interval of 2-5µm. For time-lapse experiments, embryos were mounted to be viewed dorsally, and a z-stack was captured every 5-7minutes with a depth of 5µm between z levels.

Image processing

Fixed and time-lapse images were processed as described in the general methods using ImageJ and Adobe Photoshop.

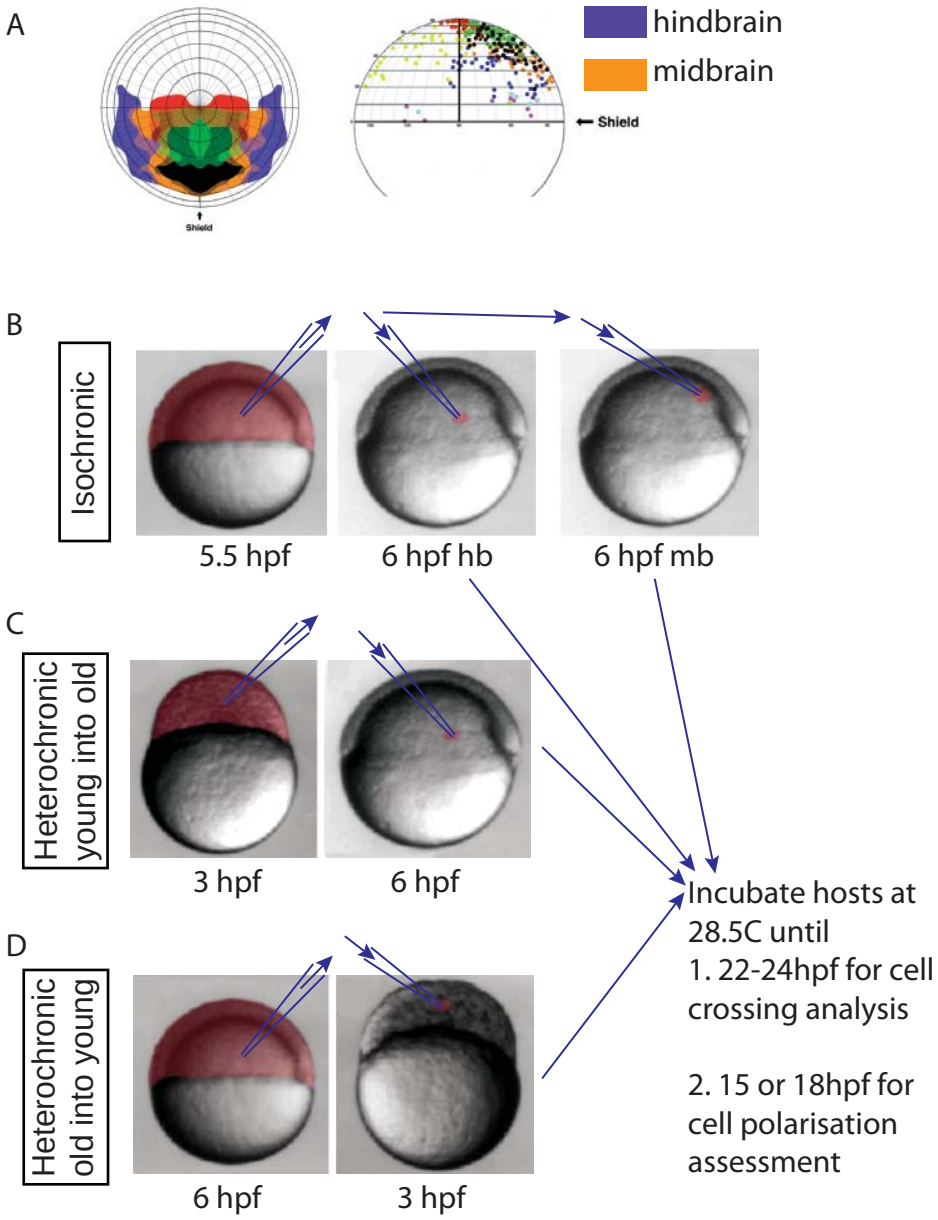

Figure 4.1 Method of heterochronic cell transplantation

A) The fate map at shield stages shows that left and right midbrain and hindbrain fated regions are non-overlapping, thus enabling unilateral targetting of transplanted cells.
B) Isochronic cell transplantation was carried out at blastula stages.
C) Embryos illustrating the approximate stages of the young donor and old host for young into old cell transplantation.
D) Embryos illustrating the approximate stages of the old donor and young host for old into young cell transplantation.
Donor embryos were coinjected with mRNA encoding H2B-RFP and either Pard3-GFP or mem-GFP at the 1-2 cell stage to obtain ubiquitous labelling (red shading).

4.4 RESULTS

In this chapter I use heterochronic cell transplantation to test if mirror-symmetric division and cell polarization are regulated by a timing mechanism. All heterochronic transplants were carried out at blastula and gastrula stages with a time difference of three hours between donor and host embryos. Host embryos were then left to develop until 15 or 18hpf for polarisation analysis, or 24hpf for cell crossing analysis.

Cells in different brain regions polarise at different times

Before studying the polarity of heterochronic cells after transplantation, I first investigated the relative timing of Pard3-GFP polarisation in different regions of the brain. As the exact location of transplanted cells within the host could vary, it was important to make sure that transplanted cells only located in brain regions that polarise at a similar time were included in the analysis of polarisation. Time-lapse imaging was used to compare the time of polarisation of cells during neurulation in the forebrain and midbrain of one embryo, and in the hindbrain of a simultaneously imaged separate embryo. To minimize potential variation in the time of polarisation in the dorso-ventral axis, z-levels at an equivalent depth in the different brain regions were chosen for analysis.

Figure 4.2 shows the polarisation of Pard3-GFP in eight different regions of the brain from 14.5hpf until 18.5hpf. Four regions of interest (ROIs) were located in the forebrain and midbrain of one embryo (fig 4.2A-E), and four ROIs were positioned in the hindbrain of a second specimen (fig 4.2F-J). The time at which a straight line of Pard3-GFP formed at the midline was used to compare apical polarity establishment across different ROIs. I found that the telencephalon polarised first, as midline localisation of Pard3-GFP was obvious by 15.5hpf (arrowhead in fig4.2B). The posterior midbrain and rhombomeres 1, 3 and 5 of the hindbrain polarised next by 17.5hpf (arrowheads in fig4.2D and I). Finally the midbrain and remaining rhombomere (r7) of the hindbrain polarised last at 18.5hpf (arrowheads in fig 4.2E and J). These observations indicate that all regions of the brain with the exception of the telencephalon show a strong midline polarisation of Pard3-GFP at either 17.5hpf or 18.5hpf. This one hour difference is less than the 3hours difference between young and old transplanted cells and therefore should not hinder the analysis of polarisation in heterochronic transplants. However the earlier polarisation of the telencephalon indicates that transplanted cells located in the telencephalon should be excluded from the analysis of Pard3-GFP polarisation.

Figure 4.2 Pard3-GFP becomes polarised to the midline at a similar time in different brain regions, except in the telencephalon.

A-E) Frames from a dorsal view confocal time-lapse of neurulation showing different anterior brain regions. The embryo is ubiquitously labelled with Pard3-GFP.

F-J) Frames from a dorsal view confocal time-lapse of neurulation showing different hindbrain regions. The embryo is labelled ubiquitously with Pard3-GFP and was simultaneously imaged with the embryo in A-E.

A-J) Arrowheads highlight the first time that Pard3-GFP is strongly localised to the midline of the neural rod in each of the different regions. Cells in the telencephalon show polarised Pard3-GFP at the midline by 15.5hpf, whereas cells in the midbrain, anterior hindbrain and rhombomeres 3 and 5 are polarised by 17.5hpf. Cells in the diencephalic/midbrain area and anterior diencephalon polarise last by 18.5hpf.

tel, telencephalon; ant di, anterior diencephalon; di/mb diencephalon/midbrain; mb, midbrain; ant hb, anterior hindbrain; r, rhombomere

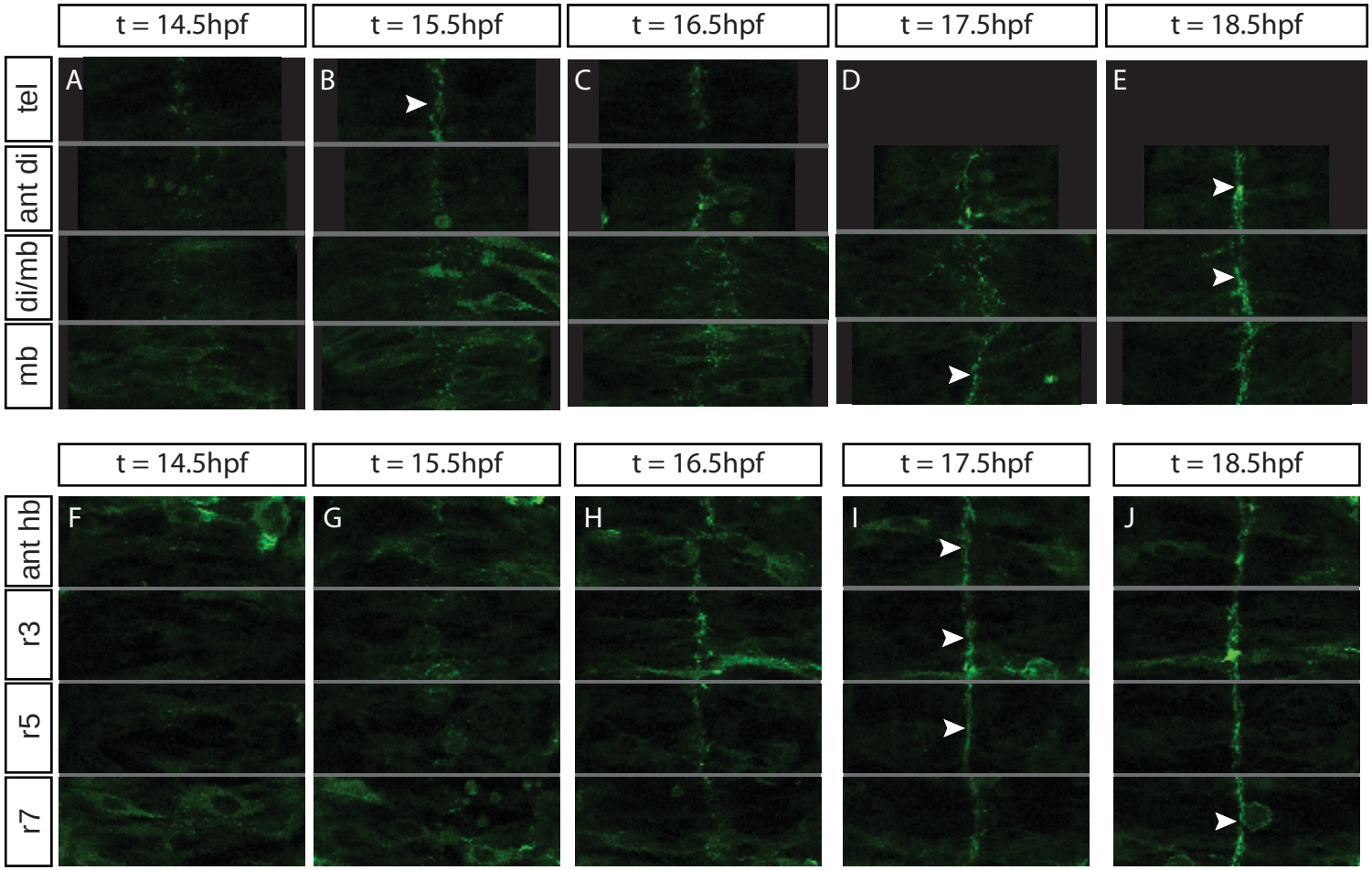

Figure 4.2 Pard3-GFP becomes polarised to the midline in different brain regions at a similar time, except in the telencephalon.

Isochronic transplanted cells integrate into the neuroepithelium and show normal apico-basal polarity at 24hpf

Cell transplantation in zebrafish has been used in many published experiments as a method to create chimeric embryos for the study of cell autonomy (Woo *et al.* 1998; Pezeron *et al.* 2008). Although a commonly used technique, it was important first to characterise the behaviour of transplanted cells in our system, and confirm that cell transplantation is a suitable technique for studying cell polarity and cell division during neurulation. Therefore, before carrying out any heterochronic cell transplantations, I first transplanted 10-30 isochronic cells at mid blastula stages into the prospective hindbrain territory (fig 4.1), and imaged the transplanted embryos at 24hpf. By this stage, the host embryo has completed neurulation, and the location, shape and polarity of the isochronic transplanted cells can be assessed (fig 4.3). I found that isochronic transplanted cells integrate well into the host neural tube, as shown by their full extension across the apico-basal width of the neuroepithelium, dispersal among host cells and spindle shaped morphology that is typical of neuroepithelial cells (fig 4.3A). Apical polarity of the transplanted cells was also assessed by labelling the cells with Pard3-GFP (fig 4.3B). At 24hpf, isochronic transplanted cells showed localisation of Pard3-GFP at the ventricular surface of the neural tube indicating that they have established correct apico-basal polarity (fig 4.3B). Time-lapse imaging of the transplanted cells during neurulation confirmed that they divided close to the midline at neural keel and rod stages and that the medial daughter cell crossed the midline to the contralateral side of the neural rod (data not shown). Therefore transplanted cells show normal behaviours of neural progenitor cells confirming that transplantation is a suitable method for studying the polarisation of neural progenitor cells.

Heterochronic transplanted cells are able to integrate into the host neuroepithelium, but some generate ectopic lumens

I next carried out heterochronic cell transplants and analysed the distribution of cells within the host neuroepithelium at 24hpf. Transplanted cells were labelled with H2B-RFP and Pard3-GFP to visualise their apico-basal organisation within the host neuroepithelium. I found that the distribution of heterochronic transplanted cells within the host could be classified into four main phenotypes (fig 4.3A-D), summarised in the tree diagram in figure 4.3E. Some transplanted cells integrated into the host neuroepithelium and either dispersed among host cells (fig 4.3C), or clustered together (fig 4.3D). A distribution was classified as dispersed when gaps were present between the transplanted cells, or clustered when greater than 10 cells were located adjacent to each other.

Figure 4.3 Isochronic and heterochronic transplanted cells can integrate into the host neural tube

A-F) Confocal micrographs of transplanted cells labelled with H2B-RFP and Pard3-GFP or mem-GFP overlaid onto bright field images of the host tissue. All images show a dorsal view and anterior is up. White arrows indicate the midline of the host neural tube.

A) Isochronic transplanted cells display a spindle-shaped morphology typical of neuroepithelial cells showing that they are integrated into the host neural tube.

B) By 24hpf, isochronic transplanted cells have established apico-basal polarity, as revealed by Pard3-GFP localised to the ventricular surface of the neuroepithelium.

C-F) Confocal projections of heterochronic transplanted cells labelled with Pard3-GFP and H2B-RFP, overlaid on brightfield images of the host embryo at 22-24hpf.

C) Heterochronic cells can integrate into the host neuroepithelium and disperse among host cells.

D) Heterochronic cells can integrate into the host neuroepithelium but remain clustered together.

E) Some clusters of heterochronic cells do not fully integrate into the neuroepithelium but generate an ectopic apical surface as an outpocket of the host neuroepithelium.

F) Some clusters of heterochronic cells can even form a rosette-like structure and generate an ectopic apical surface that is independent of the host neuroepithelium.

G) A tree diagram illustrates the four different phenotypes of transplanted cells: integrated dispersed or clustered, or ectopic lumen outpocket or independent lumen.

H) Frequency histogram to show the proportion of each of these four phenotypes for isochronic and heterochronic transplanted cells

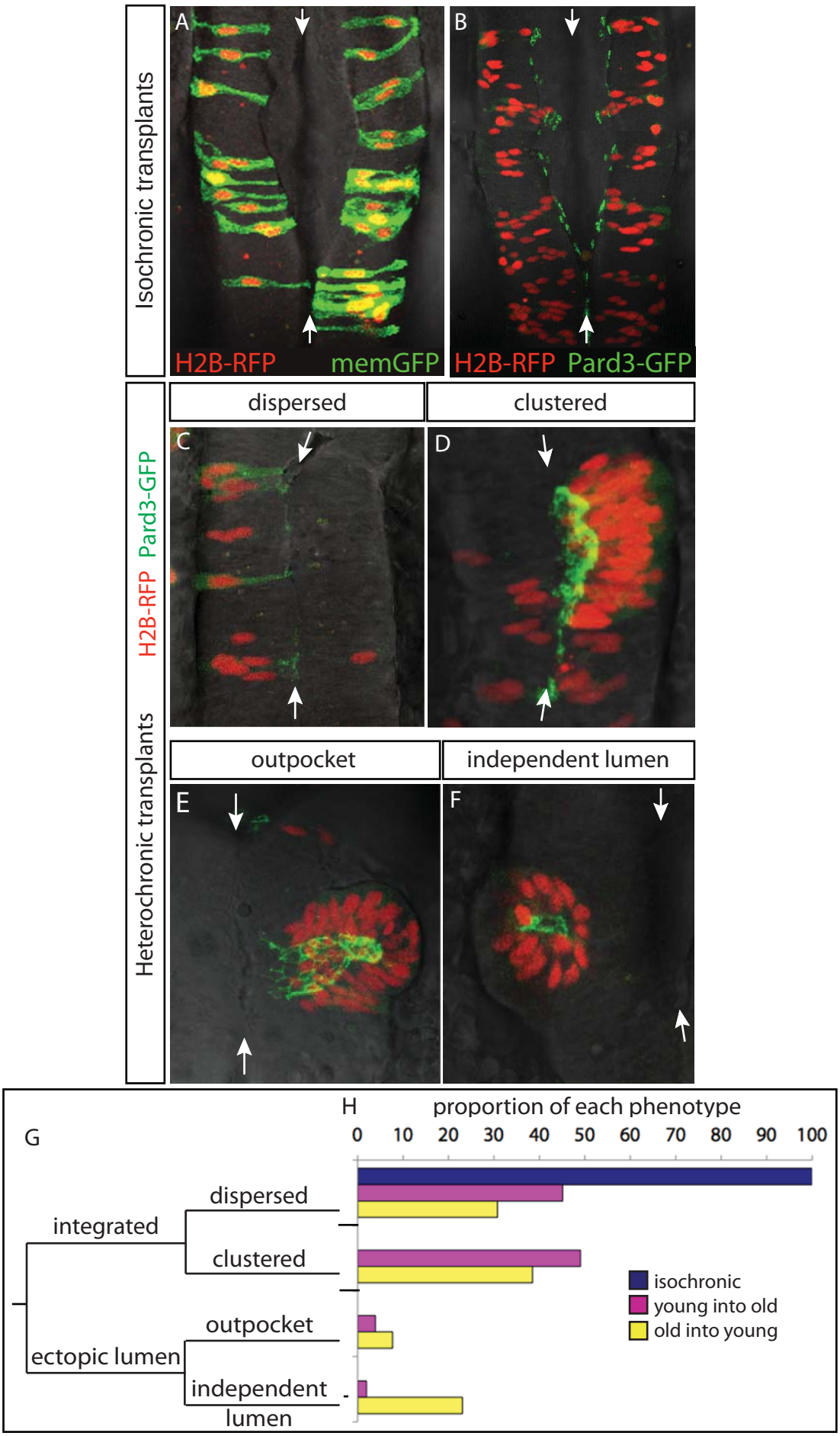

Figure 4.3 Isochronic and heterochronic transplanted cells can integrate into the host neural tube

Secondly some clusters of transplanted cells did not fully integrate into the host neuroepithelium, as the Pard3-GFP of the transplanted cells was located ectopically, i.e. not at the host apical surface (fig 4.3E,F). These ectopic lumen phenotypes could then be divided into two categories: when Pard3-GFP was continuous with the host lumen the cells were classified as an outpocket (fig 4.3E), and when Pard3-GFP was completely separated from the host apical surface the cells were classified as an independent lumen (fig 4.3F).

The histogram showing the different distributions of heterochronic transplanted cells alongside isochronic transplanted cells reveals a clear difference between behaviours of isochronic transplanted cells and both types of heterochronic transplanted cells (fig 4.3H). In all isochronic transplanted embryos, the cells integrated into the host, and dispersed among the host cells (blue in fig 4.3H). In contrast, in both types of heterochronic transplants a much greater proportion of embryos showed clustering of donor cells, such that clustered and dispersed distributions occurred at similar frequencies (fig 4.3H). The formation of ectopic lumens was most frequent for old transplanted cells (yellow in fig 4.3H).

These different types of distributions of the heterochronic transplanted cells were considered together in the analysis of polarisation, but ectopic apical lumens were not included in the division orientation or crossing analysis as the cells were not properly integrated into the neuroepithelium.

Transplanted older cells polarise on time, and prematurely compared to the surrounding younger host cells

Before investigating if heterochronic transplanted cells polarise according to their age or at the same time as their local environment, I first checked that the technique of cell transplantation did not affect the timing of polarisation by assessing the level of polarisation of isochronic transplanted cells labelled with Pard3-GFP at 15hpf and 18hpf. If isochronic transplanted cells behave the same as non-transplanted cells, they should be unpolarised or only weakly polarised at 15hpf, but should show strong polarisation by 18hpf. Indeed, isochronic donor cells at 15hpf were either not polarised Pard3-GFP (fig 4.4A), or only showed a few small puncta of Pard3-GFP close to the midline (arrowheads in fig 4.4A). Isochronic transplanted cells at 18hpf similarly showed polarisation typical of their age, as Pard3-GFP was strongly localised to the midline (fig 4.4B). This shows that cell transplantation does not affect the timing of Pard3-GFP cell polarisation.

Figure 4.4 Older transplanted cells polarise on time, and prematurely compared to host tissue.

A) Isochronic transplanted cells at 15hpf show Pard3-GFP localised within the cytoplasm of the cells, with a few small puncta (arrowheads) at the medial ends of the cells.

B) Isochronic transplanted cells at 18hpf are polarised with Pard3-GFP localised to the midline of the neural rod (arrowheads).

C) A stage matched donor embryo at 18hpf shows Pard3-GFP polarised at the midline of the neural rod.

D) A stage matched host embryo at 15hpf shows Pard3-GFP diffusely localized within the cytoplasm of the neural rod cells.

E) A cluster of older donor cells shows Pard3-GFP localised to the centre of the cluster (arrowheads).

F) A pair of older cells shows polarised Pard3-GFP localised between the two cells (arrowhead).

G-G'') Older transplanted cells in a 15hpf host embryo stained for ZO-1.

G) ZO-1 (cyan) is more strongly polarised next to the older transplanted cells than in the rest of the host tissue. All nuclei are labelled with sytox-green. Older transplanted cells are labelled with H2B-RFP

G') Older transplanted cells are labelled in red.

G'') ZO-1 is more strongly polarised next to the transplanted cells (arrowhead) than in the rest of the host tissue. Bracket shows location of most transplanted cells with H2B-RFP.

H) Graph showing the proportions of isochronic or heterochronic transplanted embryos with strongly polarised, weakly polarised or unpolarised transplanted cells. Older transplanted cells in a young host have similar polarity to 18hpf isochronic cells, but their level of polarisation is significantly different to 15hpf isochronic cells ($p<0.01$, χ^2 test). N=number of embryos analysed, n=number of groups of cells with each level of polarisation.

All images show a dorsal view and anterior is up. White arrows indicate the embryonic midline.

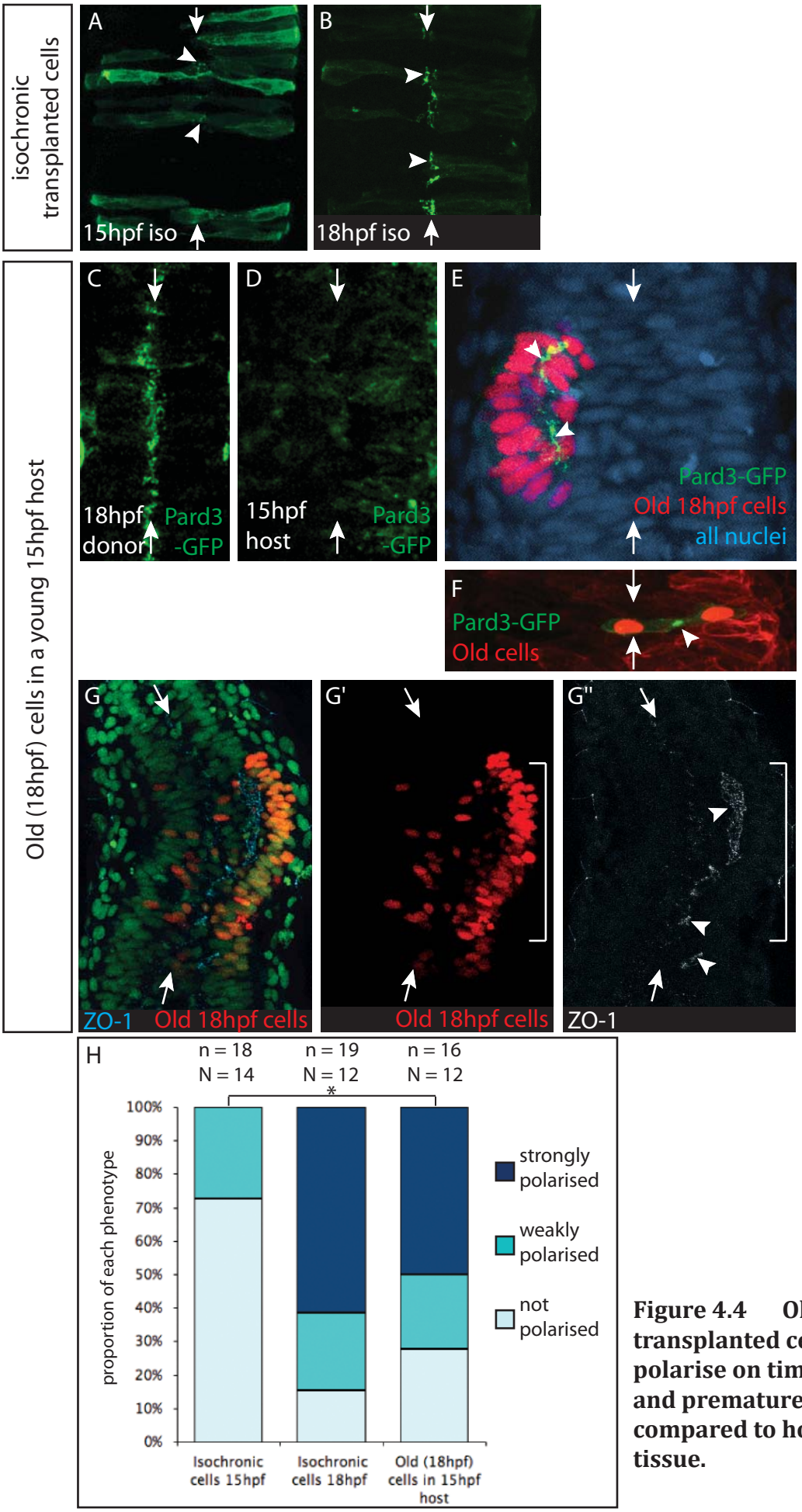

Figure 4.4 Older transplanted cells polarise on time, and prematurely compared to host tissue.

I next examined the polarity of older transplanted cells in a younger host embryo. At 15hpf, the younger host embryo does not have a strong polarisation of Pard3-GFP at the midline (fig 4.4D), but in contrast, the older donor embryo at 18hpf does show polarised Pard3-GFP at the midline (fig 4.4C). If the timing of neural cell polarisation depends on a cell's age, then the 18hpf older donor cells should show polarised Pard3-GFP even though the 15hpf host remains unpolarised. This is exactly what I observed. Figure 4.4E shows a cluster of old transplanted cells situated towards one side of the neural rod with strongly polarised Pard3-GFP located in the centre of the cluster, forming an ectopic apical surface (arrowhead in fig 4.4E). Similarly, in a separate embryo, Pard3-GFP was strongly localised to the medial ends of a pair of old transplanted cells that were isolated from other transplanted cells within the host neural rod (arrowhead in fig 4.4F). Moreover, the mirror-symmetric arrangement of the pair of cells suggests that they have arisen from a mirror-symmetric cell division. These experiments all show that older cells polarise according to their age, and prematurely compared to surrounding host tissue.

As a complementary approach to studying the polarity of cells using Pard3-GFP, I compared the polarity of donor cells to host cells using ZO-1 immunohistochemistry (fig 4.4G-G''). This had the added advantage of allowing direct comparison of the polarity of old transplanted cells with adjacent host cells in the same embryo, thus overcoming any variability in the timing of Pard3-GFP polarisation across different embryos. The donor cell nuclei (labelled in red in fig 4.G, G') are predominantly located on the right side of the host embryo (labelled in green in fig 4.4G). ZO-1 immunohistochemistry reveals that ZO-1 is strongly polarised next to the older transplanted cells (arrowheads in fig 4.4G''), but in regions where donor cells are not present, the host tissue only shows faint ZO-1 puncta (outside bracketed region in fig4.4G''). This experiment therefore confirms the results with Pard3-GFP, and shows that older transplanted cells are more strongly polarised than their surrounding host tissue.

Finally, I compared the level of polarity of old transplanted cells to isochronic transplanted cells at 15hpf and 18hpf, instead of to the host tissue. For all transplanted embryos, the level of polarisation of donor cells was categorised either as strongly polarised when Pard3-GFP was localised to the midline, weakly polarised when a few puncta of Pard3-GFP were visible, or unpolarised when Pard3-GFP was diffusely distributed within the cells. Although there is some variability in the level of polarisation of transplanted cells, there is a clear difference in the level of polarisation of isochronic transplanted cells at 15hpf compared to isochronic transplanted cells at 18hpf (compare first 2 columns in fig 4.4H). Importantly no significant difference is detected in the polarisation of older transplanted

cells to isochronic transplanted cells at 18hpf (fig 4.4H) but the polarisation level of old transplanted cells (18hpf in 15hpf host) compared to isochronic transplanted cells in a 15hpf host is significantly different (χ^2 test, $p<0.01$). In summary, these heterochronic cell transplantation experiments show that older transplanted cells show a level of polarity typical of their age not their host, thus suggesting that the timing of polarisation is intrinsic to cells.

Younger cells polarise later than isochronic transplanted cells

The above experiments indicate that older transplanted cells polarise according to their age. To investigate if younger transplanted cells likewise polarise according to their age and not their environment, I assessed the level of polarisation of younger donor cells labelled with Pard3-GFP in an older 18hpf host. If an intrinsic timer also controls when these young transplanted cells polarise, they should remain unpolarised even though the older 18hpf host has well-defined apico-basal polarity. Indeed, I found that young transplanted cells remained unpolarised in an older embryo (fig 4.5A), as Pard3-GFP was largely diffusely distributed throughout the cytoplasm of the cells. The young cells showed a similar distribution of Pard3-GFP to isochronic transplanted cells at 15hpf (fig 4.5B), and in both of these experiments the cells were much less polarised than 18hpf isochronic transplanted cells that show strongly polarised Pard3-GFP at the midline (fig 4.5C). Young cells in an old host were also more similar in morphology to isochronic cells at 15hpf, as they were not stretched across the full apico-basal extent of the neuroepithelium, and the nuclei were concentrated towards the basal edge of the neuroepithelium (fig 4.5A). This basal location of nuclei may be a characteristic of young cells because the movements of neighbouring host cells towards the midline to undergo C-division may push the nuclei of the younger cells away from the midline. This passive movement of interphase nuclei away from the future apical midline fits with recent observations of interkinetic nuclear migration (IKNM) of retinal cells, which have revealed that IKNM is largely a stochastic process except for an active apically-directed movement driven by Myosin II that bring cells close to the ventricular surface to undergo mitosis (Norden *et al.* 2009).

When the polarity of younger transplanted cells was assessed in several embryos, I found that 56% of embryos contained unpolarised transplanted cells, 39% of embryos showed weakly polarised cells, and only 5% of embryos showed young transplanted cells with strongly polarised Pard3-GFP (fig 4.5D). This distribution of polarisation of young transplanted cells was significantly different to the polarisation of 18hpf isochronic

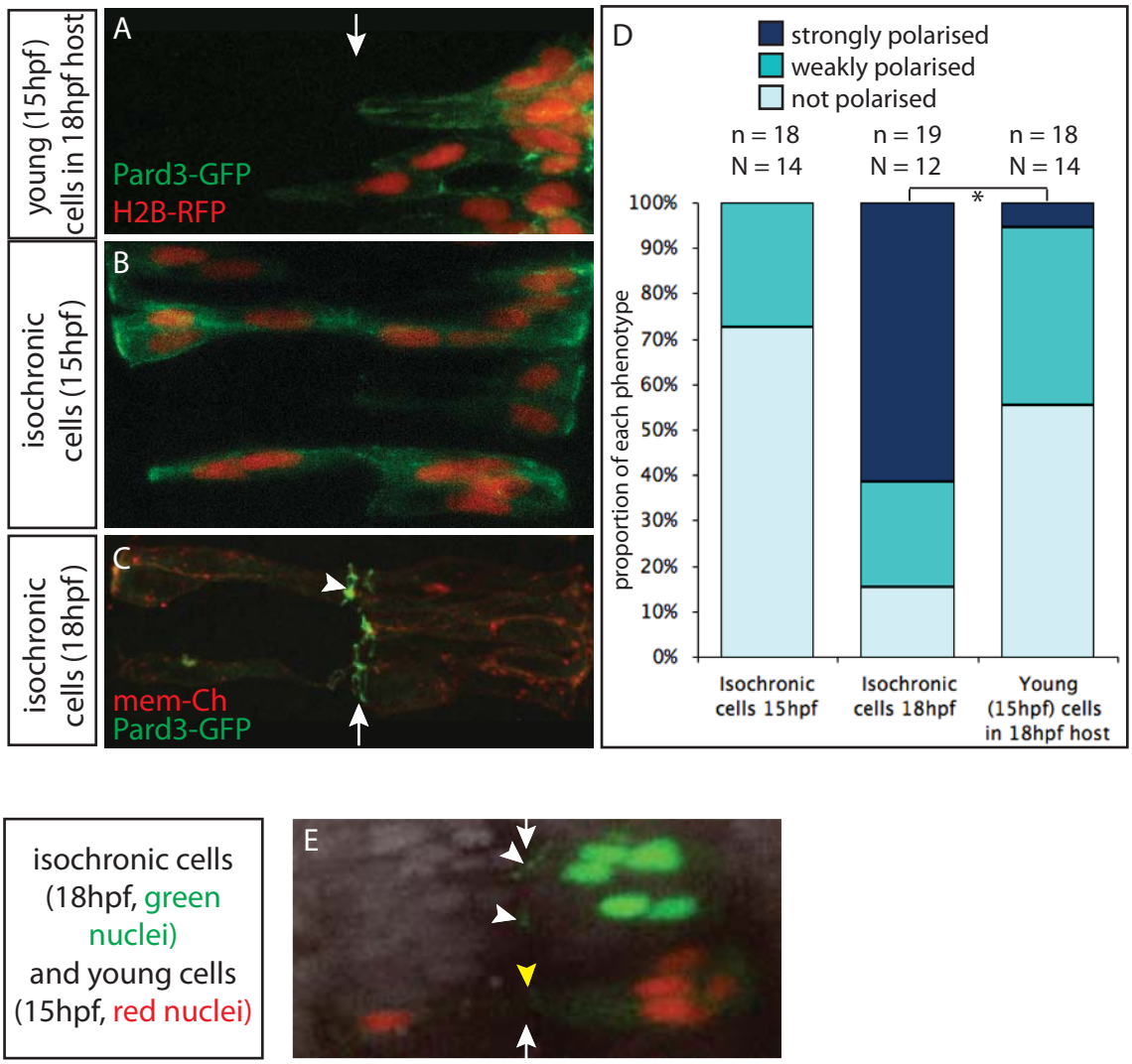

Figure 4.5 Younger transplanted cells polarise according to their age.

A-C) Confocal micrographs of transplanted cells labelled with Pard3-GFP and H2B-RFP (A,B) or Pard3-GFP and mem-Ch (C).
A) Young (15hpf) transplanted cells in an older host do not have polarised Pard3-GFP at the midline.
B) Isochronic transplanted cells at 15hpf are not polarised as Pard3-GFP is localised within the cytoplasm of the cells.
C) Isochronic transplanted cells at 18hpf are polarised with Pard3-GFP localised to the midline of the host embryo (arrowhead).
D) Graph showing the proportions of isochronic or heterochronic transplanted embryos with strongly polarised, weakly polarised or unpolarised transplanted cells. Younger transplanted cells in a older host have similar polarity to 15hpf isochronic cells, but their level of polarisation is significantly different to 18hpf isochronic cells ($p<0.01$, χ^2 test)
E) Confocal micrograph of an embryo transplanted with both isochronic (green nuclei, 18hpf) and young (red nuclei, 15hpf) cells. Isochronic cells show polarised Pard3-GFP (white arrowhead), whereas the adjacent isochronic cells remain weakly polarised (yellow arrowhead). Grey nuclei are the host nuclei.
All confocal images are from a dorsal view and anterior is up. White arrows indicate the embryonic midline.

transplanted cells (χ^2 test, $p<0.01$), but no significant difference was detected between young cells and isochronic 15hpf cells. This indicates that younger cells show a level of polarisation typical of their age. In this experiment, 5% of young transplanted cells showed strong polarisation of Pard3-GFP, which shows that a small number of cells have been induced to polarise early by the older surrounding environment. This potential modification of the intrinsic timer by the environment is considered in the discussion.

All of the analysis above compares the level of polarisation of younger transplanted cells to isochronic cells transplanted cells in different embryos. To directly compare the polarity of young and isochronic cells in the same embryo, I carried out cotransplantation of younger and isochronic cells. The two differently aged cell types were both labelled with Pard3-GFP, and also with different nuclei markers to distinguish between the two types of cells. I found that isochronic transplanted cells (green nuclei) showed polarised Pard3-GFP at the midline (arrows in fig 4.5E), but that Pard3-GFP remained mostly diffusely distributed with the cytoplasm of younger transplanted cells, with a few faint puncta of Pard3-GFP at the midline (arrowheads in fig 4.5E). Overall, I found that isochronic cells were more strongly polarised than younger cells in 73% of double transplanted embryos (N=22). The two types of transplanted cells showed the same level of polarisation in the remaining 27% of embryos, leaving zero cases when younger transplanted cells were more polarised than isochronic transplanted cells.

In summary, the lack of polarisation of most younger cells in a polarised environment shows that environmental cues are rarely able to accelerate polarisation within the younger transplanted cells, thus suggesting that age is more important than the environment for determining the timing of Pard3-GFP polarisation.

Heterochronic transplanted cells can generate ectopic apical surfaces in the host neural tube

As introduced in figure 4.2, some clusters of transplanted heterochronic cells did not integrate properly into the neuroepithelium and generated ectopic apical surfaces (fig 4.2E,F). These ectopic apical specialisations were either continuous with the host apical (lumenal) surface of the epithelium, thus named as outpockets (fig 4.6A), or completely separate from the host apical surface, forming an independent lumen (fig 4.6B). The outpockets often displayed a reticular network pattern of Pard3-GFP (fig 4.6A), which is characteristic of ZO-1 protein localisation and represents the network of rings of junctional proteins at the apical ends of cells. Optical reconstruction of a section through

the outpocket reveals that the apical surface is continuous through the cluster, and is likely to join the host apical surface at its medial extremity (fig4.6D). In contrast, clusters of cells with an independent lumen formed a rosette-like structure within one side of the host neuroepithelium, with Pard3-GFP localised to the centre of the cluster outlining a small lumen (fig4.6B,E). To confirm that the cells of the cluster were located within the host neuroepithelium, I carried out wholemount immunohistochemistry of an independent lumen for the basal marker GFAP. This revealed that the cluster of cells is indeed inside the host neuroepithelium, as GFAP staining is present around the outer edge of the cluster, continuous with the outer edge of the neural tube (fig 4.6C).

Although both old and young transplanted cells were able to form ectopic lumens, the frequency with which this occurred differed between young or old cells (fig 4.2F). I found that young transplanted cells only formed ectopic lumens in 6% of cases. However old transplanted cells formed independent lumens in 23% of embryos, and outpockets in 7% of embryos. This striking difference in the behaviour of old cells compared to young or isochronic cells is interesting as it suggests that old cells self-organise more readily than young cells within the host tissue. I reasoned that older cells may form independent structures within the host tissue because they polarise earlier than the host, and therefore there is no polarised host neuroepithelium with which to organise and align their apical specialisations. To investigate if this was true, I analysed the polarity of a cluster of older transplanted cells (red nuclei in fig 4.6F) and the surrounding host tissue (red nuclei in fig 4.6F) by whole-mount ZO-1 immunohistochemistry. This revealed that ZO-1 is strongly polarised in the centre of the small cluster of older transplanted cells (yellow arrow in fig 4.6F'), but that there are only faint spots of ZO-1 within the host tissue. This shows that the older donor cells have established apico-basal polarity ahead of the host embryo, which itself is only just beginning to polarise.

Formation of ectopic lumens is dependant on cell division

As it appears that older cells polarise earlier than the host tissue, and that the ectopic apical surface is located in the centre of the cluster of cells, we wondered if the apical specialisations were generated by cells undergoing mirror-symmetric C-division. If cell division is important for generating symmetric pairs of cells with apical specialisations located in the centre of the cluster, then blocking cell division over the period of neurulation should decrease the formation of independent lumens. Indeed, I found that blocking cell division completely abolished the formation of independent lumens by older transplanted cells (fig 4.6G). This shows that the ability of heterochronic cells to form

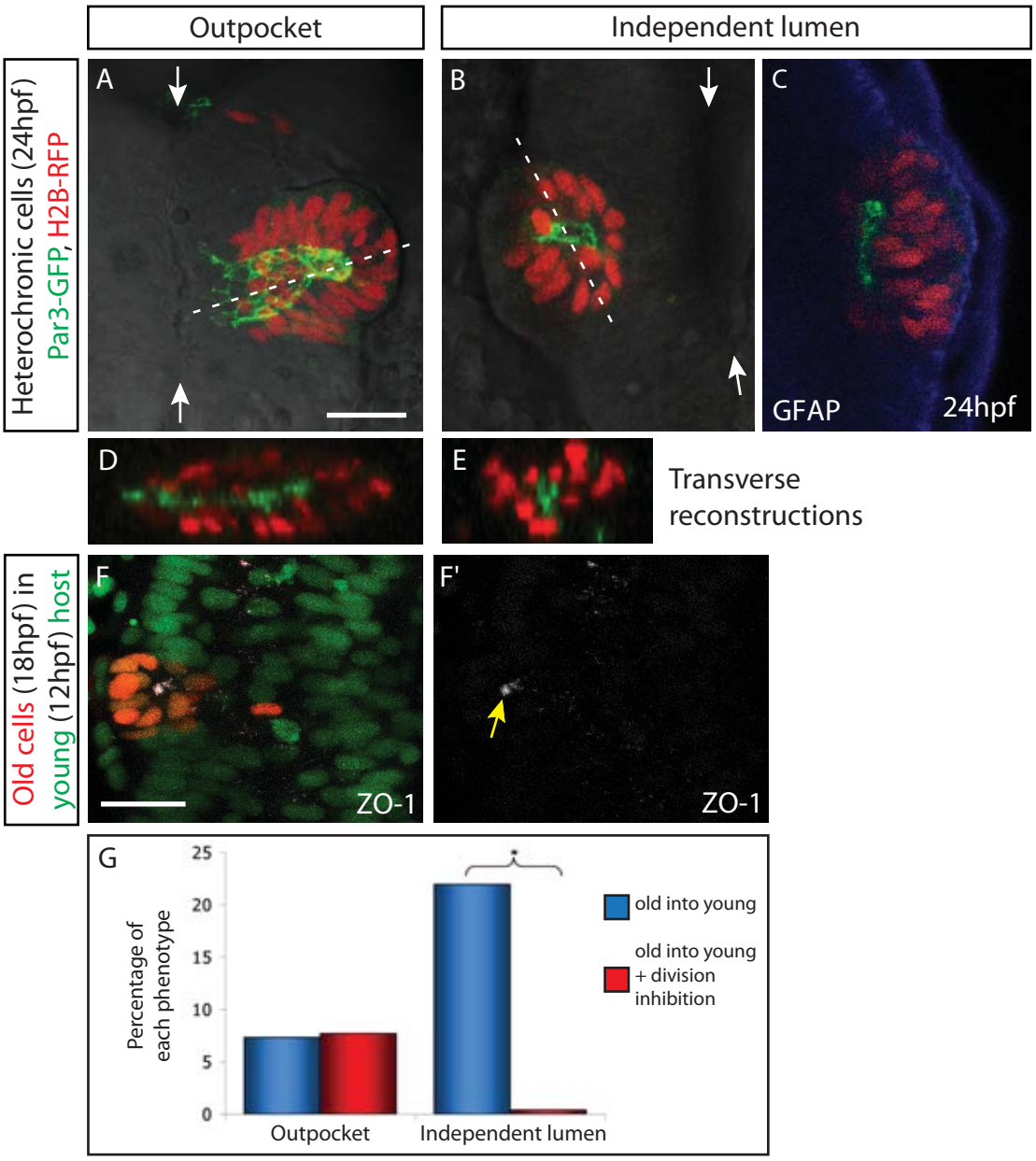

Figure 4.6 Heterochronic cells can form ectopic lumens within the host neuroepithelium.

A) Clusters of heterochronic transplanted cells can form outpockets of the host neuroepithelium. Scale bar is 25µm.

B) Some clusters of heterochronic transplanted cells form independent lumens within one side of the host neuroepithelium.

C) Whole-mount immunohistochemistry of transplanted embryos using an antibody to GFAP (blue) to reveal the basal edge of the neural tube, shows that the clusters are located within the host neuroepithelium.

D) Optical sectional reconstruction of the outpocket in A, at the level of the dotted line. Pard3-GFP is localised to the centre of the cluster and outlines a continuous lumen.

E) Optical sectional reconstruction of the cluster of cells with an independent lumen in B, at the level of the dotted line. Pard3-GFP is localised to the centre of the cluster and outlines a small lumen in the centre of the cluster.

F) Older transplanted cells (red nuclei) form a small cluster within the host tissue (green nuclei) stained for the apical marker ZO-1. ZO-1 is strongly polarised in the centre of the small cluster of older transplanted cells (yellow arrow in F'), whereas in the rest of the tissue only faint spots of ZO-1 are evident. Scale bar is 25 µm.

G) Histogram showing that the formation of independent lumens of old transplanted cells is abolished when cell division is blocked ($p<0.05$, χ^2 test).

independent lumens depends on cell division, and I assume mirror-symmetric division. It suggests that older transplanted cells undergo mirror-symmetric division precociously compared to host cells, and then self-organise by cell-cell interactions to form an ectopic apical surface in the centre of the cluster of transplanted cells.

Younger cells divide with an orientation typical of their age

As it has been shown that establishment of apico-basal polarity is tightly linked to C-division during neurulation (Tawk *et al.* 2007), I next examined the cell division behaviour of heterochronic transplanted cells during neurulation. To do this I carried out time-lapse imaging of young cells labelled with H2B-RFP, transplanted into an older host embryo, which was labelled with H2B-GFP and Pard3-Cherry. At the start of the time-lapse, the nuclei of the young cells were all strikingly positioned on one side of the host neural rod at the basal edge (fig 4.7A'). At this time point the host neural rod was not yet polarised, as shown by the arrangement of host nuclei in the midline of the neural rod (fig 4.7A), and the diffusely distributed Pard3-Ch in the host cells (fig 4.7A'). However, throughout the time-lapse as the host neural rod polarised, some young cells moved away from the basal surface towards the midline, where they divided (movie 1). This shows that the young cells were properly integrated into the host neural rod, and that they display normal interkinetic nuclear migration. By the time however that the neural rod had polarised (fig 4.7B'), the young cells were still mostly unilateral, but the nuclei were more evenly distributed throughout the apico-basal width of the neuroepithelium (fig 4.7B').

During the keel and rod stages of neurulation, neural cells divide in C-division mode in which daughter cells separate along the medio-lateral axis (fig 4.7C). However, once the apical midline has formed and the lumen has begun to open, the cell division orientation changes by 90°, so that chromosomes separate during anaphase in an axis parallel with the midline, named D-divisions (fig 4.7C). I have monitored the cell division orientation of both young transplanted and host cells after apical midline formation and classified cell divisions as C-mode, D-mode, or as O-mode if the separation of chromosomes was oriented at an oblique angle to the midline (fig 4.7C). I found that 65% of host cell divisions were D-divisions, and only 17% were C-divisions (fig 4.7D). In marked contrast however, the majority (51%) of young cells divided with an orientation typical of C-divisions, not D-divisions (fig 4.7D). This difference between the distribution of C, D, and O divisions of isochronic and young transplanted cells is highly significant ($p<0.01$), showing that the division orientation of young transplanted cells is characteristic of their

Figure 4.7 Young transplanted cells divide with an orientation typical of their age.

A,B) Confocal projections of a host embryo labelled with H2B-GFP and Pard3-Ch transplanted with young cells labelled with H2B-RFP. All images show a dorsal view and anterior is up. Scale bar in A is 25μm.

A) At early rod stage (16hpf), before Pard3-Ch has accumulated at the midline, young transplanted cells (red nuclei in A') are distributed unilaterally and nuclei are restricted to the lateral edge of the neural rod.

B) By late rod stage (18hpf), when Pard3-Ch is localised at the midline, most young transplanted cells (red nuclei in B') are still distributed unilaterally although not all nuclei remain restricted to the lateral edges of the neural rod.

C) Schematic illustrating the three different categories of cell division orientation.

D) Graph showing the number of cell divisions that follow a C mode of division, D mode of division or had an oblique angle of cleavage for host cells and young transplanted cells. A greater proportion of young cells divide with a C-mode of division orientation. The young cell division orientations are significantly different to host cell divisions $*p<0.01$, χ^2 test.

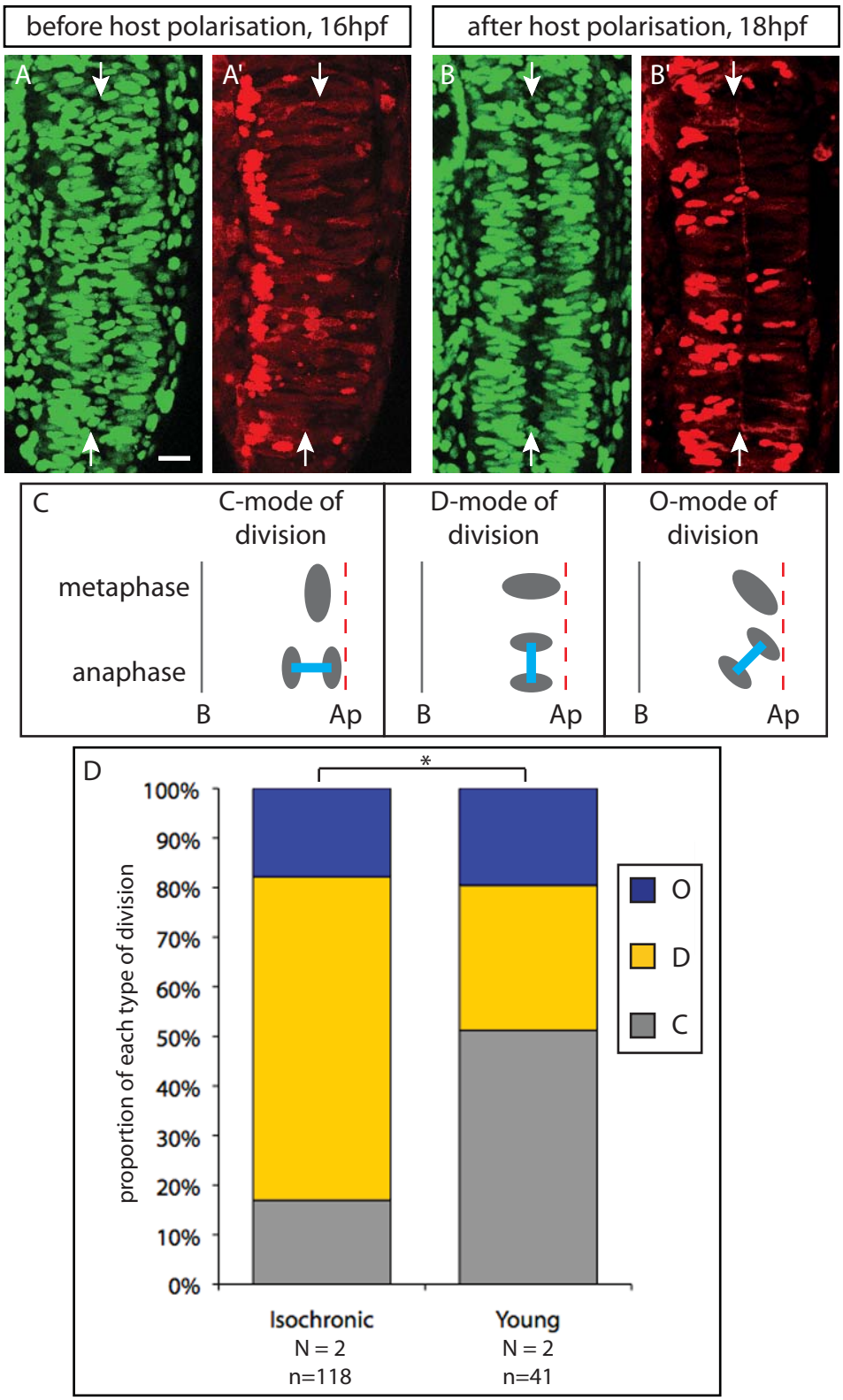

Figure 4.7 Young transplanted cells divide with an orientation typical of their age.

age despite being surrounded by an environment in which cells are dividing in a D-mode of division.

Isochronic transplanted cells cross the midline following cell division

To extend the analysis of the cell division behaviours shown by transplanted cells during neurulation I first analysed if isochronic transplanted cells behave similarly to cells *in situ*, and are able to cross the midline after cell division. Assessing midline crossing is an indirect way of measuring if cells have undergone C-division at the right time and place, because it has previously been observed that cells in the hindbrain can only cross over to the contralateral side of the neural rod after undergoing C-division close to the midline (Concha *et al.* 1998; Tawk *et al.* 2007). I analysed the location of transplanted cells within the host neural tube at 24hpf and found that isochronic transplanted cells were distributed bilaterally in the host neural tube (fig 4.8A). As cells were initially transplanted into one side of the prospective brain, this indicates that many cells have crossed the midline.

To test that cells only cross the midline after cell division, I incubated transplanted embryos in pharmacological inhibitors of cell division during the time period of neurulation. As expected, most transplanted cells remained on one side of the neural tube (fig 4.8B), and were unable to cross the midline. To further analyse the efficiency of midline crossing in embryos with and without division inhibitors, I counted how many transplanted cells were present in each side of the neural tube and calculated the percentage of successful midline crossing divisions per embryo. This calculation relies upon the assumptions that all cells will have had the chance to undergo a midline crossing division by the time of analysis at 24hpf. It has been shown that the cell cycle length of neural progenitors progressively increases during gastrulation and neurulation and is quite consistent across all cells (the standard deviation in cycle length was 9mins for divisions at gastrulation stages, and 71mins for the cell cycle leading up to the C-division, (Kimmel *et al.* 1994). This study enables us to confidently assume that by 24hpf, all cells will have gone through their midline crossing (16^{th}) cell division.

Without transplantation, tracking of neural progenitor cells through neurulation revealed that clonal progeny form bilateral pairs of sister cells in the neural tube at the end of neurulation (Kimmel *et al.* 1994). For example, in one specimen 8 out of 8 cells underwent a midline crossing division, and in a second specimen 7 out of 8 cells formed bilateral pairs (fig 4 in Kimmel *et al.* 1994). This data indicates that almost every cell in the hindbrain

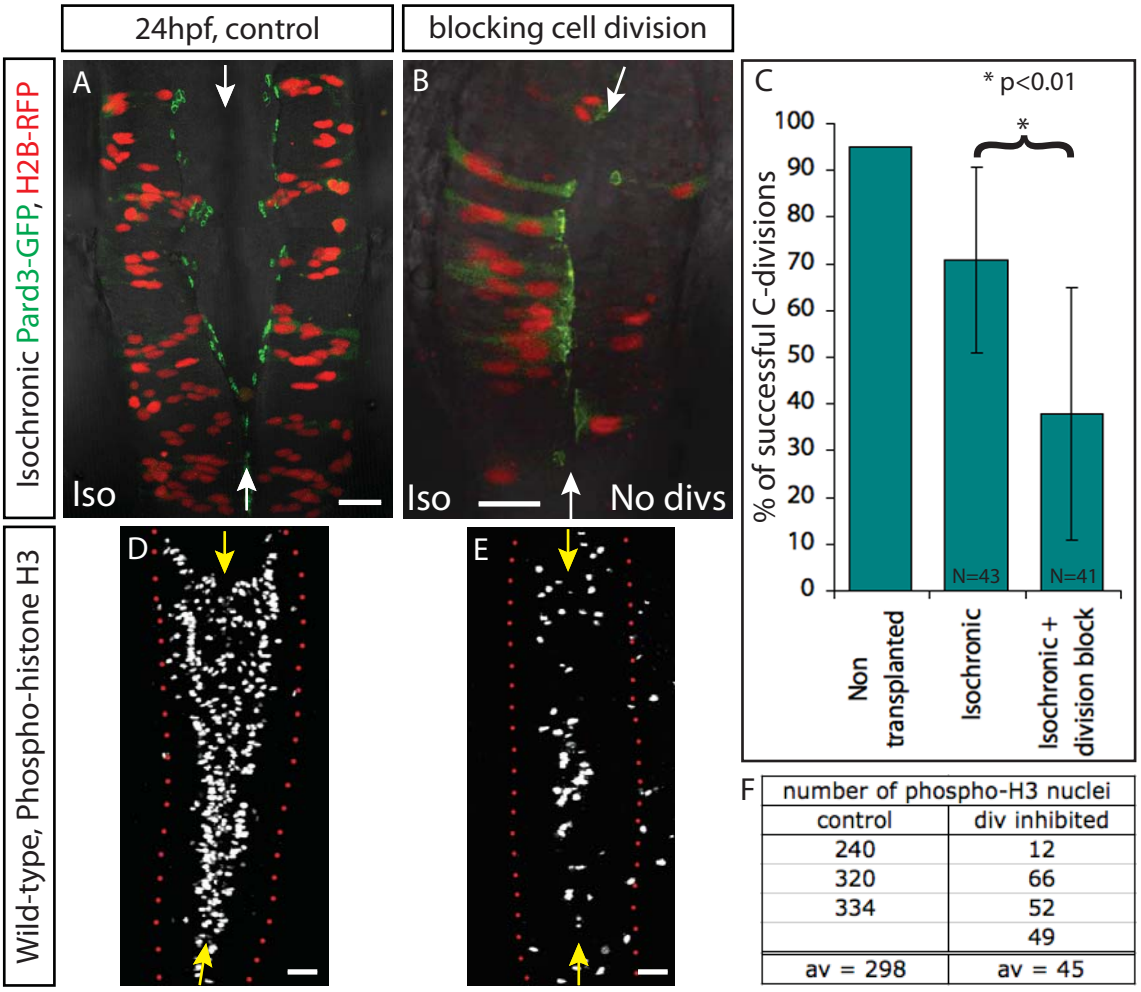

F

number of phospho-H3 nuclei	
control	div inhibited
240	12
320	66
334	52
	49
av = 298	av = 45

Figure 4.8 Isochronic transplanted cells are able to cross the midline, and inhibiting cell division reduces the efficiency of midline crossing.

A,B) Dorsal view confocal projections of isochronic transplanted cells labelled with Pard3-GFP and H2B-RFP overlaid onto brightfield images of the host embryo at 22-24hpf.
A) The bilateral distribution of transplanted cells shows that many are able cross the midline.
B) Fewer isochronic transplanted cells cross the midline when cell division is inhibited in the whole embryo during neurulation.
C) Graph showing the average number of successful C-divisions per embryo for non-transplanted cells, isochronic cells, and isochronic cells with division inhibition. Inhibiting cell division significantly reduces the number of successful C-divisions, *p<0.01, t-test. Error bars show the standard deviation.
D) Dorsal view confocal projection of a control embryo at 24hpf stained with Phospho-histone H3. Many mitotic figures are present at the apical surface of the neural tube. Red dots outline the basal edge of the neural tube.
E) Dorsal view confocal projection of a division inhibited embryo at 24hpf stained with Phospho-histone H3. The number of mitotic figures is greatly reduced compared to control embryos. Red dots outline the basal edge of the neural tube.
F) Table to show the variability in the number of phospho-histone H3 positive cells in control and division inhibited embryos.
Scale bars in each image are 25μm.

divides close to the midline at neural keel and rod stages, and that one daughter cell crosses the midline (Kimmel *et al.* 1994; Geldmacher-Voss *et al.* 2003). This is represented as an average of 95% successful C-divisions per embryo on the graph in figure 4.8C. The number of successful C-divisions of isochronic transplanted cells was slightly lower than this, at 70% on average (fig4.8C, N=43), showing that transplantation does have some affect on this behaviour of neural progenitors. Importantly though, inhibiting cell division using a mix of aphidicolin and hydroxyurea in isochronic transplanted embryos significantly reduced the number of successful C-divisions to an average of 35% (fig4.8C, N=41, t-test $p<0.01$), indicating that transplanted cells have a reduced ability to cross if cell division is inhibited.

In the presence of cell division inhibition however, the number of successful C-divisions is only halved compared to the average for isochronic transplanted embryos. If cells can only cross the midline after cell division, this percentage would be predicted to be much closer to zero. The reason why there are still 35% of successful C-divisions may be because the pharmacological inhibitors are inefficient at blocking cell division. To assess the efficiency of division block, I compared the number of mitotic figures in the neural tube at 24hpf of embryos incubated in inhibitors during the period of neurulation to control embryos. Whole-mount immunohistochemistry for phospho-histone H3 revealed that the number of cell divisions is greatly decreased in division inhibited embryos (fig 4.8E) compared to control embryos (fig 4.8D). Quantification of the reduction by counting the number of mitotic figures in control and division-inhibited embryos showed that cell division was decreased by an average of 85% in division-inhibited embryos (average number of mitotic figures in control = 298, N=3, average number of mitotic figures in division inhibited = 45, N=4). The extent of division inhibition was also variable across embryos, as the number of mitotic figures was as low as 12 in one embryo but as high as 66 in another (fig 4.8F). The inefficient division block and the variability of this inhibition across embryos could explain why the number of cells that have crossed the midline is not closer to zero.

Heterochronic transplanted cells cross the midline less efficiently than isochronic transplanted cells.

Having characterised the midline crossing behaviour of isochronic transplanted cells, I next carried out heterochronic cell transplantations to test whether the age of a cell or its environment controls midline crossing and cell division during neurulation. I assessed midline crossing of heterochronic cells at 22-24hpf. If heterochronic cells cross the

midline with the same frequency as isochronic cells, this shows that the environment controls this behaviour. However, if heterochronic cells have a reduced ability to cross the midline, this suggests that the age of cells is critical to midline crossing behaviour. As introduced in figure 4.2 I found that both ages of heterochronic transplanted cells were able to integrate into the host neuroepithelium. The transplanted cells spanned the whole apico-basal width the neuroepithelium (fig 4.9A-C), and showed normal apico-basal polarity with Pard3-GFP localised to the ventricular surface of the host neural tube by 24hpf (arrowhead in fig 4.9B,C). Moreover, in both types of heterochronic transplants, cells were predominantly located on one side of the neural tube (fig 4.9A-C), suggesting that they have a reduced ability to cross the midline.

To determine the defects in cell crossing behaviour of heterochronic transplanted cells in a quantitative manner, I counted the number of heterochronic transplanted cells on each side of the neural tube and calculated the percentage of successful C-divisions for each embryo. Only heterochronic transplanted cells that were properly integrated into the host neuroepithelium were counted to ensure a valid comparison to data from isochronic transplanted embryos. The histograms show the distribution of isochronic (fig 4.9D) or heterochronic (fig 4.9E,F) transplanted embryos according to the number of successful C-divisions per embryo. In most isochronic transplanted embryos, between 60 and 90% of transplanted cells per embryo had undergone a successful C-division. In contrast, for both types of heterochronic transplants, 50% of embryos showed transplanted cells of which only 0-9% had undergone a successful C-division. The box plot (fig 4.9G) summarises this crossing efficiency data, and clearly shows the higher median percentage of 73% of isochronic cells that have undergone a successful C-divisions compared to the 8% for young transplanted cells and 17% for old transplanted cells. Furthermore, the interquartile range for isochronic cells (IQR, central rectangle in each plot) is much higher for isochronic transplants and does not even overlap with the IQR for either type of heterochronic transplant. Statistical tests confirm that embryos transplanted with older or younger cells show a significantly lower number of cells that have undergone a successful C-division compared to isochronic transplanted embryos (KS test, $p<0.01$). This reduction in successful C-divisions shows that heterochronic transplantation effectively reduces midline crossing behaviour, and implies that heterochronic cells are unable to undergo a mirror-symmetric division at the midline of the host neural keel or rod.

Figure 4.9 Heterochronic transplanted cells have a reduced ability to cross the midline.

A-C) Confocal projections of heterochronic transplanted cells labelled with Pard3-GFP and H2B-RFP, overlaid on brightfield images of the host embryo at 22-24hpf. All images show a dorsal view and anterior is up. White arrows indicate the midline. Arrowheads indicate Pard3-GFP localised at the ventricular surface of the neural tube. Scale bars are 25μm.

A) Young transplanted cells can integrate and disperse within the host neural tube.

B) Young transplanted cells sometimes cluster within the host neural tube.

C) Old transplanted cells can integrate and disperse within the host neural tube.

D-F) Histograms showing the distribution of isochronic transplanted embryos according to the percentage of successful C-divisions per embryo.

D) In most embryos transplanted with isochronic embryos cells, between 60 and 90% of transplanted cells have undergone a successful C-division.

E) In over 50% of embryos transplanted with young cells, only 0-9% of transplanted cells have undergone a successful C-division.

F) Similar to young cells, in 50% of embryos transplanted with old cells, only 0-9% of transplanted cells have undergone a successful C-division.

G) Box plot summarising the distribution of isochronic and heterochronic transplanted embryos according to the percentage of successful C-divisions per embryo. Embryos transplanted with older or younger cells show a significantly lower number of cells that have undergone successful C-divisions compared to isochronic transplanted embryos. *$p<0.01$, KS-test. Unfilled circles represent suspected outliers.

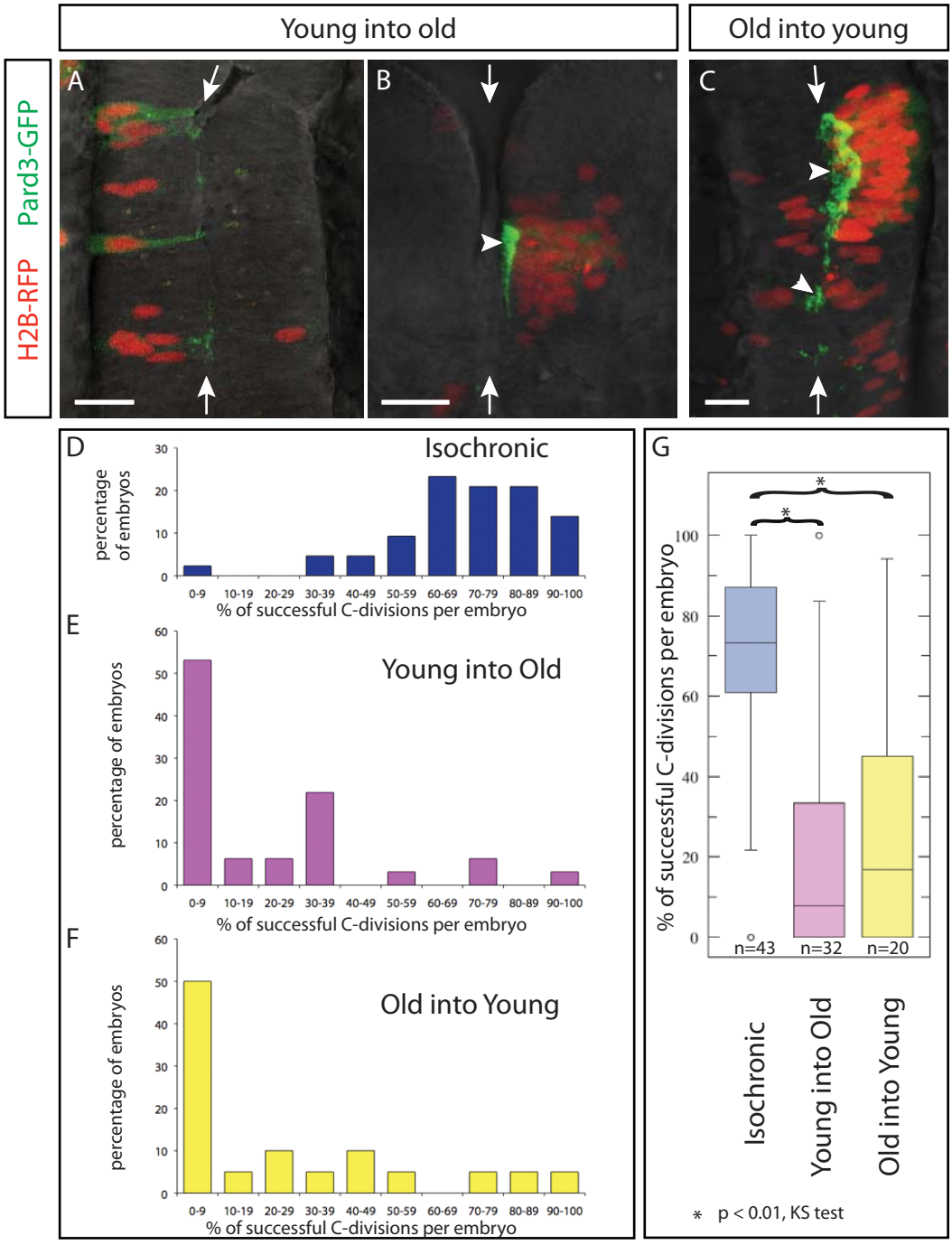

Figure 4.9 Heterochronic transplanted cells have a reduced ability to cross the midline.

Cell clustering or the number of cells does not affect the midline crossing behaviour of heterochronic transplanted cells

Although heterochronic transplanted cells showed a reduced ability to cross the midline, it was necessary to carry out several controls to ensure that this result was reliable. One of the main concerns with the data focused on the possible effect of cell clustering in the heterochronic transplants. If cells cluster together they could create their own microenvironment and this would not then test the intrinsic nature of the crossing behaviour of heterochronic cells. To determine if cell clustering affected the ability of transplanted cells to cross the midline I compared the percentage of successful C-divisions between clustered and dispersed phenotypes in both types of heterochronic transplants. The frequency histograms show that the probability of midline crossing is the same for clustered cells as it is for unclustered cells, as for both clustered and dispersed phenotypes, the highest proportion of embryos contained only 0-9% of successful C-divisions in both types of heterochronic transplants (fig 4.10A,B). Finally, statistical tests comparing the percentage of C-divisions in dispersed and clustered phenotypes found no difference between the two groups (KS test). These comparisons show that clustering does not alter the ability of cells to cross the midline.

In conjunction with the analyses of clustered versus dispersed phenotypes, I also analysed if the number of transplanted cells per embryo affected the number of successful C-divisions. This was especially a concern for the heterochronic transplants in which a larger group of transplanted cells may have a greater tendency to cluster together which would not be a stringent test of the timer hypothesis. To investigate if the total number of transplanted cells affected the percentage of successful C-divisions per embryo, I plotted the number of transplanted cells in each embryo against the corresponding percentage of successful C-divisions values for that embryo on a scatter plot (fig 4.10C-E). This should reveal any potential correlation between the two variables. The broad scattering of points on all three graphs show that there is no correlation between the number of transplanted cells and the percentage of C-divisions for isochronic of heterochronic transplants. Calculation of the Pearsons Rank Correlation Coefficients (r) for each set of data confirm that there is no correlation between the total number of transplanted cells and the percentage of successful C-divisions in each embryo, as an r value of 0 indicates no correlation (isochronic: r=0.03, young into old: r=0.005, old into young: r=0.06).

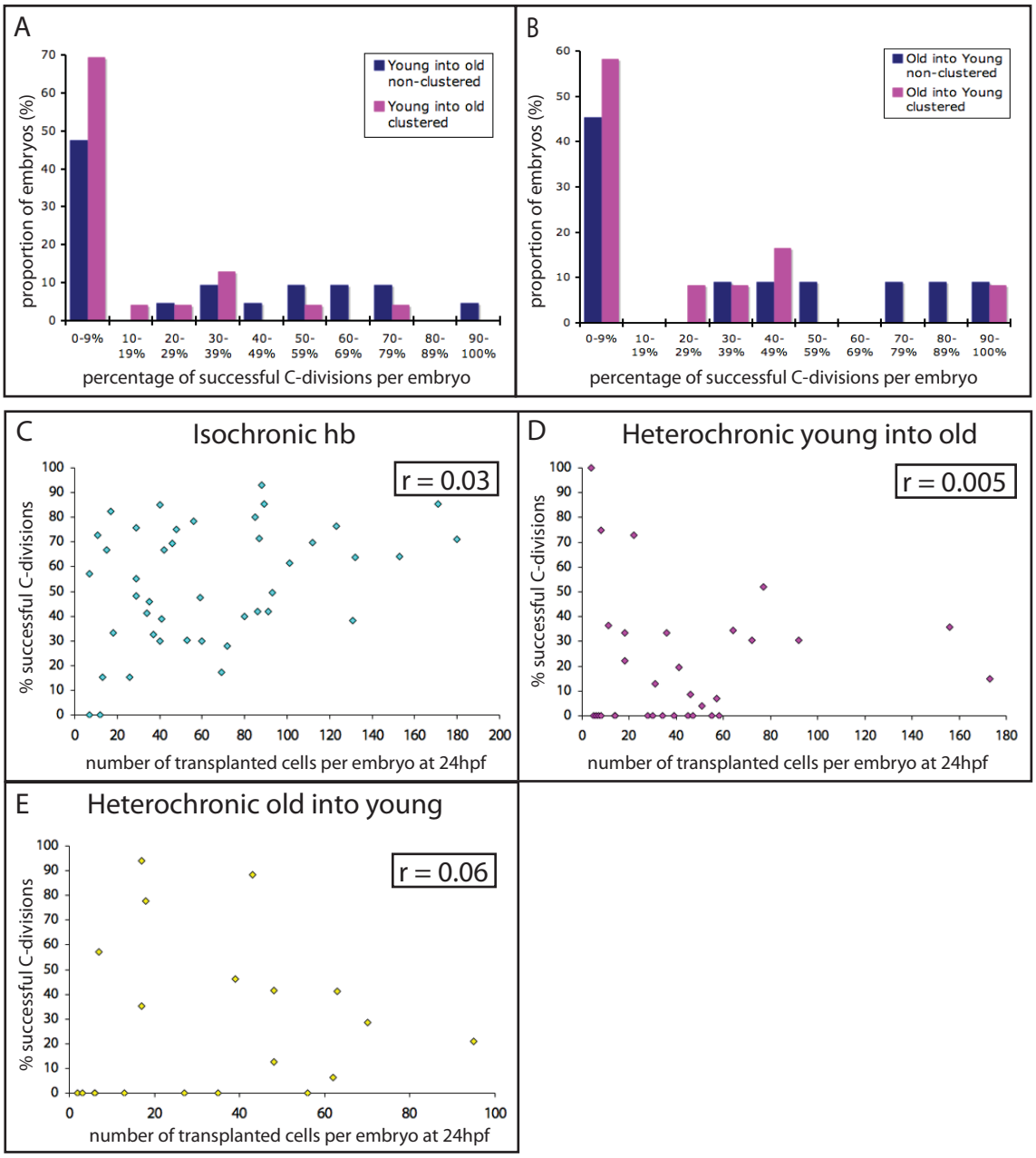

Figure 4.10 Clustering and the total number of transplanted cells does not affect the crossing behaviour of heterochronic transplanted cells.

A,B) Histograms comparing the proportions of embryos (in %) against the number of successful midline crossing divisions for clustered and dispersed phenotypes in each type of heterochronic transplant.
A) In embryos transplanted with young cells, the greatest number of embryos had 0-9% of successful C-divisions in both clustered and dispersed phenotypes.
B) Similarly, in embryos transplanted with old cells, the greatest number of embryos had 0-9% of successful C-divisions in both clustered and dispersed phenotypes, showing that clustering does not affect the efficieny of midline crossing.
C-E) Scatter graphs showing that the number of transplanted cells does not affect the efficiency of midline crossing. Each point represents a single specimen and shows the number of successful C-divisions of transplanted cells plotted against the total number of transplanted cells for that embryo. There is no correlation between the number of transplanted cells and efficiency of midline crossing for isochronic transplants, for young cells transplanted into an older embryo or for old cells transplanted into a young embryo. r indicates the Pearson's rank correlation coefficient for each data set.

The antero-posterior location of transplanted cells affects midline crossing, but heterochronic cells still show a reduction in midline crossing

A second concern raised in the analysis of cell crossing in heterochronic transplants was that the anterior-posterior location of transplanted cells could affect the ability of midline crossing. It was important to investigate this possibility because I observed that heterochronic transplanted cells, particularly old cells, were often located in the midbrain and diencephalic regions of the brain. This was in contrast to isochronic cells, which were mostly located in the hindbrain. Although I did attempt to target heterochronic cells to the hindbrain, it proved technically difficult to do this reliably because of the time difference between donor and host embryos at the time of transplantation. As most studies of the behaviour of neural progenitor cells during neurulation have focused on hindbrain and anterior spinal cord regions, it is not clear if cells in more anterior regions of the brain show a similar midline crossing behaviour. Therefore I transplanted isochronic cells into prospective midbrain and diencephalic territories at gastrula stages, and assessed midline crossing at 24hpf.

I found that isochronic transplanted cells targeted to the midbrain and diencephalon can integrate into the host neural tube (fig 4.11A), as shown by their spindle-shaped morphology that is similar to transplanted cells located in the hindbrain (fig 4.11B). Initially cells were transplanted into one side of the prospective midbrain or diencephalon, so the bilateral distribution of transplanted cells reveals that they are able to cross the midline (fig 4.11A). I also found that transplanted cells in the midbrain and diencephalon tend to disperse less than isochronic cells targeted to the hindbrain (compare fig 4.11A to B), which has also been observed before in fate-mapping studies of neural progenitor cells (Kimmel *et al.* 1994).

To further assess the crossing behaviour of cell in the midbrain and diencephalon, I calculated the number of transplanted cells that undergo a successful C-division per embryo. This revealed that the average percentage of successful C-divisions in midbrain and diencephalic brain regions is 53% (fig 4.11C), which is significantly lower than the efficiency of midline crossing in hindbrain isochronic transplants ($p<0.01$, t-test and KS-test). As this analysis showed that anterior-posterior location could affect the crossing behaviour of cells, I then compared the midline crossing frequency of isochronic midbrain/diencephalon transplants back to the heterochronic transplant data (fig 4.11D). The box plot displays the distribution of isochronic midbrain/diencephalon and

heterochronic transplanted embryos according to the number of successful C-divisions per embryo. The median percentage of successful C-divisions for isochronic cells in midbrain/diencephalic areas is 57% (reduced from 73% for hindbrain regions), and the IQR is also now closer to the IQR of the heterochronic transplants. Nonetheless, heterochronic transplanted cells still show a significant reduction in the number of successful C-divisions compared to isochronic midbrain and diencephalon transplanted cells ($p<0.01$, KS test).

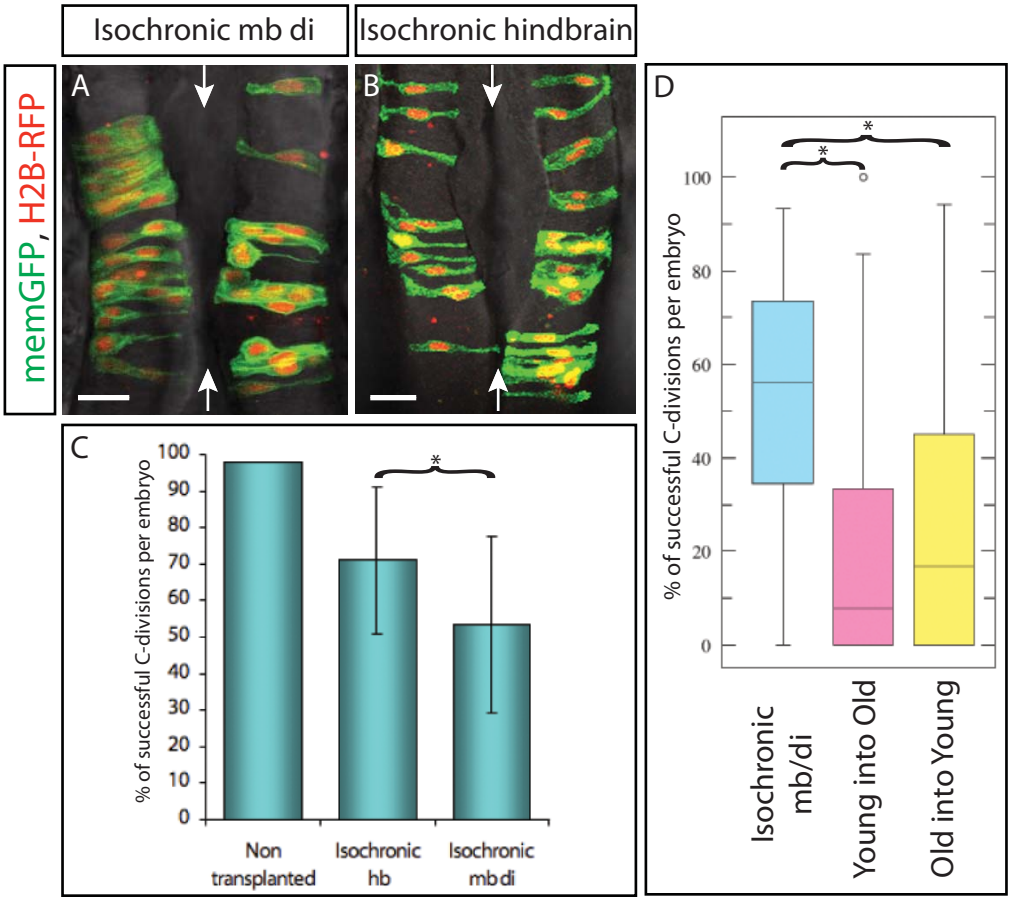

Figure 4.11 The antero-posterior location of isochronic transplanted cells affects the efficiency of midline crossing, but heterochronic transplanted cells still show an impairment in midline crossing.

A,B) Confocal micrographs of isochronic transplanted cells labelled with memGFP and H2B-RFP overlaid onto the bright-field image of the host neural tube. In both images are from a dorsal view and anterior is up. Scale bars are 25µm.
A) Isochronic transplanted cells in the midbrain and diencephalon integrate into the host neural tube, but tend to disperse less than hindbrain targeted cells.
B) Isochronic transplanted cells in the hindbrain.
C) Graph showing the average number of successful C-divisions of isochronic cells transplanted into the hindbrain (hb) or midbrain and diencephalon (mb di). The number of successful C-divisions is significantly lower in the midbrain and diencephalic areas than the hindbrain. *p<0.01, t-test and KS test. Error bars indicate the standard deviation.
D) Box plot displaying the distribution of the number of successful C-divisions per embryo in isochronic midbrain/diencephalon and heterochronic transplanted embryos. Embryos transplanted with older or younger cells still show a significantly lower number of cells that have undergone successful C-divisions compared to isochronic midbrain/diencephalon transplanted embryos. *p<0.01, KS-test.

4.5 DISCUSSION

The main aim of this chapter was to use heterochronic cell transplantation to address if apical polarisation and the mirror-symmetric cell division are regulated by an intrinsic timing mechanism rather than environmental signals. I assessed three cell behaviours of the transplanted cells during neurulation: the time of establishment of apico-basal polarity in transplanted cells, the orientation of cell division, and the ability of the cells to cross the midline.

An intrinsic timer can explain heterochronic cell behaviour during neurulation

My findings are consistent with the intrinsic timer hypothesis, as heterochronic cells showed behaviours typical of their age, not the age of their surrounding environment. I found that firstly, young cells are delayed in their polarisation compared to the host embryo, secondly that they divide with an orientation typical of C-divisions when the host cells divide with D-division orientation, and thirdly, that young cells have a reduced ability to cross the midline. I also found that old cells polarise prematurely compared to the host embryo, that they have a reduced ability to cross the midline, and also that they can self-organise within the host neuroepithelium to generate ectopic apical surfaces. These heterochronic transplant results are summarised in the schematic diagram in figure 4.12, which proposes a model to explain the observations of transplanted cell behaviours during neurulation.

When older cells are transplanted into younger hosts (fig 4.12A), older donor cells (grey) undergo mirror-symmetric division and cell polarisation prematurely compared to host cells (white). They thus form a precocious ectopic apical specialisation as the host cells are not yet polarised. They then either integrate fully into the host neural tube, and their polarity aligns with that of the host, or the apical surface remains ectopic and forms an independent lumen or outpocket within the host neuroepithelium. Conversely, younger cells (grey) transplanted into an older embryo undergo C-division late, after the host cells (white) have already established well-defined apico-basal polarity and when a host lumen may even be present (fig 4.12B). The younger cells are therefore unable to cross to the contralateral side of the neural tube, even if they do attempt to undergo a mirror-symmetric C-division.

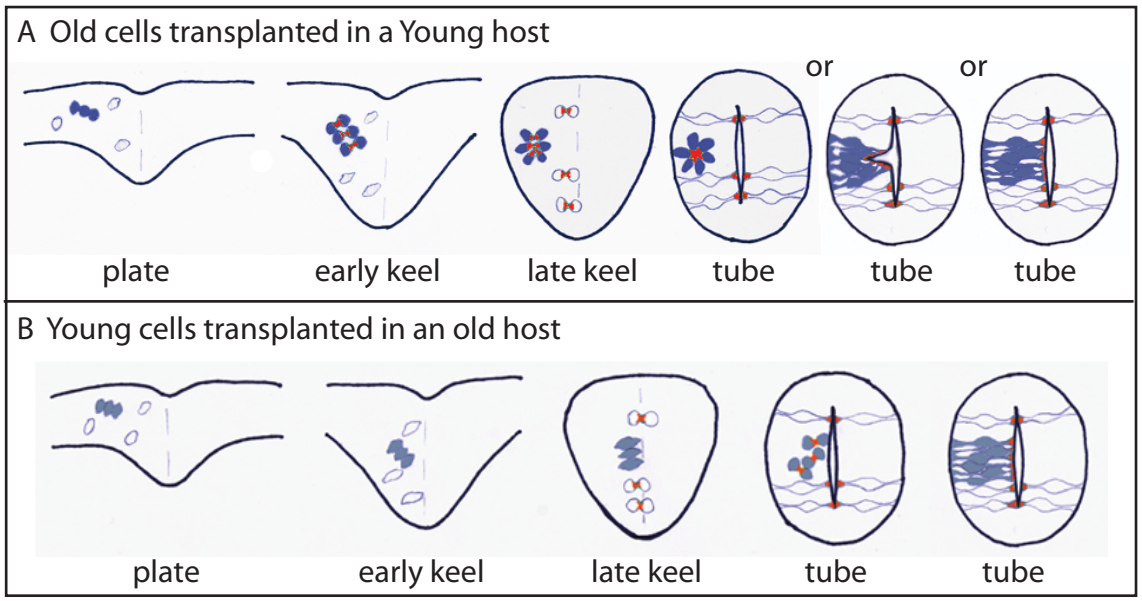

Figure 4.12 Schematic diagram to illustrate the cell behaviours of heterochronic transplanted cells.

A) Schematic showing the early polarisation behaviour of older cells transplanted into a younger host embryo. The older cells polarise and undergo mirror-symmetric cell division early. They can form ectopic lumens within the host neuroepihtelium that are either independent from the host lumen, form an outpocket of the host neuroepithelium. They also can integrate fully into the host neuroepithelium but most cells remain unilateral.

B) Schematic showing the late polarisation of young transplanted cells in an older host embryo after the lumen has begun to open in the host tissue. The young cells undergo mirror-symmetric cell division later than host cells, and therefore cannot cross the midline. They are able to integrate fully into the host neuroepithelium but most cells remain unilateral.

Properties of the intrinsic timer

All heterochronic transplants were carried out early in zebrafish development, mostly even before gastrulation. Firstly, this implies that the timer is therefore initiated before cells are committed to a neural fate and that it is unrelated to the process of neural induction. The commitment of hindbrain precursor cells to a neural lineage occurs after shield stage, because when moved from their dorsal location to a ventral region where cells are fated to become neural crest, epidermis or somites, they changed fate to match their new location (Woo *et al.* 1998). Secondly, it is surprising that the timer is able to resist the many environmental signals and cell-cell interactions that take place during the extensive morphogenetic movements of epiboly, gastrulation and neurulation that could reset it. Finally, the timer must continue to operate through several rounds of cell division after transplantation. Using the careful documentation of the average cell cycle length at these stages (Kimmel *et al.* 1994), it is possible to estimate that cell younger cells are likely in their 12th cell cycle at the time of transplantation, and that older cells are probably in their 14th cell cycle. Therefore, as cells often undergo C-division on their 16th cell cycle (Kimmel *et al.* 1994), the timer must be able to operate through at least 4 rounds of cell division.

The formation of ectopic lumens by older transplanted cells shows the power of mirror-symmetric division for generating polarity.

Older transplanted cells are able either to integrate fully into the younger host neuroepithelium or form ectopic lumens. The reasons why older cells form one type of phenotype or the other are not obvious, but there are several possible explanations. It may depend on the clustering of the transplanted cells. If they form a compact group of cells that divide and polarise in coordination with each other, then the cluster might form an independent lumen within the host neural tissue. If the cells are more dispersed, or polarise in a less ectopic location, then the group of donor cells may be able to integrate better into the host neuroepithelium and align their apical surface with the host cells (fig 4.12A). It is not likely that the formation of an ectopic lumen or integrated phenotype depends on the number of cells in the cluster, because the number of cells in an ectopic lumen or outpocket can vary, as can the number of cells in an integrated cluster, and these numbers are overlapping (data not shown). However, it could depend on the location of polarising cells within the neural plate. If donor cells are more lateral in the neural plate, they may polarise in a more ectopic location compared to more medially located cells, and thus form an ectopic lumen rather than an outpocket or fully integrated cluster.

Both old and young heterochronic transplanted cells can form ectopic lumens within the host neuroepithelium, but older transplanted cells show this phenotype more frequently than young transplanted cells that polarise more often with the correct orientation. As the older donor cells polarise precociously compared to host tissue, they are perhaps more than young cells able to form independent lumenal surfaces because the host embryo is not yet polarised and therefore they do not have an apico-basal axis into which they have to integrate. Early polarisation may then be maintained by the establishment of stable junctional complexes with neighbouring donor cells also polarising at the same time, which persist even when the host embryo neuroepithelium forms. Even a single transplanted cell isolated from other transplanted cells would have a sister cell with which it could maintain contact once it had undergone cell division. In contrast, younger cells may be aligned by extrinsic cues from the already polarized older host tissue and are thus more likely to integrate without making ectopic luminal surfaces.

Interestingly, I found that cell division affected the frequency of formation of ectopic lumens. Older transplanted cells formed independent lumens more often than outpockets but when division was inhibited this abolished the formation of independent lumens. This suggests that mirror-symmetric division is required to form pairs of sister cells with the apical specialisations aligned in the centre of the cluster during independent lumen generation. If mirror-symmetric division is blocked then the cells may still polarise, but in a less coordinated fashion, so that apical specializations are not organised to the centre of the cluster. Then later as the host polarises, the apical edge of the donor cells can join up with the host apical surface to generate an outpocket, not a completely independent lumen.

The best way to analyse transplants and resolve some of this speculation about how the transplanted cells actually behave would be to carry out time-lapse imaging during neurulation. It is however technically difficult to do this type of analysis as it is difficult to find the small number of transplanted cells and follow then for long periods of time during this embryonic period of extensive morphogenesis.

Why do some heterochronic cells behave the same as isochronic cells?

In all heterochronic transplant assays, the transplanted cells showed some variability in their behaviour, and some behaved similarly to isochronic cells. There are several reasons that could account for why transplanted cells show this variability. The technique of cell transplantation itself may increase variability in the behaviour of heterochronic

transplanted cells, as even in isochronic transplants the average number of successful C-divisions per embryo was less than non-transplanted cells. I am not sure why transplantation affects cell behaviour in this way, but perhaps transplanted cells take time to recover from the procedure, although it does not seem disruptive enough to cause cell death in most cases.

Relative difference between heterochronic donor and host cell behaviours in time

Some heterochronic transplanted cells may behave the same as isochronic cells because of the natural variation in the timing of cell behaviour during neural tube development. In wild-type embryos, the time period over which mirror-symmetric C-division takes place is 2-3 hours (Kimmel *et al.* 1994). Cell polarisation in the neural rod also occurs over a certain time period, it is not instantaneous. Therefore as heterochronic transplanted cells are only three hours older or younger compared to cells in the host embryo, there is likely to be an overlapping period in which donor and host cells are undergoing cell division and polarisation at the same time. This natural host heterochrony can explain why some heterochronic cells appear to act the same as isochronic cells, and also explains why in all of the assays there is a variation in the behaviour of cells of a particular age.

Moreover, embryos do not all develop synchronously, and there must be variation among the actual time difference of donor and host cells, which could affect the phenotype of the transplanted cells. Cells are transplanted early in development to give them sufficient time to recover from any stress associated with the transplantation procedure. However after the point of transplantation, the exact age of donor cells within the host cannot be monitored. If transplantation does slightly delay donor cells in their development, the time difference between young transplanted cells and the older host embryo would be increased, but the time difference would be decreased between older cells and a young host embryo. This would therefore increase the likelihood of older transplanted cells undergoing midline crossing and polarisation coincidentally with host cells. Indeed the midline crossing efficiency of old into young heterochronic transplants is slightly higher compared to young cells transplanted into an older embryo.

Another factor contributing to the slightly higher percentage of midline crossing divisions for older transplanted cells could be that when older cells undergo C-division and polarise early there is nothing preventing the medial daughter cell from crossing over the midline in terms of the structure of the neural keel. Later when the host neuroepithelium becomes

polarised, the donor cell apical specialisations may become aligned with the host apical surface resulting in pairs of sister cells separated across the midline.

Possible influence of the environment on cell polarisation

I cannot rule out the possibility that extrinsic factors could have a small influence the behaviour of heterochronic cells as a small number of heterochronic cells do behave similarly to host cells. The environment of the neural rod may influence the polarisation and orientation of division of heterochronic transplanted cells, especially young cells. In order to establish apico-basal polarity, cells must make junctional contacts with neighbouring cells that are also becoming polarised at the same time. Therefore it would not be surprising if the polarised host environment surrounding young transplanted cells could partially induce them to polarise. This may be true in a small number of heterochronic transplants, because in 5% of embryos young cells in an 18hpf host are strongly polarised, whereas no isochronic cells at 15hpf show strong polarisation (fig 4.5D). However, the polarisation level of young cells and isochronic 15hpf cells are not significantly different ($p>0.4$), showing that in general young cells show cell polarisation typical of their age.

Potential caveats to using the technique of cell transplantation

In some heterochronic transplanted embryos donor cells showed a clustered phenotype at 24hpf, presumably having remained clustered together from the time of transplantation through to 24hpf. This clustering of donor cells never occurs in isochronic transplants and could be a concern because clustered heterochronic cells could create their own microenvironment and therefore this would not be a stringent test of the timing hypothesis. It has been shown that when neural cells do not express the appropriate Eph or Ephrin combination for their hindbrain rhombomere, cells could form tight clusters restricted to the lateral edge of one side of the neural rod and were not able to cross the midline after cell division (Kemp *et al.* 2009b). I only included integrated heterochronic cells that spanned the whole width of the neuroepithelium at 24hpf in my midline crossing analysis, to avoid this complication. Moreover my analysis has shown that there is no difference in the efficiency of midline crossing between clustered and dispersed phenotypes, and that the number of transplanted cells also does not affect the efficiency of midline crossing.

I also investigated if the antero-posterior location of transplanted cells could affect midline crossing. Although I found that the number of successful C-divisions of transplanted cells

located in the midbrain and diencephalon was significantly lower than those located in the hindbrain, the efficiency of midline crossing of heterochronic transplanted cells was still significantly lower than midbrain and diencephalic isochronic cells.

Speculation on the mechanism of the intrinsic timer

As noted in chapter 3, the polarisation of neural cells on time but in ectopic locations in embryos with delayed convergence suggests that the local environment of the neural tissue is not important for regulating cell polarisation. The precocious polarisation of older transplanted cells also shows that a younger neural environment is permissive for early polarisation if cells have reached the right age, even if they are located ectopically. In addition, the my results argues against a timed signal from the surrounding environment that directs neural cell polarisation at a particular developmental time, because older cells polarise in a young host embryo and younger cells show a delayed polarisation in an older host. These experiments do not however rule out that neural cells have to reach a certain age (or competence) to be able to respond to an environmental signal. However this itself could be part of the intrinsic timer.

Interestingly the cell autonomy of directed and random migration of endodermal cell movements during gastrulation has been examined using heterochronic transplantation. In these experiments, older or younger transplanted cells always showed movements typical of the host embryo age (Pezeron *et al.* 2008), thus demonstrating that these movements are governed by environmental signals. This may indicate that the environment might generally controls cell movements, whereas a timer could control cell division and polarisation, and fits with the observation that cell division and polarisation become uncoupled from morphogenetic movements in the embryos with delayed convergence. Alternatively, the relative contribution of the extrinsic and intrinsic factors for controlling cell behaviour during development may be different for endoderm precursors and neural precursors. I have begun to test a possible role for the neural environment in polarisation in more depth in the next chapter.

CHAPTER 5 TESTING THE ROBUSTNESS OF THE POLARISATION TIMER

5.1 INTRODUCTION

Abnormal neural environment

My previous results suggest that an intrinsic timer may be more important than the local environment in regulating neural cell polarisation. One way to test the importance of the structure of the neural environment for the correct timing of neuroepithelial cell polarisation is to study the generation of polarity in mutants that have abnormal neural tube morphogenesis. There are several zebrafish mutants suitable for this study, including *trilobite,* and Maternal Zygotic *one-eyed pinhead* (MZ*oep*). As a result of abnormal morphogenesis, both mutants show a disorganised neural tube at 24hpf (fig 5.1), but importantly the neuroepithelial cells are polarised as assessed by immunohistochemistry for the basal marker GFAP and the apical marker ZO-1 (fig 5.1).

The *trilobite* mutant

The *trilobite* mutant line has a mutation in *vangl2*, a component of the PCP signalling pathway that is required for efficient convergent extension movements during gastrulation and neurulation (Sepich *et al.* 2000). *tri* mutants have a wider neural plate than wild-type embryos at the beginning of neurulation, and neural cell movements towards the midline are delayed throughout neurulation. By the end of neurulation, the Z*tri* neural primordium displays an abnormal structure of duplicated neural tubes side by side (fig 5.1B,E,H) (Tawk *et al.* 2007). The duplications are caused by ectopic mirror-symmetric divisions occurring in the superficial-deep axis of the delayed neural plate (Tawk *et al.* 2007). The pairs of sister cells from these divisions remain in register, and as apical proteins are targeted to the abscission plane of the sister cells, an apical plane is generated sandwiched between the superficial and deep surfaces of the delayed primordium (Tawk *et al.* 2007). The cells seem to divide roughly on time even though they are in the wrong place, but the precise timing of the establishment of apico-basal polarity in *tri* mutants remains to be determined.

The MZ*oep* mutant

Figure 5.1 *tri* and MZ*oep* mutants generate abnormal neural tubes with defective apico-basal organisation.

A-C) Dorsal view confocal projections of a whole-mount wild-type, *tri* and MZ*oep* embryos stained for the apical marker ZO-1 (green) and the basal marker GFAP (red). Anterior is up in all pictures.

A) The neural tube of a wild-type embryo shows well-organised apico-basal polarity with ZO-1 at the ventricular surface, and GFAP lining the outer edge of the tube.

B) The neural tube of a *tri* embryo has relatively well-organised apico-basal polarity, but in the posterior hindbrain and anterior spinal cord regions (bracket), the apical surfaces are duplicated (yellow arrows), and GFAP is localised ectopically sandwiched between the two midlines (white arrow) in addition to its basal location at the edges of the tube.

C) MZ*oep* mutant embryos generate aberrant neural tube morphology and abnormal apico-basal polarity organisation (arrowheads indicates ectopic apical foci of ZO-1 expression).

D-I) Transverse cryostat sections through the neural tube of wild-type, *tri* and MZ*oep* embryos at 24hpf stained for ZO-1 (D,F) aPKC (E) or GFAP (G-I). Yellow dots indicate the basal edge of the neural primordium in D-F, while green dots indicate the apical surface in G and H.

D) In wild-type embryos, ZO-1 is restricted to a single apical midline.

E) At hindbrain levels, *tri* embryos have bilateral domains of aPKC (arrows), revealing the duplicated apical surfaces of the neuroepithelium.

F) MZ*oep* embryos have ectopic apical foci (arrowheads) indicating that the neural primordium is highly disorganised. Yellow dots indicate the edge of the neural tube

G) In wild-type embryos, GFAP is localised to the edge of the neural tube.

H) *tri* embryos show GFAP localised either side of the duplicated apical surfaces, forming mirror-image domains (arrows).

I) In MZ*oep* embryos, GFAP is expressed in ectopic locations (arrowheads) within the neural primordium.

All images kindly provided by Claudio Araya.

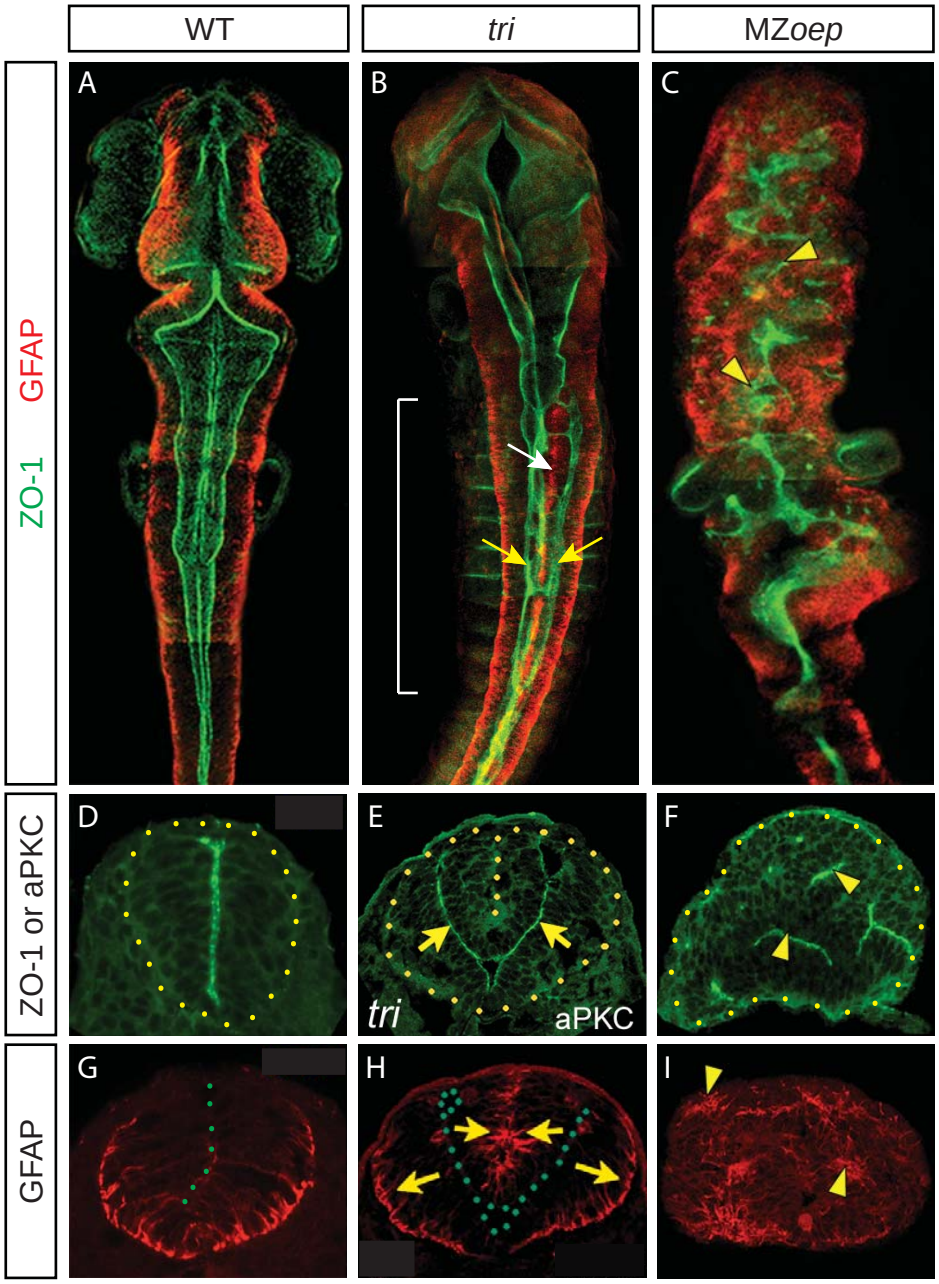

Figure 5.1 ***tri*** **and MZ*oep*** **mutants generate abnormal neural tubes with defective apico-basal organisation.**

MZ*oep* mutants lack Nodal signalling during gastrulation and anterior mesendodermal cells are not specified. Consequently, MZ*oep* embryos lack all mesodermal and endodermal structures that would normally lie adjacent to the anterior brain (Gritsman *et al.* 1999). Thus, during neurulation, the brain develops in the absence of any signals emanating from the mesoderm that could affect neural patterning and cell polarisation. Also during neurulation in MZ*oep* embryos, both the tissue movements as a whole, and individual cell movements are highly disorganised. Even as neurulation begins, the neural plate is abnormally thick, and the cells display chaotic movements as they converge towards the midline (C. Araya, unpublished observations). The mutant does attempt to make a neural tube, but shows abnormal cell movements during neurulation, and the brain has a highly disorganised structure at 24hpf (fig 5.1C,F,I). Therefore MZ*oep* embryos offer a suitable system for the test the robustness of a timer, both in the presence of gross morphogenetic deficiencies, and in the absence of any anterior mesoderm.

Step-wise model of polarisation during zebrafish neurulation

It has been proposed that the establishment of polarity during neurulation occurs in two steps (Yang *et al.* 2009). At neural plate stages, aPKC and Pard3 are either localised in an unpolarised fashion, or are not expressed at all (Geldmacher-Voss *et al.* 2003). ZO-1 and N-Cad however, are present in puncta in the neural plate (Yang *et al.* 2009), though it is unclear where these puncta are localised in individual cells. During neural keel stages as the two halves of the neural plate meet, aPKC, Pard3, Par6, ZO-1, Nok and Lin7c all become enriched at the midline, with the ventral most cells polarising first (Geldmacher-Voss *et al.* 2003; Tawk *et al.* 2007; Munson *et al.* 2008; Yang *et al.* 2009). The density of midline labelling increases over time, and by rod and tube stages all junctional and polarity proteins studied become localised to the apical ends of neuroepithelial cells (Geldmacher-Voss *et al.* 2003; Tawk *et al.* 2007; Munson *et al.* 2008; Yang *et al.* 2009). Thus ZO-1 and N-Cad puncta appear earlier in time compared to other apical-proteins, and may constitute the first step in the process in the establishment of polarity, with the other polarity proteins stabilising the early ZO-1 and N-Cad puncta after cell rearrangements of neurulation have largely finished (Yang *et al.* 2009). I have assessed the early establishment of polarity in this chapter using immunohistochemistry to ZO-1, and the later phase of polarisation using Pard3 fusion proteins.

Culture of cells in ectopic locations

An absolute test of the robustness of the cell intrinsic timer is to see if cells can polarise on time outside the brain. To do this, neural cells can placed either in ectopic locations in the

embryo, or in cell culture. The determination of hindbrain progenitors to a hindbrain fate has been tested by transplanting cells to ectopic locations within the embryo (Woo *et al.* 1998), suggesting that transplantation of cells to an ectopic location is a potential way to test the cell autonomy of the polarisation timer of neural cells. The optic vesicle has also been successfully cultured in an ectopic location on the lateral yolk (Picker *et al.* 2009), further showing that ectopic culture of zebrafish cells is a feasible approach. The technique of *in vitro* cell culture has previously been used in the study of developmental timers of both neural and non-neural cell types. Culture systems provide an environment devoid of many of the normal environmental signals that cells receive during development, so provide an excellent way to test the intrinsic nature of specific cell behaviours. Furthermore, it is easy to manipulate aspects of the environment in culture that may influence cell behaviour during morphogenesis, such as growth factor signals or the composition of the substrate, providing a more accessible system than is often possible in the embryo.

Culture systems for epithelial cells

Polarised epithelial cell lines deriving from a number of different organs, including the gut, kidney and mammary glands have traditionally been cultured on 2D substrates. However both the flatness and composition of the substrate are highly artificial compared to a cell's *in vivo* environment, and therefore cellular behaviours shown in culture may not occur during organogenesis. Moreover, recent studies showing that the transcription profiles of cells grown as 2D monolayers is different to cells cultured in spheroid cultures (Chang *et al.* 2009) has revealed how important the culture medium may be for the correct function of the cells. Three-dimensional culture systems provide both a more organotypic environment while maintaining the advantage of accessibility of culture systems.

Types of 3D culture systems

Three dimensional culture systems commonly used for culturing epithelial cells can be classed into three main types: tissue can be explanted into culture, such that the transferred intact tissue largely keeps its original architecture, cells can be cultured as large aggregates, or spheroids and finally cells can be dissociated and embedded in a matrix (Pampaloni *et al.* 2007). Explant culture has been an invaluable tool for increasing our understanding of cellular behaviours in biological processes as diverse as gastrulation and brain connectivity (Keller *et al.* 1985; Keller *et al.* 1988; Gahwiler *et al.* 1997). Hanging drop culture systems rely on gravity to form a large aggregation of cells, which then differentiates and generates a 3D-architecture in the absence of direction from any

external substrate (Pampaloni *et al.* 2007). They have been used successfully for culturing a number of different cell types, including zebrafish mesodermal and ectodermal cells (Kelm *et al.* 2003; Schotz *et al.* 2008; Carreira-Barbosa *et al.* 2009). The third way of culturing cells is in flexible 3D gels, such as Matrigel which are made of purified extracellular matrix components, or synthetic fibrous scaffolds (Tibbitt *et al.* 2009). The 3D environment that the gels provide allows cells to form structures more typical of their *in vivo* arrangement, and it has been shown that both physical and biochemical properties of the gel are important for morphogenesis (Roskelley *et al.* 1994).

The steps of cell polarisation and lumen formation have been successfully investigated in 3D culture systems using MDCK cells (Martin-Belmonte *et al.* 2007b) and Caco-2 cells (Jaffe *et al.* 2008). In both studies, fluorescently labelled fusion proteins were stably expressed to enable the development of polarity and cyst morphogenesis to be observed over time. Therefore 3D culture is arguably more appropriate than 2D systems for studying lumen formation during organogenesis, and is why we chose Matrigel as the culture medium for studying the polarisation of zebrafish neural cells.

Matrigel

Matrigel (BD Biosciences) is a solubilised preparation of basement membrane, and so consists of mainly laminin, collagen IV and heparin sulphate proteoglycans. Matrigel has been used successfully to promote attachment and differentiation of many cell types, including mammary epithelial cells (Debnath *et al.* 2003), hepatocytes (Castell *et al.* 2009) and neurons (Ferri *et al.* 1995). In Matrigel, epithelial cells such as MDCK and Caco cells develop into spherical cysts that closely resemble the acini or ducts of many organs *in vivo*. The gel mimics the basal environment of the basement membrane *in vivo* (Simmons 1982), and thus the cells of the cysts polarise with the apical surface in the centre of the cyst outlining a lumen.

Cell culture and intrinsic timers

Different types of glia differentiate at specific times during brain development *in vivo*, a schedule that is precisely followed when glial precursors are dissociated and cultured (Abney *et al.* 1981). The differentiation of optic nerve oligodendrocyte precursors in culture also occurs after a set time that is specific to the clonal lineage of the cell (Temple *et al.* 1986). Similarly, cardiac myocyte precursors in culture divide a certain number of times before differentiating, and clonal progeny differentiate at the same time (Burton *et al.* 1999). These studies show that developmental timers can continue to operate in

culture, and therefore the culture of zebrafish neural cells over the time period of neurulation should provide a system for us to investigate the role of the embryonic environment on the time of establishment of polarity in these cells.

5.2 AIMS

1. To determine the robustness of a timer for establishment of polarity by comparing the time at which polarity first appears in two different morphogenetic mutants, namely *trilobite* and MZ*oep*. If polarity occurs at the same time, even though the tissue architecture and cell organisation is abnormal then this is good evidence that the timing of polarisation is intrinsic to neural cells and independent of the surrounding tissue.

2. In parallel to aim 1, the role of the mesoderm in the timing of establishment of apico-basal polarity can be investigated using the MZ*oep* mutant. If polarity develops on time, then this rules out that neural cells polarise by responding to a signal from the mesoderm.

3. To test the importance of the dorsal midline of the embryo for the establishment of polarity, by placing neural cells into extreme ectopic environments in the embryo.

4. To test the importance of the embryonic environment for establishment of polarity, by placing neural cells into 3D culture.

5.3 METHODS

Specific protocols for quantifying the appearance of ZO-1 puncta

For analysis of the appearance of ZO-1 puncta in MZ*oep*, *tri* and wt embryos, the following steps were taken in an attempt to ensure that staining and imaging across specimens was as consistent as possible.

Fixation and immunohistochemistry

At the time of fixation, wt and *tri* embryos were staged under the dissecting microscope according to the number of somites. Embryos were fixed in 4% PFA from the same aliquot, and fixed overnight at 4˚C for the same time period. Embryos were then washed in fresh PBS, dehydrated into methanol, and put at -20˚C to permeabilise the embryos. When all embryos of all stages had been placed at -20˚C for at least an hour, the normal immunohistochemistry protocol was followed with all tubes of embryos being treated identically. For all stages, the same aliquot of antibody was used at the same dilution.

Imaging

After washing of the secondary antibody, all embryos were mounted for dorsal view imaging through the hindbrain. Confocal settings including laser power, gain, offset, pinhole and averaging were set at the beginning of imaging and left unchanged throughout. All embryos were imaged on the same day, and the same z-stack was taken for each embryo (25 z-slices at 3µm intervals), starting from the dorsal most part of the neural primordium (fig 5.3D).

Data analysis

A histogram of all pixels intensities (256 gray levels) was derived from a large ROI (100µm x 100µm) in each of three different z-levels per specimen (fig5.3E). Z-levels at comparable dorso-ventral depths were chosen for analysis across embryos to minimize the change in intensity that occurs with z-depth. Care was taken to avoid sampling any signal from the polarised EVL, and from ventral most z-levels because in wild-type embryos these polarise earlier than the rest of the tissue, and are not present in MZ*oep* mutants due to the loss of ventral midline specified cells (Gritsman *et al.* 1999). For each time point, 2-8 mutant or wild-type embryos were analysed.

The average maximum background pixel intensity was calculated from maximum intensity measurements at five locations in each chosen z-slice. Background pixel intensity was sampled from a smaller ROI (10µm x 10µm), avoiding obvious real signal (fig5.3E). Pixels below this cut-off value were regarded as background, and any pixels above were counted as signal (fig5.3F). Finally, as the sampled number of pixels was the same for every measurement, the average number of pixels above background was calculated for MZ*oep*, *tri* or wild-type embryos at each stage.

Specific protocols for quantifying the appearance of Pard3 puncta

Pard3 polarisation time-lapse imaging

Time-lapse imaging for the analysis of Pard3 polarisation in several different wild-type embryos was carried out simultaneously. To obtain embryos without mesoderm, wild-type embryos were incubated in 150µM SB-431542 (Tocris Bioscience) in embryo medium from 2hpf to block Nodal signalling and thus mimic the MZ*oep* phenotype (Inman *et al.* 2002; Sun *et al.* 2006). Then wild-type and SB-treated embryos were imaged simultaneously on the same confocal microscope from 13-20hpf. For both experiments, embryos with similar cytoplasmic expression levels of Pard3-GFP at 11hpf (before establishment of polarity) were chosen for imaging. All embryos were mounted for transverse imaging through the hindbrain.

Pard3-GFP polarisation analysis

The appearance of Pard3-GFP puncta was analysed by marking puncta of Pard3 at each time frame with a small dot. Time-lapse series at z-levels through the hindbrain at the level of the otic vesicle in both SB-treated and wild-type embryos were chosen for analysis. Then the number of Pard3-GFP puncta observed over a 20 or 30 minute period (depending on the experiment) at a particular z-level was counted. The number of puncta in each period was normalised to the maximum number in any one period for each embryo, and plotted against time. Normalising to the maximum facilitates the comparison of traces plotted on the same graph. For comparison of wild-type and SB-treated embryos, the average number of Pard3 puncta in each time period was calculated from the normalised data from 3 or 4 z-levels in each embryo.

Ectopic yolk transplants

1. MZ*oep* mutant, HuC:GFP transgenic or wild-type embryos were injected at 1-4 cell stage with H2B-RFP RNA alone or in combination with Pard3-GFP RNA, and incubated at 28.5˚C until about 11hpf. When MZ*oep* embryos were not available, wild-type

embryos were incubated in 150µM SB-431542 to mimic the MZ*oep* phenotype (Tocris Bioscience).

2. Some wild-type embryos were not injected, but incubated at the same temperature until 11hpf to be the host embryos.
3. The most uniformly fluorescent embryos were chosen to be the donor embryos. Both donor and host embryos were manually dechorionated in agarose coated petri dishes and then transferred to an agarose transplant plate filled with fish water supplemented with penicillin/streptomycin (diluted 1:100, P4458 Sigma).
4. Cells were taken out of the donor neural plate using a glass capillary needle (without filament) attached to an oil-filled transplant rig mounted on a micromanipulator (fig 5.2A).
5. The cells were quickly transferred to the host, which was oriented lateral facing up. The needle was pushed through the enveloping layer and 20-30 cells were placed above the yolk in a central lateral location (fig 5.2B).
6. After transplantation the host embryos were left to heal on the bench for 1 hour, and then transferred back to an agarose lined petri dish for incubation overnight in fish water supplemented with penicillin and streptomycin, until fixing or live confocal imaging.

Three-dimensional culture using Matrigel

Preparation of Matrigel and donor embryos

Matrigel matrix Phenol Red-free was used for all experiments (Catalogue number: 356237, BD biosciences). Matrigel is a basement membrane extract taken from the Engelbreth-Holm-Swarm (EHS) mouse sarcoma (Kleinman *et al.* 1982; Kleinman *et al.* 1986). Matrigel also contains growth factors such as TGF-β, epidermal growth factor, insulin-like growth factor, fibroblast growth factor, tissue plasminogen activator (McGuire *et al.* 1989; Vukicevic *et al.* 1992), and any others that occur naturally in the EHS tumour.

On the day of the experiment donor embryos were injected exactly as described for ectopic yolk transplants with Pard3-GFP and H2B-RFP. A 1ml aliquot of Matrigel was defrosted on ice during the day, and 1ml and 200ml filter tips were chilled at -20˚C for handling the Matrigel, as it gels quickly when the temperature becomes too warm.

The following solutions were prepared prior to selecting donor embryos:
Solution A: 500µl of media with supplements for mixing with Matrigel 1:1

350µl L-15 media without phenol red (Gibco)

100µl Fetal Calf Serum (FCS) to make final concentration of 10%

10µl Penicillin Streptomycin solution (P4458, Sigma)

Solution B: 15ml 2% Matrigel in L-15

300µl of Matrigel

750µl FCS (final concentration 5%)

150µl Penicillin streptomycin solution (P4458, Sigma)

13.8ml L-15 media

Cell-culture method

1. Donor embryos were prepared as described for ectopic yolk transplants to be ready for transplantation at 11hpf.
2. 15µl of solution A was taken and placed in drop either directly into the bottom of a 35mm petri dish, or onto a small (22mm x 22mm) glass coverslip supported on a slide. 15µl of Matrigel was mixed with this drop, to make a 50% Matrigel solution, and it was kept on ice to keep it liquid (fig 5.3C). It is advised not to dilute Matrigel more than 1 part Matrigel to 2 parts L-15, otherwise Matrigel may not keep the gel consistency needed for culture (M. Parsons, personal communication).
3. Then 20-30 cells were taken from the donor neural plate into the capillary needle using a micromanipulator (fig 5.2A).
4. The chilled drop of Matrigel was then transferred to the dissecting microscope and the needle tip lowered into the drop. As the cells were expelled slowly from the needle, the drop was moved around to disperse the cells within the matrix (fig 5.2C).
5. This procedure was repeated for several Matrigel drops, using different donor embryos.
6. The Matrigel drops were left to gel on the bench for 30-60mins.
7. Finally the Matrigel was covered with a solution of 2% Matrigel in L15 (solution B) to prevent drying out (fig 5.2C), and incubated at 28.5˚C until the cells were imaged.

Transferring the cells into Matrigel using a transplant needle worked well because it was possible to obtain purely neural cells without contamination with cells from the enveloping layer. It also avoided the use of trypsin to dissociate cells from the embryo, which may increase the likelihood of cells subsequently dying in the culture process. Lastly small numbers of cells could be dispersed within the gel, to overcome the concern that too many cells located in close proximity could cause also result in cell death.

Immunohistochemistry

Antibodies used and their concentrations are detailed below:
Anti ZO-1 at 1:500 (Invitrogen, 33-9100)
Anti Laminin at 1:500 (Sigma, L9393)
Anti GFAP at 1:400 (Dako, Z0344)

Confocal and time-lapse imaging

All confocal images in this chapter were acquired using an SP5 Leica laser scanning confocal microscope. Fixed antibody stained embryos were mounted in a dorsal or lateral view, and a stack of z-slices through the neural tissue or ectopic cluster of cells was collected. The z-interval depth was 2-4μm depending on the experiment. Matrigel clusters were imaged live, by dipping a water immersion lens into the L-15 medium. For time-lapse imaging of ectopic clusters, embryos were mounted laterally so that the cluster was easily accessible for imaging. A z-stack with a z depth interval of 5μm was captured every 5minutes.

Image processing

Fixed and time-lapse images were processed as described in the general methods using ImageJ and Adobe Photoshop.

Statistical analysis

All statistical analyses were carried out in GraphPad Prism. To test for differences between the number of pixels of ZO-1 between wild-type and MZ*oep* or *tri* embryos, a two way ANOVA test was used. To check that the data was of a Gaussian distribution and thus that the ANOVA test was appropriate, a frequency histogram was plotted of the number of ZO-1 puncta in wild-type or MZ*oep* for a time point with a great enough sample size. The histogram showed an approximate bell shape indicating a Gaussian distribution, and in addition, data sets at each time point passed the D'Agostino & Pearson test for normality. A significant difference was classified as $p<0.05$. For the ANOVA test comparing MZ*oep* and wild-type ZO-1 puncta, there were no detectable puncta of ZO-1 at 11.5hpf, so this was time-point was not included in the analysis.

Many of the experiments in this chapter were carried out in collaboration with Claudio Araya.

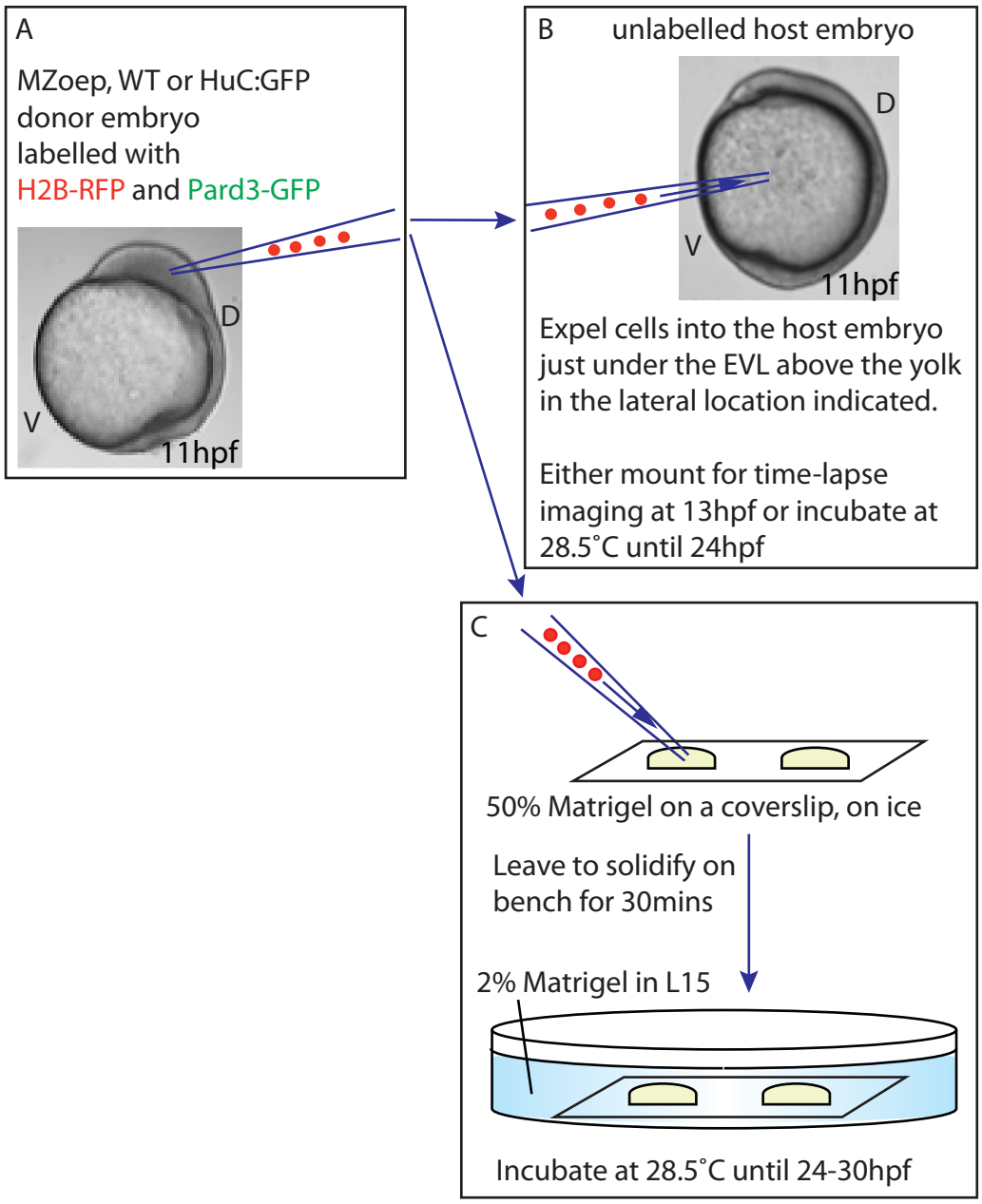

Figure 5.2 Schematic illustration showing the method used for extreme ectopic transplants and Matrigel culture.

A) Neural plate cells co-injected with Pard3-GFP and H2B-RFP mRNA were removed from wild-type or SB-treated (Nodal-deficient) embryos at 11hpf using a capillary needle.
B) For ectopic transplants, cells were expelled into an unlabelled host embryo of similar age just under the EVL next to the yolk, away from the embryo's dorsal axis.
C) For three-dimensional culture, cells were embedded in Matrigel.
In A and B, D (dorsal side of the embryo), V (ventral side of the embryo).

5.4 RESULTS

The aim of these experiments is to determine the effect, if any, of abnormal neural tube morphogenesis and the surrounding tissues on the timing of the establishment of apico-basal polarity during neurulation. Firstly I test if correct tissue morphogenesis is important. Secondly I test if the dorsal midline environment of the embryo is important for polarisation. Lastly, I examine if the embryonic environment as a whole is important for polarisation by placing cells in 3D culture.

Determination of the timing of establishment of apico-basal polarity using ZO-1 immunohistochemistry

ZO-1 is usually associated with tight junctions in epithelia, and therefore is useful as a marker for apical polarity. It is proposed that to be one of the first apical proteins to be expressed during zebrafish neurulation (Yang *et al.* 2009). At the start of neurulation at 10hpf, ZO-1 is not detectable by immunohistochemistry in the neural tissue (Geldmacher-Voss *et al.* 2003; Yang *et al.* 2009). However by 11.5hpf, one study has reported the presence of small puncta of ZO-1 in neural plate cells (Yang *et al.* 2009), whereas another has reported no local accumulation of ZO-1 (Geldmacher-Voss *et al.* 2003). Thus the exact timing of the appearance of puncta of ZO-1 remains unclear. However it is agreed that by neural keel stages, ZO-1 is localised to small puncta, which become concentrated at the midline as neurulation progresses (Geldmacher-Voss *et al.* 2003; Yang *et al.* 2009).

I have developed a reliable and unbiased method for assessing ZO-1 puncta at the tissue level by immunohistochemistry to determine when puncta of ZO-1 first become evident during neural tube formation. I have taken care to be consistent in the immunohistochemistry protocol and confocal imaging for all embryos at different stages (see methods), to enable small faint spots of ZO-1 to be reliably detected across different embryos and distinguished from the background staining. Alexa-fluor 633 was used as the secondary antibody, because it gave less background staining compared to alexa-fluor 488 minimal in whole-mount preparations (fig5.3A,B). ZO-1 staining is only present at the apical ventricular surface of control embryos at 24hpf, consistent with its localisation at tight junctions in epithelia (fig 5.3B). At 24hpf, non-specific staining of the secondary antibody was low as shown by the lack of any detectable fluorescence in the control staining when the primary antibody was omitted (fig 5.3C). Confocal z-stacks were collected through the neural primordium of embryos at several different stages (fig 5.3D),

Figure 5.3 Method for assessing the establishment of polarity by ZO-1 immunohistochemistry.

A-C) Confocal projections of the hindbrain neural tube in 24hpf zebrafish embryos from a dorsal view. In all pictures anterior is up and red dots indicate the basal edge of the neural tube. The otic vesicle (OV) is used as landmark for the hindbrain.

A) Whole mount ZO-1 immunostaining using the alexa fluor 488 secondary antibody reveals some background staining in the neural tissue.

B) Whole mount ZO-1 immunostaining using the alexa fluor 633 secondary antibody reveals very little background staining in the neural tissue.

C) Whole mount immunostaining using the alexa fluor 633 secondary antibody without primary antibody incubation shows that the 633 secondary antibody alone produces no detectable background staining in the embryo.

D) Brightfield image of a neurula stage wild-type embryo illustrating the orientation for imaging through the hindbrain and the details for imaging (antero-dorsal is left).

E) Example of a single confocal z-slice through a wild-type embryo at 13hpf revealing ZO-1 puncta. Anterior is to the left. The large box shows the region of interest (ROI) for the pixel intensity histogram. The smaller boxes are example ROIs for maximum background measurements, positioned where there are no obvious puncta of ZO-1. Anterior is left.

F) Example histogram of pixel intensities from the large ROI with the limit between background and ZO-1 signal shown.

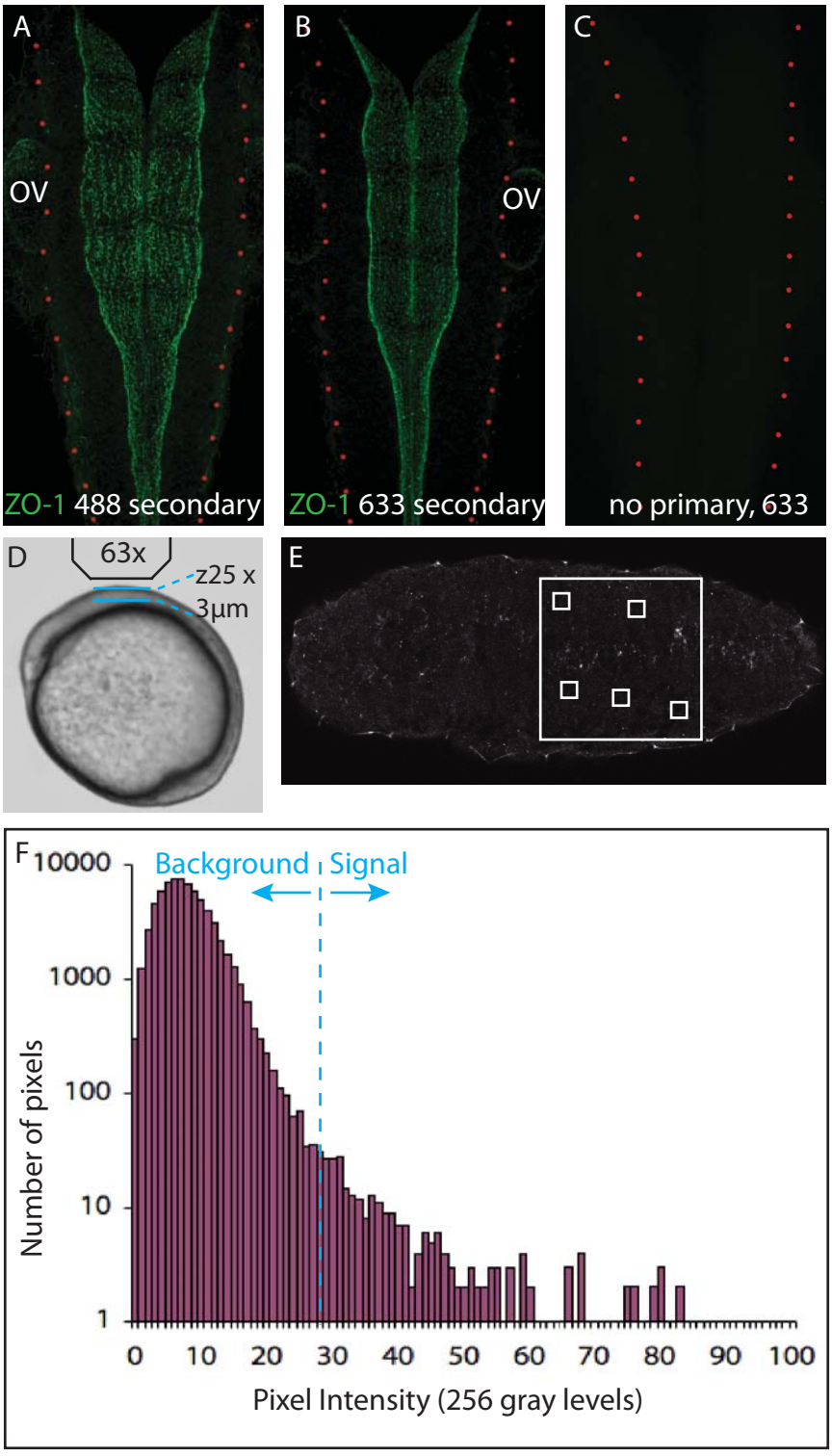

Figure 5.3 Method for assessing the establishment of polarity by ZO-1 immunohistochemistry.

and the presence of puncta of ZO-1 in single z-slices was analysed using fluorescence intensity measurements. A histogram of all pixels intensities within a large region of interest (ROI, large box in fig 5.3E) was derived (fig 5.3F), for three z-slices in each embryo. To determine which intensity range in the histogram represented background, and which range represented signal, the average maximum intensity was calculated in several ROIs in each z-level from areas of no obvious signal (small boxes in fig 5.3E). Pixels below this cut-off value were regarded as background, and any pixels above this value were counted as signal (fig 5.3F).

ZO-1 polarises at the same time in *tri* and wild-type embryos

To determine if focal accumulations of ZO-1 appear on time even though neural tube morphogenesis is abnormal, I analysed the appearance of ZO-1 puncta in Z*tri* and wild-type embryos by immunohistochemistry. It is already known that apico-basal polarity is generated in ectopic locations in *tri* embryos (Tawk *et al.* 2007), but the precise timing of the establishment of polarity has not previously been investigated. Figure 5.4 shows representative maximum projections of ZO-1 staining from a subset of z-levels through the posterior hindbrain from wild-type and *tri* embryos of different ages. At 12hpf, although the neural tissue is wider in *tri* embryos compared to wild-type, puncta of ZO-1 are scattered throughout the neural tissue (between the dotted lines) in both wild-type (fig 5.4A) and *tri* (fig 5.4E) embryos.

The progressive coalescence of ZO-1 puncta over time is also similar in wild-type and *tri* embryos. At 13hpf, the puncta are still scattered throughout the neural tissue, in both wild-type (fig 5.4B) and *tri* (fig 5.4F) embryos. However by 14hpf, the puncta are slightly concentrated towards the future apical surface in both wild-type (fig 5.4C) and *tri* embryos (fig 5.4G). By 17hpf, ZO-1 puncta have coalesced towards a single midline in wild-type embryos (fig 5.4D). In *tri* embryos, puncta have coalesced towards a midline, but this apical specialization is bifurcated (fig 5.4H), as expected if convergence is delayed and neural tube duplications occur (compare to fig 5.1B). Overall these images reveal that the appearance and progression of the localisation of ZO-1 is similar in wild-type and *tri* embryos.

To quantify the appearance of puncta of ZO-1 in wild-type and tri embryos, I calculated the average number of pixels of ZO-1 fluorescence in a fixed area from several z-levels in different embryos (fig 5.4I). In wild-type embryos, the number of pixels increases steadily over time, from an average of 200 pixels at 12hpf to an average of 350 pixels by 17hpf.

Figure 5.4 Puncta of ZO-1 appear at the same time in wild-type and *trilobite* embryos.

A-H) Representative images of whole-mount ZO-1 staining in wild-type (A-D) and *trilobite* (E-H) embryos at different stages of neurulation. Images are maximum confocal projections of 6 consecutive z-levels through the neural tissue including the z-levels chosen for analysis. All embryos were imaged from a dorsal view at posterior hindbrain or anterior spinal cord regions. In all pictures anterior is up. White dotted lines indicate the lateral boundaries of the neural tissue. Arrows indicate the approximate positions of the future apical midlines of the developing neural tube. Insets show higher magnification of the small boxed areas to illustrate the presence of puncta of ZO-1. Scale bar is 50μm.

A) At 12hpf, puncta of ZO-1 are present in wild-type embryos, and are scattered throughout the tissue.

B) At 13hpf, puncta of ZO-1 are more numerous but remain scattered throughout the neural tissue of wild-type embryos.

C) By 14hpf, there is little change in the distribution of puncta of ZO-1 in wild-type embryos compared to13hpf.

D) By 17hpf, puncta of ZO- have coalesced towards the midline in wild-type embryos.

E) At 12hpf, puncta of ZO-1 are also present in *tri* embryos, scattered throughout the neural tissue, which is wider compared to wild-type embryos at 12hpf.

F) At 13hpf, puncta of ZO-1 are present, but remain scattered throughout the neural tissue of *tri* embryos.

G) By 14hpf, the neural tissue of *tri* mutants is still wider compared to wild-type, and puncta remain scattered throughout the tissue.

H) By 17hpf, the puncta have coalesced towards the duplicated apical surfaces of the *tri* mutant neural primordium.

I) The average number of pixels of Z0-1 staining over time for wild-type embryos and *tri* mutants. For wild-type embryos, the number of pixels increases over time, from an average of 200 pixels at 12hpf to an average of 350 by 17hpf. For *tri* embryos, the number of pixels of ZO-1 staining also generally increases over time, from 220 at 12hpf to 370 at 17hpf, although there is a slight increase at 13hpf. At each time point there is no significant difference between the number of puncta in wild-type and *tri* embryos (two way ANOVA). Error bars indicate the standard deviation.

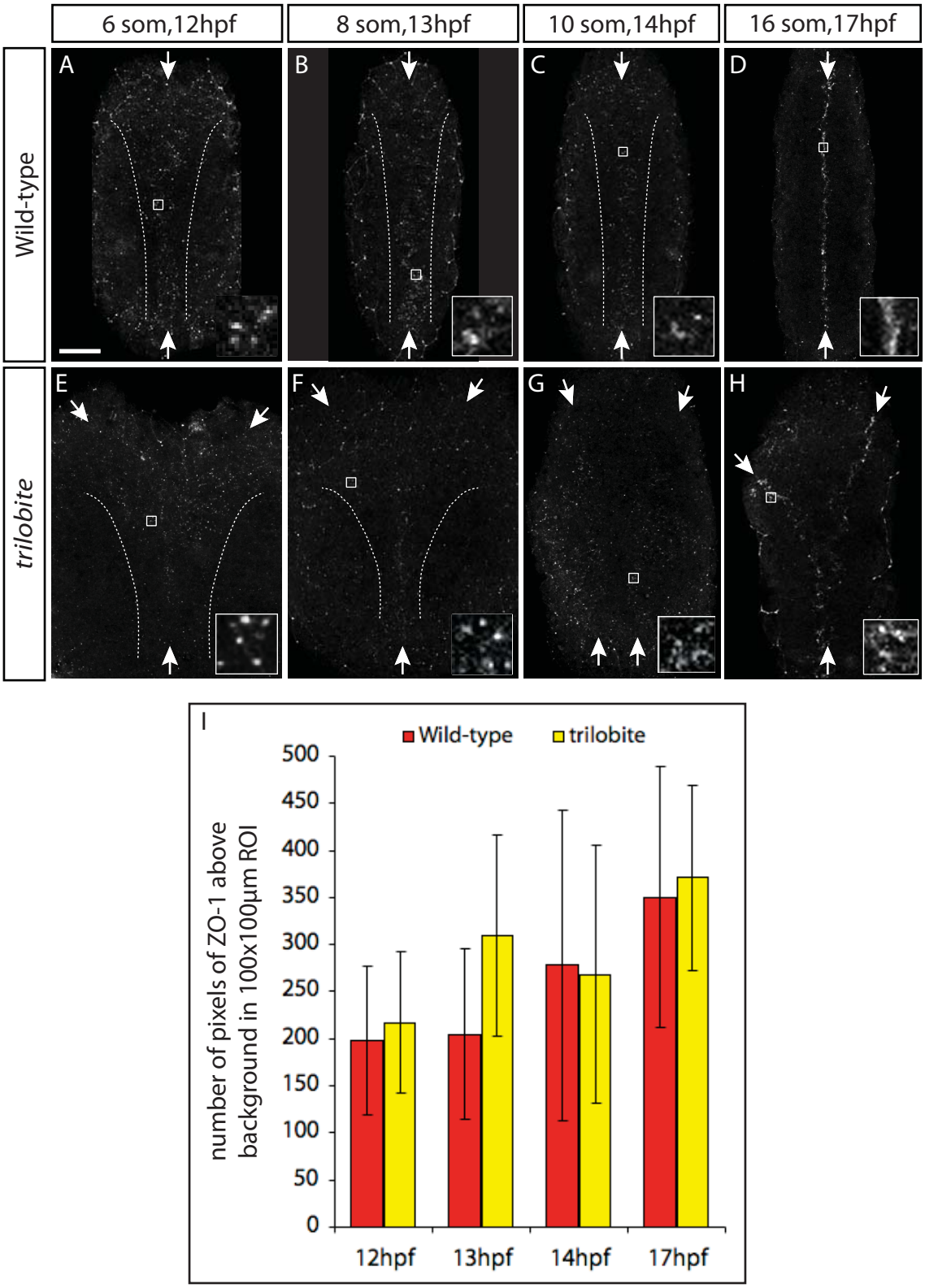

Figure 5.4 Puncta of ZO-1 appear at the same time in wild-type and *trilobite* embryos.

This is consistent with increasing numbers of cells becoming polarised as ZO-1 protein coalesces to form brighter puncta over time. For *tri* embryos, the number of pixels of ZO-1 staining also generally increases over time, from 220 pixels at 12hpf to 370 pixels at 17hpf. At each time point, I did not detect any significant difference in the number of pixels of ZO-1 between wild-type and *tri* embryos (two way ANOVA, $p>0.05$) and therefore I conclude that the development of apical polarity as assessed by ZO-1, occurs on time in *tri* embryos.

The time of ZO-1 polarisation in MZ*oep* embryos is delayed by thirty minutes compared to wild-type

To investigate if polarity is established on time in a more disorganised neural primordium than *tri* mutants, I analysed the time at which puncta of ZO-1 first appear in MZ*oep* embryos. By the end of neurulation, at 24hpf, MZ*oep* mutants display an extremely disorganised neural primordium (fig 5.1C), although importantly apico-basal polarity within the tissue is still present (fig 5.1F,I). This experiment tests the contribution of midline structures such as the notochord, and also the mesoderm for determining the time of polarisation of neuroepithelial cells, because MZ*oep* embryos lack all these tissues in the anterior regions of the embryo (Gritsman *et al.* 1999).

Immunohistochemistry for ZO-1 in the hindbrain reveals that at 11.5hpf neither wild-type nor MZ*oep* embryos exhibit many puncta of ZO-1 (fig 5.5A,E). However by 13.5hpf, wild-type embryos show scattered puncta of ZO-1 mostly localised towards the midline of the tissue (fig 5.5B), whereas in MZ*oep* embryos there are still only a few puncta present (fig 5.5F). By 15hpf midline localisation of ZO-1 puncta is clear in wild-type embryos (fig 5.5C), but the number of puncta of ZO-1 have increased in MZ*oep*, although they are still scattered throughout the tissue (fig 5.5G). Finally at 16.5hpf, nearly all ZO-1 protein is localised at the midline in wild-type embryos (fig 5.5D), and in MZ*oep* embryos puncta of ZO-1 have coalesced into ectopic apical surfaces (arrows in fig 5.5H). Overall the images reveal that apical polarity is generated at a similar time in wild-type and MZ*oep* embryos, even though the structure of the neural rod of MZoep embryos is highly disorganised.

Quantification of the ZO-1 staining in wild-type and MZ*oep* embryos reveals that ZO-1 polarisation is delayed by 30 minutes in the MZ*oep* mutant compared to wild-type (fig 5.5I). In wild-type embryos, the number of pixels of ZO-1 over time increases in two stages. The first increase occurs from 11.5hpf to13hpf when the average pixel count changes from 70 at 11.5hpf to 230 at 13hpf. The number of pixels remains roughly

Figure 5.5 The appearance of ZO-1 puncta is delayed by 30minutes in MZ*oep* mutants compared to wild-type embryos.

A-H) Representative images of whole-mount ZO-1 staining in wild-type (A-D) and MZ*oep* (E-H) embryos at different stages of neurulation. Images are maximum confocal projections of 6 consecutive at equal z-levels through the neural tissue of wild-type and MZ*oep* embryos. All embryos were imaged from a dorsal view at posterior hindbrain or anterior spinal cord regions. In all pictures, anterior is up. White arrows indicate the approximate positions of the future apical midline of the embryo. The ZO-1 staining surrounding the edge of the neural tissue is from the polarised EVL overlying the neural tissue. Scale bar is 50μm. At 11.5hpf, neither wild-type or MZ*oep* embryos show any puncta of ZO-1 (A,E). At 13.5hpf, puncta of ZO-1 become present within the neural tissue of wild-type embryos (red arrows, B). Similarly, within the abnormal MZ*oep* neural tissue some scattered ZO-1 puncta begin to be expressed (red arrows, F). At 15hpf, puncta of ZO-1 are present in both wild-type and MZ*oep* embryos (C,G). At this stage, ZO-1 puncta have coalesced towards the midline in wild-type embryos (C), but remain scattered throughout the tissue of MZ*oep* embryos (yellow arrow, G). Finally by 16.5hpf, puncta of ZO-1 are localised at the maturing apical midline of wild-type embryos (D) and have coalesced to ectopic apical foci in the aberrant neural tissue of MZ*oep* mutants (yellow arrows, H).

I) The average number of pixels of Z0-1 staining over time for MZ*oep* and wild-type embryos. At 13.5hpf the number of ZO-1 puncta in MZ*oep* embryos is significantly different to wild-type (*$p<0.01$, two way ANOVA), indicating that ZO-1 polarisation is delayed by 30mins in MZ*oep* embryos. At subsequent time points (14, 15 and 16hpf), there is no significant difference between the wild-type and MZ*oep* embryos. Error bars indicate the standard deviation.

J) The average number of pixels of Z0-1 staining over time for wild-type embryos from 12.5hpf to 13.5hpf. ZO-1 polarisation is low at 12.5hpf but increases at 13hpf, and again at 13.5hpf to reach an average of 200pixels, similar to the level at 13.5hpf in I. Error bars indicate the standard deviation.

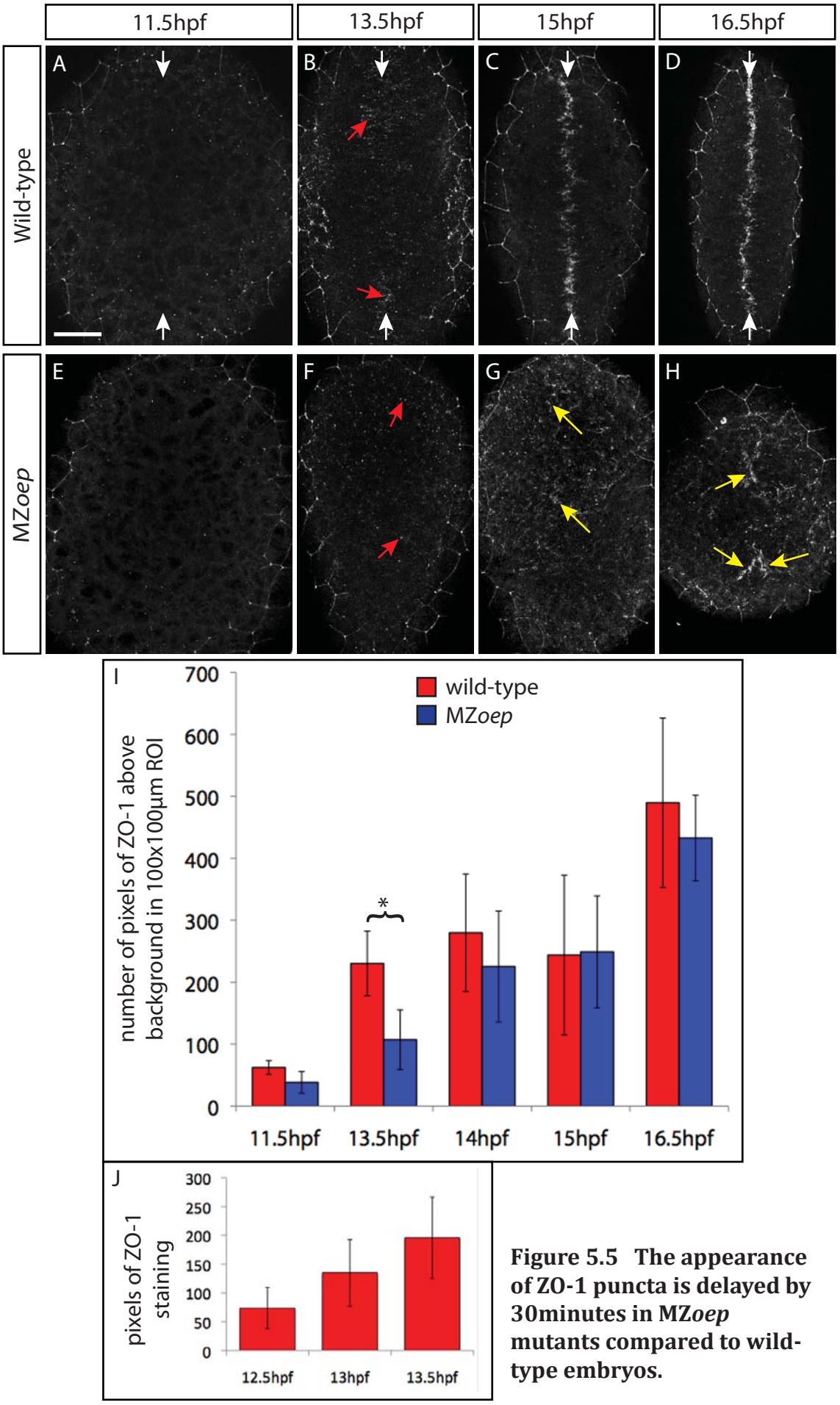

Figure 5.5 The appearance of ZO-1 puncta is delayed by 30minutes in MZ*oep* mutants compared to wild-type embryos.

constant until 16.5hpf when the number of ZO-1 pixels doubles to approximately 500 on average. At 13.5hpf, the polarisation level of ZO-1 is lower in MZ*oep* embryos compared to wild-type indicating that MZ*oep* embryos are delayed in the first step of polarisation. MZ*oep* embryos do however show a similar increase in ZO-1 pixels from 15hpf to 16.5hpf, indicating that the later progression of polarisation is similar to wild-type. To accurately determine the delay in the initial step in polarisation of MZ*oep* embryos compared to wild-type, I carried out ZO-1 intensity analysis from 12.5hpf to 13.5hpf in wild-type embryos to fill in the gap in the data from 11.5hpf and 13.5hpf. I found that at 12.5hpf, the number of pixels of ZO-1 was still low at background levels, but at 13hpf it increased to an average of 150 pixels, and similar to the previous experiment, reached just over approximately 200 pixels at 13.5hpf (fig 5.5J). This confirms that in wild-type embryos ZO-1 only begins to become polarised at 13hpf, which is 30 minutes prior to the start of polarisation in MZ*oep* embryos.

Assessing the variability in the appearance of Pard3-GFP puncta in different dorso-ventral z-levels and across different embryos during neurulation

Having assessed the early polarisation of neural cells using the apical marker ZO-1, I next investigated if the later event of Pard3 polarisation occurs on time in mutants with abnormal neural tube morphogenesis. During zebrafish neurulation, the localisation of Pard3-GFP changes from a non-polarised cytosolic distribution into puncta located near the midline, which then finally coalesce to form a single midline seam (Tawk *et al.* 2007). To analyse Pard3 polarisation, I simultaneously imaged wild-type and Nodal deficient (SB-treated) embryos ubiquitously labelled with Pard3-Cherry (Pard3-Ch) or Pard3-GFP by time-lapse confocal microscopy over the time period of neurulation. The appearance of puncta of Pard3 over time was quantified by counting the number of puncta of Pard3 present in regular time intervals. I used Pard3 tagged with Cherry for time-lapse comparisons of wild-type embryos, but I have not detected any difference in behaviour between the GFP and Cherry (Ch) fusion proteins.

The analysis of the appearance of Pard3 puncta is useful as it gives one measure of the later events of establishment of apico-basal polarity, but it does however have several technical difficulties associated with it. The classification of a puncta of Pard3 as a localised accumulation above the cytoplasmic levels of Pard3 present in the tissue involves a judgement by eye, and therefore is liable to bias and inconsistency across different embryos. This is further complicated by variation in the levels of fluorescence of tagged -

Pard3 across different embryos, presumably as a result of variable efficiencies in Pard3-Ch RNA injection at the 1-4cell stage. To reveal the inherent variability in this method of analysis, I assessed the number of puncta of Pard3-Ch over time in consecutive z-levels of a time-lapse from a single embryo. The variability caused by different fluorescence levels of Pard3-Ch should be minimized and Pard3-Ch should become polarised at the same time in each z-level. From this analysis, general features about the time-course of the appearance of Pard3-Ch puncta are also revealed.

Pard3 puncta appear at similar times in different dorso-ventral z-levels

Frames taken at hourly intervals from one z-level of a time-lapse movie show the progression of the establishment of polarity of Pard3-Ch at the tissue level (fig 5.6A-E). At 15 and 16hpf, Pard3-Ch is only polarised at the midline at the ventral extremity of the nascent lumen (yellow arrowheads in fig 5.6A,B). By 17hpf, the region of Pard3-Ch polarisation at the midline has extended more dorsally (between the arrowheads in fig 5.6C). By 18hpf, puncta of Pard3-Ch are present at the midline at all dorso-ventral levels (yellow arrowheads in fig 5.6D), but in some areas Pard3-Ch remains cytoplasmic. Finally by 19hpf, most Pard3-Ch is localised at the midline, forming a straight apical surface (fig 5.6E).

To quantify the appearance of Pard3-Ch puncta, I placed a dot over every spot of Pard3-GFP in each frame of the time-lapse movie. This is illustrated in figures 5.6A'-E', which show each of the images in fig 5.6A-E with blue dots over Pard3-Ch puncta. Finally for each z-level the number of puncta present in 20minute periods were counted and normalised to the maximum number of puncta (fig 5.6F). The graph reveals that there are two main phases to each trace. The first is from 13h20mins post fertilisation until 16h 40mins, when puncta of Pard3 are at a low level that is fluctuating but stays below 20% of the maximum number of puncta. These puncta of Pard3-Ch are mostly those located at the midline in the ventral extremity of the nascent lumen (fig 5.6A,B). The second phase begins just before 17hpf when the number of puncta increases above the low level (arrow on fig 5.6F). The number of puncta then steadily increases over the next hour before reaching a maximum (100% on graph) between 18hpf and 19hpf. This second phase represents puncta of Pard3 forming at or near the midline of the neural rod in all dorso-ventral positions as apico-basal polarity is established throughout the whole depth of the neural rod.

The shapes of the traces from the 4 different z-levels in figure 5.6F are similar, and all

Figure 5.6 The timing of Pard3-GFP polarisation during neurulation shows variation within and across different wild-type embryos.

A-E) Frames at hourly intervals taken from a single z-level time–lapse movie of wild-type neurulation showing the polarisation of Pard3-GFP in transverse view. Red dots outline the neural rod, white arrows indicate the midline of the rod, and yellow arrowheads point to Pard3-GFP puncta. Scale bar is 25μm and applies to all images.

A) At 15hpf, puncta of Pard3-GFP first appear at the most ventral position of the future apical midline of the neural rod.

B) Puncta of Pard3-GFP are still only present at the ventral midline at 16hpf

C) By 17hpf, Pard3-GFP puncta are present in the ventral half of the neural rod between the arrowheads.

D) Pard3-GFP puncta are present at the midline at all dorso-ventral levels at 18hpf, some cytoplasmic Pard3-GFP remains.

E) By 19hpf, most Pard3-GFP is localised to puncta at the midline.

A'-E') The same frames from the time–lapse as A-E, but with blue dots overlaid onto the puncta of Pard3-GFP. Red dots outline the neural rod.

F,G) Graphs showing the variation in the appearance of Pard3-GFP puncta in the neural rod over time. Puncta appear in two phases during neurulation: first the number of puncta is low and represents puncta at the ventral extremity of the nascent lumen, but then at approximately 17hpf, the number of puncta increases as Pard3-GFP puncta appear at all dorso-ventral levels of the neural rod. The horizontal dotted line indicates the maximum percentage of dots that occurs in the first phase of ventral polarisation. The arrow indicate the transition between the two phases of polarisation. The bracket indicates the hour over which the greatest increase in Pard3-GFP puncta occurs.

F) Pard3-GFP polarisation over four different z-levels. The arrowhead indicates the faster appearance of Pard3-GFP puncta in one z-level.

G) Pard3-GFP polarisation in three different wild-type embryos. The transition to a large increase in Pard3-GFP puncta is earlier for wild-type 2 than wild-types 1 and 3 (arrows), but hour of the largest increase of puncta appears at 17-18hpf for all three embryos.

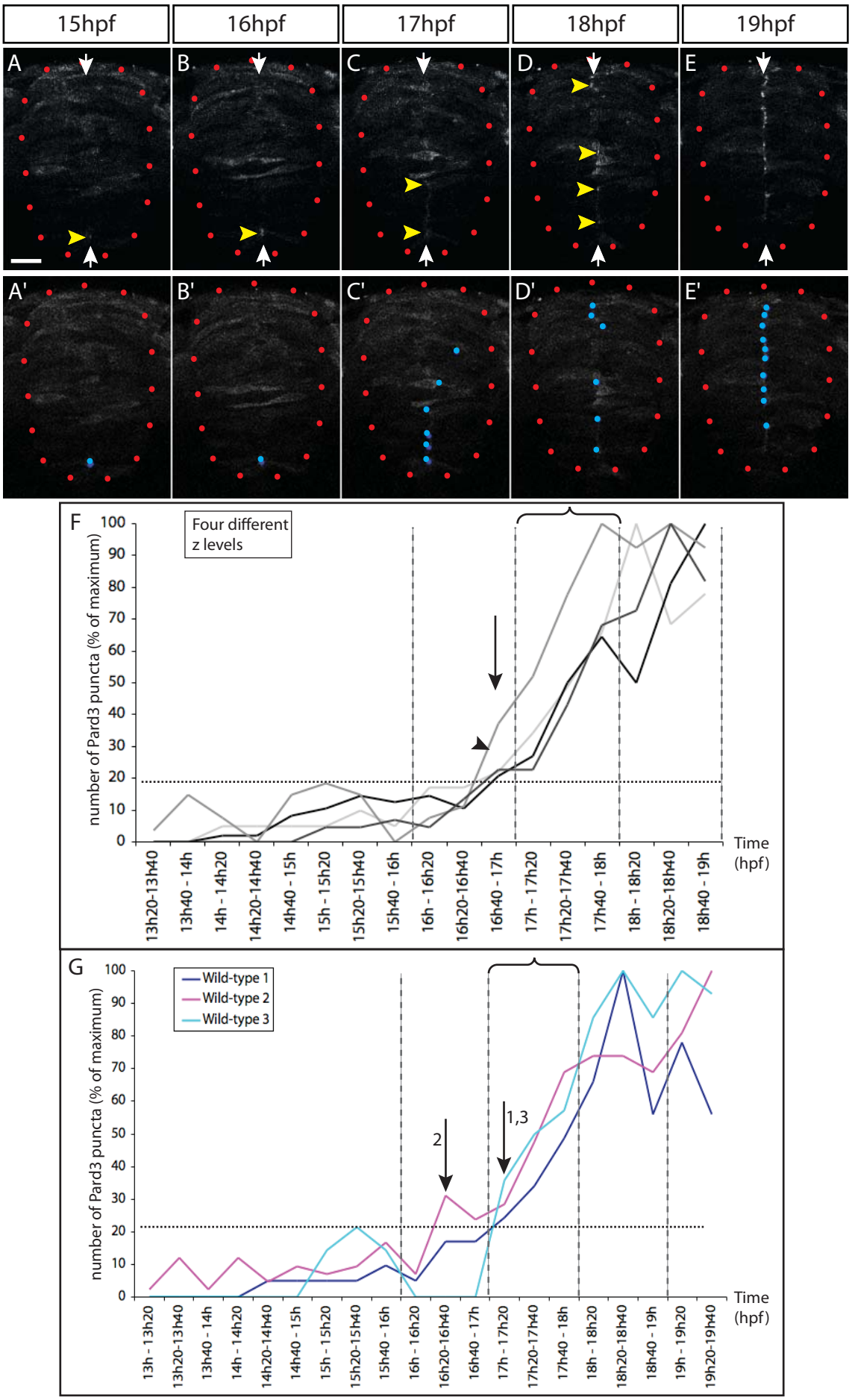

Figure 5.6 The timing of Pard3-GFP polarisation during neurulation shows variation within and across different wild-type embryos.

show the two phases of polarisation. Importantly the transition between the low level of Pard3-Ch puncta and the increase in puncta (arrow in fig 5.6F) occurs in the same period of 16h40 to 17h post fertilization in all 4 z-levels. This indicates Pard3-Ch begins to become polarised throughout the whole neural rod at the same time. The hour over which the greatest increase in puncta occurs is 17-18hpf in all z-levels, and the rate of increase is also similar during this hour. However the traces do show variation in several aspects including the rate at which puncta appear at the beginning of the increase. One z-level especially shows a more rapid increase compared to the others (arrowhead in fig 5.6F). There is also variation in when the maximum number of puncta is reached, ranging from 17h40mins post fertilization to 19hpf across the different z-levels. These two differences could represent real variation in the timing of the appearance of Pard3 puncta in different cells, or may result from inconsistent labelling of cells with Pard3-Ch at the cellular level. This variation should be considered when comparing between wild-type and mutant embryos, together with the other technical difficulties previously mentioned. Overall though, the analysis shows that puncta of Pard3-Ch appear at a similar time and rate in all z-levels analysed within this one embryo.

Pard3 puncta appear at similar times in different wild-type embryos

Before comparing the timing of Pard3-GFP polarisation between wild-type and MZ*oep* embryos, I first determined the variation in the time of Pard3-GFP polarisation across different wild-type embryos. Three wild-type embryos labelled with Pard3-GFP were simultaneously imaged over the time period of neurulation. In an attempt to minimize the variation in Pard3-GFP intensity across embryos, only embryos with approximately the same level of Pard3-GFP fluorescence at 11hpf (before Pard3 begins to become polarised) were chosen for imaging. One z-level from each of these embryos at the level of the hindbrain can be viewed as a single time-lapse sequence in supplementary movie 2.

For one z-level in each embryo, the number of Pard3-GFP puncta present every 20mins was summed, normalized to the maximum number of puncta, and plotted over time (fig 5.6G). The three traces from the different embryos all exhibit the two phases of polarisation of low level ventral polarisation and the later phase of polarisation at all dorso-ventral levels revealed in the previous section. However, the time of the transition between the two phases varies by 40 minutes, as it occurs at 16h20-16h40pf for wild-type 2 compared to 17h-17h20pf for wild-types 1 and 3. As wild-type 2 shows a slow start to this phase of polarisation, the largest increase in Pard3-GFP puncta (indicated by the bracket) occurs at 17-18hpf for all three embryos. Finally the time at which the maximum

number of Pard3-GFP puncta occurs also varies slightly between embryos, as it occurs at 18h20-18h40 for wild-type 1 and 3 but at 19h20-19h40 for wild-type 2. This amount of variation is similar to that of the three different z-levels in fig 5.5F. In summary this analysis shows that the progression of Pard3-GFP puncta is similar across the three different wild-type embryos.

Pard3-GFP puncta appear 1.5hours later in Nodal-deficient embryos than in wild-type

To obtain embryos with abnormal tube morphogenesis, wild-type embryos were treated with SB drug to block Nodal signalling and mimic the MZ*oep* phenotype. Both wild-type and SB-treated embryos were labelled with Pard3-GFP, and then simultaneously imaged throughout neurulation by time-lapse microscopy. Figure 5.7 shows frames taken from the time-lapse movies of Pard3-GFP polarisation in wild-type (fig 5.7A-D) and Nodal-deficient (fig 5.7E-H) embryos. The whole time-lapse can be viewed as a movie in supplementary movie 3. At 16hpf, the wild-type embryo has puncta of Pard3-GFP at the midline of the ventral extremity of the nascent lumen (fig 5.7A), but no puncta of Pard3-GFP are present in the Nodal-deficient embryo (fig 5.7E). This is probably because the ventral midline cells are not specified in embryos lacking Nodal signalling (Gritsman *et al.* 1999). By 17.5hpf however, puncta of Pard3-GFP have formed at several dorso-ventral levels in wild-type embryos (arrows in fig 5.7B), and puncta are also present Nodal-deficient embryos (arrows in fig 5.7F). By 19hpf, these puncta are more numerous in both wild-type (fig 5.7C) and Nodal-deficient embryos (fig 5.7G), and are localised to the embryonic midline in wild-type embryos. The neural primordium of Nodal-deficient embryos is highly disorganised so puncta of Pard3-GFP are randomly located at 19hpf (fig 5.7G). Finally by 20.5hpf, Pard3-GFP localises to the apical surfaces at the midline in wild-type embryos (fig5.7D) and to ectopic apical foci in Nodal-deficient embryos (fig5.7H).

The number of Pard3-GFP puncta was quantified over time by calculating the average number of puncta in each time period from three z-levels each of two wild-type and two Nodal-deficient embryos (fig 5.7I). To avoid the complication of the lack of ventral midline specification in Nodal-deficient (SB) embryos, I have only compared when the large increase in Pard3-GFP puncta occurs. Although there is some variation in the progression in the appearance of Pard3-GFP puncta between the two wild-type embryos, both lines of the Nodal-deficient (SB) embryos are shifted to the right compared to wild-type, indicating that they have a delay in polarisation of Pard3-GFP. The hour over which the largest increase in puncta of Pard3-GFP occurs (brackets in fig 5.8I) is 16-17hpf for WT1,

Figure 5.7 Puncta of Pard3-GFP appear 1.5hours later in Nodal-deficient embryos compared to wild-type.

A-D) Frames from a transverse view time-lapse movie of neurulation of a wild-type embryo labelled with Pard3-GFP. White arrows indicate puncta of Pard3-GFP at 16phpf and 17.5hpf, and Pard3-GFP polarisation at the midline reveals a single midline plane at 19 and 20.5hpf. Red dots outline the edge of neural rod. Scale bar is 25μm.

E-H) Frames from a transverse view time-lapse movie of neurulation of a Nodal-deficient (SB) embryo labelled with Pard3-GFP. Puncta of Pard3-GFP (yellow arrows) are present at 17.5hpf, and become more numerous at 19hpf. Red dots outline the edge of disorganised Nodal-deficient neural rod. Scale bar is 25μm.

I) The average number of Pard3-GFP puncta over time for each of two wild-type (WT) and two Nodal deficient embryos. The brackets indicate the hour period when the largest increase in puncta Pard3-GFP appears for each of the embryos. This is from 16-17hpf for WT 1, from 17-18hpf for WT 2, but the greatest increase in Pard3-GFP puncta in Nodal-deficient embryos occurs from 18-19hpf.

J) The average number of Pard3-GFP puncta over time for wild-type (WT) and Nodal deficient (SB) embryos. The progression of appearance of Pard3-GFP puncta in SB embryos is delayed by 1.5hours compared to WT. Length of grey arrows is equivalent to 1.5hours. Error bars show the standard deviation.

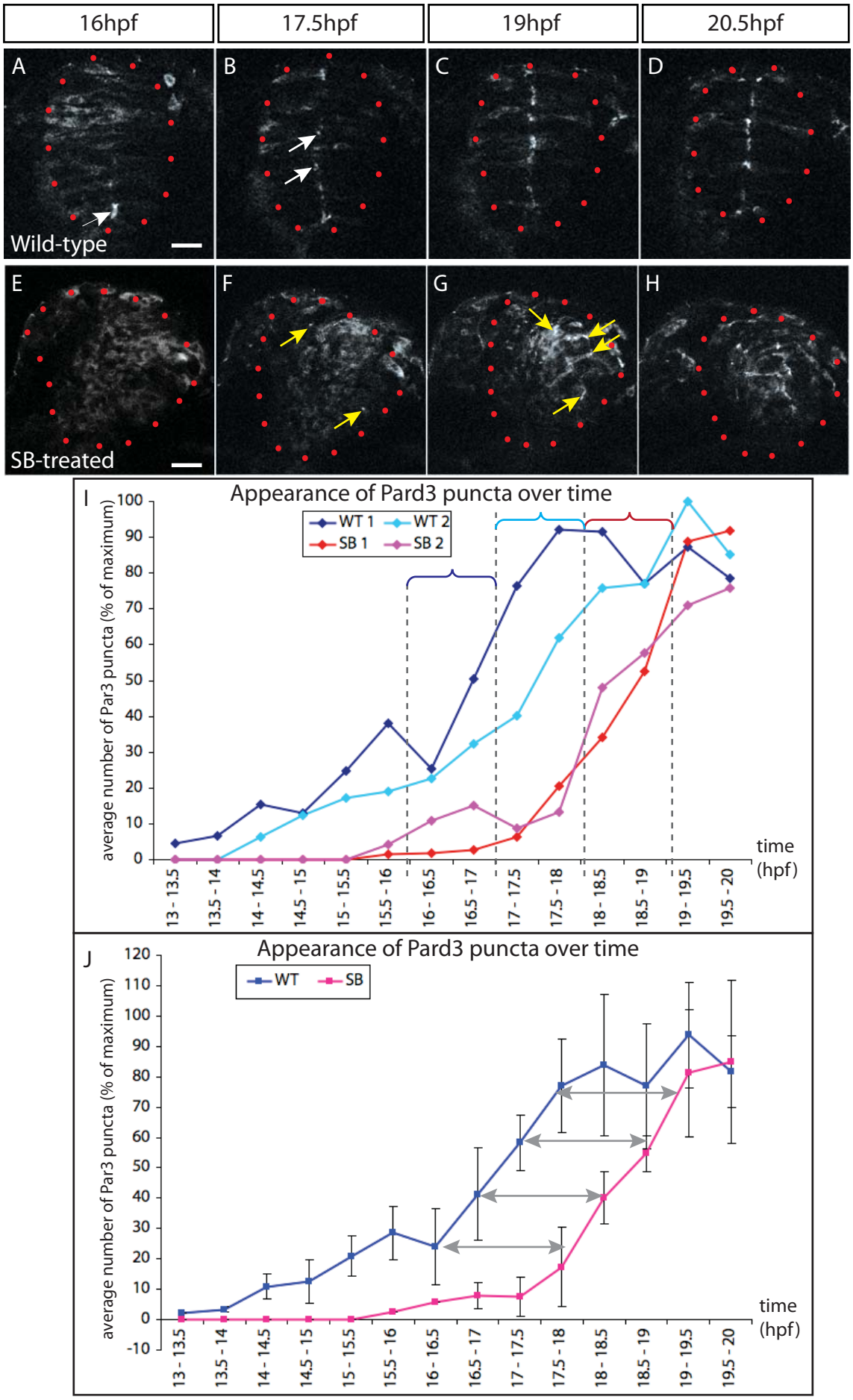

Figure 5.7 Puncta of Pard3-GFP appear 1.5hours later in SB-treated (Nodal-deficient) embryos compared to wild-type.

17-18hpf for WT2, but between 18 and 19hpf for the 2 Nodal-deficient embryos. This difference between WT and Nodal-deficient embryos is outside the limits of the variation seen across different wild-type embryos and therefore likely represents a real delay in the polarisation of Pard3-GFP in Nodal-deficient embryos.

To obtain an estimate of the average delay between wild-type and Nodal-deficient embryos, the normalised data for each z-level from the two embryos was averaged for wild-type and Nodal-deficient embryos (fig 5.7J). This graph shows that there is a consistent average delay of 1.5hours between the WT and Nodal-deficient embryos (grey arrows in fig 5.7J), from the beginning of the large increase in puncta up until the time at which the maximum number of puncta is reached. This difference is again outside the limits of the variation seen in different wild-type embryos and shows that the late stage of Pard3-GFP polarisation is delayed in Nodal-deficient embryos compared to wild-type.

Neural cells in extreme ectopic locations in the embryo form clusters with a central lumen

The studies above show that the generation of apical polarity in neural progenitors cells is delayed in Nodal-deficient embryos, suggesting that abnormal morphogenesis of the neural tube can affect cell polarisation. To further investigate the influence of the environment on the timing of cell polarisation, I have tested if neural cells can polarise outside their normal neural environment. To do this I transplanted neural plate cells onto the yolk under the EVL of host embryos in a lateral location (fig 5.2B), and analysed the polarisation of the ectopic cluster of cells at 28hpf. By this time, the donor neuroepithelial cells in the neural tube have well-established apico-basal polarity (fig 5.1A). I found that the transplanted cells often stay in a tight cluster, which remained in an ectopic location by 28hpf (fig 5.8A,D). I found that Pard3-GFP localised to the centre of the cluster, outlining a small lumen (fig 5.8B). In this smaller cluster, the cells appear to be organised into a spheroid monolayer, with each cell stretched from the apical surface to the outer edge of the cluster (fig 5.8B). Immunohistochemistry of the cluster revealed that ZO-1 was localised to the centre of the cluster indicating the presence of tight junctions (fig 5.8C), and laminin surrounded the cluster (fig 5.8C), most likely having been secreted by the neural cells. The arrangement and polarity of cells within the cluster is overall very similar to the structure of the neural tube and suggests that even in these extreme ectopic locations, the cluster of neural cells attempt to make a neural tube.

There are however some differences in the tissue structure of the clusters with respect to

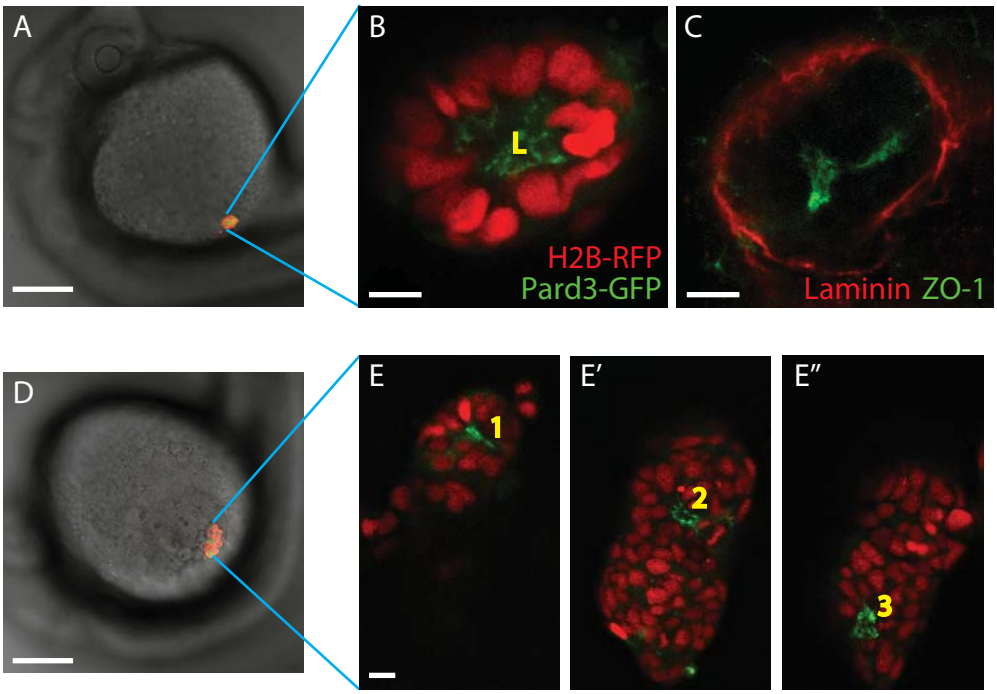

Figure 5.8 Clusters of ectopically located neural cells form polarised cysts with one or more central lumens by 24hpf.

A) A cluster of transplanted cells labelled with H2B-RFP in a 24hpf host embryo. The cluster of cells is located ectopically, distant from the brain. Scale bar represents 100µm.
B) Higher magnification of the ectopic cluster of A that shows that Pard3-GFP (green) is located at internal surfaces and demarcates a single lumen (L), revealing that the cells of the cluster are polarised. Scale bar represents 10µm.
C) Similarly, cluster of cells immunostained for the tight junction component ZO-1 (green) and the basal lamina component, Laminin (red). The cluster has distinct tight junctions as ZO-1 located at the centre of luminal surface of the cluster, while Laminin surrounds the cluster.
D) A larger cluster of transplanted cells labelled with H2B-RFP and Pard3-GFP is located ectopically, away from brain territories. Scale bar represents 100µm.
E–E'') Three z-slices through this larger cluster reveal multiple lumens outlined by Pard3-GFP (green). 1, 2, and 3 indicate three different lumens. within the cluster. Scale bar represents 10µm.

the neural tube. The cells of both the small and large cluster do not display the typical elongated morphology of polarised neuroepithelial cells (fig 5.8B,E). Furthermore, the large cluster of cells has a much more disorganised structure with multiple lumens, and irregularly shaped and positioned nuclei within the cluster (fig 5.8E–E''). In contrast to the small cluster, the cells have not formed a monolayer and do not appear to extend from the lumen to the outside edge of the cluster (fig 5.8E–E''). Therefore although Pard3-GFP outlines small lumens within the large cluster, the ectopic location of the cells results in some defects in neuroepithelial cell morphology and lumen formation. Nonetheless the generation of apical polarity appears to be a robust behaviour of neural cells even in this ectopic environment.

Ectopic clusters of neural cells establish apico-basal polarity on time

As clusters of cells in ectopic locations show well-defined apico-basal polarity by 24hpf, I next investigated if cells in ectopic locations polarise at the same time as in the neural rod by carrying out time-lapse imaging of a cluster of cells labelled with Pard3-GFP and H2B-RFP from 13hpf to 22hpf. At the beginning of the time-lapse at 13hpf, the cluster was located on the yolk of the embryo, just under the EVL, distant from the neural keel (fig 5.9A), where it remained until 24hpf (fig 5.9B). By 24hpf the cells were arranged in a long thin cluster with Pard3-GFP localised to the centre (fig 5.9C). Importantly for this study of the timing of polarisation, at the start of the time-lapse (13hpf, fig 5.9D) there were no bright puncta of Pard3-GFP within the cluster indicating that the cells of the cluster were not polarised. During the next 6hours, the cells of the cluster established apico-basal polarity, illustrated in the frames of Pard3-GFP from the time-lapse movie of the cluster (fig 5.9D-H). The whole time-lapse series can be viewed as supplementary movie 4. At 14hpf, small puncta of Pard3-GFP were already present at random locations within the cluster (arrows in fig 5.9E). By 15hpf, the puncta of Pard3-GFP were more numerous, slightly brighter and larger (fig 5.9F). Then over the next 2 hours, the puncta of Pard3-GFP coalesced towards each other to form larger and brighter puncta, especially in the centre of the cluster (yellow arrows in fig 5.9G). This is the same period over which puncta of Pard3-GFP coalesce towards the midline in the neural rod. By 19hpf, when neural rods have formed a single midline seam of Pard3-GFP, the puncta of Pard3-GFP in the ectopic cluster were likewise mostly organised in the centre of the cluster, forming two main concentrations of Pard3-GFP (fig 5.9H). Presumably the two accumulations then join together to form a continuous central lumen that is present by 24hpf (fig 5.9C). These observations show that Pard3-GFP polarity is established within the ectopic cluster with the same timing as Pard3-GFP polarity is generated within the neural rod during neurulation.

The normal timing of the establishment of polarity in the cluster is remarkable considering the disorganised movements of the cluster revealed in the time-lapse movie (movie 4). During the time-lapse, the cluster as a whole undergoes extensive movements on the yolk, and changes shape dramatically over time from an initial circular shape, to become highly elongated. Large cell rearrangements also occur within the cluster over time, as cells regularly change location within the cluster, and are highly mobile. These movements are very different from the organised convergence, invagination and intercalation movements that cells usually undergo during neurulation.

Ectopic clusters of neural cells may polarise by an alternative mechanism to mirror-symmetric cell division

In the neural rod, most neural cells undergo a highly regulated and stereotypical cell division at the midline of the neural rod. Moreover polarity is often generated during this cell division when Pard3-GFP is mirror-symmetrically localised to the abscission plane of the two daughter cells (Tawk *et al.* 2007). To explore whether the cells in ectopic clusters similarly polarised by mirror-symmetric division, I investigated if firstly, cell division shows any organisation within the cluster, and secondly if it is coordinated with the establishment of polarity. I analysed the location and orientation of cell divisions from the time-lapse movie in six 1hour periods, by plotting the positions of the two daughter cell nuclei immediately after division at anaphase of mitosis. These are shown overlaid on a projection of all nuclei of the cluster within each hour (fig 5.9I-M). In total, 19 cell divisions were observed from 14hpf to 19hpf, the time at which polarity is being established in the cluster. From this analysis, the cell division location and orientation in the cluster appears close to random, although there may be a slight tendency for cells to divide towards the edges of the cluster, especially at 14 and 15hpf (fig 5.9I,J). This is in stark contrast to the stereotypical locations of C-divisions during neural keel and rod stages (15-17hpf) that always occur close to the midline of the neural primordium with a medio-lateral orientation (fig 1.8).

As Pard3-GFP often becomes localised to the abscission plane of cells undergoing C-division in the neural rod (Tawk *et al.* 2007), I looked directly for the appearance of Pard3-GFP puncta between daughter cell nuclei after cell division at 15-17hpf in the cluster. Two examples of short time lapse sequences of potential mirror-symmetric divisions are shown in figure 5.9N and 5.9O. In the cell division at 15hpf, Pard3-GFP appeared between the two daughter nuclei (blue dots) as they separated (arrow at 5minutes after division in fig 5.9N). This punctum of Pard3-GFP did not remain in the next frame, so was either unstable, or moved out of the frame with the two daughter cell nuclei. In the division at 16hpf,

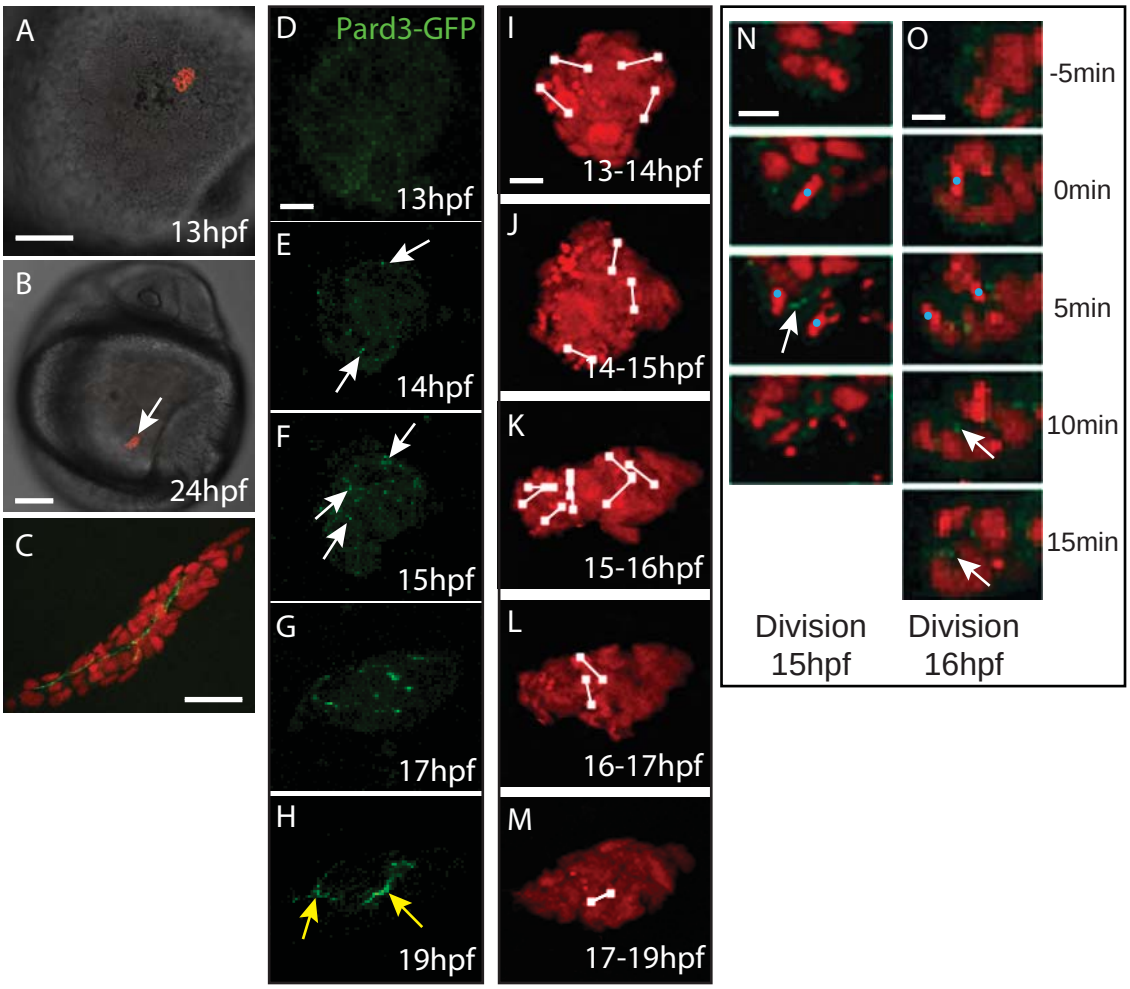

Figure 5.9 Time-lapse analysis of Pard3-GFP localisation in an ectopic cluster reveals that apical polarity is established on time.

A) The ectopic cluster of cells (red) is located above the yolk at 13hpf. Scale bar is 100µm.
B) The ectopic cluster of cells (arrow) has remained in an ectopic location by 24hpf. Scale bar is 100µm.
C) The cells of the cluster have polarised with an apical surface outlined by Pard3-GFP (green) in the centre of a large cluster by 24hpf. Scale bar is 100µm.
D-H) Maximum confocal projections of Pard3-GFP at all z-levels through the cluster at hourly time points. White arrows indicate Pard3-GFp puncta. Scale bar is 10µm.
D) At 13hpf the cells of the ectopic cluster are not polarised, as Pard3-GFP is diffusely localised in the cytoplasm.
E) Puncta of Pard3-GFP first appear at 14hpf.
F) The puncta of Pard3-GFP are more numerous at 15hpf and are scattered throughout the cluster.
G) By 17hpf, the puncta have coalesced into larger aggregates in the centre of the cluster.
H) By 19hpf, puncta of Pard3-GFP have coalesced at the centre of the cluster in two locations (yellow arrows).
I-M) Cell divisions indicated by the white dots and lines overlaid on maximum confocal projections of H2B-RFP at all z-levels and time points within the indicated 1hour periods. There is no pattern to the location or orientation of cell divisions. Scale bar is 10µm.
N,O) Time-lapse sequences of cell divisions with puncta of Pard3-GFP (arrows) located between daughter nuclei after cell division. Blue dots label the mother cell in metaphase and the two daughter cells. Time begins at metaphase of mitosis. Scale bar is 10µm.

Pard3- GFP only became localised between the two daughter cells 10 minutes after division (arrow in fig 5.9O), although in this example the spot remained present in the next frame (arrow at 15mins in fig 5.9O). These examples show that some cells may polarise by mirror-symmetric inheritance of Pard3-GFP, but as the cells within the cluster are highly mobile and the cells rearrange rapidly after cell division this is impossible to confirm definitively. In other cell divisions (not shown) Pard3 was not observed at the abscission plane, suggesting that cells are able to polarise by other mechanisms other than mirror-symmetric cell division.

Neural cells differentiate into neurons on time in extreme ectopic locations in the embryo

In the ectopic transplants, cells were taken from the neural plate of wild-type or MZ*oep* embryos, and therefore were already specified as being neural prior to transplantation. To verify that these ectopically located cells remained fated as neural, and also to investigate if the differentiation program of these cells could continue in ectopic locations, I used donor neural plate cells from the tg(HuC:GFP) line, in which all neurons express GFP (Park *et al.* 2000). The neural tube of a 28hpf wild-type embryo is organised with the GFP-positive neurons at the basal edge and ZO-1 localised at the midline (fig 5.10A,B). I imaged ectopic clusters at 24hpf (n=1 fig 5.10C,D) and 30hpf (n=7 fig 5.10E-G) and found that even as early as 24hpf, groups of cells located at the periphery of the cluster expressed cytoplasmic GFP (arrows in fig 5.10D,E), indicating that they had begun to differentiate into neurons. By 30hpf, 6 out of the 7 ectopic clusters examined contained GFP-positive cells (fig 5.10E-G), some of which now showed neuronal-like morphology with long processes resembling axons or dendrites (fig 5.10G). The location of the neurons at the outer (basal) edge of the cluster, coupled with the ZO-1 localisation at the centre of the cluster surrounding a small lumen (fig 5.10F), is highly reminiscent of the organisation of the neural tube (fig 5.10B). Overall these experiments show that when transplanted into ectopic locations, neural cells not only polarise on time, but can also differentiate on time into neurons that exhibit typical neuronal morphology and are spatially organised at the edge of the cluster similar to their basal location at the edge of neural tube *in vivo*.

Neural progenitor cells form polarised cysts when cultured in Matrigel

One of the most robust tests of an intrinsic timer is to determine if it still operates *in vitro*. We focused on developing a three dimensional (3D) culture protocol for zebrafish neural cells because polarisation and lumen formation of several types of epithelial cells has been successfully investigated in 3D culture (Bryant *et al.* 2008). To test if neural plate cells were

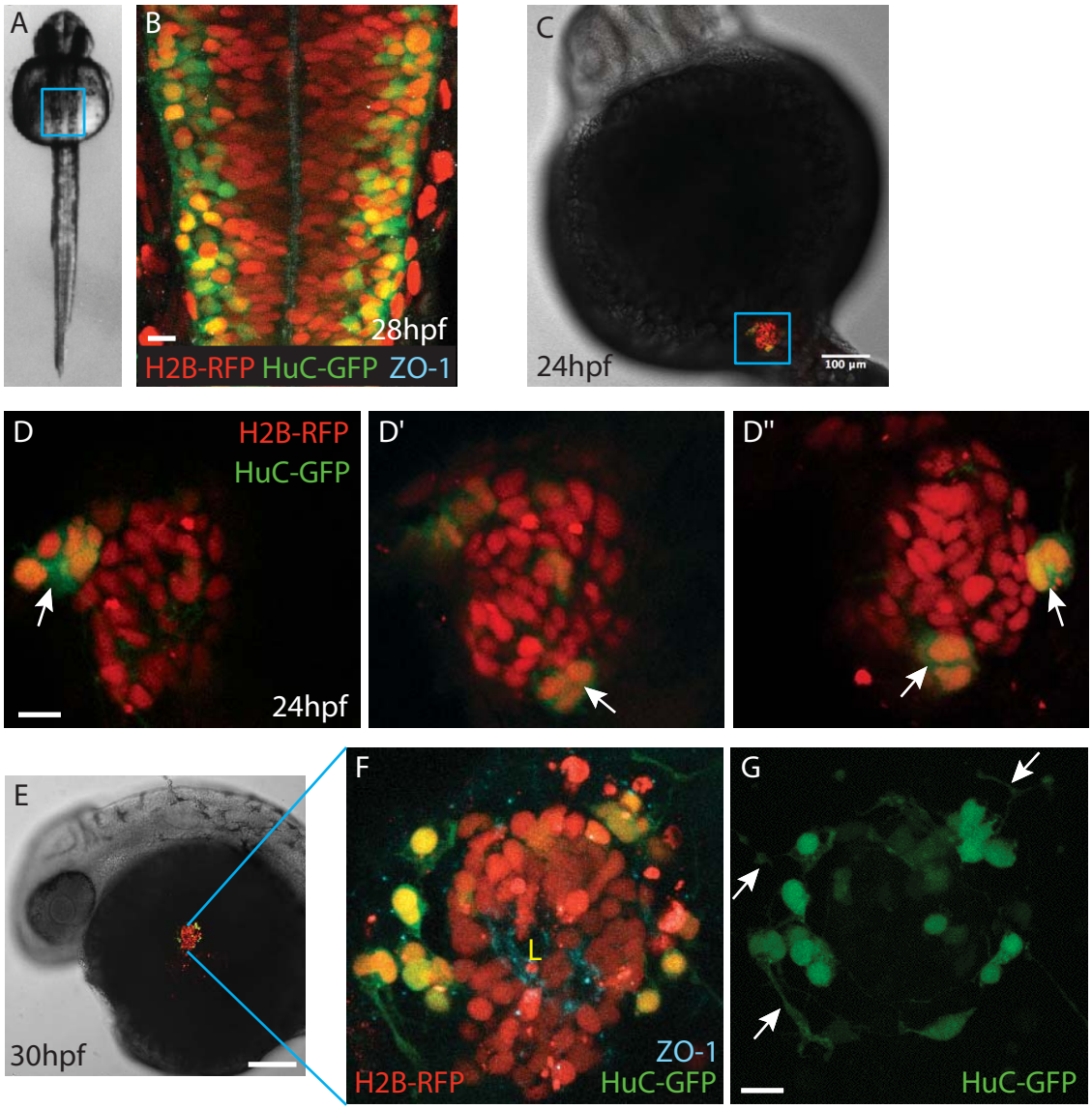

Figure 5.10 Ectopically located cells can differentiate into neurons outside the neural tube by 24hpf.

A) 30hpf brightfield dorsal view of a zebrafish. The blue box shows the approximate location of the photomicrograph in B.
B) Dorsal confocal section through the neural tube of a HuC:GFP transgenic embryo stained for ZO-1 at 28hpf. All cell nuclei are labelled with H2B-RFP. Pale blue ZO-1 is located at the apical midline showing that the neuroepithelial cells are polarised, and HuC:GFP expression reveals that neurons are located at the basal edge of the tube.
C) A cluster of transplanted cells labelled with H2B-RFP is located ectopically.
D-D'') Different z-levels through an ectopic cluster of cells at 24hpf. Some cells of the cluster are expressing GFP (green) showing that neurons are differentiating on time even in ectopic locations. Arrows indicate presence of differentiating neurons.
E) A large cluster of transplanted cells is located ectopically at 30hpf.
F) Maximum projection of confocal z-slices taken through the centre of the cluster. At 30hpf, the cells of the cluster expressing GFP that have differentiated into neurons are usually located towards the edge of cluster. ZO-1 is polarised to the centre of the cluster demarcating the luminal surface (L indicates the lumen).
G) Single GFP channel of the merge picture in F shows that some neurons have extended long thin processes resembling dendrites (arrows), which usually project away from the cluster.
Scale bar indicates 100µm in C and E, 10µm in B, D and G.

able to polarise in culture they were embedded in Matrigel and analysed at approximately 28hpf, the time at which neuroepithelial cells within the embryo have well-defined apico-basal polarity (fig 5.10B). I found that the cells survived well within the matrix and by 28hpf they had formed small cysts (fig 5.11A,D). The shape of the cyst was either spherical (fig 5.11A-C) or more irregular (fig 5.11D-G). In the spherical clusters, Pard3-GFP was localised to the centre of the cluster and outlined a single lumenal space (fig 5.11B), which is equivalent to its localisation close to the ventricular surface of the neural tube *in vivo*. However the cells of the cyst did not display the typical elongated shape of neuroepithelial cells (fig 5.11B), as the depth of the cyst wall is little more than the size of a single cell nucleus. Nonetheless the formation of a single central lumen indicates that the cells have developed well-organised apical polarity within the cluster.

In a larger more elongated cluster, Pard3-GFP outlined two lumens within the cluster (arrows in fig 5.11E), but both lumens were located centrally within the cluster as a whole (fig 5.11F). The brightfield image of this particular cluster (fig 5.11G) reveals that it could consist of two small clusters close together, which correlates with the position of the two lumens. It is currently unclear which factors determine the organisation and shape of the lumen within each cluster, but it may depend on the size and/or the shape of the cluster. However in all examples of clusters that have polarised Pard3-GFP, Pard3-GFP is located in the centre of the cluster (n=4) indicating that the apical surface is always in the interior of the cluster.

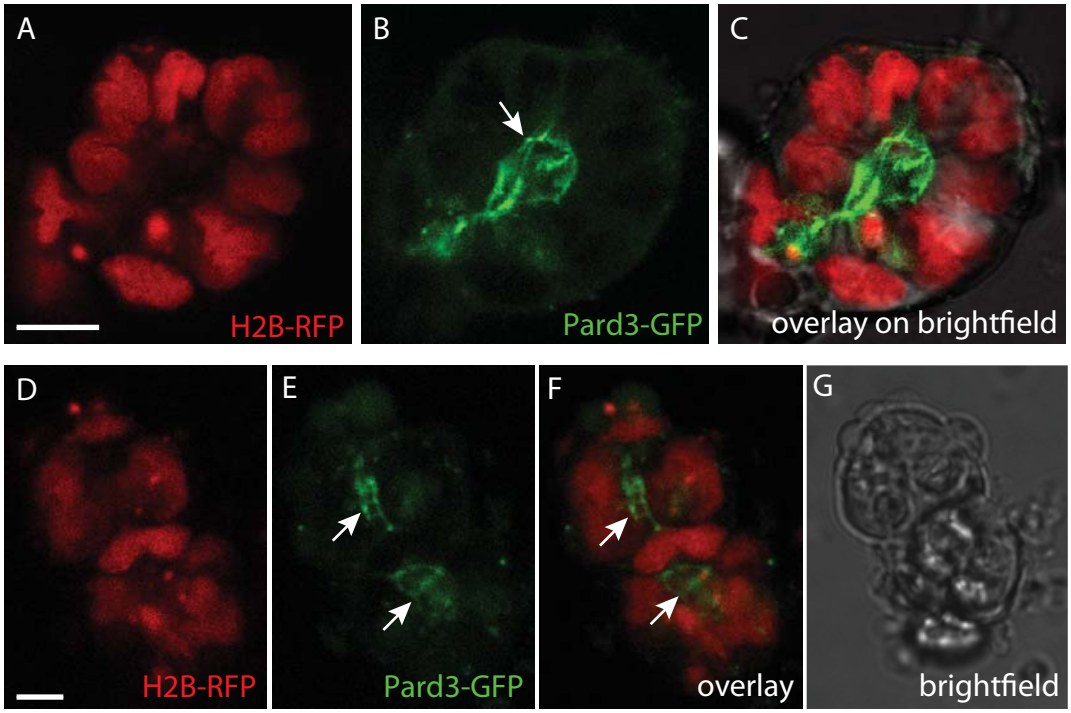

Figure 5.11 Neuroepithelial cells form polarised cysts by 24hpf when cultured in three dimensions.

Neuroepithelial cells were taken from an embryo at 11hpf, and cultured in Matrigel until 24hpf.
A-C) A small projection of z-slices though the centre of a cluster of neuroepithelial cells expressing H2B-RFP (red, A) and Pard3-GFP (green, B). The cells of the cyst are polarised with the apical marker Pard3-GFP localised to the centre of the cyst outlining a single central lumen (arrow in B).
D-F) A small projection of z-slices though the centre of a second cluster of neuroepithelial cells expressing H2B-RFP (red, D) and Pard3-GFP (green, E). There are two distinct patches of apical membrane (arrows), indicating the presence of two lumens in the centre of the cluster.
G) Brightfield image of the cluster of cells in D-F.
Scale bar indicates 10μm.

5.5 DISCUSSION

My analysis of the establishment of polarity during neurulation using ZO-1 immunohistochemistry shows that *tri* embryos polarise at the same time as wild-type embryos. This indicates that the establishment of apico-basal polarity is independent of the abnormal neural tube morphogenesis of this mutant and also planar cell polarity signalling. My analysis of apical polarisation in MZ*oep* embryos revealed a small 30minute delay in the initiation of polarisation of ZO-1, and a 1.5hour delay in the later stage of Pard3-GFP polarisation compared to wild-type. This signifies that one of the several abnormalities in Nodal-deficient embryos affects the development of apical polarity during zebrafish neurulation, which could be the loss of co-ordinated movements of neurulation, the lack of Nodal and midline signals, or the absence of mesodermal tissue.

I also found that neural cells are able to polarise in ectopic locations in the embryo, and in Matrigel 3D culture. In the ectopic location in the embryo (above the yolk), apical polarity was first generated as small puncta of Pard3-GFP, which then became organised to the centre of the cluster to form one or more lumens. I found that some cells may polarise by mirror-symmetric inheritance of Pard3-GFP during cell division, but many Pard3-GFP puncta did not correlate with the locations of cell divisions, suggesting that the generation of polarity can occur by an alternative mechanism to mirror-symmetric division. In 3D culture, clusters of cells also established apico-basal polarity with the apical polarity organised to the centre of the cluster outlining one or more central lumens. This indicates that the clusters of neural cells can self-organise into a hollow cyst similar in organisation to the neural tube in the absence of many aspects of their normal environment.

Generation of apical polarity is independent of PCP signalling and normal convergent extension

trilobite embryos have defective PCP signalling that results in slow convergence of the neural tissue towards the dorsal midline. Despite this abnormal neural tube morphogenesis, I have shown that apical polarity is generated on time in this mutant. The simplest conclusion of this experiment is that PCP signalling is not required for apical polarity to be established on time. However the neural tube morphogenesis defects of *tri* embryos also reveals other information about which factors are, and are not, important for neural cell polarisation.

The cells in the *tri* neural primordium have a different environment to wild-type neural rod cells firstly because the primordium is not located at the embryonic midline. The cells are therefore distant from the notochord and associated midline signals such as Shh, suggesting that a local midline signal is not important for cell polarisation. Secondly, the basal lamina is only present on the deep side of the neural primordium at the time of polarisation, in contrast to the neural rod where the basal lamina surrounds the lateral outer edges. This implies that neural cells are able to polarise in the absence of a bilateral basal lamina. Thirdly, although the tri primordium is still adjacent to the mesoderm, the mesoderm only underlies the *tri* neural primordium on the deep side of the neural primordium. Thus bilateral mesoderm does also not seem to be important for correct cell polarisation. Simply the presence mesoderm may however be enough to allow cell polarisation, as the mesoderm may direct the timing of cell polarisation, for example by sending a diffusible signal. Another similarity of the *tri* neural primordium to the wild-type neural rod is that the cellular arrangements within the *tri* neural plate may not be too dissimilar to the wild-type neural rod, even though with respect to the embryonic axes and midline, the *tri* neural primordium is abnormally shaped. For example, the cells seem to be elongated in the *tri* neural plate similar to within the wild-type neural rod, and thus this similar cellular morphology may produce a local environment typical of the neural rod and might allow for the neural cells to divide and polarise on time. Evidence supporting this idea comes from the observation that transplanted older cells polarise early in a young environment, indicating that the shape of a younger neural primordium is permissive for cell polarisation.

Cell polarisation can occur on time independently of the dorsal environment of the embryo

My results show that neural progenitors are to able polarise on time in extreme ectopic locations within the embryo, as puncta of Pard3-GFP first appear at 14hpf (fig 5.9), similar to the time at which they appear in the wild-type neural rod (fig 5.6). Moreover the puncta coalesce towards the centre of the cluster to form two apical foci by 18hpf (fig 5.9), which is when puncta of Pard3-GFP have coalesced at the midline of the neural rod to outline the apical surfaces of the neuroepithelium. This polarisation of cells in the absence of the normal environmental signals present at the dorsal midline of the embryo shows that the ability to polarise is a robust property of zebrafish neural cells. In this environment the cells are sitting on the yolk cells, just under the enveloping layer (EVL) with which they probably contact. They are however far away from other embryonic tissues, such as the notochord, somites and paraxial mesoderm and the signals they may

produce to induce cell polarisation. This strongly suggests that the polarisation timer of neural progenitors can run independently of all these tissues. The cells are however surrounded by some extracellular matrix components, such as laminin. The possible contribution of the ECM is discussed below, as cells in 3D culture are also surrounded by the ECM components of Matrigel.

Cell polarisation is delayed in Nodal-deficient embryos.

Although neural cells show robust polarisation on time in several abnormal environments, in Nodal-deficient (SB-treated) or MZ*oep* embryos, ZO-1 polarisation is delayed by half an hour, and Pard3-GFP polarisation is delayed by 1.5hours compared to wild-type. These results do not seem to fit in with the other data as they suggest that the intrinsic timer regulating polarisation can be modified in the Nodal-deficient embryos. One or more of several different defects may cause the delay in polarisation such as a lack of a specific tissue such as mesoderm, ventral midline cells, the notochord or endoderm, a lack of Nodal signalling itself, or the abnormal cell organisation and morphogenesis of the neural tissue during neurulation.

It is unlikely that the delay in polarisation in Nodal-deficient embryos is caused by a lack of Nodal signalling during neurulation, because inhibiting Nodal signalling with the SB drug just over the time course of neurulation does not disrupt neural tube morphogenesis (C. Araya, unpublished observations). It is also unlikely that a lack of a polarising signal from a missing tissue before neurulation causes the delay because cells cultured in ectopic yolk locations were taken from the neural plate of a Nodal-deficient embryo and they are able to polarise on time. Furthermore this suggests that something during neurulation acts to inhibit apical specialisations forming on time.

The severe defects in neural tube morphogenesis in MZ*oep* embryos seem the most likely cause of the delay. Defects in neural tube morphogenesis are apparent from the beginning of neurulation, when the tissue fails to invaginate at the midline, and the neural plate becomes much thicker than in wild-type embryos (C. Araya, unpublished observations). During the later stages of neurulation, cellular arrangements within the neural primordium are also highly disorganised, and cell trajectories of individual cell movements are much more random than normal (C. Araya, unpublished observations). In addition, cell divisions occur in many orientations and locations contributing to the disorganised movements of the cells during neurulation. This lack of coordination between cells both in their movements and divisions is likely to inhibit the generation of

stable contacts between cells that are necessary for the formation of an epithelium. Thus the appearance of stable Pard3 puncta may be delayed.

The delay in the appearance of foci of ZO-1 may be less than the delay in Pard3-GFP polarisation because ZO-1 puncta appear earlier in neurulation before some of the defects in neural tube morphogenesis become so severe in MZ*oep* mutants. For example, the cell movements seem to become progressively more chaotic during the course of neurulation (C. Araya, unpublished observations). Moreover the mechanism by which Pard3-GFP becomes polarised in MZ*oep* mutants is currently unclear because it is difficult to spot any mirror-symmetric divisions with Pard3-GFP localised to the abscission plane between daughter cells. This may be because the disorganised cell movements and random division orientations make it hard to observe mirror-symmetric divisions in time-lapse movies, or alternatively there is the possibility that polarity is generated by another mechanism, other than mirror-symmetric division. Whatever the mechanism of Pard3-GFP polarisation, the delay in polarisation in MZ*oep* embryos suggests that grossly disorganised cell movements can affect the establishment of apical polarity. The precise factors that can modify the timing of cell polarisation are unclear from these experiments, but when considered with evidence of an intrinsic timer from chapter 4, it seems likely that the neural environment must be permissive for the timer and cell polarisation to occur.

Finally, there is a possibility that the delays in polarisation in MZ*oep* and SB embryos may be caused by a general delay in embryo development. It is difficult to accurately determine the age of these embryos because they do not form anterior somites to count, and have such gross abnormalities in embryogenesis that their age cannot be determined from general embryo morphology.

Limitations to the polarisation analysis

Analysis of the changes in ZO-1 intensity or puncta over time provides an unbiased readout of tissue polarization. Nonetheless there are several limitations to this approach. We are looking at the appearance of the protein as puncta within a tissue, not at the cellular level. It is not clear where these puncta are located within a cell; we are not even certain that they are located close to the membrane at these early stages. It seems unlikely that the ZO-1 puncta are part of functional tight junctions because at these stages of neurulation cells are very dynamic and intercalating across the two sides of the neural keel. This would require contacts and junctions to be constantly remodelled. However the

ZO-1 puncta may represent spot adherens junctions, because in the generation of apical polarity in mammalian epithelial cells in culture, ZO-1 is one of the first proteins to be localised to the point of cell-cell contact (Yonemura *et al.* 1995). The only way to confirm the junctional structures present between neuroepithelial cells at keel stages is to study the tissue structure by electron microscopy. Nonetheless, whatever the nature of structural unit of ZO-1 that accumulates in focal puncta during neurulation, it is one of the first markers to define the prospective luminal plane and therefore is a *bona fide* readout of polarity.

Pard3-GFP polarisation during neurulation was difficult to quantify, especially in MZ*oep* embryos, for a number of reasons. As Pard3-GFP was exogenously introduced into the embryo by microinjection of RNA encoding the fusion protein, it was a concern that inconsistent RNA injection could produce variations in the overall level of fluorescence intensity, which could in turn, affect the number of Pard3-GFP puncta observed. This was overcome by trying to choose embryos with similar expression levels at neural plate stages, and by normalising the number of puncta over time to the maximum for each embryo. The second concern was that the classification of a punctum of Pard3-GFP involved a judgement by eye, which was liable to bias. This was especially true of wild-type to MZ*oep* comparisons, as it was easier to observe the puncta in wild-type embryos as they appeared in a defined location close to the midline, whereas in MZ*oep* embryos puncta could appear randomly within the tissue. Moreover, the Pard3-GFP puncta seemed to be more stable over time in wild-type embryos as they often appeared in several sequential frames of the movies, compared to puncta of Pard3-GFP in MZ*oep* embryos that were often only present in a couple of frames. This is likely caused by the more uncoordinated movements of cells in MZ*oep* embryos compared to wild-type, which could then either result in the puncta being less stable in MZ*oep* embryos as neighbouring cells do not maintain contact, or simply cause cells to move in and out of the plane of focus more often in MZ*oep* embryos. This instability of Pard3-GFP puncta may account for the greater variability in the appearance of puncta between the different z-levels of the time-lapse in MZ*oep* embryos. Despite these difficulties though, repeating the analysis over several z-levels and across different embryos and then calculating the average appears to have given reliable results for this analysis.

Matrigel may promote neural progenitor cell polarisation

I have found that clusters of zebrafish neural progenitor cells form remarkably well-polarised cysts when placed in Matrigel culture. This further suggests that the program of

cell polarisation within neural progenitor cells can continue in the absence of many external signals. However, Matrigel is composed of several different basement membrane components, including laminin and collagen, which may simply adequately support cyst formation, or may actively instruct the cells to polarise as soon as they placed into the gel. It is possible that the physical properties of Matrigel such as stiffness and density may promote cyst and lumen formation, as these have been shown to affect cell signalling and behaviour (Discher *et al.* 2005; Yamada *et al.* 2007). Alternatively, the basement membrane components of Matrigel may give provide a biochemical cue to the cells to orient their polarity. When MDCK cells are embedded in ECM gels they form cysts with apical polarity at the centre of the cluster, but when they are cultured suspension by coating the substrate in poly-HEMA that prevents cell attachment to a substrate, they form clusters with apical polarity oriented on the outside of the cluster towards the culture medium (Wang *et al.* 1990b; Wang *et al.* 1990a; Liu *et al.* 2007). This shows that attachment to a substrate is important for the correct orientation of polarity, and ECM components including laminin and collagen, may be the crucial molecules in this interaction. For example, when β1-integrin receptors are inhibited in MDCK cells grown in collagen, the cysts develop inverted polarity (Yu *et al.* 2005b). It would be interesting to explore the physical and chemical contributions of the substrate for neural cell polarisation by comparing cell polarisation in different 3D gels, such as gels consisting of a single ECM component or peptides of ECM proteins, and completely synthetic gels that do not provide any biochemical cures (Tibbitt *et al.* 2009).

Cell polarisation in extreme environments may rely less upon mirror-symmetric cell division than in the neural rod

The formation of polarised cysts of zebrafish neural progenitor cells in 3D culture is similar to that of MDCK and Caco-2 cells, in that the apical lumen forms in the interior of the cluster of cells. However, the zebrafish neural cells polarise within 14 hours of the cells being placed into culture, which is much more rapid than cyst formation of Caco and MDCK cells that often takes several days (Martin-Belmonte *et al.* 2007b; Jaffe *et al.* 2008). Moreover zebrafish neural cells sometimes form clusters with multiple lumens, which is rare in MDCK and Caco-2 cell cultures (Martin-Belmonte *et al.* 2007b; Jaffe *et al.* 2008). These differences in the speed of polarity generation and cyst organisation between zebrafish and mammalian cells may have several explanations. Different types of cells undergo lumen formation by different mechanisms (Bryant *et al.* 2008), which is likely to depend on different individual cell behaviours and the initial culture conditions.

The initial culture conditions have been shown to affect both the speed and mechanism of lumen formation. When Caco-2 and MDCK cells are plated at a low density in Matrigel, cysts are generated by proliferation from single cells and take several days to form because MDCK and Caco-2 cells have a cell cycle length in the order of a day (Martin-Belmonte *et al.* 2007a; Jaffe *et al.* 2008; Schluter *et al.* 2009). Under these conditions apoptosis appears to play a small role, if any, during lumen formation (Martin-Belmonte *et al.* 2008). However when plated at a higher density, MDCK cells form aggregates that show delayed polarisation and a greater number of central apoptotic cells (Martin-Belmonte *et al.* 2008). In my experiments the cell cycle length of zebrafish cells during neurulation is approximately 4 hours (Kimmel *et al.* 1994), but even so the cysts still form too quickly for cell division to be solely responsible for generating the clusters. This indicates that the neural plate cells were probably not dispersed well within the gel and therefore the cells aggregated together quickly. If similar to the MDCK high density cultures, cell aggregation should cause cyst formation to be slowed, but in my experiments, apical polarity was generated in approximately 12hours. This indicates that neural progenitor cells are remarkably efficient in generating cysts with central apical polarity.

As mentioned above Caco-2 and MDCK cells form cysts by proliferation. Two recent studies have shown that lumen formation in these cysts is generated during the first cell division by the localisation of apical components to the abscission site of the two daughter cells (Jaffe *et al.* 2008; Schluter *et al.* 2009). Zebrafish neural progenitors cells likewise polarise polarity proteins to the abscission plane between two daughter cells during the lumen formation of the neural tube. In the extreme ectopic clusters in the embryo, the reliance upon this mechanism for generating apical polarity however seems to be decreased because cell divisions were randomly oriented, puncta of Pard3-GFP initially appeared throughout the ectopic cluster, and mirror-symmetric C-divisions were hard to identify. Over time Pard3-GFP puncta coalesced towards the centre of the cluster as the cells underwent extensive rearrangements within the cluster. In Matrigel, the zebrafish neural cells may also not rely solely upon cell division to polarise as the clusters form rapidly. This reduction in the reliance of neural cells to polarise by division might explain why cyst generation is less coordinated and why multiple lumens can be generated.

In summary, my initial experiments of culturing zebrafish neural progenitors in Matrigel suggest that 3D culture may provide a complementary approach to investigating lumen formation *in vivo*. The technique of 3D culture may be valuable for enabling investigation into the mechanism of cell polarisation and the possible contribution of the ECM, which

are experiments that may not be possible in the embryo because of the large numbers of the extracellular matrix proteins secreted from several different types of cells *in vivo* and functional redundancy between different isoforms. Moreover time-lapse imaging of cell polarisation in culture using GFP-tagged fusion proteins may reveal more information about the mechanism of polarisation and whether cell division and/or apoptosis play any role in lumen formation. It may even be possible, with more technical expertise, to observe a single neural cell undergoing cell division in culture, as a test of the cell intrinsic nature of mirror-symmetric cell division.

CHAPTER 6 THE POLARISATION TIMER IS INDEPENDENT OF CELL DIVISION

6.1 INTRODUCTION

Previous chapters have shown that the age of a neural cell is crucial for determining the time at which neural cells undergo C-division and establish apico-basal polarity. The next logical area of investigation is to consider possible mechanisms of how neural cells monitor time. In this chapter I test the hypothesis that neural progenitor cells count the number of cell cycles to know their age. This hypothesis is based on the following observations of cell behaviour and cell division during zebrafish development.

Distinguishable cellular behaviours occur at particular cell cycles

During zebrafish development the neural tube forms within the first twenty-four hours of development. During this early period of development it is has been observed that specific cell behaviours such as cellular morphogenetic movements and orientation of cell division are related to specific cell cycles (Kimmel *et al.* 1994). Kimmel and colleagues found that in the 15th cell cycle, cells generally move in a posterior-direction during epiboly and divide along the antero-posterior axis (Kimmel *et al.* 1994). However during cell cycle 16, cells change direction to move towards the dorsal midline as they undergo convergence extension movements and then divide in the neural keel or rod with a medio-lateral orientation to separate sister cells across the midline (Kimmel *et al.* 1994). Thus it is apparent that C-division during neurulation almost always occurs on a cell's 16th cell division. It is therefore an attractive hypothesis that cells count the number of cell cycles to know when to polarise.

Although the cellular morphogenesis and cycle number during zebrafish development appear to be related, there has however been little research into whether this relationship is just coincidental or if it is causally related. It may be that the environment of the neural keel determines the characteristics of C-divisions, and it just so happens that the cells are going through the 16th cell cycle leading to the 16th division at this time. However, I have previously shown by heterochronic cell transplantation that neural cell age is crucial for the timing of polarisation and division, so it seems unlikely that the environment is the sole controller of cell behaviour during neurulation. Nonetheless, the relationship of the intrinsic timer to cell division remains open for investigation.

Cell division is required for some developmental timers

The requirement of cell division for developmental timers has been investigated in the temporal transition sequence of neuroblasts in the *Drosophila* CNS. The neuroblasts undergo multiple rounds of cell division during neurogenesis, and each division is asymmetric, as the neuroblast renews itself, and buds off a smaller ganglion mother cell (GMC). During these asymmetric cell divisions, the neuroblasts sequentially express a series of transcription factors (Isshiki *et al.* 2001), which are inherited by the GMCs, and determine the identity of the neurons or glia generated from the terminal division of the GMC (Isshiki *et al.* 2001; Grosskortenhaus *et al.* 2005). Thus, in the neuroblasts, the timely switch of expression from one transcription factor to the next is important for correct temporal identity of neurons. It has been shown that the switch from Hunchback to Krüppel, which are first two transcription factors in the series, depends on cytokinesis, because neuroblasts arrested in G2 phase of the cell cycle continue to express *hunchback*, and do not switch to *Krüppel* expression (Grosskortenhaus *et al.* 2005). Further experiments showed that cytokinesis, but not cell cycle progression *per se*, was necessary for the switch because *hunchback* failed to be downregulated in neuroblasts that were impaired in cytokinesis but could continue though the cell cycle (Grosskortenhaus *et al.* 2005).

The counting of cell divisions as mechanism for measuring time has been tested for other developmental timers. It was originally proposed that oligodendrocyte precursor cells (OPCs) counted the number of cell divisions before differentiating, because during early studies of OPCs in culture, isolated clonal progeny always differentiated after the same number of cell divisions (Temple *et al.* 1986). Subsequent work however showed this not to be true as when OPCs were cultured at 33°C instead of 37°C they divided more slowly, but still differentiated at the same time, even though they had undergone fewer cell cycles (Gao *et al.* 1997). In a separate example, results from experiments using clones of cultured cardiac myocytes were consistent with an intrinsic timer controlling their time of differentiation. However, lowering the temperature to slow down the cell cycle similarly showed that the timer does not simply count the number of cell divisions (Burton *et al.* 1999). Thus many of the proposed intrinsic timers that operate during embryonic development do not seem to operate by counting the number of cell cycles, so it will be interesting to see if neural cells are different and do monitor time using this mechanism.

Is cell division a requirement for polarisation during zebrafish neurulation?

In addition to researching if cells count the number of cell cycles to know when to undergo C-division, I also wanted to investigate the possibility that cells were able to polarise on time in the absence of cell division, especially because mirror-symmetric cell division is one mechanism by which cells acquire apico-basal polarity during neurulation (Tawk *et al.* 2007). I have already shown that cell polarisation, cell division orientation and midline crossing all occur according to a cell's age, and do not seem to be influenced by the surrounding environment (Chapter 4), but I did not explore whether all of these behaviours were controlled separately by the developmental timer, or are dependent upon each other for their correct timing.

Several groups including the Clarke lab have studied the effects of inhibiting cell division for neural tube morphogenesis (Ciruna *et al.* 2006; Tawk *et al.* 2007; Nyholm *et al.* 2009). Inhibiting cell division using the pharmacological inhibitors aphidicolin and hydroxyurea at various stages of neurulation results in a relatively normal neural tube by 24hpf (Ciruna *et al.* 2006; Tawk *et al.* 2007), but the cellular behaviours during morphogenesis and the timing of polarity establishment have not been studied in detail.

Another group has investigated the effect of blocking cell division for a longer period of development by studying embryos mutant in the G2/M transition regulator *emi1* that cease mitosis in all tissues from the beginning of gastrulation (Zhang *et al.* 2008). Emi1 acts at the G2-M transition by inhibiting the Anaphase Promoting Complex/cyclosome (APC/C), which in turn allows cyclinB1 to accumulate (Reimann *et al.* 2001). Upon Emi1 depletion in cycling *Xenopus* extracts, the cyclin B1 accumulation necessary for entry into mitosis is prevented (Reimann *et al.* 2001), so it is likely that in the zebrafish *emi1* mutant the cells are arrested in G2 phase of the cell cycle. They found that surprisingly, *emi1* mutants develop relatively normally until 24hpf, although both axis elongation and somite morphogenesis are slightly impaired (Zhang *et al.* 2008), indicating that the large-scale morphogenetic movements of epiboly, gastrulation, and neurulation were not affected by blocking cell division. Deeper analysis of neurulation in the absence of cell division should reveal the importance of the mirror-symmetric division for cell polarisation.

6.2 AIMS

1. To determine if neuroepithelial cells count the number of cell cycles as a mechanism for measuring time (for C-division and polarisation).
2. To test if cells establish apical polarity on time and in the right place in the complete absence of cell division.

6.3 METHODS

Blocking cell division for at least one cell cycle prior to neurulation

Embryos were injected at the 1-cell stage with p53 morpholino (5' GCG CCA TTG CTT TGC AAG AAT TG 3', 0.75mM) and H2B-RNA (100pg). Injection of p53MO was necessary because otherwise the toxicity of the cell-division inhibitors during gastrulation caused the embryos either to die or be so unhealthy that cell division did not recover.
Labelled embryos were selected at shield stage and were incubated at 28.5°C in the cell division inhibitors aphidicolin (150µM, 2.5% DMSO) and hydroxyurea (20mM) in embryo medium for 4 hours from 60% epiboly (6hpf) to 11hpf, which covers the time of the 15th cell cycle and division. Control embryos were incubated in 2.5% DMSO in embryo medium for this time period.
At 11hpf, the inhibitors were washed out by carefully exchanging the medium with fresh embryo medium three times. Aphidicolin and hydroxyurea are reversible drugs, and so upon washing, cell division can return. The embryos were left to recover at 28.5°C until needed for imaging or fixing. Embryos that have undergone this protocol are referred to as 15th cycle embryos.
To determine the efficiency of cell division inhibition at least 4 treated and 4 control embryos were fixed at regular time period during the drug treatment and stained in wholemount for phospho-histone H3 to label mitotic figures.

N.B. Inhibiting the cell cycle for longer or earlier in development (to cover more than 1 cell cycle or block the 14th division) was not possible because the embryos did not complete epiboly normally and often died.

Blocking cell division throughout neurulation

Cell division was blocked throughout neurulation by injecting embryos at the one cell stage with 2nl of 0.5mM of emi1 translation blocking morpholino (Gene-Tools) targeted against the ATG start site of the gene (5' GTA GTT TGG ACA CTT CAT ATT GAGG 3').
Control embryos were injected with 2nl of the standard control morpholino from Gene-Tools (5'-CCT CTT ACC TCA GTT ACA ATT TATA 3') at the same concentration (0.5mM).
Morpholinos were coinjected with RNA encoding Pard3-GFP (100pg) and H2B-RFP (100pg).

Time-lapse imaging in this chapter

Time-lapse imaging of Pard3 polarisation in control and *emi1* morphant embryos was carried out simultaneously. Embryos with similar expression levels of Pard3-GFP at neural plate stages of neurulation were chosen for imaging, and the embryos mounted for transverse imaging through the hindbrain.
Time-lapse imaging of cell divisions in 15th cycle and control embryos was also carried out simultaneously.
All confocal images in this chapter were acquired using an SP5 Leica laser scanning confocal microscope.

Pard3-GFP intensity analysis to measure polarization at the apical midline

Simultaneous time-lapse movies of control and *emi1* morphant embryos ubiquitously labelled with Pard3-GFP were analysed for establishment of apical polarity.
A projection of three consecutive z-levels over time was made for each embryo choosing z-levels through the hindbrain. Then single frames of this projected time-lapse at regular time points (half hour or hourly intervals) were chosen for analysis. A line approximately 140μm in width was drawn across the neural rod in each time frame. Then the average Pard3-GFP intensity across the neural rod was measured using the line profile command in ImageJ. These fluorescence intensity profiles were then compared over time to determine the progression of Pard3-GFP polarisation at the midline.

Immunohistochemistry

Antibodies used in this chapter were:
Anti ZO-1 (1:500, Zymed)
Anti phospho-histone H3 (1:500, Upstate)

Image processing

Fixed and time-lapse images were processed as described in the general methods using ImageJ and Adobe Photoshop.

Statistical analysis

All statistical analysis was carried out using GraphPad software. As the orientation of cell division data for 15th cycle embryos was not of a Gaussian distribution (D'Agostino and Pearson test), non-parametric tests were used to compare the angles of divisions between wild-type and 15th cycle embryos. To compare all three distribution at once a Kruskal-Wallis test was used, and the data were not significantly different. A Mann-Whitney U test

was also used to separately compare division orientations in each 15th cycle embryo to division orientations in the control embryo, with a result of non-significance for both embryos ($p=0.33$ and $p=0.78$).

6.4 RESULTS

As neural cells usually undergo mirror-symmetric C-division on their 16th cycle (Kimmel *et al.* 1994), it is possible that neural cells count the number of cell cycles as a mechanism for measuring time to know when to undergo this specialized division. To test this possibility I blocked cell division for one cell cycle prior to rod and keel stages of neurulation, so that after recovery cells will then be in their 15th cycle rather than their normal 16th cycle during keel and rod stages of neurulation. The properties of these cell divisions, such as division orientation and midline crossing of daughter cells was then analysed and compared to control embryos.

Pharmacological cell division inhibitors effectively block cell division during gastrulation

Before analysing if cells count the number of cell cycles to know when to undergo C-division, I first optimised the protocol for temporarily blocking cell division before neurulation using the pharmacological inhibitors aphidicolin and hydroxyurea. It was necessary to achieve a reliable and efficient reduction in cell division from 6hpf to approximately 11hpf, because the 15th cell cycle, which occurs during this time in development is on average 150 minutes long (Kimmel *et al.* 1994). Thus this period of division block should cover at least one cell cycle. The 16th cell cycle leading up to C-division is 240minutes long on average and usually occurs at 15-17hpf, so a recovery time of 4hours after washing out of the inhibitors should be enough to allow cell division to return during neurulation (Kimmel *et al.* 1994). It was necessary to inject the division inhibited embryos with p53 morpholino (p53MO) at the 1-cell stage to achieve good survival rates of embryos, so control embryos were also injected with p53MO.

To determine the time course and effectiveness of division inhibition, I fixed embryos at different time points during and after incubation in the inhibitors and stained for Phospho-histone H3 to label mitotic figures (fig 6.1). I found that within one hour of incubation in the inhibitors, cell division was dramatically reduced compared to control embryos (fig 6.1A,B). Cell division remained inhibited until the end of the incubation period (fig 6.1C,D). Recovery of cell division after washing was slower than the initiation of cell division block after adding the inhibitors, because after one hour of washing the number of mitotic figures remained low (fig 6.1E,F).

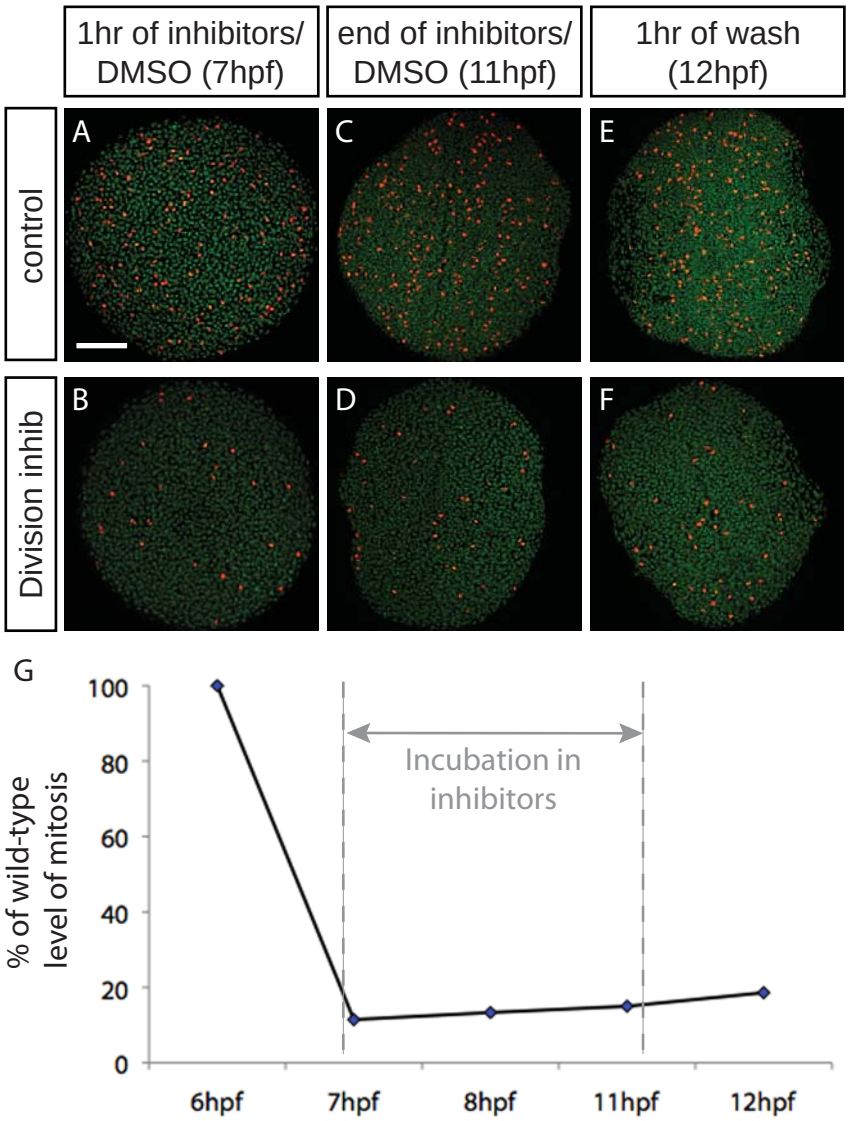

Figure 6.1 Pharmacological inhibitors can be used to reversibly block the 15th cell cycle during gastrulation

A-F) Maximum projections of control and aphidicolin and hyroxyurea treated (division-inhibited) embryos stained for Phospho-histone H3 in red to visualise cells undergoing mitosis. All nuclei are labelled in green with sytox-green.
A,B) After 1 hour of incubation in aphidicolin and hydroxyurea the number of mitotic figures was greatly reduced in these embryos (n=6) compared to control embryos (n=6).
C,D) At the end of the incubation period cell division was still markedly reduced (controls n=8, division inhibited n=8).
E,F) One hour after wash the number of mitotic figures in division-inhibited embryos remained low (n=5) compared to control embryos (n=6).
G) Graph showing that cell division is reduced to less than 20% of the wild-type level of cell divisions when embryos are treated with aphidicolin and hydroxyurea and remains reduced for 1hour after wash out of the drugs.
Scale bar in A is 100µm.

To quantify the efficiency of the division inhibition, I counted the number of mitotic figures in control and treated embryos at several time points, and calculated the average percentage of wild-type level of mitosis at each time point (fig 6.1I). The graph shows that after 1 hour of incubation in the drugs, cell division was reduced to 13% of the wild-type level, and it remained less than 15% of the wild-type level during the incubation period. One hour after washing out the inhibitors, cell division remained low at 18% of the wild-type level, but time-lapse analysis shows robust recovery of division by 15hpf (see fig6.2). In summary, I have confirmed that cell division is efficiently inhibited from 7hpf until 12hpf, and therefore using this protocol will enable me to test if cells count the number of cell cycles. I subsequently refer to embryos that have undergone this protocol as 15th cycle embryos.

Neural progenitors undergo cell divisions at rod stage of neurulation showing all the characteristics of C-divisions.

Having finalized the protocol for temporary cell division inhibition over the 15th cell cycle, I carried out simultaneous time-lapse imaging of 15th cycle embryos alongside control embryos. Embryos were labelled ubiquitously with H2B-RFP to enable cell divisions to be analysed, and mosaically labelled with membrane-GFP to reveal single cell behaviours. Time-lapse analysis of 15th cycle embryos reveals that many cells recover to undergo division at rod stage of neurulation (15-17hpf) (movie 5) showing that by 4 hours after wash out of the division inhibitors, cell divisions have returned.

I first analysed the locations of cell divisions from the time-lapse movies. These are shown overlaid onto a single image of the neural rod taken from each time-lapse (fig 6.2A-C) and reveal that in transverse section, the size and shape of the neural primordium in 15th cycle embryos (fig6.2B,C) is the same as control embryos (fig 6.2A). This indicates that the morphogenetic movements of gastrulation and neurulation have continued normally in the 15th cycle embryos. The larger nuclei in the 15th cycle embryos compared to control embryos confirm that cell division has been successfully blocked in these embryos, because at these stages of development, cell division results in a halving of cell volume. Cell divisions are indicated by the white lines and dots, which represent the separation of the two daughter cells immediately after division. The locations of most divisions in 15th cycle embryos are close to the midline of the neural rod (fig 6.2B,C), similar to the location of cell divisions in control embryos (fig 6.2A). I also analysed the division orientation and crossing behaviour of cell divisions from the two 15th cycle blocked embryos, and one control embryo (fig 6.2D-F). An angle of 0% represents daughter cells that separate in the

Figure 6.2 Neural progenitors in 15th cycle embryos undergo cell division showing many of the characteristics of C-division.

A-C) Locations of cell divisions in one control and two 15th cycle embryos overlaid onto a confocal micrograph of the embryos at rod stage of neurulation. Cell division in 15th cycle embryos was inhibited using aphidicolin and hydroxyurea from 7-11hpf and left to recover after washing out of the inhibitors. White dots indicate the location of anaphase nuclei and the lines indicate the orientation of divisions. Blue dots outline the edge of neural rod.

A) Most control cells are undergoing the 16th cell division and divide close to the midline with a medio-lateral orientation.

B) In a 15th cycle inhibited embryo, most cells are undergoing their 15th cell division but still divide close to the midline with a medio-lateral orientation.

C) A second 15th cycle inhibited embryo also shows that cells are dividing close to the midline with a medio-lateral orientation.

D-F) Graphs showing the angles of cell divisions in control and 15th cycle embryos at rod stages of neurulation. An angle of 0° represents a medio-lateral separation of daughter cell nuclei. An angle of 90° represents dorso-ventral oriented separation of daughter cell nuclei during mitosis.

D) Most 16th cycle divisions in the control embryo are oriented within 0° and 30° (n=29).

E) Most cell divisions in the first 15th cycle embryo are also oriented within 0° and 30° (n=37), similar to control embryos.

F) Most cell divisions in the second 15th cycle embryo are also oriented within 0° and 30° (n=38), indicating that these cell divisions have properties typical of 16th cell divisions.

G) Single frame from the control embryo time-lapse. Boxed area indicates the region of the cell division in I. Cells are labelled with H2B-RFP and mem-GFP.

H) Single frame from a 15th cycle embryo time-lapse. Boxed area indicates the region of the cell division in J. Cells are labelled with H2B-RFP and mem-GFP.

I) Time-lapse sequence starting at 16.8hpf showing a cell dividing in the control embryo. The sister cells separate across the midline to form a bilateral pair of cells. Cells are labelled with H2B-RFP and mem-GFP.

J) Time-lapse sequence starting at 17.5hpf showing two cells dividing in the 15th cycle inhibited embryo. After both divisions, the sister cells separate across the midline to form bilateral pairs of cells, in a manner identical to control cells in I. Cells are labelled with H2B-RFP and mem-GFP.

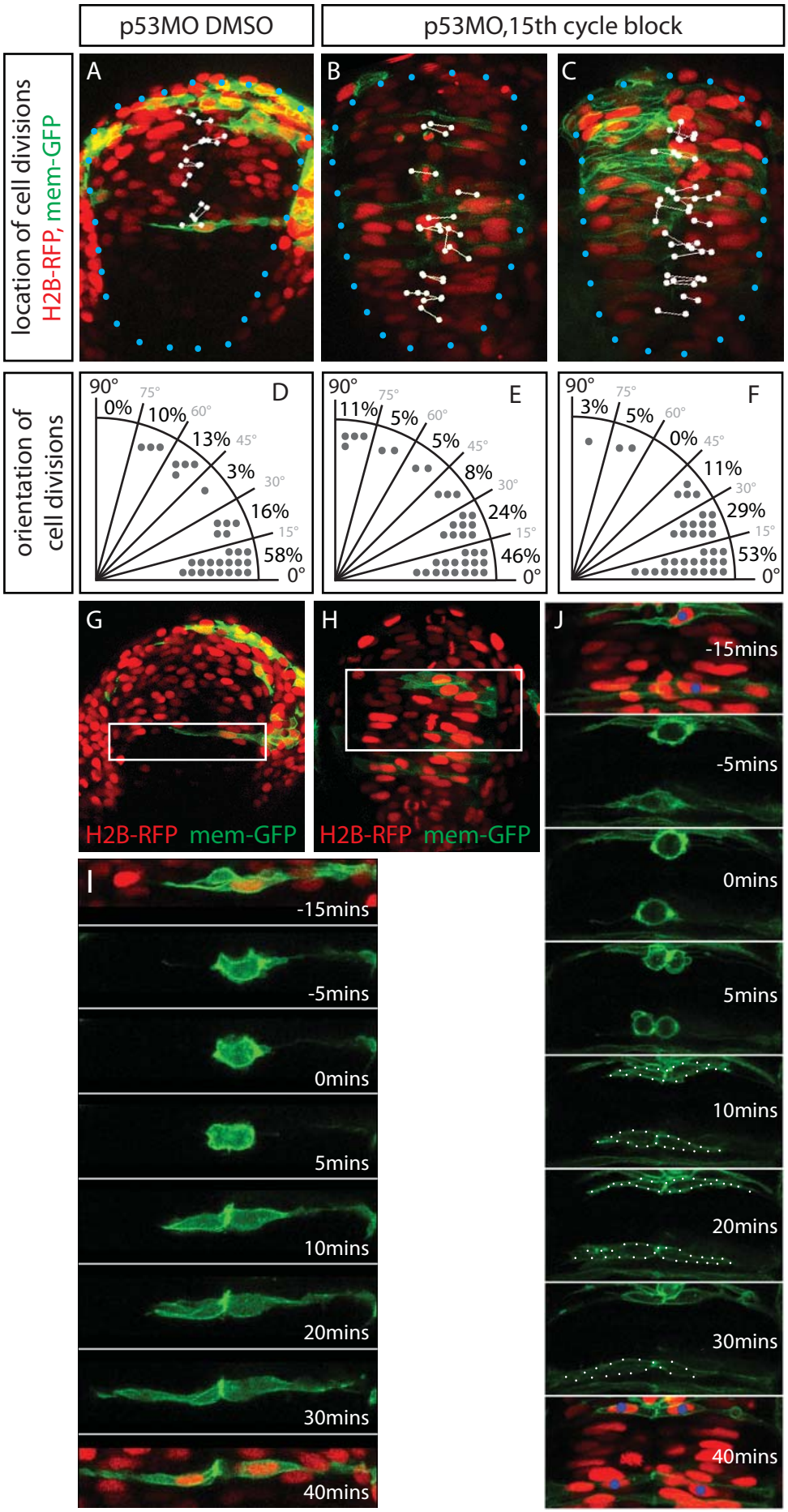

Figure 6.2 Neural progenitors in the neural rod of 15th cycle embryos undergo cell division showing many of the characteristics of C-division.

medio-lateral orientation, and an angle of 90% represents dorso-ventral oriented cell divisions. For control embryos, 58% of cell divisions were between 0° and 15° (fig 6.2E, n=29). Similarly, in the 15th cycle inhibited embryos, 46% of divisions in embryo 1 (fig 6.2E, n=37), and 53% of divisions in embryo 2 (fig 6.2F, n=38) were also between 0° and 15°. Moreover when the division orientations of 15th cycle embryos were compared to those in control embryos, they were not significantly different ($p>0.39$, Kruskal-Wallis test), showing that cell division orientation in 15th cycle embryos is the same as control cells during rod stage of neurulation.

As the location and orientation of cell division in 15th cycle embryos was normal, I next analysed if cells cross the midline after division. The series of frames from a control time-lapse movie at the position of the box in figure 4.2G shows the typical behaviour a cell undergoing the 16th cell division (fig6.2I). The cell rounds up and divides with a medio-lateral orientation close to the midline at t=0. The sister cells then proceed to separate across the midline by t=30mins, forming a bilateral pair of cells. Cells dividing in a 15th cycle embryo show exactly the same behaviour (fig 6.2J). The two cells shown both divide in aligned with the medio-lateral axis of the rod and the two sister cells separate across the midline by t=30mins (fig 6.2J, movie 6). Overall, in 85% of the 70 monitored cell divisions from the two 15th cycle blocked embryos, one daughter cell crossed the midline. In the other 15% of divisions, both daughter cells stayed on one side, and these were often the divisions oriented in the dorso-ventral axis. Dorso-ventral oriented divisions are typical of the next (17th) cell division and this may be why the cells do not cross the midline. Therefore cell divisions in 15th cycle embryos mostly show all the properties of 16th cycle cell divisions.

Neural progenitors polarise on time after the 15th cell cycle is blocked

Neural cells normally establish apico-basal polarity as they undergo C-division (Tawk *et al.* 2007). As cells divide at rod stages with all the characteristics of the 16th cell division in 15th cycle embryos, I next assessed whether apico-basal polarity is established as normal in these embryos. To study the generation of apical polarity, I fixed control and 15th cycle embryos at different stages of neurulation and carried out wholemount immunohistochemistry for ZO-1 (fig 6.3). At 15hpf, both control (fig 6.3A) and 15th cycle (fig 6.3B) embryos only showed faint puncta of ZO-1. By 16.5hpf, both control and 15th cycle embryos showed similar ZO-1 staining at the midline, both in the intensity of staining and the width of the midline (fig 6.3C,D). The later organisation of the apical midline was also normal in 15th cycle blocked embryos, because by 18.5hpf, the ventricle

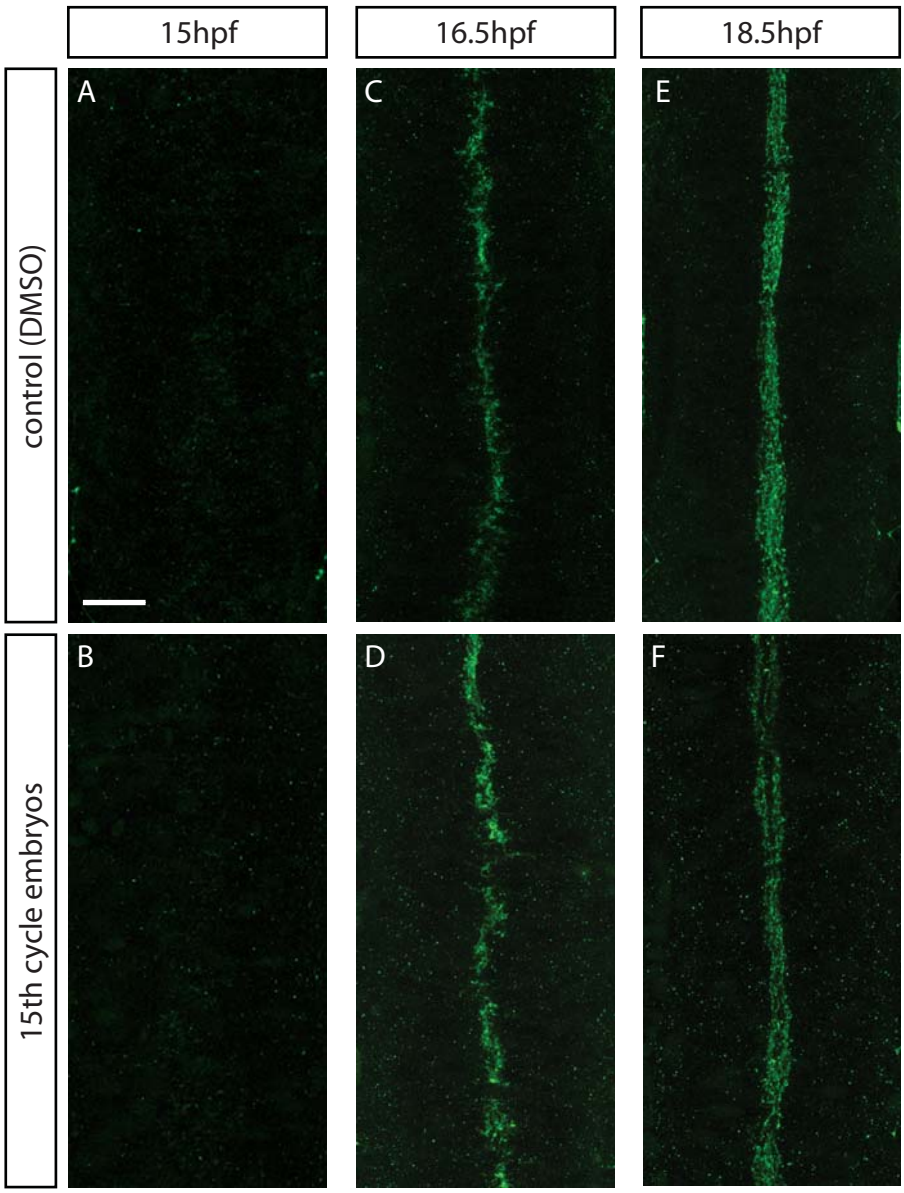

Figure 6.3 The timing of ZO-1 polarisation is the same in 15th cycle embryos compared to control embryos.

A-F) Dorsal view confocal projections through the hindbrain of control and 15th cycle embryos labelled by immunohistochemistry for ZO-1 (green).
A,B) Control and 15th cycle embryos only show a few faint puncta of ZO-1 at 15hpf.
C,D) By 16.5hpf, ZO-1 is similarly localised to the midline of the neural rod in control and 15th cycle embryos.
E,F) By 18.5hpf in both control and 15th cycle embryos, ZO-1 outlines the apical surface of the neural tube, and the ventricle has begun to open, indicating that the temporary division block does not affect the establishment of apical polarity or lumen formation.
Scale bar in A is 25μm and applies to all images.

had begun to open in both control and 15th cycle (fig 6.3E,F) embryos. This experiment demonstrates that at the tissue level, the establishment of apical polarity is not disrupted in 15th cycle embryos and when considered together with the cell division analyses, I conclude that neuroepithelial cells do not count the number of cell divisions as a mechanism of monitoring time to determine when to undergo C-division and polarise.

Emi1 morpholino successfully blocks cell division during neurulation

Having determined that neural progenitors are able to cross the midline and polarise on time during neurulation despite being in an abnormal cell cycle, I next investigated if cells are able to polarise on time without cell division at all. To inhibit cell division throughout the whole of neurulation I used a morpholino against the cell-cycle component Emi1 (*emi1*MO). An *emi1*MO has been shown to effectively block cell division from 5-11hpf with little observed toxicity (Zhang *et al.* 2008), thus potentially offering an alternative to the aphidicolin and hydroxyurea drug mix that can cause some cell death from toxicity. To confirm that the morpholino efficiently inhibited cell division in the neural primordium during neurulation, embryos ubiquitously injected with *emi1*MO were fixed at several time points, and stained by wholemount immunohistochemistry for phospho-histone H3 to reveal cell divisions (fig 6.4). I found that at 7.5hpf, the level of cell division in *emi1* morphants (n=4, fig 6.4A) was the same as in control embryos (n=2, fig 6.4A,B). However by 10hpf, the level of mitosis in the morphants (n=5, fig 6.4D) had decreased dramatically compared to control embryos (n=4, fig 6.4C), so that only a few mitotic figures remained. The number of mitotic figures in the morphants towards the end of neurulation at 17hpf (n=7, fig 6.4F) remained much lower than in control embryos (n=4, fig 6.4E), but by 21hpf it had recovered a little (fig 6.4G,H). The efficiency of the cell division inhibition is shown in figure 6.4I, with the time period at which C-divisions occur also indicated. This shows that the number of mitotic figures in *emi1* morphants is less than 10% of the number in wild-type embryos from 10hpf until 17hpf (fig 6.4I), illustrating that *emi1*MO efficiently blocks cell division throughout neurulation and importantly during the time period of C-division. Therefore emi1MO can be used to investigate if cells polarise on time in the absence of mirror-symmetric cell division and provides a good alternative to the mix of pharmacological inhibitors because it blocks cell division more efficiently, shows less variability and shows less toxicity.

Division blocked embryos polarise Pard3 at the same time and place as control embryos

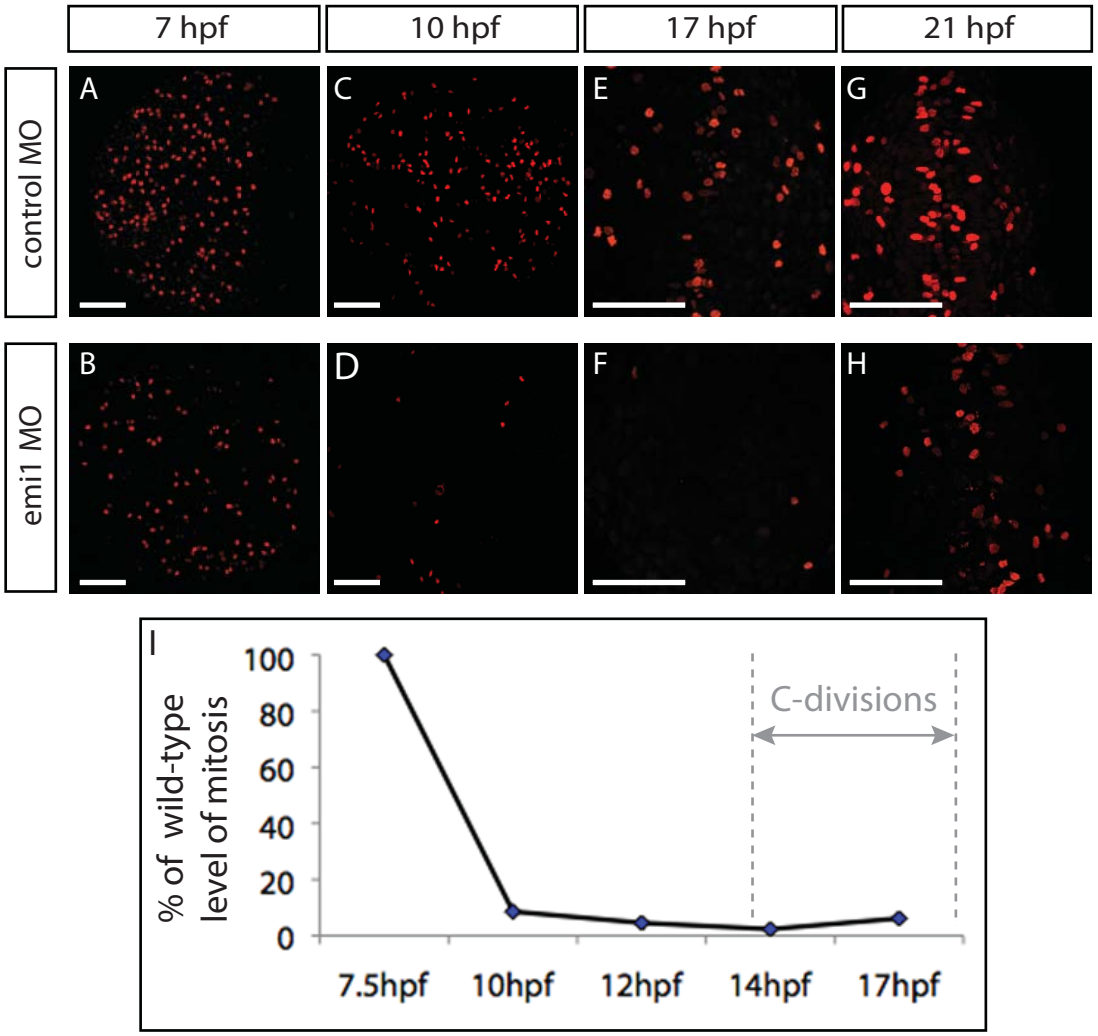

Figure 6.4 Emi1 morpholino effectively blocks cell division during neurulation.

A-H) Maximum projections of control and emi1 morphants stained for Phospho-histone H3 (red) to visualise cells undergoing mitosis (n=3-8 for each time point).

I) Graph showing that during neurulation (from 10hpf to 17hpf), the level of mitosis in emi1 morphants is less than 10% of the control level, but is unaltered before neurulation (7.5hpf).

Scale bar in each image is 100µm.
Images E-H kindly provided by X. Ren.

To assess if Pard3-GFP became polarised in *emi1* morphants at the same time as control embryos, I used time-lapse microscopy to visualise Pard3-GFP accumulation during neurulation. Control and *emi1* morphants of the same age (as assayed by counting somite number), were injected ubiquitously with Pard3-GFP and H2B-RFP and imaged simultaneously. At the start of the time-lapse, the shape of the neural primordium in *emi1* morphants was normal and the cells in the *emi1* morphant appeared healthy (movie 7) showing that blocking cell division by emi1MO did not have any effect on the gross morphogenetic movements of neurulation until 14hpf. The Pard3-GFP time-lapse of *emi1* and control embryos reveals that the progression of polarisation occurs at the same time in both embryos (movie 7). The H2B-RFP channel shows that in contrast to the control embryo in which many cells are dividing at the midline, the *emi1* morphant cells show very few divisions (movie 7). Frames taken from this time-lapse at hourly intervals (fig 6.5A-J) illustrate that at 14hpf there are a small number of Pard3-GFP puncta close to the midline of the neural rod in both control and *emi1* morphants (arrowheads in fig 6.5A,F). As time progresses, the puncta of Pard3-GFP become more numerous at the midline (arrowheads in fig 6.5B,C,G,H). By 17hpf in both control and *emi1* morphants, the puncta have mostly accumulated at the midline and the apical midline seam is beginning to form (fig 6.5D,I). Finally by 18hpf, Pard3-GFP is localised to the midline forming a continuous apical seam in control embryos (fig 6.5E). Likewise, in *emi1* morphants, Par-GFP is located at the midline, but a few gaps in the midline persist (bracket in fig 6.5J). Overall though, the timing of Pard3-GFP polarisation is similar between both embryos.

To compare the timing of Pard3-GFP polarisation more carefully I analysed the average fluorescence intensity across the width of the neural rod, illustrated in figure 6.5K, at regular time points from a projection of 3 adjacent z-levels of the time-lapse (fig 6.5L). Plotting the line profiles are the same axes shows that over time the average Pard3-GFP intensity at the midline increases as the tissue becomes polarised, and the fluorescence intensity at more lateral edges of the neural rod stays low (fig 6.5L), however it is difficult to see the detailed features of each trace. To make it easier to compare the line profiles over time, each time point is shown shifted vertically for each of two control and two *emi1* morphant embryos in figure 6.6. These graphs show that the intensity of Pard3-GFP at 15hpf is relatively uniform across the width of the neural rod for most embryos, but in *emi1*MO 1 there is a small peak in the centre of the neural rod (arrowhead in fig 6.6C). This suggests that Pard3-GFP could be becoming polarised even a little earlier in division blocked embryos. By the next time point at 16hpf, all embryos show a low broad peak of fluorescence in the centre of the neural rod (red trace). Then from 16hpf to 18hpf, the peak becomes narrower and increases in intensity across all 4 embryos, as Pard3-GFP

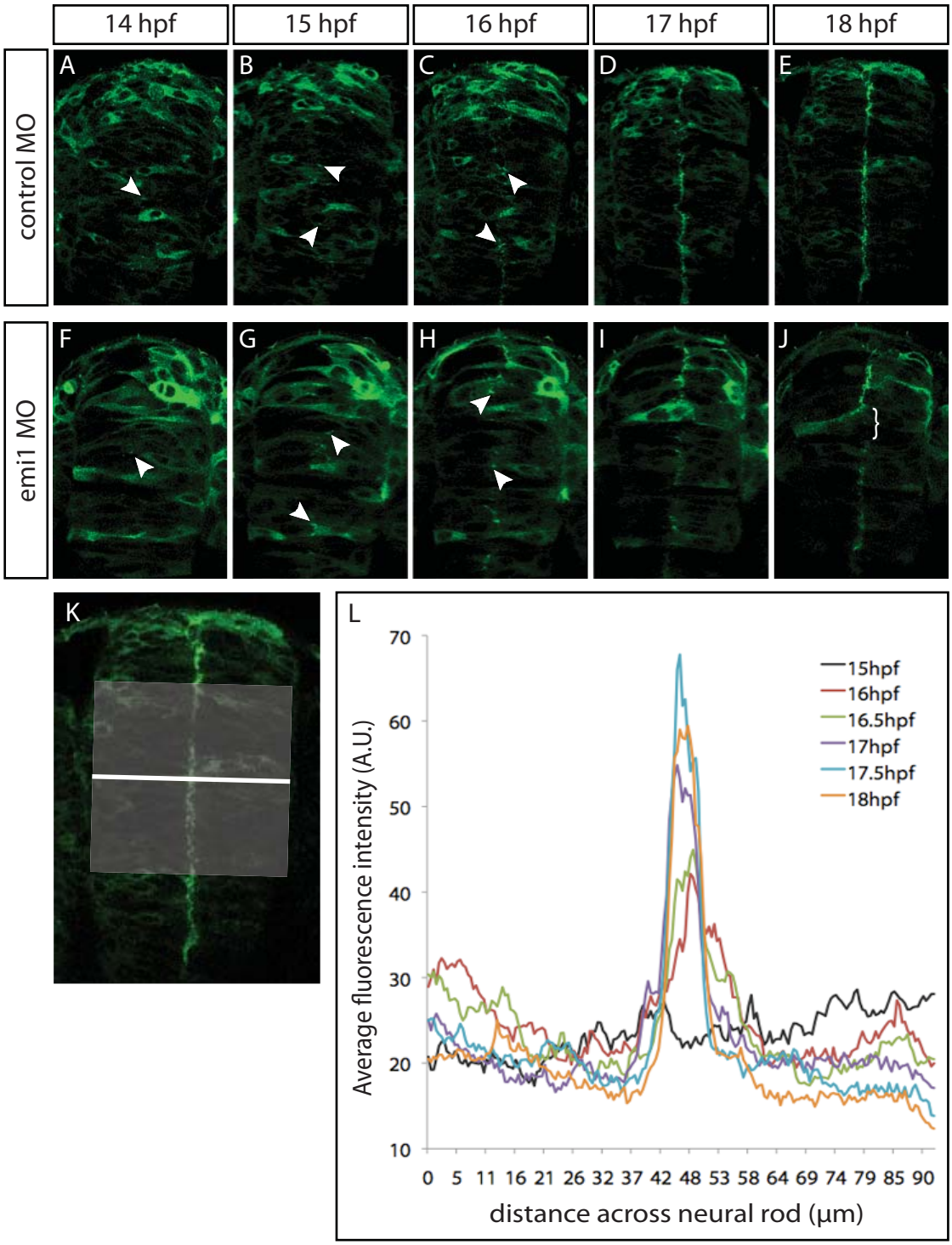

Figure 6.5 Neural progenitors polarise on time in the absence of cell division

A-J) Frames from simultaneous time-lapse movies of control and emi1 morphant embryos undergoing neurulation. Both embryos ubiquitously express Pard3-GFP (green) to show the establishment of apical polarity. Puncta of Pard3-GFP occur close to the midline in both embryos at 14hpf (white arrowheads). Puncta become more numerous over time and both embryos have a fairly straight midline seam of Pard3-GFP by 18hpf. Bracket in J indicates a gap in the midline localisation of Pard3-GFP.
K) Single frame from a time-lapse overlaid with a line across the width of the neural rod to indicate how the average plot profiles of Pard3-GFP intensity were obtained.
L) Graph showing the plot profiles of the Pard3-GFP intensity across the neural rod over time for one control embryo.

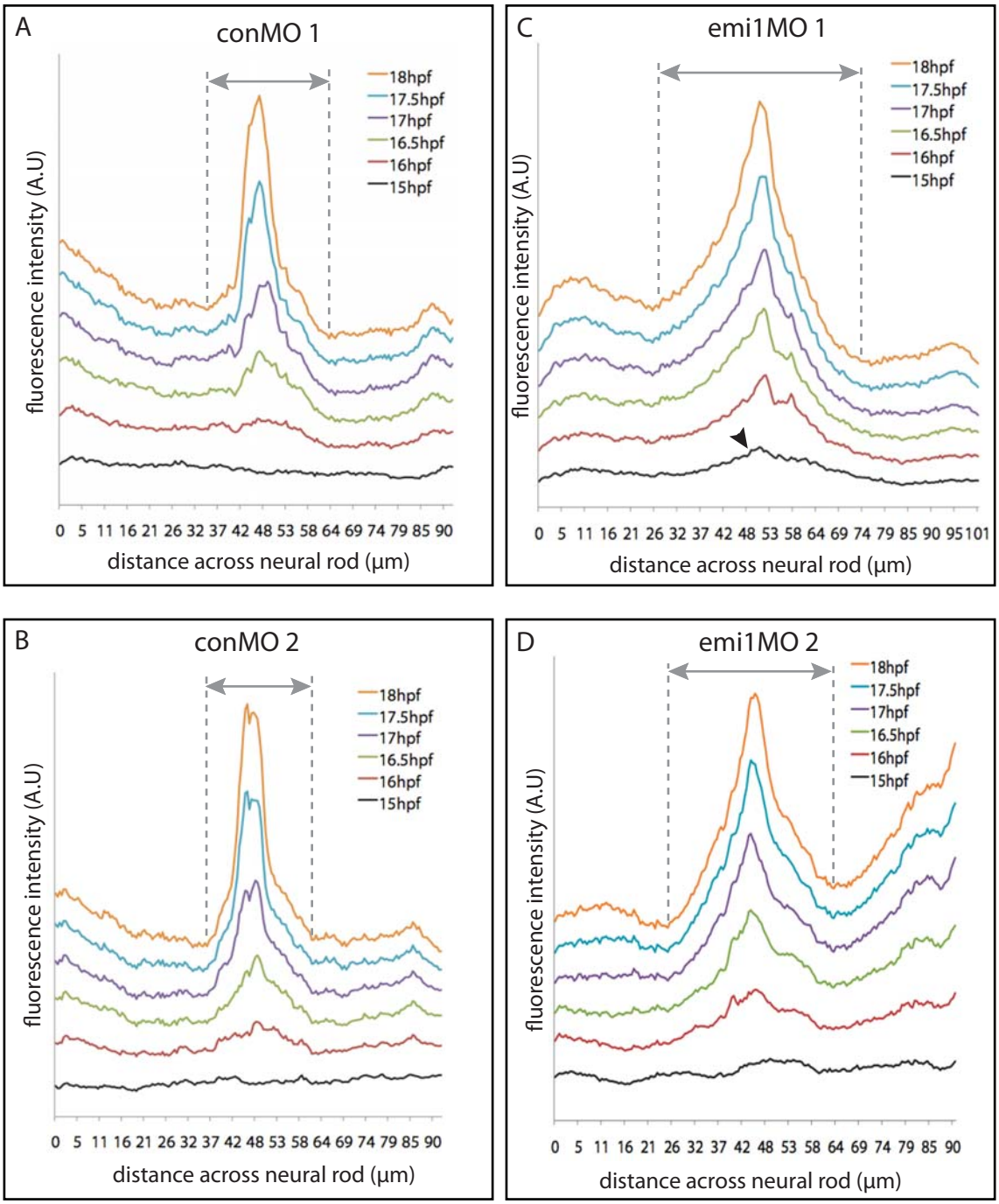

Figure 6.6 In the absence of cell division, Pard3-GFP localisation at the midline of the neural rod at18hpf is imprecise.

A-D) Plot profiles showing the fluorescence intensity across the neural rod in 2 control and 2 emi1 morphant embryos over time. The plot profiles at consecutive time are shifted vertically. The grey lines show the breadth of the peak at 18hpf for easy comparison. At 15hpf the intensity of Pard3-GFP is relatively uniform across the width of the neural rod for most embryos. Arrowhead in fig 6.6C highlights a small peak in the centre of the neural rod in emi1MO 1. By 16hpf, all embryos show a low broad peak of Pard3-GFP fluorescence in the centre of the neural rod (red trace). From 16hpf to 18hpf, as Pard3-GFP coalesces towards the midline of the neural rod, the peak becomes narrower and increases in intensity across all 4 embryos. By 18hpf, all four embryos show a tall peak of fluorescence in the centre of the neural rod, although the broader peaks of emi1 morphants compared to control embryos (grey arrows) suggests that the formation of the apical surfaces at the midline of the rod is slightly disorganised in division-blocked embryos. The fluorescence intensity of Pard3-GFP increases at the lateral edges of some traces (A,D) because some particularly bright cells are located on one side of the neural rod.

coalesces towards the midline of the neural rod (fig 6.6). By 18hpf, all four embryos show a tall peak of fluorescence in the centre of the neural rod, showing that all embryos have made an apical midline seam. The peak however is different in shape at 18hpf for control and *emi1* morphants, as it is slightly narrower for the two control embryos (25µm and 28µm) compared to the two *emi1* morphants (38µm and 46µm). The broader peak indicates that Pard3-GFP localisation at midline is slightly more disorganised in division-blocked embryos. In summary, this data shows that apical polarisation is not delayed by blocking cell division, although the midline organisation is slightly disrupted.

Division blocked embryos show a disorganised apical midline

To take a closer look at the defects in midline organisation in division-blocked embryos, fixed emi1 morphant and control embryos of different ages were stained for the apical marker ZO-1 and for the mitotic marker phospho-H3 (small insets). Confocal projections of ZO-1 reveal that puncta of ZO-1 are broadly scattered near the centre of the neural rod in both control and *emi1* morphant embryos at 14hpf (fig 6.7A,B) and 15.5hpf (fig 6.7C,D). We found no difference in the pattern of ZO-1 staining along the midline at these stages, which is in agreement with the Pard3-GFP time-lapse observations. At 17 and 18.5hpf, the midline staining in *emi1* morphant embryos (fig 6.7F,H) is slightly wider and more disorganised than in control embryos (fig 6.7E,G), which again fits with the broader midline peak of Pard3-GFP in the time-lapse observations (fig 6.6). Finally at 20hpf, the ZO-1 staining reveals that the ventricle of *emi1* morphants is less uniform in width compared to control embryos (fig 6.7I,J) and that the apical surfaces remain in close apposition at certain points (arrowhead in fig 6.7J), indicating that ventricle opening is delayed and disorganised in *emi1* morphants.

Division blocked cells stretch across the whole width of the neural rod and form ectopic bridges of tissue.

To investigate further the apical midline defects we analysed neuroepithelial cell organisation and the tissue structure of the rod at the end of neurulation. We found that at 18.5hpf, when the control embryos have a continuous midline of ZO-1 staining (fig 6.8A,A'), often the *emi1* morphants have gaps in the midline ZO-1 staining (fig 6.8B,B'). Counterstaining of *emi1* morphants to show the positions of all nuclei revealed that the gaps in ZO-1 staining coincided with abnormally positioned nuclei at the midline (fig 6.8B,B'). This shows that cells are still spanning the midline, forming ectopic bridges of tissue that interrupt the apical midline. As these gaps occur at regular intervals in the hindbrain in accordance with its segmental organisation, we also investigated if gaps in

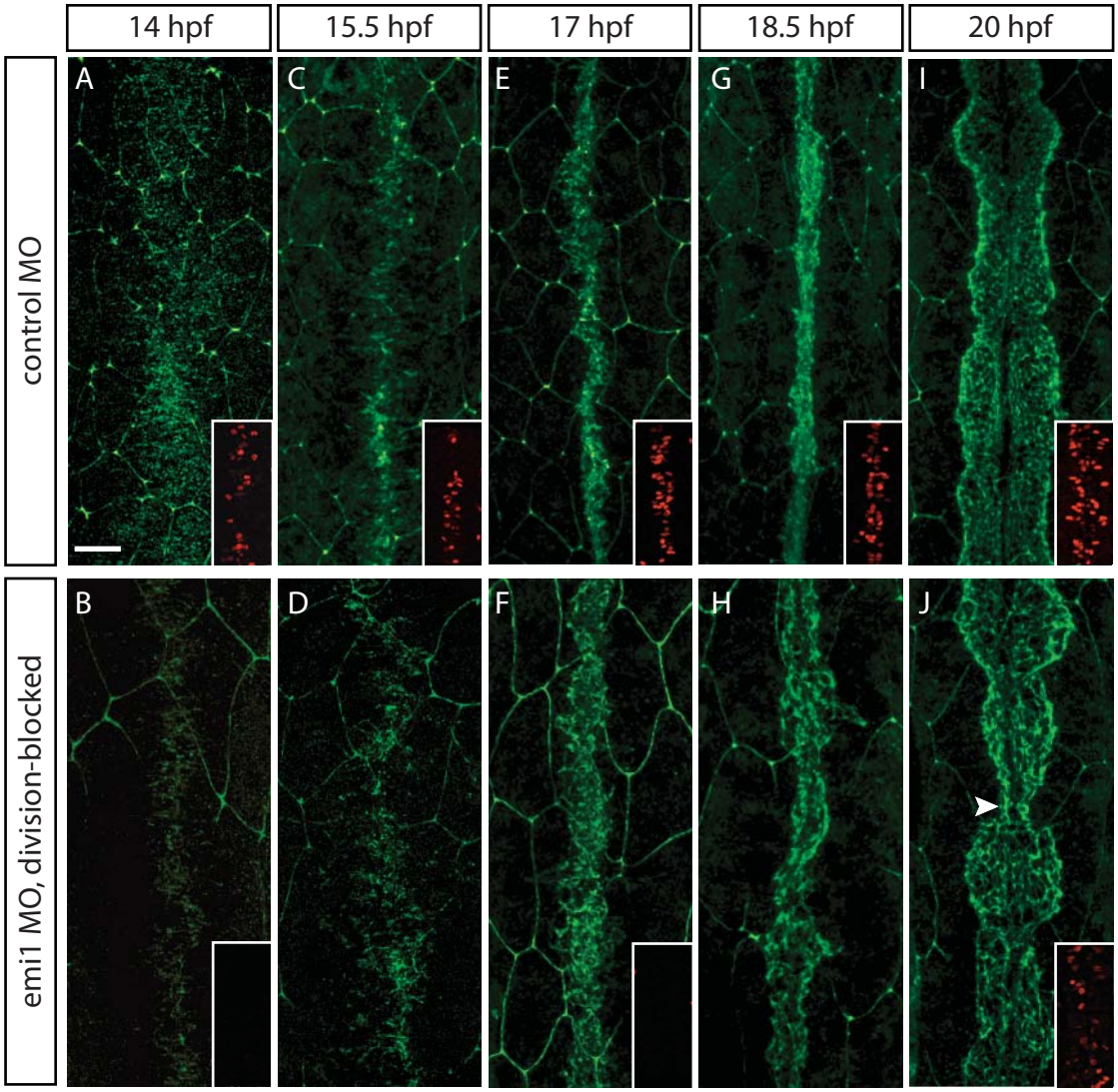

Figure 6.7 Division-blocked embryos have a disorganised midline.

A-J) Control and emi1 morphants were fixed and stained for ZO-1 (green) to show the organisation of the apical midline, and most were stained for phospho-H3 to show mitotic cells (red in insets). All images are confocal projections taken from a dorsal view through the hindbrain. Anterior is up in all images.
A,B) Puncta of ZO-1 are broadly scattered near the centre of the neural rod in both control and emi1 morphant embryos at 14hpf.
C,D) Puncta of ZO-1 are more numerous but remain scattered near the centre of the neural rod in both control and emi1 morphant embryos at 15.5hpf
E,F) At 17hpf the puncta have coalesced at the midline in both control and emi1 morphant embryos, although the midline staining is slightly wider in emi1 morphant embryos
G,H) At 18hpf the midline staining is less uniform in width in emi1 morphant embryos compared to controls.
I,J) Finally at 20hpf, when the ventricle has begun to open, the ZO-1 staining reveals that ventricle opening is less organised in emi1 morphants compared to controls, as the two apical surfaces of each side of the neural tube remain in close apposition at certain points (arrowhead).
Scale bar in A is 25μm. All images kindly provided by X. Ren.

ZO-1 staining similarly occur in the non-segmented spinal cord (fig 6.8C,C'). Cells in spinal cord regions also spanned with width of the neural rod indicated by nuclei stuck in the midline of the spinal cord and interruptions in the ZO-1 staining (fig 6.8C,C'). In summary, blocking cell division during neurulation causes some defects in the organisation of the apical midline, which probably lead to delayed ventricle opening.

In summary these experiments show that the cellular behaviour of apical polarisation can occur on time in the absence of mirror-cell division, but that cell division is important to generate the correct cellular organisation of the neural rod necessary for efficient lumen formation.

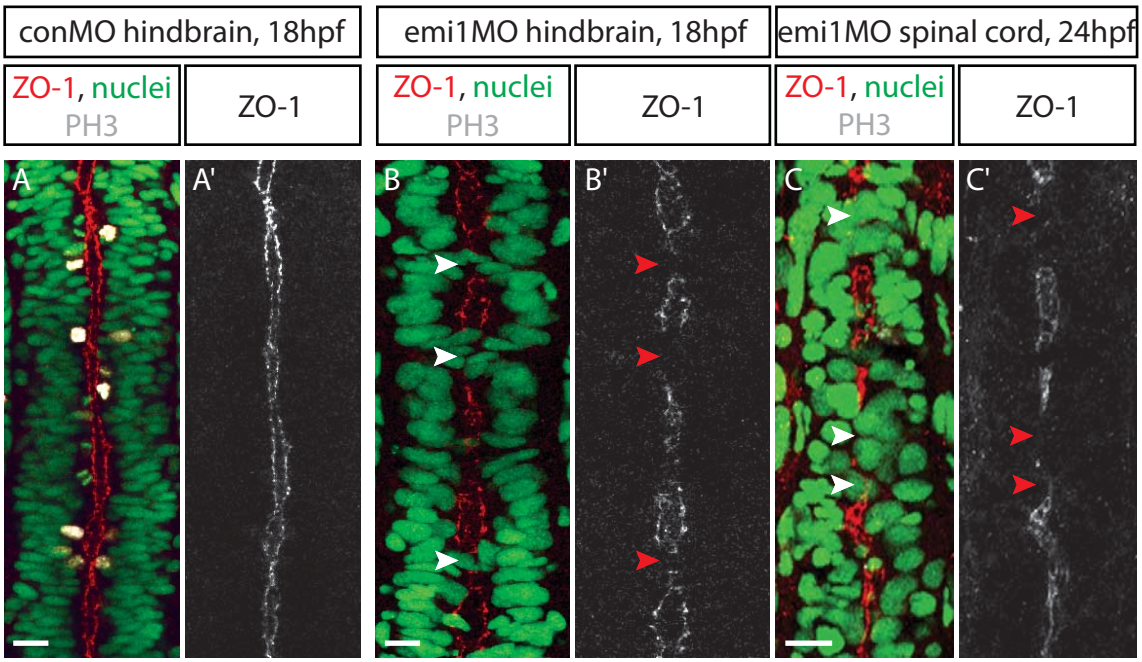

Figure 6.8 Cells and nuclei lie across the midline in division-blocked embryos causing interruptions in the apical surfaces.

All images are dorsal view confocal projections of several z-levels covering a depth of 20-30µm. Anterior is up in all images. Scale bars are 25µm.
A,B,C) Immunohistochemistry of control and emi1 morphant embryos for ZO-1 (red), Phospho-H3 (white), and counter-stained with sytox green to label all nuclei (green). In all images anterior is up. White arrowheads show nuclei spanning the midline of the neural rod in B and C.
A',B',C') The ZO-1 channel of A-C only, red arrowheads highlight gaps in ZO-1 staining.

A) Nuclei lie either side of the apical surfaces and several mitotic cells are present close to the apical surfaces in control embryos.
A') The apical surfaces at the midline of the neural tube of control embryos are continuous. No mitotic cells are visible.
B) In the hindbrain of emi1 morphants at 18hpf, some cells stretch across the midline of the neural tube and their nuclei remain in the middle (white arrowheads).
B') This results in periodic interruptions in the apical ZO-1 staining (red arrowheads).
C) Nuclei are also positioned in the middle of the neural tube in spinal cord regions in emi1 morphants at 18hpf (white arrowheads).
C') These ectopic cells cause similar interruptions in the apical surfaces in the spinal cord.
All images kindly provided by X. Ren.

6.5 DISCUSSION

The polarisation timer is not dependent upon cell division

My results show that when cell division was blocked temporarily for at least one cell cycle prior to neurulation, neural cells in 15th cycle embryos undergo cell divisions displaying all the properties of C-division at rod stage of neurulation. They divide at the midline with the same medio-lateral orientation as control cells, and one daughter cell crosses the midline after division. Moreover polarity is established on time, as ZO-1 staining at the tissue level is indistinguishable from control embryos. Taking all these observations together, they show that temporarily blocking cell division has no effect on neural cell behaviour or morphogenesis. Therefore I conclude that cells do not count the number of cell divisions to know when to undergo C-division.

Next I investigated the requirement cell division for cell polarisation during neurulation. My observations of division-blocked embryos undergoing neurulation show that Pard3-GFP and ZO-1 polarise at the same time as in control embryos. Division-blocked embryos do however show a less precise localisation of Pard3-GFP at the midline than wild-type embryos, and do have some defects in midline organisation due to abnormal cell arrangements within the neural rod. These observations show that although neural progenitors do not require cell division to polarise, the process is less precise and midline formation is less efficient without cell division. The polarisation of Pard3-GFP on time shows that if a timer controls cell polarisation during neurulation, then it can continue to act completely independently of cell division.

How is cell division and polarisation controlled in 15th cycle embryos?

In 15th cycle embryos, neural rod cells divide with properties of the 16th cell division. If this result is considered upon its own, there are two alternatives for how cell division and behaviour are controlled. It could be argued that the local environment of the neural rod promotes mirror-symmetric C-division and polarisation, or alternatively, that division and polarisation are controlled by an intrinsic timer that does not rely upon counting the number of cell cycles. Evidence in support of the timer hypothesis comes from my studies of young cells transplanted into an older embryo (Chapter 4). These cells are not induced to behave differently by their surrounding environment of the neural rod as they show apical polarisation typical of their age, they divide with a different orientation compared to neighbouring host cells that again is typical of their age, and also show a reduced ability

to cross the midline. If then the results of the 15th cycle embryos are considered with those of Chapter 4, it appears that polarisation and mirror-symmetric division are regulated by a timing mechanism that does not rely on counting the number of cell cycles cells have undergone during embryogenesis.

Many other cell intrinsic timers have also been shown to operate independently of counting cell divisions, including the oligodendrocyte differentiation timer (Gao *et al.* 1997) and circadian clock. Research to date indicates that the circadian clock is able to keep time while cells are both dividing and differentiating in cyanobacteria (Dong *et al.* 2008) in many types of cells in culture (Tamai *et al.* 2005) and most importantly during early zebrafish embryogenesis (Ziv *et al.* 2006b). It has also been proposed that, instead of being part of a developmental timer, cell division is actually a source of noise during the somitogenesis clock (Zhang *et al.* 2008). Interestingly sometimes we begin to see spots of Pard3-GFP accumulating at the midline slightly earlier in division-blocked embryos, but this is inconsistent. Therefore it is maybe not surprising that a timer does not rely upon counting cell divisions, but there are several other mechanisms for measuring time, such as the increase or decrease in concentration of an intracellular factor, or sequential switches to change state over time. Possible mechanisms for the zebrafish polarisation timer are considered further in the general discussion of Chapter 7.

Although the results of cell division orientation and polarisation in 15th cycle embryos could be consistent with an intrinsic timing hypothesis, they could also indicate that the environment influences cell behaviour, in particular the orientation of cell division. Observations of cellular behaviour and cell division orientation during zebrafish gastrulation have shown that certain behaviours are correlated with specific cell cycles (Kimmel *et al.* 1994), but these behaviours are also correlated with specific morphogenetic movements (Concha *et al.* 1998). Therefore it is possible that cells could respond to the structure of the tissue to know how to behave. The mechanical properties of the cell such as its shape, or its interaction with adjacent cells or the ECM could determine the orientation of cell division and midline crossing behaviour in the neural rod. During zebrafish neurulation, the neural primordium changes shape from a plate to a keel to a rod. In the early neural keel, cell divisions are aligned with the superficial-deep axis of the neural primordium that is perpendicular to the basal surface. This division orientation is maintained relative to the basal surface as the keel gradually rounds up, such that at rod stages the cells divide in a medio-lateral orientation (Concha *et al.* 1998; Geldmacher-Voss *et al.* 2003; Tawk *et al.* 2007), suggesting that the structure of the neural primordium can control division orientation.

Studies of how cell shape and the ECM can influence cell division orientation have also been carried out using micro-contact printing of ECM components in 2D culture systems. ECM components can be printed onto a coverslip in a specific pattern and when single cells adhere to these patterns they adopt a specific shape (Thery *et al.* 2005). The shape of the ECM contact area and elongation of the cell in interphase influenced the orientation of the division axis, even though the cells rounded up upon entering mitosis (Thery *et al.* 2005). The authors propose that the ECM contacts cause heterogeneity in cortical actin, which in turn predetermines spindle orientation (Thery *et al.* 2005). Whether this influence upon division orientation happens *in vivo*, when the surrounding environment is more complex is unclear, because in studies of the relationship between cell division orientation, cell movement and cell shape during zebrafish gastrulation, neither the axis of elongation of a cell nor its direction of movement directly determined the cleavage orientation during cell division (Concha *et al.* 1998). Therefore cell elongation does not always influence division orientation during zebrafish development. However at keel and rod stages of neurulation, it has been documented that during mitosis, the spindle itself rotates by 90° to become aligned with the medio-lateral axis (Geldmacher-Voss *et al.* 2003), indicating that the final mitotic spindle orientation correlates with the shape of the cell before division. Therefore the possibility that the properties of a cell in the neural rod determine its angle of cleavage cannot be completely ruled out.

Redundant mechanisms other than mirror-symmetric cell division must exist for generating polarity during neurulation

During normal neural tube morphogenesis, Pard3-GFP accumulates at the abscission plane of cells undergoing mirror-symmetric C-division (Tawk *et al.* 2007). However, here I show that even without cell division, cells are able to polarise roughly at the right place, though the midline polarisation is not quite as precise. Therefore a second mechanism, other than cell division, must exist to target apical proteins to the right place within a cell at the right time, thus indicating that apical polarisation and lumen formation is a robust process in CNS development. This redundant mechanism may act together with abscission plane targeting as part of the mechanism for polarity establishment during normal development, or be a backup mechanism for when cells do not divide. Interestingly in the eye and anterior forebrain, cells in wild-type embryos can polarise without dividing (Kenzo Ivanovitch, personal communication) so neural cells are able to polarise independently of cell division in brain regions other than the hindbrain.

What is the advantage of generating apical polarity by mirror-symmetric cell division for neural tube morphogenesis?

As it appears that cells are able to polarise on time during neurulation in the absence of cell division, what then is the advantage of using the mirror-symmetric cell division as a mechanism for targeting of polarity proteins to the abscission plane of the separating two daughter cells? From the study of division-blocked embryos it appears that there are at least two advantages. The wider midline polarisation of Pard3-GFP in division-blocked embryos (fig 6.6) suggests that midline division helps to align all apical specialisations to the midline of the tissue. In wild-type embryos pairs of sister cells stretch equally across the width of the neural rod to form two columns of cells, and so targeting apical proteins to the abscission site of each pair of cells neatly and efficiently aligns apical proteins to the midline of the tissue. The second advantage is that separation of sister cells across the midline by cytokinesis ensures that cells are not stuck at the midline. In division-blocked embryos cells remain stretched across the whole width of the neural rod, forming ectopic bridges of tissue across the midline. This causes interruptions in the apical staining at the midline and disrupts subsequent lumen formation. In summary, generating a midline by mirror symmetric C-division organises the cellular architecture of the neural rod so that continuous apical surfaces form at the midline and the ventricle can then open efficiently.

My results have shown that blocking cell division throughout the whole embryo from 10-24hpf does not appear to affect the large-scale morphogenetic movements of epiboly, gastrulation, and neurulation, or the timing of neural progenitor cell polarisation. This is in agreement with published studies that show the formation of a neural tube in division-blocked embryos with correct apico-basal polarity by 24hpf (Ciruna *et al.* 2006; Tawk *et al.* 2007; Zhang *et al.* 2008; Nyholm *et al.* 2009). In contrast to these studies however, we have found that cell division is important for correct midline organisation and cellular architecture of the neural rod and tube. This apparent difference in the importance of cell division for zebrafish neurulation may result from a lack of careful analysis of the whole of neural tube morphogenesis in the published work. We have found that by 24hpf, the organisation of the neural tube has begun to recover so if only this time point was studied, then the observations we have made may have been missed. The most detailed study shows that at the tissue level, ZO-1 and phospho-myosin localise at the midline of the neural rod at 19hpf when cell division was inhibited for the time period of C-divisions (from 15hpf until 19hpf) (Nyholm *et al.* 2009). However analysis of polarisation at the cellular level, or the cellular architecture of the rod was not studied.

We have used a morpholino against *emi1* to block the mirror-symmetric C-division effectively with little toxicity. However as cell division begins to be blocked before neurulation (fig 6.4), it was possible that some of the differences in our results compared to published work could result from the block of additional cell divisions (before and after C-division). Moreover, the *emi1*MO likely blocks the cell cycle in G2, which is in a different phase to the pharmacological inhibitors that block DNA replication so this may be a second reason why our results differ from published work. To address both of these concerns we blocked cell division just over the period of C-division using pharmacological inhibitors to check that we obtain the same phenotypes as the *emi1*morphants. We have seen the same defects in the midline organisation and cellular arrangements (X. Ren, unpublished observations), confirming that these defects are likely to arise from a lack of mirror-symmetric C-division.

CHAPTER 7 GENERAL DISCUSSION

In this thesis, I have explored how cell division and cell polarisation are coordinated with the morphogenetic movements of zebrafish neurulation. I have focused upon the hypothesis that a mechanism intrinsic to neural cells controls the time of mirror-symmetric cell division during the keel to rod transition. I have also considered the importance of correctly regulating cell division and polarisation for neural tube morphogenesis. The main conclusions from my work are:

- Neural tube duplications arise by uncoupling the morphogenetic movements of the neural tissue from mirror-symmetric cell division and polarisation. This result argues that PCP pathway does not have additional roles in the repolarisation of cells after division nor in contralateral intercalation as previously proposed (Ciruna *et al.* 2006)
- Heterochronic transplanted cells behave according to their age, not the age of their surrounding environment, which indicates that an intrinsic timer controls neural progenitor cell division and polarisation during zebrafish neural tube morphogenesis.
- The timer can be modified by the extreme morphogenetic abnormalities caused by a lack of mesoderm in MZ*oep* embryos, but that cell polarisation can occur on time in the absence of PCP signalling.
- Many of the environmental signals present at the dorsal midline of the embryo are not required for neural cell polarisation, as progenitors are able to polarise and differentiate on time in extreme ectopic locations within the embryo, and generate small cysts with a central lumen in 3D culture.
- The polarisation timer is independent of cell division.

What is the basis of the polarisation timer?

My experiments show that the timer does not rely upon the oscillatory behaviour associated with cell division to monitor time (Chapter 6). Therefore the mechanism by which the embryo or neural cells use to measure time remains to be discovered. It is possible that the zebrafish embryo has a global mechanism for monitoring time, a master timer that simultaneously controls the timing and synchrony of developmental events across many different tissues, like the heterochronic genes in *C. elegans* that seem to fulfil this function (Moss 2007). Integration of this timing information with extrinsic signals could then provide specificity of cell behaviour in different tissues. In addition a master timer could drive individual timers in each tissue, that in turn regulate the timing of cell-specific behaviours. Alternatively, intrinsic timers may exist in series or parallel with each

other in different tissues, which would then interact with each other to ensure coordination of development across the embryo.

Which broad type of timing mechanism is most likely?

Out of the three main types of timer presented in the introduction, i.e. clock, switch or egg-timer, I can only speculate on which type is likely to be the basis of the polarisation behaviour. It is possible that an egg-timing like mechanism could control the time of polarisation during zebrafish development. This type of timer would be non-oscillatory and activate a response after a defined time period, which in this case, would be mirror-symmetric cell division and establishment of apical polarity. A timer of this type has been shown to operate during oligodendrocyte development, as a gradual increase in the concentration of p27 and p57 proteins to a threshold level controls the time of differentiation of optic nerve oligodendrocyte precursors *in vitro* (Raff 2006)

It seems unlikely that a clock type of timer regulates neural cell polarisation because there are few obvious cyclical cell behaviours during gastrulation and neurulation, apart of course from cell division that I have already shown not to be required for the timer. A switch timing mechanism involving step-wise and progressive changes between different phases of development could be more likely, especially as timers like this have been proposed to act during neural development in other species, such as *Drosophila*. In the temporal transition sequence of *Drosophila* neuroblasts, changes in expression of transcription factors are related to the cell cycle (Brody *et al.* 2005), but the upstream factors that regulate the progression of the switches remain largely unknown. During gastrulation and neurulation in zebrafish specific cell behaviours occur on specific cell cycles (Kimmel *et al.* 1994; Concha *et al.* 1998), suggesting that different cell behaviours may be controlled by a series of switches. As these observations are just correlations, the link to the cell cycle may be coincidental especially as embryogenesis can proceed relatively unaffected without cell division until 24hpf in zebrafish (Zhang *et al.* 2008). The series of switches may well control other different cell behaviours during embryogenesis, such as morphogenetic movements.

Finally the progenitors of the neural tube could have an intrinsic programme controlling their progressive maturation of which cell polarisation could be the first step. This may be similar to the progressive and sequential change in the production of different types of retinal cells from retinal progenitors over time (Marquardt *et al.* 2002). Intrinsic timing mechanisms are important in this process as retinal precursors in dissociated cell culture

can recapitulate many of the cell division and fate behaviours of retinal progenitors *in vivo* (Cayouette *et al.* 2003). Whatever the basis of the timer, it must be operational before or at 3.5hpf, because cells transplanted at this time mostly behave according to their age (Chapter 4).

Could microRNAs be the molecular basis of the timer?

MicroRNAs (miRNAs) have been shown to be important components of several intracellular timers. miRNAs are small 22 nucleotide RNAs that function to repress gene function, either by binding to their target mRNA and inhibiting translation, or by directing the cleavage of the target mRNA (Bagga *et al.* 2005; Valencia-Sanchez *et al.* 2006). The first gene discovered to encode an miRNA was actually the heterochronic gene *lin-4* in *C. elegans* (Lee *et al.* 1993). Since this discovery, a second heterochronic gene in *C. elegans,* the miRNA let-7 (Reinhart *et al.* 2000), has been shown to have homologues in many species and to be expressed at a time consistent with a function in regulating late developmental events (Pasquinelli *et al.* 2000).

miRNAs have also recently been shown to be part of a tissue specific timing mechanism in the *Xenopus* retina. The adult retina of the eye contains many different cell types, which are formed in a specific order and at certain times during embryogenesis (Marquardt *et al.* 2002; Cayouette *et al.* 2003). This indicates that the fate of a retinal cell largely depends on its birth date. Experiments in a number of species, including *Xenopus*, strongly suggest that intrinsic timing mechanisms play an important role in retinal histogenesis (Rapaport *et al.* 2001; Cayouette *et al.* 2003; Kay *et al.* 2005). For example, heterochronic transplant experiments in *Xenopus* have shown that young cells are not influenced to progress through neurogenesis early, either when transplanted into an older host retina, or when co-cultured with older cells (Rapaport *et al.* 2001). Research into the molecular mechanism of the timer has again implicated miRNAs as part of the timing mechanism. In the *Xenopus* retina, progenitor cells divide with a short cell cycle in early histogenesis, while at later stages the cell cycle is longer and the progenitor cells generate specific types of neurons that express the homeobox genes *otx2* and *vsx1*. *otx2* and *vsx1* are switched on in the neural precursors by an increase in the cell cycle length, because when progenitors are forced to proliferate faster, *otx2* and *vsx1* fail to become expressed (Decembrini *et al.* 2006). It has been proposed that the early expression of *otx2* and *vsx1* is inhibited by four specific miRNAs that are expressed early in neurogenesis when the cell cycle is shorter (Decembrini *et al.* 2009). These miRNAs likely inhibit translation of *otx2* and *vsx1* by binding to regulatory sequences of the genes (Decembrini *et al.* 2009). The causal link

between the increase in cell cycle length and decrease in miRNA expression remains unclear, but nonetheless, it is likely that miRNAs are part of the intrinsic timer that couples the birth date of neurons to cell fate.

Several experiments have shown that miRNAs have an important role during embryogenesis in zebrafish. One approach taken to determine the global role of miRNAs in zebrafish embryogenesis has been to create a mutant deplete of all maternal and zygotic Dicer activity, the MZ*dicer* mutant. In MZ*dicer* embryos, the formation of all miRNAs is abolished (Giraldez *et al.* 2005) because a crucial step in miRNA biogenesis, is the cleavage of larger pre-miRNA into short 22nt duplex RNAs by Dicer (Elbashir *et al.* 2001). MZ*dicer* embryos display a range of defects, which are mainly in morphogenetic processes such as epiboly and neurulation as axis formation and cell specification remain unaffected (Giraldez *et al.* 2005). The abnormal morphogenesis of the neural tube is manifest in the shape and size of the brain ventricles, which are much reduced in size and do not show the midbrain hindbrain boundary restriction despite normal antero-posterior brain patterning (Giraldez *et al.* 2005). Morphogenesis during epiboly is disrupted because the prechordal plate migrates too fast relative to the extent of epiboly (Giraldez *et al.* 2005). This suggests that during epiboly, cell behaviours across different tissues are not correctly synchronised. It is tempting to speculate that the brain morphogenesis defects could arise from a similar disruption in the coordination of cell behaviour with morphogenesis, especially considering there is a strong precedent from both my work and other work from the Clarke lab that coordinating cellular and tissue behaviours in time and space during neurulation is essential (Tawk *et al.* 2007). Interestingly the brain morphogenesis defects are rescued by overexpression of RNA encoding the miR-430 family of miRNAs (Giraldez *et al.* 2005), suggesting that a possible route for further investigation could be to knock down these miRNAs using modified morpholinos that inactivate miRNAs.

Finally, a second paper has shown that the miR-430 miRNA that rescues the brain morphogenesis defects in MZ*dicer* embryos (Giraldez *et al.* 2005) is also essential for degrading maternal RNAs at the maternal to zygotic transition (MZT) in zebrafish (Giraldez *et al.* 2006). Therefore it is possible that the efficient degradation of mRNAs at the MZT is essential for the setting up of other developmental timers that could act later in zebrafish development. As zygotic transcription is activated at the MZT (Tadros *et al.* 2009), the concentration of a polarisation timer component may begin to gradually increase from the MZT onwards until directing the polarisation of neural cells after a certain amount of time has elapsed. The transcription and/or translation of polarity genes could be one of the later components of such a timer. To determine if the timer is

dependent upon protein translation, embryos could be incubated in a reversible inhibitor of translation, such as cycloheximide for a specific time period in development. However, the incubation period would have to be during late gastrulation or neurulation because cycloheximide treatment from 5hpf results in all cells undergoing apoptosis and embryo death by 13hpf (Negron *et al.* 2004).

Could the polarisation timer be related to other timers that operate during zebrafish development?

Observations of the cell cycle length of neural progenitors also suggest that a cell's local environment is not important for controlling this aspect of cell behaviour. During convergence and extension, clonally related cells intercalate among other cells and therefore can become widely separated in the anterior-posterior axis, forming clonal strings (Kimmel *et al.* 1994). Nonetheless, cells within a clone surprisingly exhibit highly synchronous cell divisions, often only a few minutes apart (Kimmel *et al.* 1994). Moreover, even when clonal progeny are lineage-restricted at cycle 14 to different fates such as mesoderm and ectoderm (but not including EVL or YSL), they still maintain synchronous cell cycles up until the early part of cycle 16 (Kane *et al.* 1992). These observations argue that a cell's clonal history is more important than either the local environment or eventual fate of a cell for determining its cell cycle characteristics during early zebrafish development.

The polarisation timer is unlikely to be related to the circadian clock

Zebrafish cells have circadian rhythms that operate in early embryogenesis (Carr *et al.* 2006). It is logical to ask if the timing mechanism I have uncovered relates in any way to a circadian rhythm. Within the first 24 hours of development, zebrafish cells can show an increase in expression of the clock gene, *per2*, in response to light, but only after the MBT (Ziv *et al.* 2006a). Moreover the time and length of the period for which zebrafish cells are exposed to light during this first day affects the rhythmic expression of a circadian gene in the pineal gland 3 days later. These two observations suggest that the clock is set up in the first day of embryogenesis, and so could interact with other timing processes. However, importantly for my work, they also found that if the embryos were raised in constant darkness, or were only exposed to light for 3 hours during the first day, then the rhythm 3 days later was either completely absent or much weaker respectively (Ziv *et al.* 2006a). During my experiments I only exposed the embryos to light for about 3 hours while carrying out the cell transplantation, and therefore according to these previous experiments, the experimental embryos would not have a strong circadian rhythm. This

suggests that a potential interaction between the polarisation timer and circadian clock does not seem likely, although further experiments are needed to rule out this possibility completely.

Integrating the intrinsic polarisation timer with external factors

During retinal histogenesis, a single progenitor cell is capable of generating all of the different cell types in the retina (Turner *et al.* 1987; Holt *et al.* 1988; Wetts *et al.* 1988), but the type of cells produced can be influenced by secreted factors such as Sonic Hedgehog (Neumann *et al.* 2000). In order to link the influence of the environment on cell fate, it has been proposed that an intrinsic timer regulates the ability of cells to respond to secreted signals over time (Watanabe *et al.* 1990; Livesey *et al.* 2001). This responsiveness to signals may be controlled by timed receptor expression, since expression of the EGF receptor increases during late retinal histogenesis (Lillien *et al.* 1998), and overexpression of the receptor alters retinal cell fate (Lillien 1995). It is possible that a mechanism similar to this acts to control the time of neural progenitor cell polarisation, as the ability of the cells to respond to a polarising cue from the ECM or a diffusible signal may only occur during the late stages of neurulation.

I have shown that the timer is delayed in the extreme morphogenetic mutant MZ*oep*, and it is not surprising that the polarisation timer of neural cells is affected at least in part by the surrounding environment of the cells. Extrinsic signals may work in conjunction with the normal mechanism of timed mirror-symmetric cell division to direct cell polarisation. Alternatively the environment may be more responsible for organising cell and tissue behaviour during neurulation, rather than directing the time of polarisation itself. The gradual coalescence of the apical specialisations to form lumens in the centre of the ectopic clusters suggests that something biases the localisation of apical components to the interior, not the exterior of the cluster. Moreover apical proteins are localised to the centre of the cluster of neural cells in Matrigel. It seems likely that the interaction of neural cells with ECM components may direct the orientation of cell polarisation both in the ectopic locations, because in 3D culture laminin is crucial for directing the orientation of polarity (O'Brien *et al.* 2001; Yu *et al.* 2005b). The basal lamina may also be important for neural tube formation in the embryo, as a basal lamina lies under the neural tissue from early as neural plate stage, and knock down of *laminin c1* and *fibronectin* together leads to abnormal neural tube morphogenesis (C. Araya, unpublished observations). Interaction with the basal lamina throughout neurulation may give the neural cells some

level of polarity, even though the formation of a proper neuroepithelium is a late event in neurulation.

Finally it is likely that the mesoderm has an important role in coordinating neural cell behaviour during wild-type neurulation as revealed by the extremely disrupted neural tube morphogenesis in MZ*oep* mutant embryos. The mesoderm could organise neural cell behaviour mechanism by providing a mechanical support for the morphogenetic movements of neurulation, or it could secrete diffusible factors that direct cell polarisation and behaviour. Interestingly, in the extreme ectopic clusters of cells both in Matrigel and on the yolk of the embryo, the cells do not have the elongated morphology characteristic of neuroepithelial cells in the brain. This suggests that factors are missing that promote cells to adopt this morphology in the ectopic locations. The mesoderm is one potential candidate, and this could be investigated by co-culturing mesodermal cells with neural cells in the ectopic locations. The mesoderm might help to organise cell divisions and polarisation within the cluster more effectively, and this may then enable neuroepithelial cells to adopt their normal elongated morphology.

How do cells locate the midline of the neural rod?

Comparisons of wild-type and split-brain embryos

As mentioned above, in addition to polarising on time, neural cells must also assemble apical proteins in the right place, i.e. at the midline of the neural rod. During normal neurulation, neural keel and rod cells have an elongated morphology as they usually extend from one basal side past the midline into the contralateral side of the rod (fig 7.1A). Mirror-symmetric cell division at the midline of the rod generates pairs of cells that stretch equally across the width of the rod (fig 7.1A''). As apical proteins are targeted to the abscission site of sister cells, then the apical surface is thus defined at the embryonic midline where sister cells contact at their medial ends (Tawk *et al.* 2007). Similarly neural progenitors in split-brain and *tri* embryos also divide halfway between the superficial and deep surfaces of the delayed neural plate (fig 7.1B') and subsequently form pairs of sister cells that are elongated, but across one side of the neural primordium only (fig 7.1B''). The targeting of apical proteins to the abscission site between daughter cells generates ectopic apical surfaces that are sandwiched between superficial and deep surfaces of the primordium (fig 7.1B'').

One striking observation about mirror-symmetric cell divisions in the neural rod is that they always occur close to the midline (fig 7.1A'), indicating that the cells are able to detect

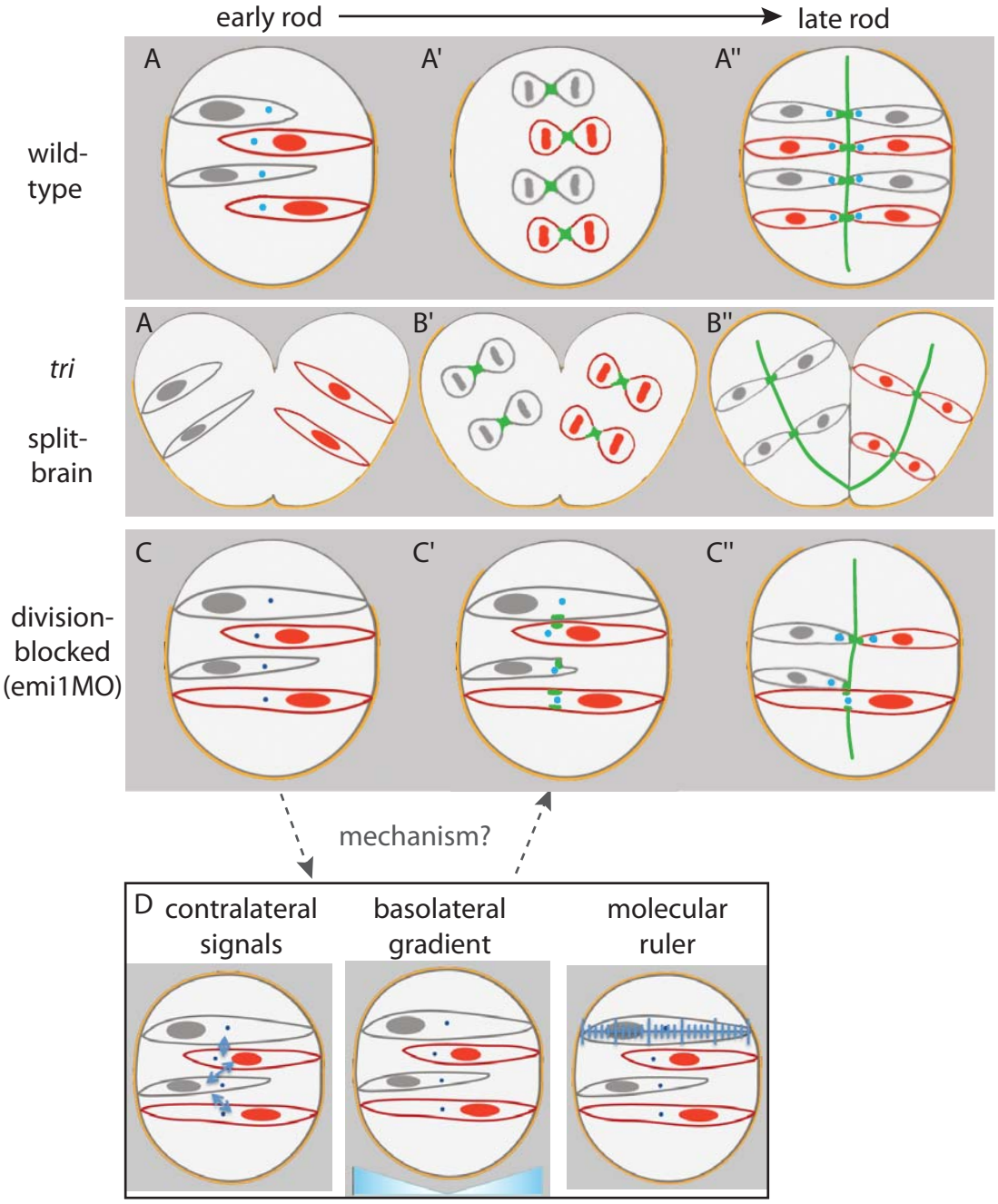

Figure 7.1 Model of cell polarisation in wild-type, delayed-convergence and division-blocked embryos.

A) In wild-type embryos cells establish apical polarity as divide at the midline of the rod. The two daughter cells from each division extend equally across each side of the rod such that apical proteins are localised to the midline.

B) In embryos with delayed convergence (*tri* and split-brain), cells undergo mirror-symmetric cell division in ectopic lateral locations. This leads to the generation of bilateral apical seams and duplicated neural tubes.

C) In division-blocked embryos cells stretch across the neural rod, but Pard3 still polarises close to the midline of the rod. The formation of a straight apical seam is disrupted as cells remain stretched across the midline and the localisation of Par3 to the midline is imprecise.

D-F) Three potential mechanisms for how cells are able to locate the midline of the neural in the absence of cell division.

Green represents Pard3-GFP, blue dots are centrosomes, orange represents the basal lamina. Cells are coloured grey and red to illustrate left and right sides.

Images adapted from a figure by Una Ren

the location of the midline. Similarly neural progenitors in split-brain and *tri* embryos also divide halfway between the superficial and deep surfaces of the delayed neural plate (fig 7.1B', Tawk *et al.* 2007). In both cases, cells are able to locate the halfway point between the edges of the neural primordium. This indicates that bilateral mesoderm and a bilateral basal lamina are not necessary for this process, as in split-brain and *tri* embryos mesoderm and a basal lamina are only present on the deep side of the delayed neural plate.

Possible mechanisms for how cells in division-blocked embryos polarise apical proteins to the midline of the neural rod

In division-blocked embryos (emi1 morphants) cells also extend across the midline of the neural rod, and they are also able to locate the midline of the neural rod, not to divide, but to localise Pard3-GFP (fig 6.5). Pard3-GFP is seen to accumulate only at the midline in cells in division-blocked embryos even at the time when many cells are extended past the midline of the neural rod (fig 7.1C'). This localisation of Pard3-GFP half way along the long axis of a cell instead of at the end of the cell is surprising because in migrating cells, apical polarity proteins are usually localised to the leading edge of the cell (Schmoranzer *et al.* 2009). Moreover, although division-blocked embryos also do not have an inbuilt mechanism of determining the midline by forming mirror-symmetric pairs of cells, they do generate a fairly straight apical plane at the embryonic midline. How apical proteins are polarised to the midline in the absence of cell division is not clear, but there are several hypotheses.

One hypothesis is that cells on one side of the neural rod may contact cells on the opposite side to make a pair of cells and thus define the middle in a similar manner to normal (fig 7.1D). We have observed neural rod cells in division-blocked embryos making connections with contralateral partners (X. Ren, unpublished observations), so this may be part of the mechanism. Although why cells only form connections at the midline, rather than at any other point of contact between cells in the medio-lateral axis, suggests that another mechanism is at least acting in parallel with this one to define the midline of the neural rod.

Another mechanism may be that cells measure the distance across the neural rod using a type of molecular ruler (fig 7.1E), in an analogous way that nebulin might act as a molecular ruler to determine the length of thin filaments in striated muscle sarcomeres (Littlefield *et al.* 2008). This may be mediated in concert with microtubules, as stabilized

microtubules extend along the long axis of neural rod cells (Hong *et al.* 2010). A third mechanism is that a gradient of a molecule exists across the neural rod with its highest concentration at the basal edge of the rod (fig 7.1F). Cells could then sense the middle of the rod as the location of the lowest concentration of the molecule. Fission yeast detect when they are large enough to split into two daughter cells through the dose dependent G2/M inhibitor Pom1. Pom1 exists in a polar gradient in each cell that is highest at each end of the cell and decreases towards the centre. Only when the cell reaches a certain length is the concentration of Pom1 is low enough in the middle of the cell for the inhibition upon mitosis to be relieved (Martin *et al.* 2009; Moseley *et al.* 2009).

It would be interesting to test which of these hypotheses, if any, are true, but experimentally how to do this is not immediately obvious. In all these mechanisms it is possible that if a few cells can "set up" the location of the midline, other cells could take their midline cue from neighbouring cells. If any or all of these mechanisms rely upon the neural rod cells being in tension across the width of the rod, then this would require cells to make contralateral connections to form a pair of cells, or for them to stretch all the way across the width of the neural rod from one basal edge to the other contralateral basal edge. In division-blocked embryos, many cells stretch the whole way across the neural rod (X. Ren, unpublished observations), so perhaps the middle of these cells could be defined as the location furthest away from the two basal points of reference. However many only reach part way across the width of the rod and therefore are only attached to the basal edge of the rod at one end. The contribution of tension to the generation of the apical surface during neural tube formation remains to be investigated both in wild-type and division-blocked embryos.

The centrosome may also play a role in neural cell polarisation as it has been shown to be sufficient to determine neuronal polarity *in vitro* (de Anda *et al.* 2005). During neurulation in zebrafish, the centrosomes are initially located close to the nucleus in neural plate cells, but they gradually move more distant from the nucleus to become concentrated at the future midline in keel and rod stages (Hong *et al.* 2010). It has been shown that apical positioning of the centrosome is partly controlled by Par3, because in embryos depleted of Par3, many centrosomes are abnormally located at the basal edges of the cells (Hong *et al.* 2010). This indicates that Pard3 may be upstream of centrosome localisation during neurulation, which is similar to observations of centrosome positioning in migrating cells (Schmoranzer *et al.* 2009). Interestingly in *emi1* morphants, localisation of the centrosomes to the future midline in neural rod stages is normal (X. Ren, unpublished observations). If the centrosome or microtubule cytoskeleton is important

for trafficking apical proteins towards the midline then this may explain how division-blocked cells are still able to polarise fairly well. In summary, further characterisation of the cell biology of neural cells during neural tube morphogenesis may answer the apparently simple question of how a cell is able to locate the midline of the neural rod, that turns out not to be so simple after all. Moreover it will be interesting to investigate further the mechanisms of how apical proteins are directed to the midline and abscission site of cells during zebrafish neural tube formation. Finally, the contribution of the centrosome remains to be determined, especially as previous work has shown that the centrosome does not appear to be crucial for neuronal polarity *in vivo* (Zolessi *et al.* 2006).

Future perspectives

There are several possible directions for future work to follow up on the results presented in this thesis. One of the most obvious and intriguing questions concerns the details of the intrinsic timer controlling neural polarisation: what is the molecular mechanism of the timer? This may not be an easy question to answer but a sensible first step might be to investigate the brain morphogenesis defect of the MZ*dicer* mutant more carefully, especially as miRNAs are central components of many developmental timers. My results of 15th cycle embryos in which cell division is temporarily blocked prior to neurulation are consistent with the timer not relying upon counting the number of cell cycles to operate, but it would be good to complement these observations by carrying out the reverse experiment of decreasing the length of the cell cycle, possibly by manipulating specific components of the cell cycle. In this situation cells would be undergoing their 16th cell division in the neural plate so it would be interesting to find out if what effect, if any, this has on neural tube morphogenesis, as it might be predicted that early mirror-symmetric divisions might cause neural tube duplications.

Another possible direction could be to investigate further the role of the environment for neural cell behaviour during neurulation. Similar analyses of the timing of ZO-1 and Pard3-GFP polarisation could be carried out in other morphogenetic mutants to determine if other signalling pathways have any effect on the polarisation timer. For example, the BMP signalling mutant *swirl* has a dorsalised phenotype and the ectoderm is neuralised (Hammerschmidt *et al.* 1996; Kishimoto *et al.* 1997; Barth *et al.* 1999). Patterns of neurogenesis are affected in the neural plate (Barth *et al.* 1999), so it would be interesting to investigate neural tube morphogenesis and polarisation in this mutant.

A final direction could be to use the 3D cell culture technique to learn more about the role of the ECM in cell polarisation of neural progenitor cells. Several different hydrogels are commercially available that allow precise control over both the composition and physical properties of the ECM substrate. These gels range from consisting of a single ECM component such as collagen, peptides of ECM proteins within a synthetic gel, through to completely synthetic gels that do not provide any biochemical cures and are thus only permissive rather than instructive for cell function (Tibbitt *et al.* 2009). These might also enable research into whether the physical or chemical composition of the environment is important for neural cell polarisation.

Concluding remarks

The main result of this thesis is that the age of a neural progenitor cell is more important than the surrounding environment for determining the timing of cell division and polarisation during zebrafish neural tube formation. This highlights the importance of factors controlling convergence and extension, such as the planar cell polarity pathway, for ensuring that the morphogenetic movements of neurulation occur on time and at the right speed, thus avoiding defects in neural tube formation. My results show that tissue morphogenesis must be tightly regulated in time and space so that it is coordinated with the timed behaviours of individual cells for embryogenesis to proceed successfully.

LIST OF ABBREVIATIONS

ANOVA	Analysis of Variance
aPKC	a-typical Protein Kinase C
C-division	Crossing division
Ch	Cherry
DLHP	Dorso-lateral hinge point
Dll1	Delta-like 1
ECM	Extracellular matrix
EVL	Enveloping layer
FCS	Fetal Calf Serum
GC	Granule cell
GFAP	Glial fibrillary acidic protein
GMC	Ganglion mother cell
IQR	Interquartile range
KS-test	Kolmogorov-Smirnov test
MBT	Mid-blastula transition
MDCK cells	Madin Darby Canine Kidney cells
MHP	Median hinge point
MZ*oep*	Maternal Zygotic *one-eyed pinhead*
MZT	Maternal to Zygotic transition
N-Cad	N-Cadherin
NTD	Neural Tube Defect
OPC	Oligodendrocyte precursor
OV	Otic vesicle
PBS	Phoshate buffered saline
PCP	Planar Cell Polarity
PH3	Phospho-histone H3
PSM	Presomitic mesoderm
PtdIns-Ps	Phosphatidylinositol phosphate
ROI	Region of Interest
Shh	Sonic Hedgehog
siRNA	Small interfering RNA
tri	*trilobite*
WT	Wild-type
ZO-1	Zonula occludens -1

BIBLIOGRAPHY

Abney, E. R., P. P. Bartlett and M. C. Raff (1981). "Astrocytes, ependymal cells, and oligodendrocytes develop on schedule in dissociated cell cultures of embryonic rat brain." Dev Biol **83**(2): 301-310.

Adler, P. N., J. Charlton and J. Liu (1998). "Mutations in the cadherin superfamily member gene dachsous cause a tissue polarity phenotype by altering frizzled signaling." Development **125**(5): 959-968.

Ahringer, J. (2003). "Control of cell polarity and mitotic spindle positioning in animal cells." Curr Opin Cell Biol **15**(1): 73-81.

Akimenko, M. A., M. Ekker, J. Wegner, W. Lin and M. Westerfield (1994). "Combinatorial expression of three zebrafish genes related to distal-less: part of a homeobox gene code for the head." J Neurosci **14**(6): 3475-3486.

Albrecht-Buehler, G. (1977). "Daughter 3T3 cells. Are they mirror images of each other?" J Cell Biol **72**(3): 595-603.

Ambros, V. (1989). "A hierarchy of regulatory genes controls a larva-to-adult developmental switch in C. elegans." Cell **57**(1): 49-57.

Ambros, V. and H. R. Horvitz (1984). "Heterochronic mutants of the nematode Caenorhabditis elegans." Science **226**(4673): 409-416.

Ando, R., H. Hama, M. Yamamoto-Hino, H. Mizuno and A. Miyawaki (2002). "An optical marker based on the UV-induced green-to-red photoconversion of a fluorescent protein." Proc Natl Acad Sci U S A **99**(20): 12651-12656.

Andrew, D. J. and A. J. Ewald (2009). "Morphogenesis of epithelial tubes: Insights into tube formation, elongation, and elaboration." Dev Biol.

Andrew, D. J., K. D. Henderson and P. Seshaiah (2000). "Salivary gland development in Drosophila melanogaster." Mech Dev **92**(1): 5-17.

Aulehla, A., C. Wehrle, B. Brand-Saberi, R. Kemler, A. Gossler, B. Kanzler and B. G. Herrmann (2003). "Wnt3a plays a major role in the segmentation clock controlling somitogenesis." Dev Cell **4**(3): 395-406.

Baena-Lopez, L. A., A. Baonza and A. Garcia-Bellido (2005). "The orientation of cell divisions determines the shape of Drosophila organs." Curr Biol **15**(18): 1640-1644.

Bagga, S., J. Bracht, S. Hunter, K. Massirer, J. Holtz, R. Eachus and A. E. Pasquinelli (2005). "Regulation by let-7 and lin-4 miRNAs results in target mRNA degradation." Cell **122**(4): 553-563.

Balklava, Z., S. Pant, H. Fares and B. D. Grant (2007). "Genome-wide analysis identifies a general requirement for polarity proteins in endocytic traffic." Nat Cell Biol **9**(9): 1066-1073.

Balsalobre, A., F. Damiola and U. Schibler (1998). "A serum shock induces circadian gene expression in mammalian tissue culture cells." Cell **93**(6): 929-937.

Barrantes, I. B., A. J. Elia, K. Wunsch, M. H. Hrabe de Angelis, T. W. Mak, J. Rossant, R. A. Conlon, A. Gossler and J. L. de la Pompa (1999). "Interaction between Notch signalling and Lunatic fringe during somite boundary formation in the mouse." Curr Biol **9**(9): 470-480.

Barres, B. A., I. K. Hart, H. S. Coles, J. F. Burne, J. T. Voyvodic, W. D. Richardson and M. C. Raff (1992). "Cell death and control of cell survival in the oligodendrocyte lineage." Cell **70**(1): 31-46.

Barres, B. A., M. A. Lazar and M. C. Raff (1994). "A novel role for thyroid hormone, glucocorticoids and retinoic acid in timing oligodendrocyte development." Development **120**(5): 1097-1108.

Barth, K. A., Y. Kishimoto, K. B. Rohr, C. Seydler, S. Schulte-Merker and S. W. Wilson (1999). "Bmp activity establishes a gradient of positional information throughout the entire neural plate." Development **126**(22): 4977-4987.

Bayless, K. J. and G. E. Davis (2002). "The Cdc42 and Rac1 GTPases are required for capillary lumen formation in three-dimensional extracellular matrices." J Cell Sci **115**(Pt 6): 1123-1136.

Betschinger, J., K. Mechtler and J. A. Knoblich (2003). "The Par complex directs asymmetric cell division by phosphorylating the cytoskeletal protein Lgl." Nature **422**(6929): 326-330.

Bilder, D., M. Li and N. Perrimon (2000). "Cooperative regulation of cell polarity and growth by Drosophila tumor suppressors." Science **289**(5476): 113-116.

Bolton, V. N., P. J. Oades and M. H. Johnson (1984). "The relationship between cleavage, DNA replication, and gene expression in the mouse 2-cell embryo." J Embryol Exp Morphol **79**: 139-163.

Brennan, K., G. Offiah, E. A. McSherry and A. M. Hopkins (2010). "Tight junctions: a barrier to the initiation and progression of breast cancer?" J Biomed Biotechnol **2010**: 460607.

Brody, T. and W. F. Odenwald (2000). "Programmed transformations in neuroblast gene expression during Drosophila CNS lineage development." Dev Biol **226**(1): 34-44.

Brody, T. and W. F. Odenwald (2005). "Regulation of temporal identities during Drosophila neuroblast lineage development." Curr Opin Cell Biol **17**(6): 672-675.

Brouns, M. R., S. F. Matheson, K. Q. Hu, I. Delalle, V. S. Caviness, J. Silver, R. T. Bronson and J. Settleman (2000). "The adhesion signaling molecule p190 RhoGAP is required for morphogenetic processes in neural development." Development **127**(22): 4891-4903.

Bryant, D. M. and K. E. Mostov (2008). "From cells to organs: building polarized tissue." Nat Rev Mol Cell Biol **9**(11): 887-901.

Burton, P. B., M. C. Raff, P. Kerr, M. H. Yacoub and P. J. Barton (1999). "An intrinsic timer that controls cell-cycle withdrawal in cultured cardiac myocytes." Dev Biol **216**(2): 659-670.

Carr, A. J., T. Katherine Tamai, L. C. Young, V. Ferrer, M. P. Dekens and D. Whitmore (2006). "Light reaches the very heart of the zebrafish clock." Chronobiol Int **23**(1-2): 91-100.

Carreira-Barbosa, F., M. Kajita, V. Morel, H. Wada, H. Okamoto, A. Martinez Arias, Y. Fujita, S. W. Wilson and M. Tada (2009). "Flamingo regulates epiboly and convergence/extension movements through cell cohesive and signalling functions during zebrafish gastrulation." Development **136**(3): 383-392.

Castell, J. V. and M. J. Gomez-Lechon (2009). "Liver cell culture techniques." Methods Mol Biol **481**: 35-46.

Cayouette, M., B. A. Barres and M. Raff (2003). "Importance of intrinsic mechanisms in cell fate decisions in the developing rat retina." Neuron **40**(5): 897-904.

Cenci, C. and A. P. Gould (2005). "Drosophila Grainyhead specifies late programmes of neural proliferation by regulating the mitotic activity and Hox-dependent apoptosis of neuroblasts." Development **132**(17): 3835-3845.

Chang, T. T. and M. Hughes-Fulford (2009). "Monolayer and spheroid culture of human liver hepatocellular carcinoma cell line cells demonstrate distinct global gene expression patterns and functional phenotypes." Tissue Eng Part A **15**(3): 559-567.

Chen, C. S., M. Mrksich, S. Huang, G. M. Whitesides and D. E. Ingber (1997). "Geometric control of cell life and death." Science **276**(5317): 1425-1428.

Christians, E., E. Campion, E. M. Thompson and J. P. Renard (1995). "Expression of the HSP 70.1 gene, a landmark of early zygotic activity in the mouse embryo, is restricted to the first burst of transcription." Development **121**(1): 113-122.

Cinquin, O. (2007a). "Repressor dimerization in the zebrafish somitogenesis clock." PLoS Comput Biol **3**(2): e32.

Cinquin, O. (2007b). "Understanding the somitogenesis clock: what's missing?" Mech Dev **124**(7-8): 501-517.

Ciruna, B., A. Jenny, D. Lee, M. Mlodzik and A. F. Schier (2006). "Planar cell polarity signalling couples cell division and morphogenesis during neurulation." Nature **439**(7073): 220-224.

Clarke, J. (2009). "Role of polarized cell divisions in zebrafish neural tube formation." Curr Opin Neurobiol **19**(2): 134-138.

Classen, A. K., K. I. Anderson, E. Marois and S. Eaton (2005). "Hexagonal packing of Drosophila wing epithelial cells by the planar cell polarity pathway." Dev Cell **9**(6): 805-817.

Clute, P. and Y. Masui (1995). "Regulation of the appearance of division asynchrony and microtubule-dependent chromosome cycles in Xenopus laevis embryos." Dev Biol **171**(2): 273-285.

Colas, J. F. and G. C. Schoenwolf (2001). "Towards a cellular and molecular understanding of neurulation." Dev Dyn **221**(2): 117-145.

Concha, M. L. and R. J. Adams (1998). "Oriented cell divisions and cellular morphogenesis in the zebrafish gastrula and neurula: a time-lapse analysis." Development **125**(6): 983-994.

Conlon, R. A., A. G. Reaume and J. Rossant (1995). "Notch1 is required for the coordinate segmentation of somites." Development **121**(5): 1533-1545.

Cooke, J. and E. C. Zeeman (1976). "A clock and wavefront model for control of the number of repeated structures during animal morphogenesis." J Theor Biol **58**(2): 455-476.

Copp, A. J., F. A. Brook and H. J. Roberts (1988a). "A cell-type-specific abnormality of cell proliferation in mutant (curly tail) mouse embryos developing spinal neural tube defects." Development **104**(2): 285-295.

Copp, A. J., J. A. Crolla and F. A. Brook (1988b). "Prevention of spinal neural tube defects in the mouse embryo by growth retardation during neurulation." Development **104**(2): 297-303.

Copp, A. J. and N. D. Greene (2010). "Genetics and development of neural tube defects." J Pathol **220**(2): 217-230.

Copp, A. J., N. D. Greene and J. N. Murdoch (2003). "The genetic basis of mammalian neurulation." Nat Rev Genet **4**(10): 784-793.

Curtin, J. A., E. Quint, V. Tsipouri, R. M. Arkell, B. Cattanach, A. J. Copp, D. J. Henderson, N. Spurr, P. Stanier, E. M. Fisher, P. M. Nolan, K. P. Steel, S. D. Brown, I. C. Gray and J. N. Murdoch (2003). "Mutation of Celsr1 disrupts planar polarity of inner ear hair

cells and causes severe neural tube defects in the mouse." Curr Biol **13**(13): 1129-1133.

da Silva, S. M. and J. P. Vincent (2007). "Oriented cell divisions in the extending germband of Drosophila." Development **134**(17): 3049-3054.

Davis, G. E. and C. W. Camarillo (1996). "An alpha 2 beta 1 integrin-dependent pinocytic mechanism involving intracellular vacuole formation and coalescence regulates capillary lumen and tube formation in three-dimensional collagen matrix." Exp Cell Res **224**(1): 39-51.

de Anda, F. C., G. Pollarolo, J. S. Da Silva, P. G. Camoletto, F. Feiguin and C. G. Dotti (2005). "Centrosome localization determines neuronal polarity." Nature **436**(7051): 704-708.

DeBiasio, R. L., G. M. LaRocca, P. L. Post and D. L. Taylor (1996). "Myosin II transport, organization, and phosphorylation: evidence for cortical flow/solation-contraction coupling during cytokinesis and cell locomotion." Mol Biol Cell **7**(8): 1259-1282.

Debnath, J., S. K. Muthuswamy and J. S. Brugge (2003). "Morphogenesis and oncogenesis of MCF-10A mammary epithelial acini grown in three-dimensional basement membrane cultures." Methods **30**(3): 256-268.

Decembrini, S., M. Andreazzoli, R. Vignali, G. Barsacchi and F. Cremisi (2006). "Timing the generation of distinct retinal cells by homeobox proteins." PLoS Biol **4**(9): e272.

Decembrini, S., D. Bressan, R. Vignali, L. Pitto, S. Mariotti, G. Rainaldi, X. Wang, M. Evangelista, G. Barsacchi and F. Cremisi (2009). "MicroRNAs couple cell fate and developmental timing in retina." Proc Natl Acad Sci U S A **106**(50): 21179-21184.

Dekens, M. P., C. Santoriello, D. Vallone, G. Grassi, D. Whitmore and N. S. Foulkes (2003). "Light regulates the cell cycle in zebrafish." Curr Biol **13**(23): 2051-2057.

Dekens, M. P. and D. Whitmore (2008). "Autonomous onset of the circadian clock in the zebrafish embryo." EMBO J **27**(20): 2757-2765.

Delaunay, F., C. Thisse, O. Marchand, V. Laudet and B. Thisse (2000). "An inherited functional circadian clock in zebrafish embryos." Science **289**(5477): 297-300.

Dequeant, M. L., E. Glynn, K. Gaudenz, M. Wahl, J. Chen, A. Mushegian and O. Pourquie (2006). "A complex oscillating network of signaling genes underlies the mouse segmentation clock." Science **314**(5805): 1595-1598.

Deschene, E. R. and M. J. Barresi (2009). "Tissue targeted embryonic chimeras: zebrafish gastrula cell transplantation." J Vis Exp(31).

Devenport, D. and E. Fuchs (2008). "Planar polarization in embryonic epidermis orchestrates global asymmetric morphogenesis of hair follicles." Nat Cell Biol **10**(11): 1257-1268.

Discher, D. E., P. Janmey and Y. L. Wang (2005). "Tissue cells feel and respond to the stiffness of their substrate." Science **310**(5751): 1139-1143.

Dong, G. and S. S. Golden (2008). "How a cyanobacterium tells time." Curr Opin Microbiol **11**(6): 541-546.

Dugas, J. C., A. Ibrahim and B. A. Barres (2007). "A crucial role for p57(Kip2) in the intracellular timer that controls oligodendrocyte differentiation." J Neurosci **27**(23): 6185-6196.

Durand, B., M. L. Fero, J. M. Roberts and M. C. Raff (1998). "p27Kip1 alters the response of cells to mitogen and is part of a cell-intrinsic timer that arrests the cell cycle and initiates differentiation." Curr Biol **8**(8): 431-440.

Durand, B., F. B. Gao and M. Raff (1997). "Accumulation of the cyclin-dependent kinase inhibitor p27/Kip1 and the timing of oligodendrocyte differentiation." EMBO J **16**(2): 306-317.

Ebnet, K., A. Suzuki, Y. Horikoshi, T. Hirose, M. K. Meyer Zu Brickwedde, S. Ohno and D. Vestweber (2001). "The cell polarity protein ASIP/PAR-3 directly associates with junctional adhesion molecule (JAM)." EMBO J **20**(14): 3738-3748.

Ebnet, K., A. Suzuki, S. Ohno and D. Vestweber (2004). "Junctional adhesion molecules (JAMs): more molecules with dual functions?" J Cell Sci **117**(Pt 1): 19-29.

Edgar, B. A. (1994). "Cell cycle. Cell-cycle control in a developmental context." Curr Biol **4**(6): 522-524.

Elbashir, S. M., W. Lendeckel and T. Tuschl (2001). "RNA interference is mediated by 21- and 22-nucleotide RNAs." Genes Dev **15**(2): 188-200.

England, S. J., G. B. Blanchard, L. Mahadevan and R. J. Adams (2006). "A dynamic fate map of the forebrain shows how vertebrate eyes form and explains two causes of cyclopia." Development **133**(23): 4613-4617.

Etienne-Manneville, S. (2004). "Cdc42--the centre of polarity." J Cell Sci **117**(Pt 8): 1291-1300.

Feng, W., H. Wu, L. N. Chan and M. Zhang (2008). "Par-3-mediated junctional localization of the lipid phosphatase PTEN is required for cell polarity establishment." J Biol Chem **283**(34): 23440-23449.

Ferri, R. T. and P. Levitt (1995). "Regulation of regional differences in the differentiation of cerebral cortical neurons by EGF family-matrix interactions." Development **121**(4): 1151-1160.

Fleming, T. P., Q. Javed, J. Collins and M. Hay (1993). "Biogenesis of structural intercellular junctions during cleavage in the mouse embryo." J Cell Sci Suppl **17**: 119-125.

Foe, V. E. (1989). "Mitotic domains reveal early commitment of cells in Drosophila embryos." Development **107**(1): 1-22.

Forsberg, H., F. Crozet and N. A. Brown (1998). "Waves of mouse Lunatic fringe expression, in four-hour cycles at two-hour intervals, precede somite boundary formation." Curr Biol **8**(18): 1027-1030.

Fukata, M. and K. Kaibuchi (2001). "Rho-family GTPases in cadherin-mediated cell-cell adhesion." Nat Rev Mol Cell Biol **2**(12): 887-897.

Gahwiler, B. H., M. Capogna, D. Debanne, R. A. McKinney and S. M. Thompson (1997). "Organotypic slice cultures: a technique has come of age." Trends Neurosci **20**(10): 471-477.

Gallego, M. and D. M. Virshup (2007). "Post-translational modifications regulate the ticking of the circadian clock." Nat Rev Mol Cell Biol **8**(2): 139-148.

Gao, F. B., B. Durand and M. Raff (1997). "Oligodendrocyte precursor cells count time but not cell divisions before differentiation." Curr Biol **7**(2): 152-155.

Gassama-Diagne, A., W. Yu, M. ter Beest, F. Martin-Belmonte, A. Kierbel, J. Engel and K. Mostov (2006). "Phosphatidylinositol-3,4,5-trisphosphate regulates the formation of the basolateral plasma membrane in epithelial cells." Nat Cell Biol **8**(9): 963-970.

Geldmacher-Voss, B., A. M. Reugels, S. Pauls and J. A. Campos-Ortega (2003). "A 90-degree rotation of the mitotic spindle changes the orientation of mitoses of zebrafish neuroepithelial cells." Development **130**(16): 3767-3780.

Gervais, L. and J. Casanova (2010). "In Vivo Coupling of Cell Elongation and Lumen Formation in a Single Cell." Curr Biol **20**(4): 359-366.

Giraldez, A. J., R. M. Cinalli, M. E. Glasner, A. J. Enright, J. M. Thomson, S. Baskerville, S. M. Hammond, D. P. Bartel and A. F. Schier (2005). "MicroRNAs regulate brain morphogenesis in zebrafish." Science **308**(5723): 833-838.

Giraldez, A. J., Y. Mishima, J. Rihel, R. J. Grocock, S. Van Dongen, K. Inoue, A. J. Enright and A. F. Schier (2006). "Zebrafish MiR-430 promotes deadenylation and clearance of maternal mRNAs." Science **312**(5770): 75-79.

Giudicelli, F. and J. Lewis (2004). "The vertebrate segmentation clock." Curr Opin Genet Dev **14**(4): 407-414.

Goldstein, B. and I. G. Macara (2007). "The PAR proteins: fundamental players in animal cell polarization." Dev Cell **13**(5): 609-622.

Gomez, C., E. M. Ozbudak, J. Wunderlich, D. Baumann, J. Lewis and O. Pourquie (2008). "Control of segment number in vertebrate embryos." Nature **454**(7202): 335-339.

Gong, Y., C. Mo and S. E. Fraser (2004). "Planar cell polarity signalling controls cell division orientation during zebrafish gastrulation." Nature **430**(7000): 689-693.

Gonzalez-Gaitan, M., M. P. Capdevila and A. Garcia-Bellido (1994). "Cell proliferation patterns in the wing imaginal disc of Drosophila." Mech Dev **46**(3): 183-200.

Gritsman, K., J. Zhang, S. Cheng, E. Heckscher, W. S. Talbot and A. F. Schier (1999). "The EGF-CFC protein one-eyed pinhead is essential for nodal signaling." Cell **97**(1): 121-132.

Grosskortenhaus, R., B. J. Pearson, A. Marusich and C. Q. Doe (2005). "Regulation of temporal identity transitions in Drosophila neuroblasts." Dev Cell **8**(2): 193-202.

Grosskortenhaus, R., K. J. Robinson and C. Q. Doe (2006). "Pdm and Castor specify late-born motor neuron identity in the NB7-1 lineage." Genes Dev **20**(18): 2618-2627.

Gubb, D. and A. Garcia-Bellido (1982). "A genetic analysis of the determination of cuticular polarity during development in Drosophila melanogaster." J Embryol Exp Morphol **68**: 37-57.

Gunawardane, R. N., S. B. Lizarraga, C. Wiese, A. Wilde and Y. Zheng (2000). "gamma-Tubulin complexes and their role in microtubule nucleation." Curr Top Dev Biol **49**: 55-73.

Haigo, S. L., J. D. Hildebrand, R. M. Harland and J. B. Wallingford (2003). "Shroom induces apical constriction and is required for hingepoint formation during neural tube closure." Curr Biol **13**(24): 2125-2137.

Hammerschmidt, M., G. N. Serbedzija and A. P. McMahon (1996). "Genetic analysis of dorsoventral pattern formation in the zebrafish: requirement of a BMP-like ventralizing activity and its dorsal repressor." Genes Dev **10**(19): 2452-2461.

Hara, K., P. Tydeman and M. Kirschner (1980). "A cytoplasmic clock with the same period as the division cycle in Xenopus eggs." Proc Natl Acad Sci U S A **77**(1): 462-466.

Hardin, J. and R. Keller (1988). "The behaviour and function of bottle cells during gastrulation of Xenopus laevis." Development **103**(1): 211-230.

Harris, T. J. and M. Peifer (2004). "Adherens junction-dependent and -independent steps in the establishment of epithelial cell polarity in Drosophila." J Cell Biol **167**(1): 135-147.

Harris, T. J. and M. Peifer (2005). "The positioning and segregation of apical cues during epithelial polarity establishment in Drosophila." J Cell Biol **170**(5): 813-823.

Harris, W. A. and V. Hartenstein (1991). "Neuronal determination without cell division in Xenopus embryos." Neuron **6**(4): 499-515.

Hartley, R. S., J. C. Sible, A. L. Lewellyn and J. L. Maller (1997). "A role for cyclin E/Cdk2 in the timing of the midblastula transition in Xenopus embryos." Dev Biol **188**(2): 312-321.

Hartsock, A. and W. J. Nelson (2008). "Adherens and tight junctions: structure, function and connections to the actin cytoskeleton." Biochim Biophys Acta **1778**(3): 660-669.

Hildebrand, J. D. and P. Soriano (1999). "Shroom, a PDZ domain-containing actin-binding protein, is required for neural tube morphogenesis in mice." Cell **99**(5): 485-497.

Hirose, T., Y. Izumi, Y. Nagashima, Y. Tamai-Nagai, H. Kurihara, T. Sakai, Y. Suzuki, T. Yamanaka, A. Suzuki, K. Mizuno and S. Ohno (2002). "Involvement of ASIP/PAR-3 in the promotion of epithelial tight junction formation." J Cell Sci **115**(Pt 12): 2485-2495.

Holley, S. A., R. Geisler and C. Nusslein-Volhard (2000a). "Control of her1 expression during zebrafish somitogenesis by a delta-dependent oscillator and an independent wave-front activity." Genes Dev **14**(13): 1678-1690.

Holley, S. A., D. Julich, G. J. Rauch, R. Geisler and C. Nusslein-Volhard (2002). "her1 and the notch pathway function within the oscillator mechanism that regulates zebrafish somitogenesis." Development **129**(5): 1175-1183.

Holley, S. A. and C. Nusslein-Volhard (2000b). "Somitogenesis in zebrafish." Curr Top Dev Biol **47**: 247-277.

Holt, C. E., T. W. Bertsch, H. M. Ellis and W. A. Harris (1988). "Cellular determination in the Xenopus retina is independent of lineage and birth date." Neuron **1**(1): 15-26.

Hong, E. and R. Brewster (2006). "N-cadherin is required for the polarized cell behaviors that drive neurulation in the zebrafish." Development **133**(19): 3895-3905.

Hong, E., P. Jayachandran and R. Brewster (2010). "The polarity protein Pard3 is required for centrosome positioning during neurulation." Dev Biol.

Howe, J. A. and J. W. Newport (1996). "A developmental timer regulates degradation of cyclin E1 at the midblastula transition during Xenopus embryogenesis." Proc Natl Acad Sci U S A **93**(5): 2060-2064.

Huber, L. A., S. Pimplikar, R. G. Parton, H. Virta, M. Zerial and K. Simons (1993). "Rab8, a small GTPase involved in vesicular traffic between the TGN and the basolateral plasma membrane." J Cell Biol **123**(1): 35-45.

Hurd, T. W., L. Gao, M. H. Roh, I. G. Macara and B. Margolis (2003). "Direct interaction of two polarity complexes implicated in epithelial tight junction assembly." Nat Cell Biol **5**(2): 137-142.

Hyatt, G. A. and J. E. Dowling (1997). "Retinoic acid. A key molecule for eye and photoreceptor development." Invest Ophthalmol Vis Sci **38**(8): 1471-1475.

Iden, S. and J. G. Collard (2008). "Crosstalk between small GTPases and polarity proteins in cell polarization." Nat Rev Mol Cell Biol **9**(11): 846-859.

Inman, G. J., F. J. Nicolas, J. F. Callahan, J. D. Harling, L. M. Gaster, A. D. Reith, N. J. Laping and C. S. Hill (2002). "SB-431542 is a potent and specific inhibitor of transforming growth factor-beta superfamily type I activin receptor-like kinase (ALK) receptors ALK4, ALK5, and ALK7." Mol Pharmacol **62**(1): 65-74.

Isshiki, T., B. Pearson, S. Holbrook and C. Q. Doe (2001). "Drosophila neuroblasts sequentially express transcription factors which specify the temporal identity of their neuronal progeny." Cell **106**(4): 511-521.

Itoh, M., H. Sasaki, M. Furuse, H. Ozaki, T. Kita and S. Tsukita (2001). "Junctional adhesion molecule (JAM) binds to PAR-3: a possible mechanism for the recruitment of PAR-3 to tight junctions." J Cell Biol **154**(3): 491-497.

Jacob, J., C. Maurange and A. P. Gould (2008). "Temporal control of neuronal diversity: common regulatory principles in insects and vertebrates?" Development **135**(21): 3481-3489.

Jaffe, A. B., N. Kaji, J. Durgan and A. Hall (2008). "Cdc42 controls spindle orientation to position the apical surface during epithelial morphogenesis." J Cell Biol **183**(4): 625-633.

Janetopoulos, C., J. Borleis, F. Vazquez, M. Iijima and P. Devreotes (2005). "Temporal and spatial regulation of phosphoinositide signaling mediates cytokinesis." Dev Cell **8**(4): 467-477.

Jenny, A. and M. Mlodzik (2006). "Planar cell polarity signaling: a common mechanism for cellular polarization." Mt Sinai J Med **73**(5): 738-750.

Jessen, J. R., J. Topczewski, S. Bingham, D. S. Sepich, F. Marlow, A. Chandrasekhar and L. Solnica-Krezel (2002). "Zebrafish trilobite identifies new roles for Strabismus in gastrulation and neuronal movements." Nat Cell Biol **4**(8): 610-615.

Jiang, Y. J., B. L. Aerne, L. Smithers, C. Haddon, D. Ish-Horowicz and J. Lewis (2000). "Notch signalling and the synchronization of the somite segmentation clock." Nature **408**(6811): 475-479.

Joberty, G., C. Petersen, L. Gao and I. G. Macara (2000). "The cell-polarity protein Par6 links Par3 and atypical protein kinase C to Cdc42." Nat Cell Biol **2**(8): 531-539.

Kamei, M., W. B. Saunders, K. J. Bayless, L. Dye, G. E. Davis and B. M. Weinstein (2006). "Endothelial tubes assemble from intracellular vacuoles in vivo." Nature **442**(7101): 453-456.

Kanai, M. I., M. Okabe and Y. Hiromi (2005). "seven-up Controls switching of transcription factors that specify temporal identities of Drosophila neuroblasts." Dev Cell **8**(2): 203-213.

Kane, D. A., R. M. Warga and C. B. Kimmel (1992). "Mitotic domains in the early embryo of the zebrafish." Nature **360**(6406): 735-737.

Kay, J. N., B. A. Link and H. Baier (2005). "Staggered cell-intrinsic timing of ath5 expression underlies the wave of ganglion cell neurogenesis in the zebrafish retina." Development **132**(11): 2573-2585.

Keller, H., P. Rentsch and J. Hagmann (2002). "Differences in cortical actin structure and dynamics document that different types of blebs are formed by distinct mechanisms." Exp Cell Res **277**(2): 161-172.

Keller, R. (2002). "Shaping the vertebrate body plan by polarized embryonic cell movements." Science **298**(5600): 1950-1954.

Keller, R. and M. Danilchik (1988). "Regional expression, pattern and timing of convergence and extension during gastrulation of Xenopus laevis." Development **103**(1): 193-209.

Keller, R. E., M. Danilchik, R. Gimlich and J. Shih (1985). "The function and mechanism of convergent extension during gastrulation of Xenopus laevis." J Embryol Exp Morphol **89 Suppl**: 185-209.

Kelley, M. W., J. K. Turner and T. A. Reh (1995). "Ligands of steroid/thyroid receptors induce cone photoreceptors in vertebrate retina." Development **121**(11): 3777-3785.

Kelm, J. M., N. E. Timmins, C. J. Brown, M. Fussenegger and L. K. Nielsen (2003). "Method for generation of homogeneous multicellular tumor spheroids applicable to a wide variety of cell types." Biotechnol Bioeng **83**(2): 173-180.

Kelsch, W., C. P. Mosley, C. W. Lin and C. Lois (2007). "Distinct mammalian precursors are committed to generate neurons with defined dendritic projection patterns." PLoS Biol **5**(11): e300.

Kemp, H. A., A. Carmany-Rampey and C. Moens (2009a). "Generating chimeric zebrafish embryos by transplantation." J Vis Exp(29).

Kemp, H. A., J. E. Cooke and C. B. Moens (2009b). "EphA4 and EfnB2a maintain rhombomere coherence by independently regulating intercalation of progenitor cells in the zebrafish neural keel." Dev Biol **327**(2): 313-326.

Kesavan, G., F. W. Sand, T. U. Greiner, J. K. Johansson, S. Kobberup, X. Wu, C. Brakebusch and H. Semb (2009). "Cdc42-mediated tubulogenesis controls cell specification." Cell **139**(4): 791-801.

Kim, T. H., J. Goodman, K. V. Anderson and L. Niswander (2007). "Phactr4 regulates neural tube and optic fissure closure by controlling PP1-, Rb-, and E2F1-regulated cell-cycle progression." Dev Cell **13**(1): 87-102.

Kimmel, C. B., W. W. Ballard, S. R. Kimmel, B. Ullmann and T. F. Schilling (1995). "Stages of embryonic development of the zebrafish." Dev Dyn **203**(3): 253-310.

Kimmel, C. B., R. M. Warga and D. A. Kane (1994). "Cell cycles and clonal strings during formation of the zebrafish central nervous system." Development **120**(2): 265-276.

Kirkman, T. W. (1996). "Statistics to Use.", 2009, from http://www.physics.csbsju.edu/stats/.

Kishimoto, Y., K. H. Lee, L. Zon, M. Hammerschmidt and S. Schulte-Merker (1997). "The molecular nature of zebrafish swirl: BMP2 function is essential during early dorsoventral patterning." Development **124**(22): 4457-4466.

Kleinman, H. K., M. L. McGarvey, J. R. Hassell, V. L. Star, F. B. Cannon, G. W. Laurie and G. R. Martin (1986). "Basement membrane complexes with biological activity." Biochemistry **25**(2): 312-318.

Kleinman, H. K., M. L. McGarvey, L. A. Liotta, P. G. Robey, K. Tryggvason and G. R. Martin (1982). "Isolation and characterization of type IV procollagen, laminin, and heparan sulfate proteoglycan from the EHS sarcoma." Biochemistry **21**(24): 6188-6193.

Knust, E. and O. Bossinger (2002). "Composition and formation of intercellular junctions in epithelial cells." Science **298**(5600): 1955-1959.

Kozubowski, L., K. Saito, J. M. Johnson, A. S. Howell, T. R. Zyla and D. J. Lew (2008). "Symmetry-breaking polarization driven by a Cdc42p GEF-PAK complex." Curr Biol **18**(22): 1719-1726.

Kume, K., M. J. Zylka, S. Sriram, L. P. Shearman, D. R. Weaver, X. Jin, E. S. Maywood, M. H. Hastings and S. M. Reppert (1999). "mCRY1 and mCRY2 are essential components of the negative limb of the circadian clock feedback loop." Cell **98**(2): 193-205.

Lee, C., H. M. Scherr and J. B. Wallingford (2007). "Shroom family proteins regulate gamma-tubulin distribution and microtubule architecture during epithelial cell shape change." Development **134**(7): 1431-1441.

Lee, R. C., R. L. Feinbaum and V. Ambros (1993). "The C. elegans heterochronic gene lin-4 encodes small RNAs with antisense complementarity to lin-14." Cell **75**(5): 843-854.

Leptin, M. and B. Grunewald (1990). "Cell shape changes during gastrulation in Drosophila." Development **110**(1): 73-84.

Ligon, L. A., S. Karki, M. Tokito and E. L. Holzbaur (2001). "Dynein binds to beta-catenin and may tether microtubules at adherens junctions." Nat Cell Biol **3**(10): 913-917.

Lillien, L. (1995). "Changes in retinal cell fate induced by overexpression of EGF receptor." Nature **377**(6545): 158-162.

Lillien, L. and D. Wancio (1998). "Changes in Epidermal Growth Factor Receptor Expression and Competence to Generate Glia Regulate Timing and Choice of Differentiation in the Retina." Mol Cell Neurosci **10**(5/6): 296-308.

Littlefield, R. S. and V. M. Fowler (2008). "Thin filament length regulation in striated muscle sarcomeres: pointed-end dynamics go beyond a nebulin ruler." Semin Cell Dev Biol **19**(6): 511-519.

Liu, K. D., A. Datta, W. Yu, P. R. Brakeman, T. S. Jou, M. A. Matthay and K. E. Mostov (2007). "Rac1 is required for reorientation of polarity and lumen formation through a PI 3-kinase-dependent pathway." Am J Physiol Renal Physiol **293**(5): F1633-1640.

Livesey, F. J. and C. L. Cepko (2001). "Vertebrate neural cell-fate determination: lessons from the retina." Nat Rev Neurosci **2**(2): 109-118.

Lowery, L. A. and H. Sive (2004). "Strategies of vertebrate neurulation and a re-evaluation of teleost neural tube formation." Mech Dev **121**(10): 1189-1197.

Lowery, L. A. and H. Sive (2005). "Initial formation of zebrafish brain ventricles occurs independently of circulation and requires the nagie oko and snakehead/atp1a1a.1 gene products." Development **132**(9): 2057-2067.

Lubarsky, B. and M. A. Krasnow (2003). "Tube morphogenesis: making and shaping biological tubes." Cell **112**(1): 19-28.

Lyons, D. A., A. T. Guy and J. D. Clarke (2003). "Monitoring neural progenitor fate through multiple rounds of division in an intact vertebrate brain." Development **130**(15): 3427-3436.

Lyons, D. A., H. M. Pogoda, M. G. Voas, I. G. Woods, B. Diamond, R. Nix, N. Arana, J. Jacobs and W. S. Talbot (2005). "erbb3 and erbb2 are essential for schwann cell migration and myelination in zebrafish." Curr Biol **15**(6): 513-524.

Mailleux, A. A., M. Overholtzer, T. Schmelzle, P. Bouillet, A. Strasser and J. S. Brugge (2007). "BIM regulates apoptosis during mammary ductal morphogenesis, and its absence reveals alternative cell death mechanisms." Dev Cell **12**(2): 221-234.

Mara, A. and S. A. Holley (2007a). "Oscillators and the emergence of tissue organization during zebrafish somitogenesis." Trends Cell Biol **17**(12): 593-599.

Mara, A., J. Schroeder, C. Chalouni and S. A. Holley (2007b). "Priming, initiation and synchronization of the segmentation clock by deltaD and deltaC." Nat Cell Biol **9**(5): 523-530.

Marquardt, T. and P. Gruss (2002). "Generating neuronal diversity in the retina: one for nearly all." Trends Neurosci **25**(1): 32-38.

Martin, S. G. and M. Berthelot-Grosjean (2009). "Polar gradients of the DYRK-family kinase Pom1 couple cell length with the cell cycle." Nature **459**(7248): 852-856.

Martin, T. A., G. Watkins, R. E. Mansel and W. G. Jiang (2004). "Loss of tight junction plaque molecules in breast cancer tissues is associated with a poor prognosis in patients with breast cancer." Eur J Cancer **40**(18): 2717-2725.

Martin-Belmonte, F., A. Gassama, A. Datta, W. Yu, U. Rescher, V. Gerke and K. Mostov (2007a). "PTEN-mediated apical segregation of phosphoinositides controls epithelial morphogenesis through Cdc42." Cell **128**(2): 383-397.

Martin-Belmonte, F. and K. Mostov (2007b). "Phosphoinositides control epithelial development." Cell Cycle **6**(16): 1957-1961.

Martin-Belmonte, F., W. Yu, A. E. Rodriguez-Fraticelli, A. J. Ewald, Z. Werb, M. A. Alonso and K. Mostov (2008). "Cell-polarity dynamics controls the mechanism of lumen formation in epithelial morphogenesis." Curr Biol **18**(7): 507-513.

McFarland, K. N., R. M. Warga and D. A. Kane (2005). "Genetic locus half baked is necessary for morphogenesis of the ectoderm." Dev Dyn **233**(2): 390-406.

McGrew, M. J., J. K. Dale, S. Fraboulet and O. Pourquie (1998). "The lunatic fringe gene is a target of the molecular clock linked to somite segmentation in avian embryos." Curr Biol **8**(17): 979-982.

McGuire, P. G. and N. W. Seeds (1989). "The interaction of plasminogen activator with a reconstituted basement membrane matrix and extracellular macromolecules produced by cultured epithelial cells." J Cell Biochem **40**(2): 215-227.

Medina, E., J. Williams, E. Klipfell, D. Zarnescu, G. Thomas and A. Le Bivic (2002). "Crumbs interacts with moesin and beta(Heavy)-spectrin in the apical membrane skeleton of Drosophila." J Cell Biol **158**(5): 941-951.

Mori, K., K. Kishi and H. Ojima (1983). "Distribution of dendrites of mitral, displaced mitral, tufted, and granule cells in the rabbit olfactory bulb." J Comp Neurol **219**(3): 339-355.

Moseley, J. B., A. Mayeux, A. Paoletti and P. Nurse (2009). "A spatial gradient coordinates cell size and mitotic entry in fission yeast." Nature **459**(7248): 857-860.

Moss, E. G. (2007). "Heterochronic genes and the nature of developmental time." Curr Biol **17**(11): R425-434.

Munro, E., J. Nance and J. R. Priess (2004). "Cortical flows powered by asymmetrical contraction transport PAR proteins to establish and maintain anterior-posterior polarity in the early C. elegans embryo." Dev Cell **7**(3): 413-424.

Munson, C., J. Huisken, N. Bit-Avragim, T. Kuo, P. D. Dong, E. A. Ober, H. Verkade, S. Abdelilah-Seyfried and D. Y. Stainier (2008). "Regulation of neurocoel morphogenesis by Pard6 gamma b." Dev Biol **324**(1): 41-54.

Musch, A., D. Cohen, C. Yeaman, W. J. Nelson, E. Rodriguez-Boulan and P. J. Brennwald (2002). "Mammalian homolog of Drosophila tumor suppressor lethal (2) giant

larvae interacts with basolateral exocytic machinery in Madin-Darby canine kidney cells." Mol Biol Cell **13**(1): 158-168.

Myat, M. M. and D. J. Andrew (2000). "Fork head prevents apoptosis and promotes cell shape change during formation of the Drosophila salivary glands." Development **127**(19): 4217-4226.

Negron, J. F. and R. A. Lockshin (2004). "Activation of apoptosis and caspase-3 in zebrafish early gastrulae." Dev Dyn **231**(1): 161-170.

Nelson, W. J. (2003). "Adaptation of core mechanisms to generate cell polarity." Nature **422**(6933): 766-774.

Neufeld, T. P., A. F. de la Cruz, L. A. Johnston and B. A. Edgar (1998). "Coordination of growth and cell division in the Drosophila wing." Cell **93**(7): 1183-1193.

Neumann, C. J. and C. Nuesslein-Volhard (2000). "Patterning of the zebrafish retina by a wave of sonic hedgehog activity." Science **289**(5487): 2137-2139.

Newport, J. and M. Kirschner (1982a). "A major developmental transition in early Xenopus embryos: I. characterization and timing of cellular changes at the midblastula stage." Cell **30**(3): 675-686.

Newport, J. and M. Kirschner (1982b). "A major developmental transition in early Xenopus embryos: II. Control of the onset of transcription." Cell **30**(3): 687-696.

Nguyen, D. X. and J. Massague (2007). "Genetic determinants of cancer metastasis." Nat Rev Genet **8**(5): 341-352.

Nishimura, T. and K. Kaibuchi (2007). "Numb controls integrin endocytosis for directional cell migration with aPKC and PAR-3." Dev Cell **13**(1): 15-28.

Nishimura, T. and M. Takeichi (2009). "Remodeling of the adherens junctions during morphogenesis." Curr Top Dev Biol **89**: 33-54.

Norden, C., S. Young, B. A. Link and W. A. Harris (2009). "Actomyosin is the main driver of interkinetic nuclear migration in the retina." Cell **138**(6): 1195-1208.

Nyholm, M. K., S. Abdelilah-Seyfried and Y. Grinblat (2009). "A novel genetic mechanism regulates dorsolateral hinge-point formation during zebrafish cranial neurulation." J Cell Sci **122**(Pt 12): 2137-2148.

O'Brien, L. E., T. S. Jou, A. L. Pollack, Q. Zhang, S. H. Hansen, P. Yurchenco and K. E. Mostov (2001). "Rac1 orientates epithelial apical polarity through effects on basolateral laminin assembly." Nat Cell Biol **3**(9): 831-838.

Olsen, P. H. and V. Ambros (1999). "The lin-4 regulatory RNA controls developmental timing in Caenorhabditis elegans by blocking LIN-14 protein synthesis after the initiation of translation." Dev Biol **216**(2): 671-680.

Orona, E., J. W. Scott and E. C. Rainer (1983). "Different granule cell populations innervate superficial and deep regions of the external plexiform layer in rat olfactory bulb." J Comp Neurol **217**(2): 227-237.

Palmeirim, I., D. Henrique, D. Ish-Horowicz and O. Pourquie (1997). "Avian hairy gene expression identifies a molecular clock linked to vertebrate segmentation and somitogenesis." Cell **91**(5): 639-648.

Paluch, E., J. van der Gucht and C. Sykes (2006). "Cracking up: symmetry breaking in cellular systems." J Cell Biol **175**(5): 687-692.

Pampaloni, F., E. G. Reynaud and E. H. Stelzer (2007). "The third dimension bridges the gap between cell culture and live tissue." Nat Rev Mol Cell Biol **8**(10): 839-845.

Park, H. C., C. H. Kim, Y. K. Bae, S. Y. Yeo, S. H. Kim, S. K. Hong, J. Shin, K. W. Yoo, M. Hibi, T. Hirano, N. Miki, A. B. Chitnis and T. L. Huh (2000). "Analysis of upstream elements in the HuC promoter leads to the establishment of transgenic zebrafish with fluorescent neurons." Dev Biol **227**(2): 279-293.

Park, M. and R. T. Moon (2002). "The planar cell-polarity gene stbm regulates cell behaviour and cell fate in vertebrate embryos." Nat Cell Biol **4**(1): 20-25.

Pasquinelli, A. E., B. J. Reinhart, F. Slack, M. Q. Martindale, M. I. Kuroda, B. Maller, D. C. Hayward, E. E. Ball, B. Degnan, P. Muller, J. Spring, A. Srinivasan, M. Fishman, J. Finnerty, J. Corbo, M. Levine, P. Leahy, E. Davidson and G. Ruvkun (2000). "Conservation of the sequence and temporal expression of let-7 heterochronic regulatory RNA." Nature **408**(6808): 86-89.

Patel, A. and S. McFarlane (2000). "Overexpression of FGF-2 alters cell fate specification in the developing retina of Xenopus laevis." Dev Biol **222**(1): 170-180.

Pearson, B. J. and C. Q. Doe (2003). "Regulation of neuroblast competence in Drosophila." Nature **425**(6958): 624-628.

Pegtel, D. M., S. I. Ellenbroek, A. E. Mertens, R. A. van der Kammen, J. de Rooij and J. G. Collard (2007). "The Par-Tiam1 complex controls persistent migration by stabilizing microtubule-dependent front-rear polarity." Curr Biol **17**(19): 1623-1634.

Pezeron, G., P. Mourrain, S. Courty, J. Ghislain, T. S. Becker, F. M. Rosa and N. B. David (2008). "Live analysis of endodermal layer formation identifies random walk as a novel gastrulation movement." Curr Biol **18**(4): 276-281.

Picker, A., D. Roellig, O. Pourquie, A. C. Oates and M. Brand (2009). "Tissue micromanipulation in zebrafish embryos." Methods Mol Biol **546**: 153-172.

Plautz, J. D., M. Kaneko, J. C. Hall and S. A. Kay (1997). "Independent photoreceptive circadian clocks throughout Drosophila." Science **278**(5343): 1632-1635.

Pourquie, O. (2001). "Vertebrate somitogenesis." Annu Rev Cell Dev Biol **17**: 311-350.

Pourquie, O. (2003). "The segmentation clock: converting embryonic time into spatial pattern." Science **301**(5631): 328-330.

Prioleau, M. N., J. Huet, A. Sentenac and M. Mechali (1994). "Competition between chromatin and transcription complex assembly regulates gene expression during early development." Cell **77**(3): 439-449.

Raff, M. (2006). "The mystery of intracellular developmental programmes and timers." Biochem Soc Trans **34**(Pt 5): 663-670.

Ram, P. T. and R. M. Schultz (1993). "Reporter gene expression in G2 of the 1-cell mouse embryo." Dev Biol **156**(2): 552-556.

Rapaport, D. H., S. L. Patheal and W. A. Harris (2001). "Cellular competence plays a role in photoreceptor differentiation in the developing Xenopus retina." J Neurobiol **49**(2): 129-141.

Reimann, J. D., E. Freed, J. Y. Hsu, E. R. Kramer, J. M. Peters and P. K. Jackson (2001). "Emi1 is a mitotic regulator that interacts with Cdc20 and inhibits the anaphase promoting complex." Cell **105**(5): 645-655.

Reinhart, B. J., F. J. Slack, M. Basson, A. E. Pasquinelli, J. C. Bettinger, A. E. Rougvie, H. R. Horvitz and G. Ruvkun (2000). "The 21-nucleotide let-7 RNA regulates developmental timing in Caenorhabditis elegans." Nature **403**(6772): 901-906.

Resino, J., P. Salama-Cohen and A. Garcia-Bellido (2002). "Determining the role of patterned cell proliferation in the shape and size of the Drosophila wing." Proc Natl Acad Sci U S A **99**(11): 7502-7507.

Roh, M. H., S. Fan, C. J. Liu and B. Margolis (2003). "The Crumbs3-Pals1 complex participates in the establishment of polarity in mammalian epithelial cells." J Cell Sci **116**(Pt 14): 2895-2906.

Roskelley, C. D., P. Y. Desprez and M. J. Bissell (1994). "Extracellular matrix-dependent tissue-specific gene expression in mammary epithelial cells requires both physical and biochemical signal transduction." Proc Natl Acad Sci U S A **91**(26): 12378-12382.

Saitsu, H., S. Yamada, C. Uwabe, M. Ishibashi and K. Shiota (2004). "Development of the posterior neural tube in human embryos." Anat Embryol (Berl) **209**(2): 107-117.

Sato, T., S. Mushiake, Y. Kato, K. Sato, M. Sato, N. Takeda, K. Ozono, K. Miki, Y. Kubo, A. Tsuji, R. Harada and A. Harada (2007). "The Rab8 GTPase regulates apical protein localization in intestinal cells." Nature **448**(7151): 366-369.

Sawyer, J. M., J. R. Harrell, G. Shemer, J. Sullivan-Brown, M. Roh-Johnson and B. Goldstein (2009). "Apical constriction: A cell shape change that can drive morphogenesis." Dev Biol.

Schluter, M. A., C. S. Pfarr, J. Pieczynski, E. L. Whiteman, T. W. Hurd, S. Fan, C. J. Liu and B. Margolis (2009). "Trafficking of Crumbs3 during cytokinesis is crucial for lumen formation." Mol Biol Cell **20**(22): 4652-4663.

Schmoranzer, J., J. P. Fawcett, M. Segura, S. Tan, R. B. Vallee, T. Pawson and G. G. Gundersen (2009). "Par3 and dynein associate to regulate local microtubule dynamics and centrosome orientation during migration." Curr Biol **19**(13): 1065-1074.

Schoenwolf, G. C. (1983). "The chick epiblast: a model for examining epithelial morphogenesis." Scan Electron Microsc(Pt 3): 1371-1385.

Schoenwolf, G. C. (1984). "Histological and ultrastructural studies of secondary neurulation in mouse embryos." Am J Anat **169**(4): 361-376.

Schoenwolf, G. C. and J. Delongo (1980). "Ultrastructure of secondary neurulation in the chick embryo." Am J Anat **158**(1): 43-63.

Schoenwolf, G. C. and M. V. Franks (1984). "Quantitative analyses of changes in cell shapes during bending of the avian neural plate." Dev Biol **105**(2): 257-272.

Schoenwolf, G. C. and M. L. Powers (1987). "Shaping of the chick neuroepithelium during primary and secondary neurulation: role of cell elongation." Anat Rec **218**(2): 182-195.

Schotz, E. M., R. D. Burdine, F. Julicher, M. S. Steinberg, C. P. Heisenberg and R. A. Foty (2008). "Quantitative differences in tissue surface tension influence zebrafish germ layer positioning." HFSP J **2**(1): 42-56.

Sepich, D. S., D. C. Myers, R. Short, J. Topczewski, F. Marlow and L. Solnica-Krezel (2000). "Role of the zebrafish trilobite locus in gastrulation movements of convergence and extension." Genesis **27**(4): 159-173.

Shin, K. and B. Margolis (2006). "ZOning out tight junctions." Cell **126**(4): 647-649.

Shuster, C. B. and D. R. Burgess (2002). "Targeted new membrane addition in the cleavage furrow is a late, separate event in cytokinesis." Proc Natl Acad Sci U S A **99**(6): 3633-3638.

Simmons, N. L. (1982). "Cultured monolayers of MDCK cells: a novel model system for the study of epithelial development and function." Gen Pharmacol **13**(4): 287-291.

Skop, A. R., D. Bergmann, W. A. Mohler and J. G. White (2001). "Completion of cytokinesis in C. elegans requires a brefeldin A-sensitive membrane accumulation at the cleavage furrow apex." Curr Biol **11**(10): 735-746.

Smith, J. L. and G. C. Schoenwolf (1987). "Cell cycle and neuroepithelial cell shape during bending of the chick neural plate." Anat Rec **218**(2): 196-206.

Sohrmann, M. and M. Peter (2003). "Polarizing without a c(l)ue." Trends Cell Biol **13**(10): 526-533.

Strutt, H. and D. Strutt (2005). "Long-range coordination of planar polarity in Drosophila." Bioessays **27**(12): 1218-1227.

Sun, Z., P. Jin, T. Tian, Y. Gu, Y. G. Chen and A. Meng (2006). "Activation and roles of ALK4/ALK7-mediated maternal TGFbeta signals in zebrafish embryo." Biochem Biophys Res Commun **345**(2): 694-703.

Suzuki, A., C. Ishiyama, K. Hashiba, M. Shimizu, K. Ebnet and S. Ohno (2002). "aPKC kinase activity is required for the asymmetric differentiation of the premature junctional complex during epithelial cell polarization." J Cell Sci **115**(Pt 18): 3565-3573.

Tada, M. and M. Kai (2009). "Noncanonical Wnt/PCP signaling during vertebrate gastrulation." Zebrafish **6**(1): 29-40.

Tadros, W. and H. D. Lipshitz (2009). "The maternal-to-zygotic transition: a play in two acts." Development **136**(18): 3033-3042.

Takamiya, M. and J. A. Campos-Ortega (2006). "Hedgehog signalling controls zebrafish neural keel morphogenesis via its level-dependent effects on neurogenesis." Dev Dyn **235**(4): 978-997.

Tamai, T. K., A. J. Carr and D. Whitmore (2005). "Zebrafish circadian clocks: cells that see light." Biochem Soc Trans **33**(Pt 5): 962-966.

Tamai, T. K., V. Vardhanabhuti, N. S. Foulkes and D. Whitmore (2004). "Early embryonic light detection improves survival." Curr Biol **14**(3): R104-105.

Tanentzapf, G. and U. Tepass (2003). "Interactions between the crumbs, lethal giant larvae and bazooka pathways in epithelial polarization." Nat Cell Biol **5**(1): 46-52.

Tang, V. W. and D. A. Goodenough (2003). "Paracellular ion channel at the tight junction." Biophys J **84**(3): 1660-1673.

Tawk, M., C. Araya, D. A. Lyons, A. M. Reugels, G. C. Girdler, P. R. Bayley, D. R. Hyde, M. Tada and J. D. Clarke (2007). "A mirror-symmetric cell division that orchestrates neuroepithelial morphogenesis." Nature **446**(7137): 797-800.

Temple, S. and M. C. Raff (1986). "Clonal analysis of oligodendrocyte development in culture: evidence for a developmental clock that counts cell divisions." Cell **44**(5): 773-779.

Tepass, U., G. Tanentzapf, R. Ward and R. Fehon (2001). "Epithelial cell polarity and cell junctions in Drosophila." Annu Rev Genet **35**: 747-784.

Thery, M., V. Racine, A. Pepin, M. Piel, Y. Chen, J. B. Sibarita and M. Bornens (2005). "The extracellular matrix guides the orientation of the cell division axis." Nat Cell Biol **7**(10): 947-953.

Tibbitt, M. W. and K. S. Anseth (2009). "Hydrogels as extracellular matrix mimics for 3D cell culture." Biotechnol Bioeng **103**(4): 655-663.

Tsukita, S., M. Furuse and M. Itoh (2001). "Multifunctional strands in tight junctions." Nat Rev Mol Cell Biol **2**(4): 285-293.

Turner, D. L. and C. L. Cepko (1987). "A common progenitor for neurons and glia persists in rat retina late in development." Nature **328**(6126): 131-136.

Valencia-Sanchez, M. A., J. Liu, G. J. Hannon and R. Parker (2006). "Control of translation and mRNA degradation by miRNAs and siRNAs." Genes Dev **20**(5): 515-524.

van Eeden, F. J., M. Granato, U. Schach, M. Brand, M. Furutani-Seiki, P. Haffter, M. Hammerschmidt, C. P. Heisenberg, Y. J. Jiang, D. A. Kane, R. N. Kelsh, M. C. Mullins, J. Odenthal, R. M. Warga, M. L. Allende, E. S. Weinberg and C. Nusslein-Volhard (1996). "Mutations affecting somite formation and patterning in the zebrafish, Danio rerio." Development **123**: 153-164.

von Stein, W., A. Ramrath, A. Grimm, M. Muller-Borg and A. Wodarz (2005). "Direct association of Bazooka/PAR-3 with the lipid phosphatase PTEN reveals a link between the PAR/aPKC complex and phosphoinositide signaling." Development **132**(7): 1675-1686.

von Trotha, J. W., J. A. Campos-Ortega and A. M. Reugels (2006). "Apical localization of ASIP/PAR-3:EGFP in zebrafish neuroepithelial cells involves the oligomerization domain CR1, the PDZ domains, and the C-terminal portion of the protein." Dev Dyn **235**(4): 967-977.

Vuilleumier, R., L. Besseau, G. Boeuf, A. Piparelli, Y. Gothilf, W. G. Gehring, D. C. Klein and J. Falcon (2006). "Starting the zebrafish pineal circadian clock with a single photic transition." Endocrinology **147**(5): 2273-2279.

Vukicevic, S., H. K. Kleinman, F. P. Luyten, A. B. Roberts, N. S. Roche and A. H. Reddi (1992). "Identification of multiple active growth factors in basement membrane Matrigel suggests caution in interpretation of cellular activity related to extracellular matrix components." Exp Cell Res **202**(1): 1-8.

Wada, H. and H. Okamoto (2009). "Roles of noncanonical Wnt/PCP pathway genes in neuronal migration and neurulation in zebrafish." Zebrafish **6**(1): 3-8.

Wallingford, J. B. and R. M. Harland (2002). "Neural tube closure requires Dishevelled-dependent convergent extension of the midline." Development **129**(24): 5815-5825.

Wang, A. Z., G. K. Ojakian and W. J. Nelson (1990a). "Steps in the morphogenesis of a polarized epithelium. I. Uncoupling the roles of cell-cell and cell-substratum

contact in establishing plasma membrane polarity in multicellular epithelial (MDCK) cysts." J Cell Sci **95 (Pt 1)**: 137-151.

Wang, A. Z., G. K. Ojakian and W. J. Nelson (1990b). "Steps in the morphogenesis of a polarized epithelium. II. Disassembly and assembly of plasma membrane domains during reversal of epithelial cell polarity in multicellular epithelial (MDCK) cysts." J Cell Sci **95 (Pt 1)**: 153-165.

Wang, H. and W. Chia (2005a). "Drosophila neural progenitor polarity and asymmetric division." Biol Cell **97**(1): 63-74.

Wang, J., N. S. Hamblet, S. Mark, M. E. Dickinson, B. C. Brinkman, N. Segil, S. E. Fraser, P. Chen, J. B. Wallingford and A. Wynshaw-Boris (2006). "Dishevelled genes mediate a conserved mammalian PCP pathway to regulate convergent extension during neurulation." Development **133**(9): 1767-1778.

Wang, J., S. Mark, X. Zhang, D. Qian, S. J. Yoo, K. Radde-Gallwitz, Y. Zhang, X. Lin, A. Collazo, A. Wynshaw-Boris and P. Chen (2005b). "Regulation of polarized extension and planar cell polarity in the cochlea by the vertebrate PCP pathway." Nat Genet **37**(9): 980-985.

Wang, Y. and J. Nathans (2007). "Tissue/planar cell polarity in vertebrates: new insights and new questions." Development **134**(4): 647-658.

Watanabe, T. and M. C. Raff (1990). "Rod photoreceptor development in vitro: intrinsic properties of proliferating neuroepithelial cells change as development proceeds in the rat retina." Neuron **4**(3): 461-467.

Wei, X., Y. Luo and D. R. Hyde (2006). "Molecular cloning of three zebrafish lin7 genes and their expression patterns in the retina." Exp Eye Res **82**(1): 122-131.

Weigmann, K., S. M. Cohen and C. F. Lehner (1997). "Cell cycle progression, growth and patterning in imaginal discs despite inhibition of cell division after inactivation of Drosophila Cdc2 kinase." Development **124**(18): 3555-3563.

Wetts, R. and S. E. Fraser (1988). "Multipotent precursors can give rise to all major cell types of the frog retina." Science **239**(4844): 1142-1145.

Whitlock, K. E. and M. Westerfield (2000). "The olfactory placodes of the zebrafish form by convergence of cellular fields at the edge of the neural plate." Development **127**(17): 3645-3653.

Wolff, T. and G. M. Rubin (1998). "Strabismus, a novel gene that regulates tissue polarity and cell fate decisions in Drosophila." Development **125**(6): 1149-1159.

Wong, L. L. and P. N. Adler (1993). "Tissue polarity genes of Drosophila regulate the subcellular location for prehair initiation in pupal wing cells." J Cell Biol **123**(1): 209-221.

Woo, K. and S. E. Fraser (1998). "Specification of the hindbrain fate in the zebrafish." Dev Biol **197**(2): 283-296.

Yamada, K. M. and E. Cukierman (2007). "Modeling tissue morphogenesis and cancer in 3D." Cell **130**(4): 601-610.

Yamanaka, T., Y. Horikoshi, Y. Sugiyama, C. Ishiyama, A. Suzuki, T. Hirose, A. Iwamatsu, A. Shinohara and S. Ohno (2003). "Mammalian Lgl forms a protein complex with PAR-6 and aPKC independently of PAR-3 to regulate epithelial cell polarity." Curr Biol **13**(9): 734-743.

Yang, X., J. Zou, D. R. Hyde, L. A. Davidson and X. Wei (2009). "Stepwise maturation of apicobasal polarity of the neuroepithelium is essential for vertebrate neurulation." J Neurosci **29**(37): 11426-11440.

Ybot-Gonzalez, P., D. Savery, D. Gerrelli, M. Signore, C. E. Mitchell, C. H. Faux, N. D. Greene and A. J. Copp (2007). "Convergent extension, planar-cell-polarity signalling and initiation of mouse neural tube closure." Development **134**(4): 789-799.

Yonemura, S., M. Itoh, A. Nagafuchi and S. Tsukita (1995). "Cell-to-cell adherens junction formation and actin filament organization: similarities and differences between non-polarized fibroblasts and polarized epithelial cells." J Cell Sci **108 (Pt 1)**: 127-142.

Yu, H. M., B. Jerchow, T. J. Sheu, B. Liu, F. Costantini, J. E. Puzas, W. Birchmeier and W. Hsu (2005a). "The role of Axin2 in calvarial morphogenesis and craniosynostosis." Development **132**(8): 1995-2005.

Yu, W., A. Datta, P. Leroy, L. E. O'Brien, G. Mak, T. S. Jou, K. S. Matlin, K. E. Mostov and M. M. Zegers (2005b). "Beta1-integrin orients epithelial polarity via Rac1 and laminin." Mol Biol Cell **16**(2): 433-445.

Yu, W., A. M. Shewan, P. Brakeman, D. J. Eastburn, A. Datta, D. M. Bryant, Q. W. Fan, W. A. Weiss, M. M. Zegers and K. E. Mostov (2008). "Involvement of RhoA, ROCK I and myosin II in inverted orientation of epithelial polarity." EMBO Rep **9**(9): 923-929.

Zhang, L., C. Kendrick, D. Julich and S. A. Holley (2008). "Cell cycle progression is required for zebrafish somite morphogenesis but not segmentation clock function." Development **135**(12): 2065-2070.

Zheng, L., J. Zhang and R. W. Carthew (1995). "frizzled regulates mirror-symmetric pattern formation in the Drosophila eye." Development **121**(9): 3045-3055.

Ziv, L. and Y. Gothilf (2006a). "Circadian time-keeping during early stages of development." Proc Natl Acad Sci U S A **103**(11): 4146-4151.

Ziv, L. and Y. Gothilf (2006b). "Period2 expression pattern and its role in the development of the pineal circadian clock in zebrafish." Chronobiol Int **23**(1-2): 101-112.

Zolessi, F. R., L. Poggi, C. J. Wilkinson, C. B. Chien and W. A. Harris (2006). "Polarization and orientation of retinal ganglion cells in vivo." Neural Dev **1**: 2.